The nucleolus: a connection between cell fate and tumorigenesis in colorectal cancer

Clara Morral Martínez

DOCTORAL THESIS UPF - 2017

Director

Eduard Batlle Gómez, PhD

Tutor

Antonio García de Herreros Madueño, PhD

Institute for Research in Biomedicine, Barcelona

Colorectal Cancer Laboratory

Experimental and Life Science Department

A la mare

ACKNOWLEDGEMENTS

En primer lloc voldria donar les gràcies al meu supervisor. Gràcies Edu per haver-me donat l'oportunitat de poder formar part d'aquest gran equip. Gràcies sobretot per haver-me guiat durant tots aquests anys. Amb tu he après a desenvolupar idees, a ser crítica, a ser exigent, a ser curiosa i també ambiciosa. Recordo que un dia em vas dir que l'autèntica marató és la del doctorat, i sens dubte aquesta ha estat una de les curses més dures que he fet mai.
Elena, gràcies a tu també per haver-me ajudat en qualsevol cosa que he necessitat. La teva eficiència i professionalitat han estat clau per fer dels problemes solucions senzilles i sense importància.

Un BIG THANK YOU als meus companys de cursa de Batlle lab. I és que em sento immensament agraïda per tota l'ajuda i el suport que he rebut dia rere dia durant aquests cinc anys. Voldria mencionar primer de tot a l'Anna. Gràcies per la paciència que vas tenir amb mi quan vaig entrar al lab i no sabia gairebé ni posar una PCR. Tu em vas donar les bases que m'han servit per poder ser independent i anar desenvolupant el que ara ha acabat sent aquest projecte de tesis doctoral. Quan vas marxar, de forma quasi natural em vaig aferrar al Francisco. "Doctor", gracias por haber cuidado de mi todo este tiempo. Gracias por toda la ayuda y soporte que me has dado. Ya sabes que para mi siempre has sido todo un referente como científico y como persona.

No va fer falta que passés massa temps de la meva arribada al lab per adonar-me que tres persones eren clau per mantenir l'alt nivell de qualitat científica que m'envoltava. Marta, Sergio i Xavi, gràcies per la vostra constant implicació i ajuda en tots els projectes i per no tenir mai un no per resposta. Gràcies pel vostre bon humor malgrat les llistes inacabables de tincions o les hores infinites al estabulari.

During this long race I've also been extremely lucky to have two brilliant scientists by my side. Diana and Daniele thank you for all your help and support during these years. You have always been here when I've needed it. Not only for a protocol but also for a great advice, a simple smile or a big hug.

Carme, gràcies per la constant paciència, ajuda i energia inacabables que m'has donat durant tot aquest anys.

Mil gràcies també als Young Batlle's; Gemma, Jordi, Adrián i Adrià. Per mi sou talent i sou exemple. També sou la desconnexió, l'aire fresc, el bon rotllo i la vitalitat que m'han estat essencials per poder seguir fent quilòmetres en aquest doctorat.

I quan semblava que les cames em feien fallida va aparèixer, així com caiguda del cel, la Jelena. Gracias Jelena por confiar en mi y en este proyecto. Gracias por haber tenido la valentía de calzarte las bambas y acompañarme estos últimos años. Contigo he aprendido de ciencia y de vida. Gracias por la paciencia, por aguantar mis manías, mi pesimismo, mis agobios y problemas. No se que pasará cuando esto acabe, pero sea lo que sea estoy segura que será grande, bonito e inextinguible.

I és que cinc anys és més que suficient per veure companys que arriben però també que se'n van. Thank you to all the former membres of Batlle lab, Gavin, Peter, Alex, Mark, Enza and Elisa. You have also been part of it!

Com en qualsevol cursa, hi ha moments en que has de parar ja sigui per curar ferides o carregar piles i així poder seguir endavant. ''Ladies'', vosaltres heu estat des del primer dia el meu avituallament. Sense vosaltres hagués esta molt difícil seguir corrent. Gràcies per fer-me costat en tot moment i ser allà quan ho he necessitat. Berta, Núria, Anna i Clara, amb la mà al cor, us puc assegurar que sou un dels millors regals que m'ha donat el doctorat i només per això ja ha valgut la pena.
Victor, això també va per tu. Gràcies per els mil berenars, els dinars, els ron llimona, els bailoteos, les llargues discussions i els somriures. Gràcies per repetir-me (encara que només fos per animar-me) que la ciència em cau a mida. Pots estar tranquil que si mai tinc el meu propi lab seràs el primer tècnic que contacti! ;)
Marc, gràcies per treure'm a córrer de tant en tant, per escoltar els meus problemes, per als consells, per tenir sempre raó i per haver estat sempre disposat a ajudar-me. Gràcies a tota les resta de corredors: Ivan, Enrique, Sandra, Joana, Rosa, Irene, Frans i Konstantin. Saber que no corria sola m'ha donat els ànims per no defallir ni en les pujades més dures.

I ja puc córrer amb tot la meva energia que si no fos per tots els que des de fora m'heu animat no ho hauria aconseguit. Així doncs gràcies a les nenes de la Uni, tot això en realitat va començar allà, entre classes, pràctiques i algun que altre Apolo.

Especialment Alba i Estela, gràcies per escoltar-me i animar-me cada vegada que he saturat les nostres cerveses i cafès amb els meus problemes científics.
Marc i Artur, veure-us rondant pels passadissos de l'IRB em retorna als anys inolbidables d'Universitat i em fan treure un somriure.

Nenes d'Ullastrell, gràcies per formar part dels meus moments de desconnexió entre caps de setmana, estius, festes majors, concerts, converses inacabables per arreglar el món, comiats i aviat casaments!

Especial gràcies al meu amic fidel Joan, gràcies per ser-hi sempre en un obrir i tancar d'ulls encara que faci dies que no sàpigues res de mi. Se que puc comptar amb tu per qualsevol cosa, des de passar un dels millors estius a muntar una tesis en 48h.

Ignasi, tu has estat una de les poques persones que has viscut la Clara en el més estat pur. La Clara del mal humor, la Clara que perd la noció del temps entre experiments, la Clara que llegeix papers abans d'anar a dormir, la Clara que avui diu que serà la millor científica del món i que l'endemà desitja abandonar la ciència. La Clara que no sap separar un mal resultat d'un mal dia. Però també la Clara que estima, que valora i que es preocupa encara que no sempre ho sàpiga demostrar. Tu company de vida i de curses has aguantat tot això i molt més. Gràcies.

Finalment gràcies a la meva família. Gràcies per tot l'amor, la confiança i suport que sempre m'heu donat. Pare, Maria, gràcies per ensenyar-me a ser valenta, treballadora, constant i perseverant. De vosaltres he après que amb esforç i dedicació podem aconseguir coses meravelloses. Mariona, gràcies per pensar sempre en mi. Gràcies per no tenir en compte que hagi estat massa ocupada amb el doctorat en moments que m'has necessitat. Ricard, gràcies pels ajuts d'última hora. Vinyet, gràcies per la teva innocència que m'ajuda a relativitzar tots els meus grans problemes. Gràcies a tots per ser-hi sempre des de la sortida fins a la meta.

ABSTRACT

Colorectal cancers (CRCs) are amalgams of phenotypically distinct tumor cell populations in which only a subset of cells retain the capacity to sustain tumor growth and propagate the disease. Our laboratory and others have been able to isolate this particular group of tumor cells – termed colorectal cancer stem cells (CRC-SCs)- and characterize their genetic progra. However, the biology behind their differential tumor potential remains poorly understood. The research in this thesis has focus on the biological functions specifically enriched in this population compared with their differentiated and non-tumorigenic counterparts.

Data mining of the expression profiles of normal and cancer stem cells suggested that nucleolar function was enhanced in both types of stem cells. This biological activity is dedicated to the production of ribosomal RNA (rRNA) which in turn is used to generate ribosomes that sustain the translation rates of the cells. We have validated these in silico observations using different *in vitro* and *in vivo* models that allow us to reproduce the intestinal biology and disease. We have discovered that nucleolar activity is heterogeneously regulated in colorectal cancer (CRC) and that high levels of this activity correlate with the undifferentiated state of tumor cells. By means of CRISPR-Cas9 technology we have generated colorectal cancer organoids expressing endogenous RNA Polymerase I (RNA POL I) fused to a EGFP reporter protein. Analysis of tumor cells purified from patient derived xenografts (PDX) expressing high levels of RNA Pol I demonstrated that these cells display elevated rDNA transcriptional activity as well as tumorigenic potential. On the contrary, tumor cells with low levels of RNA Pol I represent a differentiated population with dismal tumor capacity. Furthermore, we also put forward evidence that nucleolar activity is WNT regulated and that the WNT target MYC may be essential in this scenario.

Taken together, our data provides new insights on the biology behind the differential tumorigenic behavior and fate of tumor cells in CRCs. Importantly, it also contributes to better understanding cell heterogeneity and may provide the basis for the development of new therapeutic strategies to tackle this disease.

RESUM

El càncer de colon es caracteritza per presentar una composició cel·lular heterogènia en la qual només un subgrup de cèl·lules retenen la capacitat de contribuir en el manteniment i creixement del tumor. Malgrat que el nostre laboratori i altres han aconseguit aïllar aquesta subpoblació de cèl·lules tumorals – anomenades cèl·lules mare tumorals- i caracteritzar el programa genètic que expressen, la biologia darrera el seu potencial tumoral que les caracteritza encara no s'ha descobert. L 'investigació duta a terme en aquesta tesis es focalitza en estudiar aquelles funcions biològiques que estan específicament enriquides en aquesta subpoblació tumoral comparat amb altres cèl·lules cancerígenes que no tenen potencial tumoral.

A partir de dades obtingudes en analitzar l'expressió genètica de cèl·lules mare normals i tumorals, hem descobert que l'activitat nucleolar està específicament sobre-activada en aquestes dues poblacions. Aquesta activitat biològica es basa en la transcripció d'RNA ribosomal, que és essencial per a la generació de ribosomes destinats a la síntesis proteica. Hem validat aquestes dades utilitzant diferents models *in vivo* i *in vitro* que ens permeten reproduir la biologia intestinal. Hem descobert que l'activitat nucleolar està regulada de forma heterogènia en els tumors de colon. Concretament, són les cèl·lules mare del tumor que presenten una major activació d'aquesta funció biològica. Utilitzant tècniques d'edició del genoma (CRISPR-Cas9) hem pogut generar cèl·lules tumorals de colon que expressen la proteïna RNA Polymerasa I fusionada a una molècula fluorescent (EGFP). D'aquesta manera hem pogut aïllar dels tumors de colon cèl·lules tumorals que presenten una elevada activitat nucleolar. Interessantment, hem descobert que aquestes cèl·lules tenen una elevada capacitat tumoral, mentre que altres cèl·lules tumorals amb baixa activitat nucleolar no són capaces de retenir aquest potencial cancerigen. Finalment també hem obtingut evidències de que aquesta activitat nucleolar podria estar regulada per la via de senyalització de WNT i que el oncogen MYC podria jugar un paper molt important en aquest escenari.

Els resultats obtinguts durant aquesta tesis proveeixen nova informació per al que fa a les funcions biològiques que regulen el potencial tumoral de les cèl·lules de càncer de colon. Això en permetrà entendre millor la malaltia i poder desenvolupar noves teràpies més efectives.

PREFACE

Colorectal cancers (CRCs) display a heterogeneous composition of tumor cells. Over the last decade, several studies have evidenced that not all cells present in primary CRCs are capable to sustain and regenerate the tumor as isolated entities. Instead, it has been demonstrated that CRCs contain a subset of tumor cells with elevated tumorigenic potential. This particular tumor cell population express a gene program similar to that of intestinal stem cells (ISCs) and are also able to give rise to differentiated-like progeny with dismal tumorigenic capacity (Dalerba, Dylla, Park, & Liu, 2007; Merlos-Suárez et al., 2011; O'Brien, Pollett, Gallinger, & Dick, 2007; Ricci-Vitiani et al., 2007). Hence, they have been termed colorectal cancer stem cells (CRC-SCs). Taking advantage of the CRC-SC purification strategy developed in our laboratory using the stem cell marker EPHB2 we have isolated this particular tumor cell population from various patient biopsies and further identified and studied biological functions that could play a role in their tumorigenic potential.

Bioinformatical analysis revealed that nucleolar function was clearly upregulated in CRC-SCs when compared to their differentiated-like and non-tumorigenic counterparts. Thus, we hypothesized that this biological function could explain part of the tumorigenic behavior restricted to this population. We have demonstrated that nucleolar activity is indeed heterogeneously regulated in CRCs and moreover, that it correlates with the undifferentiated state of tumor cells. Taking advantage of the recently developed genome editing technique CRISPR-Cas9, we have genetically fused a key nucleolar protein to a fluorescent reporter. Using this tool we have been able to isolate tumor cells displaying elevated nucleolar activity and prove their tumor initiating behavior. Although the specific mechanism controlling nucleolar activity in CRC-SCs still under study, we have preliminary evidence that points to WNT signaling as a likely mediator of this biological activity in CRCs. Current work performed with the tools generated during this thesis is aimed to address remaining questions regarding nucleolar activity and CRC-SCs, thus shedding additional valuable information to the understanding of tumor heterogeneity and cancer stem cell biology.

TABLE OF CONTENTS

Introduction

1. Adult stem cells

Tissue homeostasis ensures that the wear and tear of the different organs does not affect their function and it normally implies constant renewal of the cells that form a particular tissue over time. One of the most important traits to maintain tissue homeostasis is a hierarchical organization. This concept implies that the cellular heterogeneity composing adult tissues is organized both at functional and spatial level. Stem cells (SCs) reside at the apex of the hierarchy. SCs are long-lived and undifferentiated, and are able to give rise to other specialized cell types of a particular tissue. From a functional point of view stem cells are the fuel of tissue regeneration and integrity. On the other hand, mature differentiated cells ensure tissue functions.

The proportion of SCs in adult tissues is relatively low compared with other cell types. In most tissues the transition from a stem cell to a terminally differentiated cell is not driven by a direct switch. Instead, SCs first give rise to progenitor cells with high proliferation capacity but non self-renewal properties, which are already committed to differentiate. Eventually, further along the hierarchy, these progenitors will undergo terminal differentiation to functional specialized cells with physiological functions composing mature tissues (**Figure 1**).

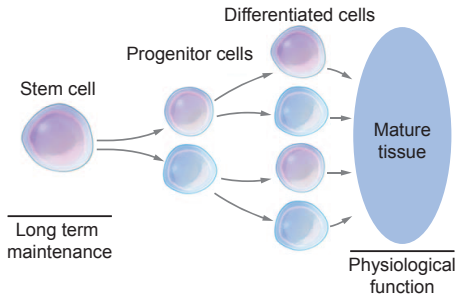

Figure 1: Schematic representation of a hierarchically organized tissue. Stem cells (SCs), defined by their ability to self-renew and give rise to differentiated cells, reside at the base of the hierarchy. Before differentiating into mature functional cells, SCs frequently give rise first to progenitor cells that undergo several rounds of division until they terminally differentiate. Adapted from (Jordan at al., 2006).

Stemness is an amazing and powerful trait that has captured the interest of biologists for many years. Already in the 60ths, Pierce showed that malignant teratocarcinomas contained highly tumorigenic cells that, as single cells, could differentiate into multiple differentiated, non-tumorigenic cell types (KLEINSMITH & PIERCE, 1964).

Later on, in the early nineties research on hematopoietic stem cells (HSCs) provided new insights about stem cell biology (Bonnet & Dick, 1997; Lapidot et al., 1994). From these studies, stem cells were defined as discrete, rare and non-dividing physical entities. This concept has dominated the stem cell field over the past two decades. Yet, more recent analysis of the behaviour of adult stem cells in several tissues

such as the intestine, has revealed that stem cells properties do not always fit in well with those originally described for the HSC. Indeed many SCs can be abundant, cycling and divide symmetrically (Clevers, 2015). These disparities suggest that stem cells should be defined based on their function rather than through a subset of hardwired properties.

1.1 Definition of Stem Cell

There are two essential properties to define SCs in adult tissues: self-renewal and multilineage differentiation capacity (Barker, van de Wetering, Clevers, Wetering, & Clevers, 2008; Fuchs, 2009; Fuchs & Chen, 2013). Moreover, SCs are able to live for long periods of time, as they are the source of all other cell types in the tissue. On the contrary, differentiated cells are short-lived with specialized functions.

1.1.1 Self-renewal

SCs self-renew constantly in order to ensure precise numbers and avoid exhaustion. SCs can divide either symmetrically or asymmetrically.

Symmetric divisions give rise to two identical daughter cells that can be specified as either two new stem cells, two early committed progenitors or two differentiated cells. In this case, the generation of differentiated progenitors relies on stochastic events or more commonly depend on the size of the SC niche so that differentiation occurs when the resulting daughter cells are displaced from the SC permissive environment. Symmetric division requires a large pool of SCs in order to self-sustain the population as at any given moment the result of SC division can lead to the formation of two differentiated cells, which would lead to the loss of parental SC clone (**Figure 2A**). By contrast, when stem cells divide asymmetrically they give rise to two different cell types, a SC and either an early committed progenitor or a differentiated cell. This kind of division usually implies the asymmetric distribution of cellular components in the two resulting daughter cells which defines different identities. In this model, a small subset of SCs is able to maintain the population since the fate of the daughter cell is deterministic (Morrison & Kimble, 2006) (**Figure 2B**).

Each type of division mode depends on the tissue and cell type. Classical examples of asymmetric division are found in model organisms such as c-elegans or Drosophila. In mammals a prime example of asymmetric cell division are the undifferentiated neural progenitors that distribute Numb asymmetrically to precursors destined to neurogenesis (Zhong et al., 1996).

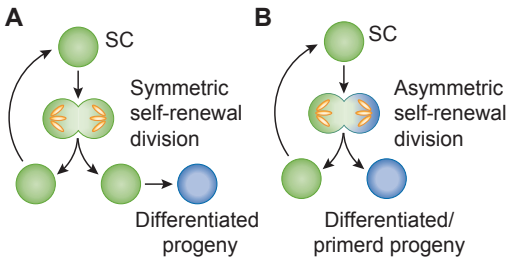

Figure 2: Symmetric and asymmetric SC division. (**A**) In symmetrical cell divisions, cellular components are equally distributed to the two daughters cells. Cell fate specification is not coupled to mitosis and differentiation relies on stochastic events or in some cases when the new daughter cell is displaced to a new microenvironment. (**B**) In asymmetrical cell division, cell fate specification is coupled to mitosis and involves unequal partitioning of cellular components to the resulting daughters. Adapted from (Fuchs & Chen, 2013).

SC identity not only relies on mechanisms such as the division mode but also on potent signals coming from the surrounding microenvironment known as the "niche" (Morrison & Spradling, 2008). The SC niche represents an anatomical compartment that provides signals to SCs. In general, the niche is composed by: stromal cells; extracellular matrix (ECM) proteins that provide structure, organization and mechanical signals; blood vessels that carry systemic signals and recruit inflammatory and other circulating cells to the niche; and neural inputs that communicate distant physiological signals to the stem cell niche (Lane, Williams, & Watt, 2014) (**Figure 3**).

In general, maintenance of stem cell identity by niche signals is achieved

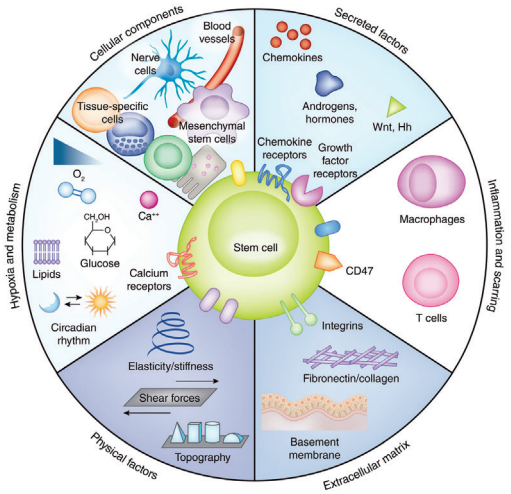

Figure 3: Niche Composition. Stem cell niches are complex, heterotypic, dynamic structures, which include different cellular components, secreted factors, immunological and metabolic control, ECM, and physical parameters. Adapted from (Lane, Williams, & Watt, 2014).

either by direct cell contact or through secretion of ligands. Examples of cell-cell contact are found in Drosophila where niche Hub cells attach to germline SCs through adherent junctions (Fuchs & Chen, 2013). Alternatively, stem cells can receive ligand mediated niche signals. A clear example are WNT proteins which in the intestine are secreted by myofibroblasts and by Paneth cells and allow the renewal of intestinal stem cells (Gregorieff et al., 2005; Sato et al., 2011).

1.1.2 Multipotency

The other fundamental stem cell property is the ability to generate multi-lineage progenitors. This is an essential requirement to maintain

tissue homeostasis since differentiated cells are responsible of ensuring tissue functionality.

The capacity of stem cells to give rise to other specialized cell types is known as “differentiation process”. Generally, differentiation is driven by signalling pathways that promote changes in the transcription profile of stem cells. In most tissues, these genetic changes consist on a global silencing of the stem cell gene program and activation of the differentiation transcriptional profile. The process of differentiation is usually accompanied by a reduction of the proliferation capacity of the differentiated progenitors that will eventually exhaust. A large proportion of the differentiation program encodes for proteins required to perform tissue function, such as digestive enzymes in the stomach, proteins that mediate contractility in muscle cells or detoxifying enzymes in the liver.

The differentiation capacity of adult SCs is restricted to specific differentiated populations of a particular tissue. This process is different from that of pluripotent property of embryonic stem cells (ESCs), which are able to give rise to all tissue types found in adult organisms (**Figure 4**).

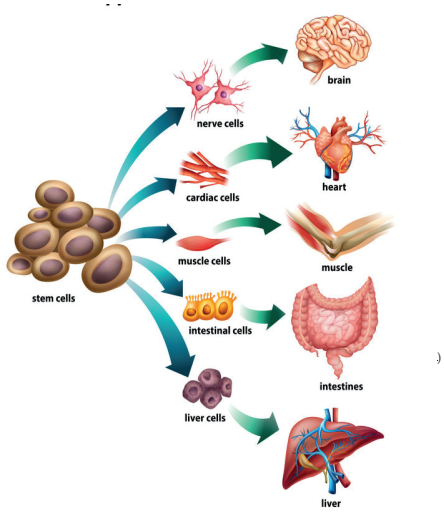

Figure 4: Stem cell multipotency. Schematic representation of the differentiation potential of cultured embryonic stem cells. Embryonic stem cells are totipotent as they can give rise to any tissue in the body. From http://mypracticalsupport.com.au/blog/wp-content/uploads/2016/07/Uses-for-stem-cells.jpg.

1.2 Examples of stem cells in adult organisms

Many tissues of the body are maintained by the presence of adult stem cells. Well-known examples are the hematopoietic system, the skin or the intestine.

The hematopoietic system was one of the first studied examples of cell heterogeneity and hierarchical organization. Between birth and death the human body produce of the order of 10^6 blood cells of different types. These specialized cells are continuously produced from precursor cells, which in turn will be replaced by cells further up the blood hierarchy. According to classical studies, the latter are the

hematopoietic stem cells (HSCs), a slow dividing rare population that fuels the entire blood system (Dick, 2003) (**Figure 5A**). Recent works have challenge this view by showing that steady-state blood cell production appeared to be maintained by the successive recruitment of thousands of clones, each with a minute contribution rather than by small number of HSCs (Busch et al., 2015; Sun et al., 2014).

The different compartments of skin epidermis such as the hair follicle (HF) are also maintained during adult homeostasis by the presence of different resident SCs. These cells are localized in a specialized microenvironment at the base of the HF called the bulge. These SCs are also slow cycling and are able to fuel the production of matrix cells that rapidly divide in the hair bulb until they terminally differentiate (Blanpain & Fuchs, 2009) (**Figure 5B**).

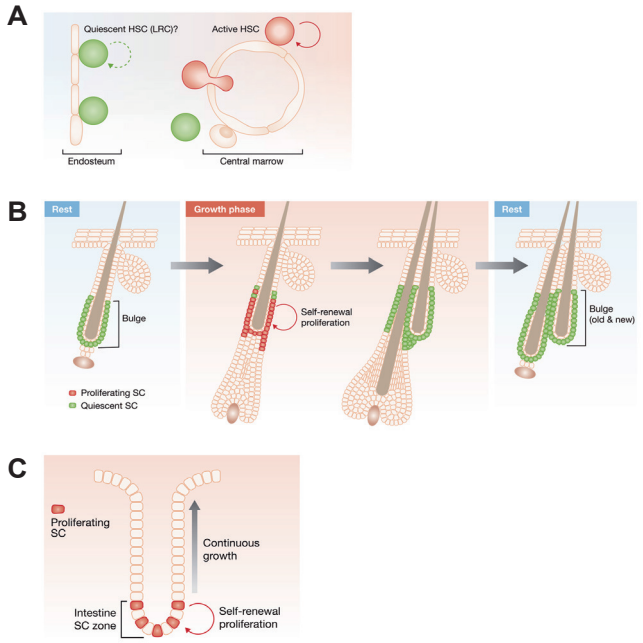

Figure 5: Examples of adult stem cells. (**A**) Activation of hematopoietic stem cells (HSCs). Most HSCs reside in the bone marrow in a quiescent state. They divide approximately once every 4-5 months during normal homeostasis. (**B**) Self-renewal of hair follicle stem cells (HFSCs). Hair follicle undergoes cycles of growth, degeneration and rest. HFSCs are located in a niche called 'the bulge' where they exist in a quiescent state in the resting periods between the cycles of growth. (**C**) Self-renewal of Intestinal Stem Cells (ISCs). The intestinal epithelium continuously regenerates with a cell turnover of 3-5 days. At the base of the crypts, ISCs continuously divide giving rise to progenitors that keep proliferating while they migrate towards the surface epithelium where differentiation takes place. Adapted from (Fuchs & Chen, 2013).

Finally, the intestine is another example of tissue maintained by adult stem cells. The entire functional epithelial layer of the intestine is replaced every 3-5 days. Regeneration is fuelled by intestinal stem cells (ISCs) located at the bottom of invaginations called intestinal crypts. Contrary to what has been described for HSCs or epidermal SCs, ISCs are active stem cells, abundant and not quiescent. During the process of differentiation these cells abandon the crypt niche and move towards the upper parts of the intestinal villus where the specialized intestinal cells reside (B. H. Clevers, 2015; H. Clevers & Batlle, 2013) (**Figure 5C**).

1.3 Functional approaches to define stem cell populations

The most common used strategies to assess stem cell properties (self-renewal and multipotency) are: lineage tracing, clonogenic cultures and transplantation assays.

1.3.1 Lineage tracing

This technique is based on genetic labelling a specific cell population in order to follow the label with time in their progeny. The most common lineage tracing strategy uses the Cre recombinase fused to the ligand binding domain of the estrogen receptor: Cre-ER fusion protein. The key feature of this technique is the expression of the fusion protein under the gene promoter of interest that, for instance, marks a particular cell population. On the other hand, a reporter allele (usually a fluorescent protein) is driven by a strong and ubiquitous promoter followed by a transcriptional stop signal that prevents the expression of the reporter gene in basal conditions. In most cases the stop signal is a tandem of three polyadenylation signals flanked by loxP sites. Upon 4-OH tamoxifen treatment, the Cre is activated specifically in cells expressing the promoter driving the Cre-ER fusion protein, and the stop signal is removed allowing reporter gene expression (**Figure 6A**).

This strategy allows the initial labelling of the population of interest. Since the reporter activation is irreversible, any cell derived from the initial labelled population will also bear the reporter signal. For instance, when the promoter of a SC marker drives Cre-ER fusion expression, the initial labelling is restricted to a few cells just after Tamoxifen induction but over time, all cells in the tissue derived from the initial labelled SC will be also marked as the genetic mark induced by Cre recombinase is permanent (**Figure 6B**).

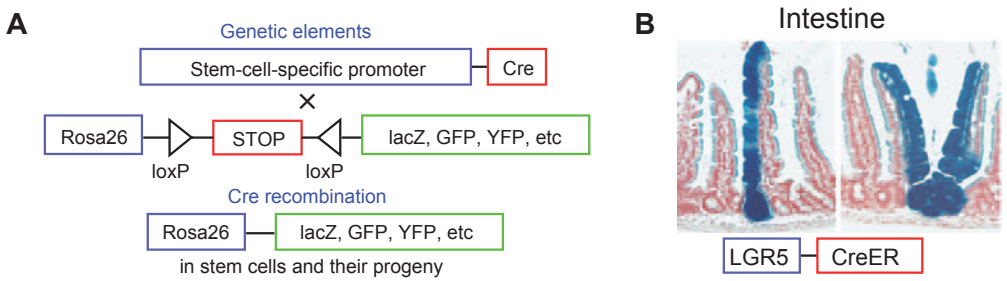

Figure 6: Genetic lineage tracing mediated by Cre recombinase. (**A**) Schematic representation of the genetic strategy to lineage-trace stem cells. A specific promoter is used to induce Cre recombination in stem cells. Animals carrying this genetic modification are crossed with animals harbouring a stop codon flanked by Cre-recombinogenic LoxP site upstream a reporter gene, such as lacZ or GFP, under the control of a ubiquitous promoter. (**B**) Genetic lineage tracing in the intestine using the Lgr5 promoter driving an inducible Cre recombinase linked to the estrogen receptor and Rosa26-lacZ reporter. By inducing nuclear translocation of Cre with tamoxifen, Lgr5-expressing cells give rise to progeny that encompass all cell types in the intestinal crypt. Adapted from (Fuchs & Horsley, 2011).

1.3.2 Clonogenic cultures

In vitro cultures are becoming increasingly popular to assess the stem cell identity of a desired population. The idea behind this technique is that when primary cells are cultured under conditions that mimic their niche only SCs will be able to sustain the cultures for extended periods of time.

The recent establishment of 3D SC culture models has allowed scientists to culture stem cells in environmental conditions close to those found *in vivo*. This technology has allowed the expansion of SCs in a non-perturbed atmosphere in order to perform detailed studies on the pathways involved in SC biology and tissue architecture.

Particularly in the field of intestinal stem cell research, the establishment of the conditions for 3D cultures has been a major step forward to reproduce intestinal biology *in vitro*. Intestinal 3D cultures, known as organoids, allow the formation of mini-guts composed by all the cell types derived from ISCs and thus, recapitulate the hierarchical organization of the tissue of origin (Sato et al., 2015; Jung et al., 2011) (**Figure 7A** and **7B**).

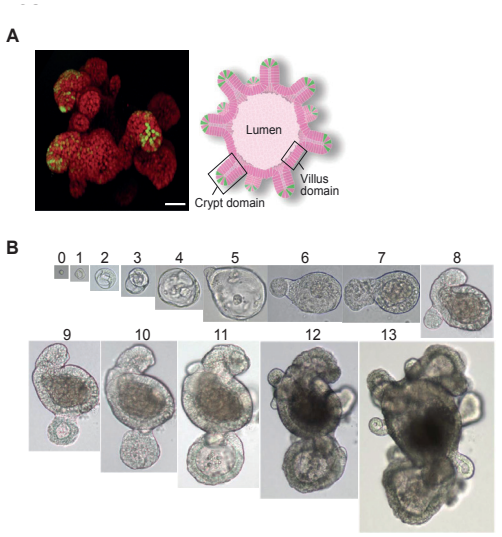

Figure 7: Intestinal crypt culture system. (**A**) Intestinal Stem Cells (ISCs) cultured *in vitro* exhibit remarkable self-organizing properties and grow tridimensional into what are known as organoids or mini-guts that in many ways reflect the structural and functional properties or the intestinal epithelium. Lgr5-GFP+ (green) ISCs are localized at the tip of crypt-like structures. (**B**) Isolated single ISCs are able to successfully grow *in vitro* giving rise to intestinal organoids. Adapted from (Sato et al., 2009).

1.3.3 Transplantation assays

Behind the concept of ‘’stem cell’’ there are the properties of long term self-renewal and multipotent capacity. Transplantation assays have been extensively used, especially in the hematopoietic stem cell field, to assess the replicative and cellular reconstitution capacity of a particular cell type. These assays have typically been used to assess the function of cell populations of the hematopoietic system. Generally, they consist on the purification of a certain cell population using surface markers and the subsequent transplantation into a host mice. Many times, the host is previously manipulated to deplete a cell population of interest destined to perform specific functions. As a way of example, a classical transplantation assay is the purification of a determined bone marrow cell population and its subsequent transplantation into a host mouse that has been previously depleted of the Hematopoietic Stem Cells (HSCs) by irradiation treatment. Only HSCs will be able to fully regenerate the bone marrow functionality for extended periods of time. (Ficara, Murphy, Lin, & Cleary, 2008).

One drawback of these type of approaches is that not all adult tissues are suitable for transplantation assays. Moreover, not all tissues can be “cleared” for SC transplantation. In this case, what is assessed is the functional engraftment in the context of normal tissue instead of the rescue of tissue function. More importantly, transplantation assays may not reveal the function of the cell type analysed in homeostasis but rather the capacity of this cell to resist the isolation and transplantation procedure. Indeed, recent analyses of haematopoiesis by lineage tracing in an intact environment has challenged the model that was build based on transplantation assays (Busch et al., 2015).

2. The mammalian intestine

The mammalian intestine has been a perfect system to study adult SC biology thanks to its cellular heterogeneity and hierarchical organization.

2.1 Intestinal structure and organization

The intestinal tract is a tubular structure that connects the end of the stomach with the anus. It divided into two main parts: the small intestine and the large intestine or colon. The first is composed of duodenum, jejunum and ileum, and is responsible for the final steps of digestion as well as nutrient uptake. The colon exerts the function of water absorption and stool compaction for excretion (**Figure 8A**).

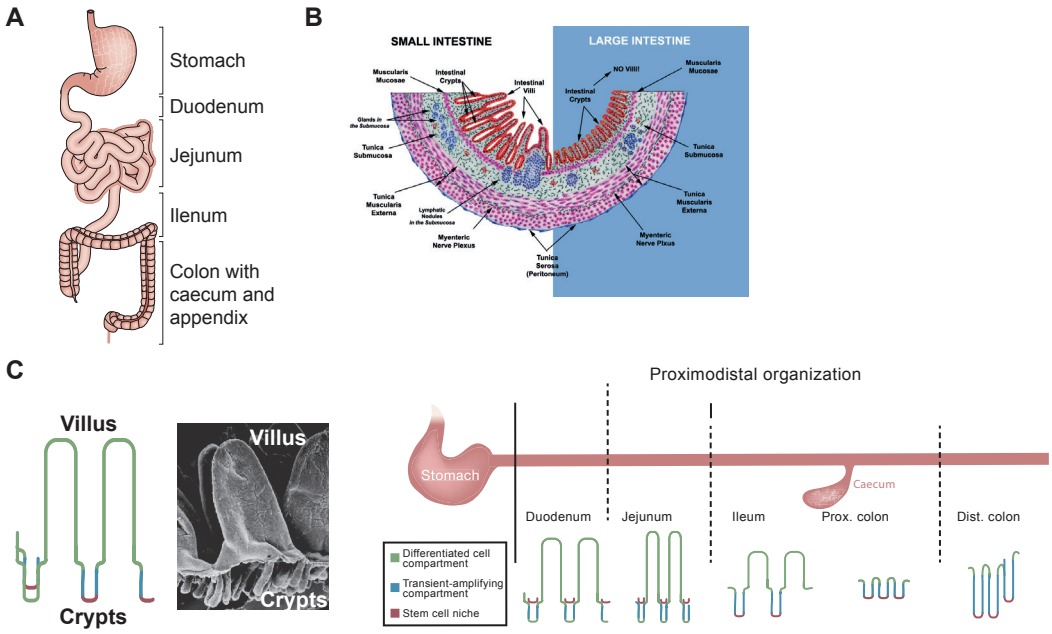

Figure 8: Anatomy of the intestinal tract and intestinal epithelium organization. (**A**) Gross anatomy of the gastrointestinal tract. The intestinal tube starts at the end of the stomach and is divided in two main parts, the small intestine where absorption of nutrients takes place, and the large intestine which function mainly is to absorb water and compact stool. (**B**) Representation of a transversal section of the small intestine and colon with the different tissue layers. The intestinal epithelium is the inner layer in contact with the lumen. Submucosa and Muscularis externa form the middle and outside layers of the intestinal wall. (**C**) Left panel. Representation of the intestinal crypt and villi structures together with a scan electron microscopy image of the small intestine. Villus are larger and are contributed by cells of different crypts. Right Panel. Proximodistal organization of the intestinal tube. Note the different size of crypts and villus along the different parts of the small intestine and the absence of villus in the colon. Adapted from (Clevers & Batlle, 2013; Mowat & Agace, 2014).

The intestinal tube is organized in different layers around a central lumen. The first layer in direct contact with the lumen is the *intestinal epithelium*. The main function of this tissue is to process and absorb nutrients of the digested food that flows through the lumen. The second layer is the *lamina propia* composed by connective tissue and stromal cells. The third layer is termed *submucosa* and contains blood vessels, nerves, lymphatic nodules and myofibroblasts. This layer is finally surrounded by a thick smooth muscle layer which is involved in peristaltic motions (**Figure 8B**).

2.2 The intestinal epithelium

The intestinal epithelium represents a prime model system to study adult stem cell biology. The high speed of cell turnover and the hierarchic organization of cellular types in the intestinal epithelium are properties that enable the study of stem cell function and behaviour. This epithelium is monostratified yet is folded into tubular invaginations termed crypts of Liberkünhn (referred to as crypts). In the intestine there are also finger-like structures that protrude into the lumen termed villi and serve to maximize the intestinal surface area for absorption. (H. Clevers & Batlle, 2013; Sancho, Batlle, & Clevers, 2004) (**Figure 8C**).

Renewal of the intestinal epithelium is a continuous process throughout lifetime. Epithelial cells of this tissue are exposed to a harsh environment and thus they must undergo rapid renewal to maintain optimal function. Regeneration relies on the activity of a small population of adult stem cells (SCs) located at the bottom of crypts. Intestinal stem cells (ISCs) constantly divide to produce transient amplifying cells (TA) that are highly proliferative progenitors. TA cells undergo through 4-5 divisions of unusually short duration that is around 12h (Marshman, Booth, & Potten, 2002). During this process, TA cells move towards the crypt-villus junction and gradually commit to the absorptive or secretory cell lineages. As these cells differentiate they continue to move upwards towards the tip of the villus. Upon reaching the villus tip after 2-3 more days, differentiated cells undergo apoptosis and are shed into the gut lumen (Bjerknes & Cheng, 2006; H. Clevers & Batlle, 2013) (**Figure 9**).

Therefore, the different epithelial cell types of both small intestine and colon are organized following a bottom-to-top axis in three compartments: the stem cell compartment located at the crypt base where the intestinal stem cells (ISCs) reside, the transient-amplifying (TA) compartment that occupies the middle portion of the crypts, and the differentiation region which extends

from the top third of the crypt to the tip of the villus (**Figure 9**).

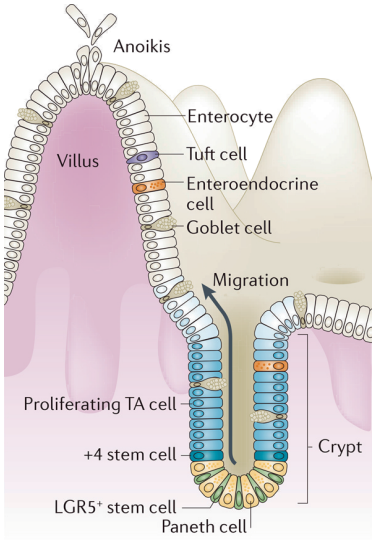

Figure 9: Self-renewal in the intestinal epithelium. Intestinal stem cells (Lgr5+) are localized at the base of the crypts intercalated with Paneth cells in the intestinal epithelium. Stem cells continuously generate rapidly proliferating transient amplifying (TA) cells, which occupy the reminder of the crypt. TA cells couple migration with differentiation into the various functional cells on the villi that eventually replace older epithelial cells shed to the lumen. Adapted from (Barker, 2014).

2.2.1 Differentiated intestinal cells

Upon leaving the crypt niche, ISCs undergo differentiation into specialized cell populations belonging to two main lineages: absorptive or secretory. (**Figure 10**).

Absorptive lineage:

- *Enterocytes* (or columnar cells) are differentiated cells of the absorptive lineage and constitute more than 80% of the epithelium. They are highly polarized cells with an apical brush border responsible for absorbing and transporting nutrients through the epithelium (Takashima, Gold, & Hartenstein, 2013). Examples of differentiation markers to distinguish this population are the Alanyl aminopeptidase (ANPEP) or the Carbonic anhydrase 1 and 2 (CA1/2).

Secretory lineage:

-*Goblet cells* are amongst the four secretory-type cells present in the differentiated epithelium. They are mucous secreting and their abundance increases towards the distal part of the small intestine and colon (Akiyama et al., 2010). Goblet cells are readily identified by well-known specific differentiation markers such as Mucin2 (MUC2), Atonal homologue 1 (ATOH1) or Delta like canonical Notch ligand 1 (DLL1).

- *Paneth cells* reside at the crypt base and have a function in innate immunity; they secrete granules containing specific proteins like lysozymes, antimicrobials, and defensins. Paneth cells are the only differentiated intestinal epithelial cell type that migrates downward to the crypt bottom and reside intermingled with ISCs. Recent works suggest that Paneth cells may constitute a niche for ISCs (Sato et al., 2011).

-*Enteroendocrine* cells are also differentiated intestinal cells that belong to the secretory lineage. Their function is to secrete hormones and neuropeptides that modulate intestinal physiology. The specification of this type of secretory cells is driven by the expression of neurogenin3 (NGN3) and NeuroD (Wang, Giel-Moloney, Rindi, & Leiter, 2007).

-*Tuft cells* are rare differentiated cells which function was unknown until very recently. Three independent studies revealed that tuft cells play a role in the initiation of type 2 immune responses, which are typically involved during intestinal protozoa or helminth parasite infections. In addition, the microtubule-linked protein kinase 1 (DCLK1) was found to be predominantly expressed in this differentiated cell population (Gerbe & Jay, 2016).

-*M cells* or *Microfold cells* are situated in the Peyer's patches (PPs) which contain immune cells. The M cells play an important role for the mucosa immunity since they transport antigens into the PPs (Neutra, 1998).

Finally, Cytokertin 20 (KRT20) is marker of terminally differentiated intestinal cells. KRT20 is a pan-differentiated gene expressed among most differentiated intestinal cell types. KRT20 antibodies label the upper part of the crypt as well as the whole villus epithelium, and have been extensively used to label the differentiated population in both normal and tumor cells (Merlos-Suárez et al., 2011).

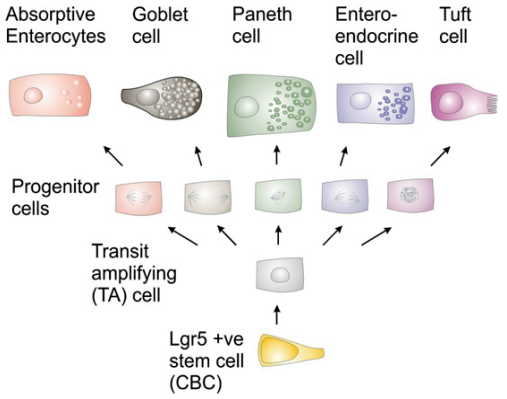

Figure 10: Schematic representation of the intestinal differentiation hierarchy. ISCs localized at the bottom of the crypts give rise to all cell lineages of the adult intestine. Most abundant lineages are absorptive enterocytes as well as goblet and Paneth cells which belong to a secretory lineage. Enteroendocrine and Tuft cells are secretory cell types found less frequently. Adapted from (Barker, Bartfeld, & Clevers, 2010).

3. Signaling pathways regulating intestinal homeostasis

Intestinal homeostasis is maintained by means of its hierarchical organization which ensures a controlled and balanced presence of different cell types with specialized functions. The major pathways that impinge on intestinal homeostasis are: WNT,

Notch, Epidermal Growth factor (EGF) and Bone Morphogenetic Protein (BMP) signalling (**Figure 11**).

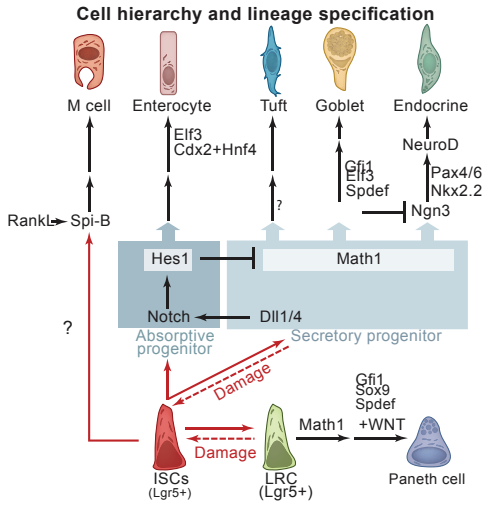

Figure 11: Main pathways regulating ISC biology. A signalling network is established between SCs and the stroma to modulate stemness and differentiation in the intestine. WNT, EGF and Notch promote stemness and proliferation whereas BMP signalling promotes proliferation. In addition Notch signalling is the main pathway controlling differentiation towards the secretory or enterocyte lineages. Adapted from (Clevers & Batlle, 2013).

3.1 WNT signalling

The WNT signalling pathway is highly conserved among many multicellular organisms. This pathway is activated by secreted WNT proteins and it has been shown to play a crucial role in organismal patterning throughout the animal kingdom.

Currently, three different signalling cascades are believed to be activated upon WNT receptor activation: the canonical Wnt/β-catenin cascade, the noncanonical planar cell polarity (PCP) pathway and the Wnt/Ca2+ pathway. The canonical WNT pathway is the best understood and the one mainly involved in intestinal stem cell homeostasis (H. Clevers, 2006). Canonical WNT signalling regulates the levels of soluble β-catenin protein, which can act as a transcriptional co-activator of the family TCF/LEF transcription factors (Cadigan, 2008).

Although WNT proteins are secreted they are relative insoluble. Once secreted, Wnts bind Frizzled (Fzds) proteins, which are seven-pass transmembrane receptors with an extracellular N-terminal cysteine-rich domain. In binding WNT, Fzds cooperate with a single-pass transmembrane molecule LRP6 or LRP5 activating the canonical signalling pathway.

Activation of the pathway leads to the activation of the protein Dishevelled (Dvl), which in turn inhibits the β-catenin destruction complex. This complex is composed by Adenomatous Polyposis Coli (APC), Axin and casein kinase I (CKI) among other proteins. The main function of the destruction complex is to degrade β-catenin in absence of WNT signalling. Thus, the major consequence of WNT binding to the receptor is the accumulation of β-catenin and its subsequent nuclear

translocation. In the nucleus this protein displaces Groucho repressor proteins from target genes and the β-catenin / TCF complex is formed. This complex is now able to drive the expression of the WNT transcriptional program (Cadigan, 2008; Klaus & Birchmeier, 2008) (**Figure 12**).

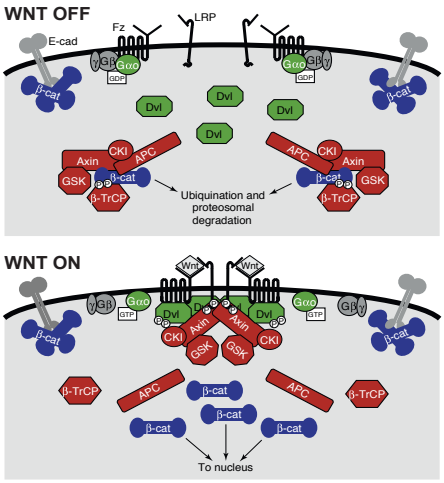

Figure 12: The canonical WNT signalling pathway. In the absence of WNT, β-catenin is phosphorylated by CKI and GSK3 leading to β-TrCP dependent ubiquitination and proteasomal degradation. The presence of WNT promotes LRP and Fz association, leading to recruitment of Dvl to the complex and GSK3 and CKI phosphorylation of LRP. This stabilizes recruitment of Axin to the receptor, which may disrupt the activity of the destruction complex, which allows accumulation of β-catenin and nuclear translocation. In the nucleus, the transcriptional β-catenin/TCF complex activates the expression of WNT target genes. From (Cadigan, 2008).

WNT signals may promote cell proliferation and tissue expansion but also control fate determination or terminal differentiation of postmitotic cells. For instance, maturation of Paneth Cells at the crypt base depend on WNT (van Es et al., 2005). There isn't a consensus WNT target gene program among all organisms, as the majority of WNT target genes appear to be cell type specific.

In the intestine, WNT signalling is the major driver of intestinal stem cell (ISC) self-renewal and proliferation (Reya & Clevers, 2005). Mouse genetic models have shown that the full knockout of TCF7L2/TCF4 leads to a complete loss of progenitor cells in the intestine (Korinek et al., 1998). In addition, overexpression of Dickkopft (DKK1) -an inhibitor of WNT binding to its receptor- in a transgenic mouse model led to the loss of proliferating cells and eventually to a loss of crypts (Pinto, Gregorieff, Begthel, & Clevers, 2003). This implies that physiological WNT signalling is required for the establishment of the progenitor compartment in the intestine.

ISC biology is not only affected by loss of WNT signalling but also by its hyperactivation. Mutations that inactivate the APC tumor suppressor gene initiate colorectal neoplasia driven by constitutive activation of β-catenin/ TCF4 signalling. Furthermore, colorectal tumors with intact APC gene were found to carry dominant activating mutations of β-catenin gene (CTNNB1) (Morin, 1997). Indeed, genetic alterations in the APC gene in mouse

models led to aberrant activation of WNT signalling (Sansom et al., 2004), which in turn imposes a stem/progenitor phenotype on epithelial mutant cells (Van de Wetering et al., 2002).

Among the WNT pathway targets, the transcription factor c-MYC was one of the first described (He et al., 1998). c-MYC has been shown to be responsible of the proliferative effects that WNT activation exerts on its target cells (Van de Wetering et al., 2002). In addition, Myc deficiency rescued the phenotype imposed by deletion of the Apc gene in mice (Sansom et al., 2007). The role of Myc in intestinal homeostasis will be further discussed in section 9.

3.2 Notch and EGF signalling

Notch signalling is another essential pathway to maintain the crypt compartment in its undifferentiated and proliferative state. Inhibition of Notch in the intestinal epithelium resulted in the complete conversion of all epithelial cells into goblet cells (Milano et al., 2004). On the contrary, overexpression of Notch1 receptor in the intestine resulted in the depletion of goblet cells and reduction in enteroendocrine and Paneth cell differentiation (Fre et al., 2005). Thus, Notch signalling in the intestine impinges in the cell fate determination between absorptive and secretory lineages through a mechanism called lateral inhibition. In this model, non-secretory cells (ISCs and absorptive cells) arise from cells in which a high level of Notch activation is maintained. These cells express high levels of the Notch target HES1 that in turn represses the transcription factor MATH1. Conversely, secretory-type cells arise from inhibition of the pathway. A mechanism to explain Notch inhibition in these cells is through the Notch ligand delta-like 1 (DLL1) which is expressed specifically in goblet cells. DLL1 expression inhibits Notch signalling and drives the goblet cell phenotype in Notch-inactivated colonic epithelial cells (Akiyama et al., 2010; H. Clevers & Batlle, 2013).

Maintenance and growth of ISCs is also achieved through signalling mediated by the mitogen Epithelial Growth Factor (EGF). EGF is the better described ligand of the family of EGF Receptors. It exist as pro-proteins that are cleaved for their activation/secretion. When bound to their ligand, EGFRs dimerize and transactivate their kinase domains. The active kinase domain is able to signal to several downstream effector pathways that overall result in mitogenic signals (Yarden & Shilo, 2007). In the intestine, EGF is indispensable for the *in vitro* growth of both normal and APC mutant ISCs (Jung et al., 2011; Sato et al., 2009a).

3.3 BMP signalling

WNT, Notch and EGF signalling pathways mainly drive maintenance of ISC identity and growth. On the contrary Bone Morphogenetic Protein (BMP) signalling is the major driver of differentiation at the top of the crypt-villus axes. BMP ligands belong to the Transforming Growth Factor (TGFβ) superfamily, and their receptors are BMPR1 and BMPR2 that upon activation phosphorylate SMAD1, SMAD5 and SMAD8. These intracellular mediators will then interact with SMAD4 and drive the expression of target genes such *ID1* or *ID3*.

In vivo ablation of BMP signalling specifically in the intestinal epithelium impairs terminal differentiation of the intestinal secretory lineage (Auclair, Benoit, Rivard, Mishina, & Perreault, 2007). On the other hand, full intestinal blockade of the BMP pathway results in ectopic SC niches in the villus and spontaneous benign overgrowth lesions called hamartomas (Haramis et al., 2004). Since BMP signalling supresses ISC growth, *in vitro* expansion of ISCs requires inhibitors of this pathway such as Noggin (Jung et al., 2011; Sato et al., 2009a). In order to maintain the undifferentiated state of ISCs, intestinal myofibroblasts may protect these cells from BMP signalling by secreting Gremlin locally (Hardwick, Kodach, Offerhaus, & van den Brink, 2008).

4. Intestinal stem cells (ISCs)

4.1 A historical perspective

It was already in the 70's when Cheng and Leblond described for the first time the existence of stem cells in the rat small intestine. These cells were termed crypt-base columnar cells (CBCs) and were identified at the bottom most positions of the crypts (Cheng & Leblond, 1974b).

They showed that CBCs phagocytised non-viable cells in their vicinity since large phagosomes appeared in their cytoplasm. To prove that these cells were the common precursors of all the differentiated intestinal cells they pulsed mice with H3-thymidine. They showed that after injection, CBCs included phagosomes containing labelled nuclei as a consequence of neighbouring CBCs that had died. Moreover they followed the appearance of radioactive signal in other cell types after different time points. For instance, 12 hours after H3-thymidine injection labelled phagosomes had appeared in partly differentiated mid-crypt columnar cells; by 18-24 hours the signal was already found in fully differentiated columnar cells and also in Paneth cells. These results were the first evidence showing that CBCs represented the ISCs of the intestine (Cheng & Leblond, 1974a). Such interesting results were

overlooked during many years in the field of intestinal biology. Instead, the accepted identity for ISCs was the "+4 model" postulated by Chris Potten. This model was based on label retaining experiments based on the assumption that the crypt cells capable of label retentions (LRCs or label retaining cells) were the ISCs.

It has been traditionally thought that stem cells divide rarely to protect their genomes. This theory was based on the observations performed in stem cell of other tissues such as hematopoietic system or the hair-follicle. In stem cells from these tissues the label retention property is tightly linked to the slow proliferative or quiescent state, i.e. slow dividing cells retain DNA labels. LRCs were found to be located around the position "+4", immediately above Paneth cells rather at the crypt base (Potten, 1977).

4.2 Identification of Lgr5 as a *bona-fide* stem cell marker

The discussion over the identity of the ISCs lasted for years, until the group of Hans Clevers identified the first bona-fide marker of ISCs. The Clevers's lab had provided previous evidence that WNT signalling was the main driver of ISC maintenance (Korinek et al., 1998). While analysing the transcriptional program driven by WNT signalling in CRC cells (Van de Wetering et al., 2002) they identified several WNT target genes that also labelled the progenitor compartment and were promising candidates to mark specifically the ISC population.

The gene Leucine rich repeat containing G protein coupled receptor 5 (*Lgr5*) was selected from the panel of intestinal WNT target genes. Lgr5 encodes for a receptor of Rspo1, a secreted protein that amplifies WNT signals (de Lau et al., 2011). Indeed Rspo1 is an essential component to maintain and expand ISCs *in vitro* suggesting that in the intestinal epithelium the highest levels of WNT signalling are found in the crypt base where the Lgr5-positive cells reside. In 2007, generation of a mouse carrying the knock-in allele EGFP-ires-CreERT2 under the control of the *Lgr5* gene promoter allowed to detect restricted Lgr5 expression in the CBCs previously described by Cheng and Leblond (Barker et al., 2007) (**Figure 13A**). This model also enabled lineage tracing experiments *in vivo* from the Lgr5 promoter. Lgr5-positive crypt base columnar cells generated all epithelial lineages over a 60-day period, suggesting that CBCs are the stem cells of the small intestine (**Figure 13B**) (Barker et al., 2007).

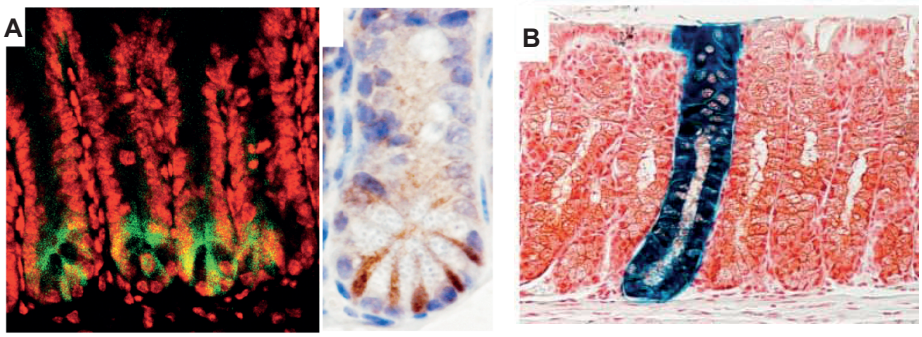

Figure 13: Lgr5 expression pattern and lineage tracing in the intestinal tract. (**A**) EGFP expression in Lgr5-EGFP-IRES-creERT2 knock in mouse shows that Lgr5 expression is restricted to the six to eight slender cells sandwiched between the Paneth cells at the crypt base of the small intestine. (**B**) Lgr5-EGFP- IRES-creERT2 knock-in mouse crossed with Rosa26-lacZ reporter mice 60 days after tamoxifen injection. The appearance of full labelled ribbons in the intestine corroborates the formation of the entire intestinal progeny from the initial label of one Lgr5+ stem cell. From (Barker et al., 2007).

Before LGR5 knock-in mice were available, one of the first studied WNT target genes was the ephrin receptor *EphB2*. This gene was also among the 120 candidates whose levels dropped upon inhibition of β-catenin/TCF-mediated transcription. Batlle and colleagues nicely showed that EphB2 was expressed in a decreasing gradient from the crypt bottom toward the top of the crypts peaking its expression in crypt base columnar cells (**Figure 14**). They also showed that the Ephb2 expression in the small intestine was inversely correlated with the expression of its ligand ephrin-B1 which was absent in the crypts and highly expressed in the villus tip (Eduard Batlle et al., 2002). As it will be commented in the following sections, the EPHB2 marker has been extensively used to isolate both normal and cancer intestinal stem cells particularly from human samples, since there are no LGR5 antibodies available and genetic approaches are not applicable to human cancers for obvious reasons (Jung et al., 2011; Merlos-Suárez et al., 2011).

With these new tools both the Clevers and the Batlle labs were able to purify and expand *in vitro* Lgr5-positive or EphB2-high CBC cells. Under appropriate *in vitro* conditions these cells were able to generate 3D intestinal organoids that recapitulated the structure and features of the intestinal epithelium. They also showed that for the maintenance of these cultures WNT and EGF signalling were required alongside the blockade of the BMP pathway (Sato et al., 2009a).

Of note, recent work has added yet another piece of important information to the identity of ISCs. Our laboratory has discovered that "+4" cells represent a subpopulation of slow dividing Lgr5+ cells that can be identified through the novel intestinal stem cell marker gene *Mex3A* (Barriga et al., 2017) (**Figure 15**). Apparently both Leblond and Potten were right in their appreciations.

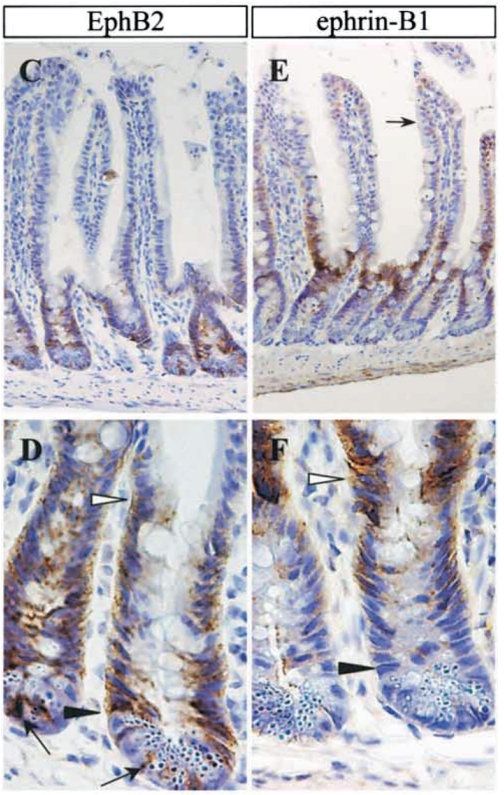

Figure 14: Complementary expression of EphB2 and ephrin-B1 in the small intestine. EphB2 is expressed in cells that localize at the bottom of the crypts of adult small intestines. EphB2 expression follows a decrease gradient from the crypt base to the villus top and it is inversely correlated with the expression of its ligand ephrin-B1. Adapted from (Eduard Batlle et al., 2002).

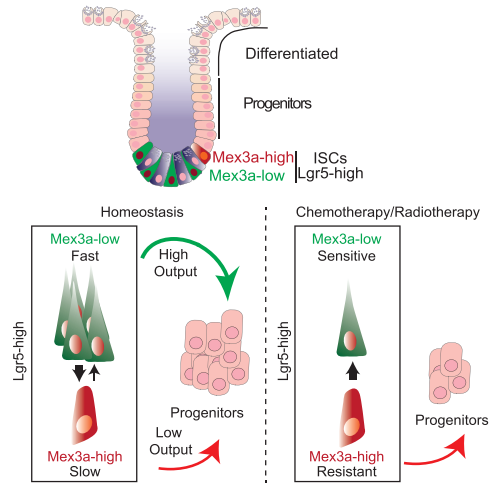

Figure 15: The RNA binding protein Mex3a defines a subset of slowly proliferating Lgr5+ cells. During intestinal homeostasis Mex3a-high cells represent a small proportion of Lgr5+ stem cells that proliferate slowly and contribute to all intestinal lineages with low kinetics. Chemotherapy and radiation mostly affects rapid proliferating Lgr5+ cells. However, Mex3a-high cells are resistant to chemotherapeutic insults and are able to regenerate the epithelium. Extracted from (Barriga et al., 2017).

4.3 The Intestinal Stem Cell gene expression signature

Identification of *Lgr5* as a marker of ISCs allowed the Clevers lab to identify other genes involved in the maintenance of the ISC phenotype. Using the Lgr5 knock-in mouse they isolated Lgr5^{hi} and Lgr5^{lo} populations from intestinal crypts and performed transcriptomic analysis in order to identify other markers specific from the Lgr5 population.

These analyses revealed that Achaete scute-like 2 (*Ascl2*) and Olfactomedin 4 (*Olfm4*) were two new candidate genes

enriched in the stem cells of the small intestine. In situ hybridization showed a clear expression of both genes at the bottom of the crypts co-localizing with *Lgr5* expression (van der Flier et al., 2009) (**Figure 16A** and **16B**). Indeed, *Ascl2* was a known WNT target gene and its conditional depletion led to disappearance of Lgr5 stem cells within days. In addition, transgenic expression of this gene induced crypt hyperplasia and ectopic crypts on villi. These results proved that Ascl2 controlled intestinal stem cell fate (van der Flier et al., 2009).

In a later study the SPARC related modular calcium binding 2 (*Smoc2*) gene was also identified as a stem cell marker. In Xenopus laevis Smoc1/2 orthologue was described as a BMP signalling inhibitor. BMP signalling is active in the intestinal villus compartment where it inhibits *de-novo* crypt formation. Thus, they proposed that *Smoc2* expression in ISCs could be a way to block BMP signalling in the stem cell niche to prevent differentiation. To confirm the stem cell-specific expression of *Smoc2* an inducible Smoc2-EGFP-ires-CreERT2 knock-in mice model was generated. The expression of EGFP was detected in crypt base columnar cells. Lineage tracing from Smoc2-KI mice resulted in classical stem cell tracing ribbons confirming *Smoc2* as another stem cell gene (Muñoz et al., 2012) (**Figure 16C**).

These genes were further validated in our laboratory by using the expression of EphB2 to isolate the stem cell population from both normal and tumor tissues (Jung et al., 2011; Merlos-Suárez et al., 2011). Altogether, *Olfm4*, *Smoc2*, *Ascl2*, *Ephb2* and *Lgr5* belong to the ISC gene expression signature

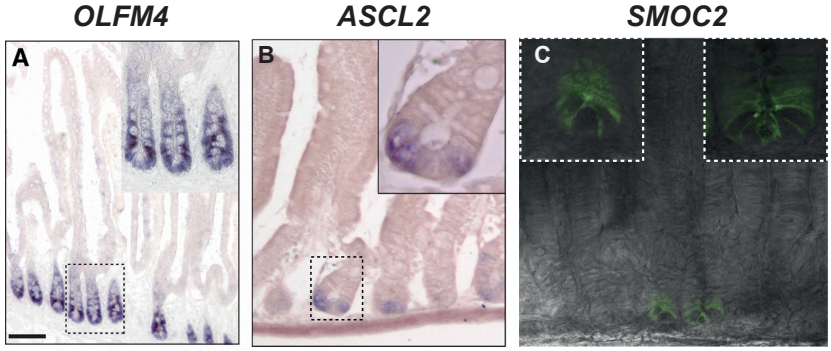

Figure 16: Expression of other intestinal stem cell markers. (**A**) In situ hybridization for *OLFM4* reveals a crypt base columnar-restricted expression pattern in human small intestinal epithelium. (**B**) In situ hybridization of *Ascl2* reveals an *Lgr5* stem cell restricted pattern. (**C**) Endogenous EGFP expression of *SMOC2* from an EGFP-ires-CreERT2 reporter mouse. *SMOC2* expression is restricted at the columnar cells of intestinal crypt base. Adapted from (Muñoz et al., 2012; van der Flier & Clevers, 2009; van der Flier, Haegebarth, Stange, van de Wetering, & Clevers, 2009).

and are considered specific markers of ISCs.

It is worth mentioning that several groups have pursued putative ISC markers other than Lgr5 to label either a different subset of cells or to potentially refine the Lgr5 population. In support of the "+4 model", several genes have been reported to be specifically expressed in the "+4 SCs" such as *Bmi1* (Park et al., 2003), *Hopx* (Takeda et al., 2011), *Lrig* (Powell et al., 2012) or *Tert* (Breault et al., 2008) (**Figure 17**). However, the overall data regarding these putative SC markers has not yielded any conclusive evidence regarding the existence of an Lgr5-independent ISCs or that any of these markers are more restricted than Lgr5 itself.

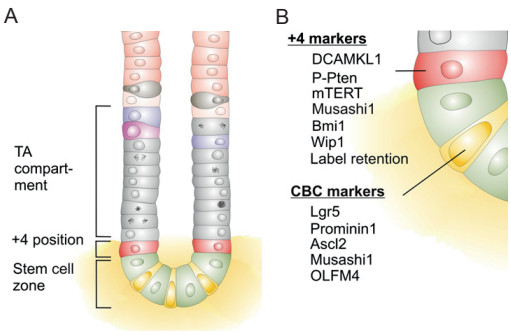

Figure 17: Crypt base columnar (CBCs) and +4 stem cell markers. (**A**) Schematic representation of the crypt base highlighting the TA compartment, the termed +4 position (in red) and the stem cell zone. Paneth cells are depicted in green and CBCs in yellow. (**B**) Described markers for CBCs and +4 cells are indicated. Extracted from (Barker et al., 2010).

5. Colorectal cancer

5.1 Development of colorectal cancer (CRC)

Colorectal cancer is the third most common cancer in the world, with nearly 1.4 million new cases diagnosed worldwide per year (www.wcrf.org). This disease is diagnosed mainly in the 65 – 75 year old population, yet some cases develop in people ranging from 30 – 40 years of age. Nowadays the overall 5 year survival of CRC patients is around 65% of all patients diagnosed, although it varies depending on the severity of the disease at the time of diagnosis.

5.1.1 Staging and disease management

The 5 years survival rate of CRC patients is related to the tumor stage at time of diagnosis, that to date, is the most robust predictor of clinical outcome. The staging system is referred to the TNM (Tumor extent, Nodal involvement and presence of Metastases) test from the American Joint Committee on Cancer (AJCC). The TNM system assigns a number based on three categories. "T" denotes the degree of invasion of the intestinal wall, "N" the degree of lymphatic node involvement, and "M" the degree of metastasis. The broader stage of a cancer is usually quoted as a number I, II, III, IV derived from the TNM value grouped by prognosis; a higher

Stage I	T2	N0	M0	T2: Tumor invades muscularis propria
Stage II - A	T3	N0	M0	T3: Tumor invades subserosa or beyond (without other organs involved)
Stage II - B	T4	N0	M0	T4: Tumor invades adjacent organs or perforates the visceral peritoneum
Stage III - A	T1-2	N1	M0	N1: Metastasis to 1 to 3 regional lymph nodes. T1 or T2.
Stage III - B	T3-4	N1	M0	N1: Metastasis to 1 to 3 regional lymph nodes. T3 or T4.
Stage III - C	Tx,	N2	M0	N2: Metastasis to 4 or more regional lymph nodes. Any T.
Stage IV	Tx,	Nx,	M1	M1: Distant metastases present. Any T, any N.

Table 1: The TNM system. Colorectal tumors are devided in IV stages based on three cathegories: degree of invasion (T), degree of lymphatic node involvement (N) and degree of metastasis (M).

number indicates a more advanced cancer and likely a worse outcome. Please find details of this system in the table below (**Table 1**).

The major cause of death in patients with CRC at stage II and III is disease relapse that can occur even years after the end of the therapy. Relapses occur in form of metastasis (preferentially in liver and lungs) and are due to the presence of residual disseminated cells that survived therapy. Stage IV CRCs are large, invasive tumors that at the time of diagnosis have already disseminated to distant organs. When the tumors are unresectable, due to large metastasis or multiple metastases, treatment involves a combination of therapies to shrink the tumor burden prior to surgery. This may be followed by further drug combination treatments post-surgery. Stage IV patients have a dismal survival rate lower than 8% (**Figure 18**).

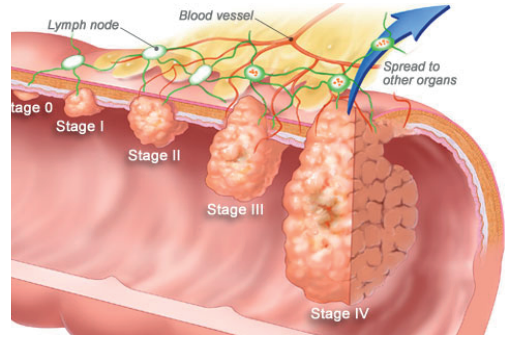

Figure 18: Colorectal cancer stages. Clinical classification of CRC staging based on the TNM system (Tumor extent, Nodal involvement and presence of Metastases). Stage I tumors have already invaded the muscle layer. Stage II cancers have invaded the serosa, the outermost layer of the intestinal wall. Stage III show lymph node metastasis, whereas stage IV already show distant metastasis at the time of diagnosis.

5.2 CRC genetics: the adenoma to carcinoma progression model

CRC is a multistep genetic process driven by the acquisition of specific mutations in a sequential and ordered manner. WNT signalling is the most commonly mutated signalling pathway in CRC. Indeed, is the first and only genetic alteration required for the

formation of benign adenomas in the intestinal epithelium. Loss of the tumor suppressor gene APC, results in hyperactivation of the WNT signalling pathway that imposes a crypt progenitor phenotype on tumor cells (Van de Wetering et al., 2002). In rare cases of colorectal cancer where APC is not mutated, AXIN2 is mutant (Krings et al., 2000), or activating point mutations in β-catenin remove its N-terminal Ser/thr destruction motif (Morin, 1997). Overall, this continuous stem-like self-renewing state gives rise to benign outgrowths of the epithelium known as adenomas.

Van de Wetering and colleagues showed that the genetic program expressed in CRC cells mutant for the WNT signalling pathway was similar to the one of normal ISCs. WNT targets such as EPHB2 were expressed both in ISCs of the normal tissue as well as in CRC lesions hyperactivated for the pathway. These were the first evidences suggesting that genes activated by aberrant β-catenin/TCF activity reflect the normal genetic program of crypt progenitors. Thus, initiation of CRC development was driven by the acquisition of a crypt stem/progenitor phenotype (Van de Wetering et al., 2002).

The progression from adenomas to fully aggressive colorectal carcinomas requires the accumulation of additional genetic alterations (Fearon & Vogelstein, 1990). Genetic studies on the development of CRCs have elucidated the main signalling pathways affected during the adenoma to carcinoma progression. The Mitogen-Activated Protein Kinase (MAPK) pathway is altered by activating mutations in the oncogene KRAS, BRAF or PIK1CA endowing cell autonomous mitogenic stimuli to cancer cells. The tumor suppressor p53 is also very frequently mutated during CRC progression which facilitates the accumulation of genomic instability. Finally, the TGF-β pathway is often silenced by loss-of-function mutations in TGFBR2, SMAD4, SMAD2 or SMAD3, which bypass the growth suppressive effects of high TGF-β levels present in the tumor microenvironment.

The accumulation of all these mutations correlates with the pathological stage of the disease and suggests a linear progression model in which the alteration all four mentioned pathways is associated with the development of aggressive adenocarcinomas (Tauriello, Calon, Lonardo, & Batlle, 2016) (**Figure 19**).

An important consideration is that acquisition of all these mutations is generally a slow process that can take decades. During this period, CRC accumulate many other mutations. Many will be passenger mutations, as

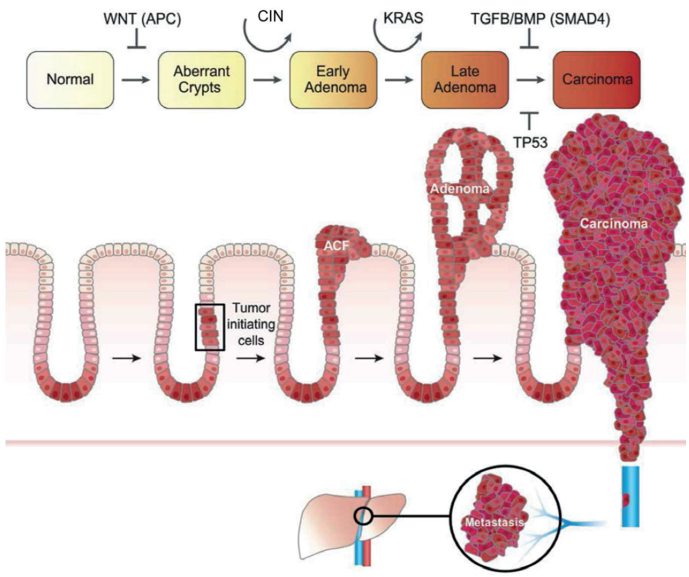

Figure 19: Genetic model of CRC progression. Schematic representation of the linear progression genetic model of CRC development. Accumulation of specific genetic alterations lead the progression from initial benign adenomas to fully malignant carcinomas. Adapted from E.Batlle lab.

they do not confer advantages to tumor cells and thus are not selected whereas other “driver” mutations gives selective advantages to tumor cells. Moreover, many studies have also evidenced that development of CRC is highly influenced by environmental factors such as lifestyle, diet or microbiota.

In addition, tumors include the existence of other cell types that are collectively referred to as tumor microenvironment (TME). These cell types include cancer-associated fibroblasts (CAFs), endothelial and immune cells. Emerging evidences of the cross-talk between cancer cells and the TME have increased the efforts to characterize stromal cell populations in order to better understand tumor progression and metastasis (Tauriello et al., 2016).

Our group showed that there is a strong association between the risk of metastasis and the expression of stromal gene programs in CRC (Calon et al., 2012). Altogether, CRC is a complex and complicated disease that has challenged the development of effective therapeutic strategies.

6. Colorectal cancer stem cells (CRC-SCs)

6.1 Cancer heterogeneity and the cancer stem cell concept

The cancer stem cell (CSC) concept arose from observations suggesting that not all tumor cells were equal. The existence of intratumoral heterogeneity (ITH) was already observed many decades ago. Classical studies using teratocarcinomas, showed that these tumors were composed by embryonal carcinoma cells and mature tissues. Only the embryonal carcinoma population displayed high malignant potential as well as multipotent capacity. Indeed, isolated embryonal tumor cells were able to undergo differentiation into the various benign tissues.

These classical studies carried out by Pierce and colleagues were the firsts evidences of the existence of stem cell-like cells within cancers (Barry Pierce & Speers, 1996). Pierce and colleagues also proposed that the heterogeneous cell types that populated tumors resembled those that populated normal tissue and so tumors were considered as caricatures of normal tissue renewal (Barry Pierce & Speers, 1996).

For many years IHT was attributed to the existence of clones within tumors with a distinct mutational profiles. Heterogeneity within these clones was explained due to environmental and stochastic influences rather than by intrinsic characteristics. Thus, the concept of tumor heterogeneity assumed that every cell within a determined clone is able to sustain tumor growth over long periods and therefore tumorigenic potential is equivalent amongst cells of identical genotype (Hanahan & Weinberg, 2000).

This concept was challenged by observations made in leukaemia. John Dick and colleagues showed that in acute myeloid leukaemia (AML) only a subset of cells were able to reconstitute the tumor when implanted into recipient mice, suggesting that cellular heterogeneity was present in genetically identical cells (Lapidot et al., 1994). Later, the same scientists showed that these tumor initiating cells (TICs) displayed features reminiscent of hematopoietic stem cells (Bonnet & Dick, 1997). These findings put forward the notion that cell heterogeneity was the consequence of cell hierarchy and suggested that cancer stem cells represent a biologically distinct subset within the malignant population which was not necessarily (**Figure 20**).

Over the past year, similar studies of tumor cell transplantation in recipient mice have demonstrated the existence of tumor initiating cells in different

cancer types including those arising in the brain, breast, colon, prostate or lung. These studies have solidified the notion that a large fraction of the phenotypic heterogeneity found in some tumors is the result of a hierarchical organization similar to the one present in their corresponding healthy tissues. In other words, tumor cells can undergo differentiation, which result in loss of tumorigenic potential despite oncogenic mutations present whereas CSCs sustain tumor growth over long term. Moreover, gene-expression signatures specific to CSCs and normal SCs revealed a high grade of similarity and were prognostic for outcome across patients with diverse driver mutations (Bartholdy et al., 2014; Gentles, Plevritis, Majeti, & Alizadeh, 2010; Merlos-Suárez et al., 2011; Ng et al., 2016).

Cancer stem cells may indeed arise from normal stem cells by mutation of genes that make the stem cells cancerous. However, it is also conceivable that more differentiated cells can, through multiple mutagenic events, acquire the self-renewal capacity and immortality that typify cancer stem cells. In this case, a differentiated cell can become a full-blown cancer stem cell (Clarke et al., 2006).

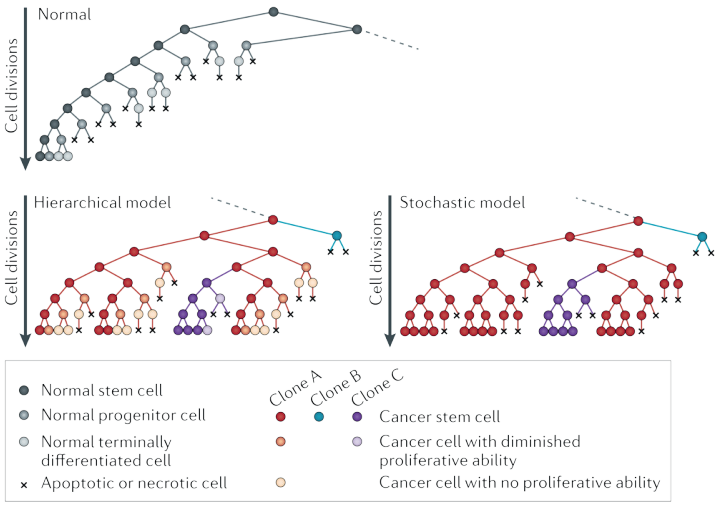

Figure 20: Hierarchical versus stochastic models of tumor cell heterogeneity. The hierarchical model assumes that cancer stem cells (CSCs) represent a biologically distinct subset within the total malignant cell population. According to this model, a pool of CSCs can only be maintained by cells that have both CSC potential and, by definition, the ability to give rise to progeny with self-limited proliferative capacity. The stochastic model assumes that every cell within a tumor has the same potential to act as a CSC, and that their variable activities are at least partially determined by some stochastically varying intrinsic factor. This means that their activities are not totally determined by the environment in which the cells are found. From (Nguyen, Vanner, Dirks, & Eaves, 2012).

Despite the different concepts and perspectives about CSC biology, there is agreement in that there is a subpopulation of cells in tumors that sustains growth, is able to self-renew and is the responsible, in most cases, of therapeutic failure.

6.2 Colorectal cancer stem cells

With the emergence of CSCs as critical players in cancer progression and therapeutic failure, increasing efforts have been dedicated into the purification and characterization of these cancer cells from colorectal tumors.

Identification and isolation of colorectal cancer stem cells (CRC-SCs) was for many years one of the main challenges in the field. Several studies demonstrated the existence of a population of tumor cells within human CRCs with the capacity to propagate the disease upon inoculation into immunodeficient mice. These cells were termed tumor initiating cells (TICs) or colorectal cancer stem cells (CRC-SCs) and were shown to give rise to the other types of cancer cells with non-tumor initiating and non-self-renewal potential. Two independent studies carried out by Ruggero de Maria and John Dick identified CD133 as a surface marker to isolate TICs. They showed that CD133+ cells were able to recapitulate the tumor upon transplantation in immunodeficient mice (O'Brien, Pollett, Gallinger, & Dick, 2007; Ricci-Vitiani et al., 2007). The same year, Dalerba and colleagues proposed CD44 as another marker highly expressed by TICs in colorectal tumors (P Dalerba, Dylla, Park, & Liu, 2007).

Later, our laboratory identified the stem cell gene EPHB2 as a candidate marker of CRC-SCs and normal SCs (Jung et al., 2011; Merlos-Suárez et al., 2011). As mentioned before, the expression of EPHB2 is driven by WNT signalling. This receptor plays a crucial role in intestinal crypt cell positioning and migration (Eduard Batlle et al., 2002). EPHB2 is expressed in a decreasing gradient from the crypt base towards the differentiated compartment in the intestine (Eduard Batlle et al., 2002). Since EPHB2 is highly expressed in the stem cell population it was successfully used to isolate SCs both from mouse and human intestine (Jung et al., 2011; Merlos-Suárez et al., 2011).

Histological analysis of CRCs according to the EPHB2 marker evidenced that cell heterogeneity in tumors is organized in a spatial and morphological manner that resembles the crypt invaginations found in the normal tissue (Merlos-Suárez et al., 2011). Similar to the normal tissue, EPHB2 expression was found in crypt-like tumor areas and absent in differentiated compartments

expressing the pan-differentiation marker KRT20 (**Figure 21**). Genetic profiling of tumor cells expressing high levels of EPHB2 (EPHB2^{hi}) revealed an enrichment of the stem cell program in this population. Tumor initiation assays also demonstrated that these cells retained tumor propagation properties as well as self-renewal and multipotent capacity. Indeed, the expression of ISC-specific genes in CRCs correlated with poor prognosis. On the contrary, differentiation of tumor cells coincided with loss of their tumorigenic potential (Merlos-Suárez et al., 2011). Therefore, CRCs maintain a hierarchical organization of tumor cells reminiscent of that found in the normal intestinal epithelium suggesting that the ISC and differentiated programs are maintained in CRC (Merlos-Suárez et al., 2011) (**Figure 22**).

Indeed, low and medium grade colorectal tumors present crypt-like glandular structures in which the stem and differentiated tumor cells are confined in clear separated compartments. Yet, this histological organization relies to some extent on the differentiation grade of these tumors since it is less evident in high grade and poorly differentiated tumors (E Batlle et al., 2005; Merlos-Suárez et al., 2011) (**Figure 23**).

In another study, single-cell transcriptomic analysis of CRC cells showed that human colon cancer tissues contained distinct cell populations whose transcriptional identities mirrored those of the different cellular lineages of normal colon. Moreover, the different gene-expression programs linked to multilineage differentiation were strongly associated with patient survival (Piero Dalerba et al., 2011).

Altogether, these studies demonstrate that colorectal tumors present a heterogeneous composition and a hierarchical cell organization. How this is controlled in an aberrant WNT signalling background remains unresolved. The balance between stemness and the differentiation phenotype in CRCs may depend on additional signalling pathways. One explanation could be the influence of signalling pathways that regulate normal ISC such as BMP and Notch signalling (Lombardo et al., 2011; Lu et al., 2013). Emerging evidences also suggest the stroma as mediator in the controlling the balance between stemness and differentiation in CRC (H.-J. Li, Reinhardt, Herschman, & Weinberg, 2012; Vermeulen et al., 2010).

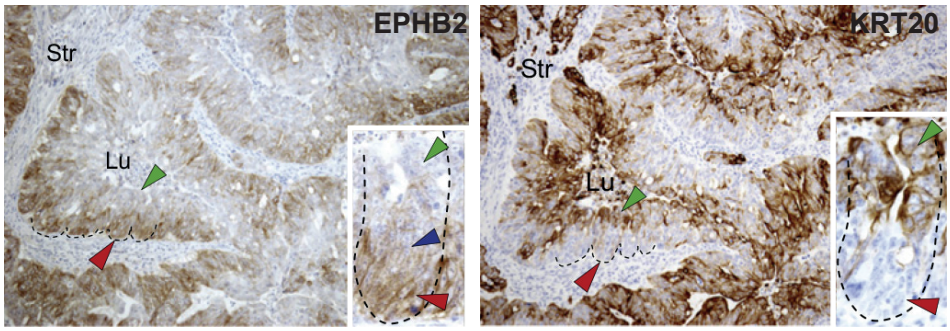

Figure 21: Histological heterogeneity of CRC. Most CRCs present a histological organization reminiscent of that found in the normal tissue, containing a population of cells with similar characteristics of normal stem cells (colorectal cancer stem cells; CRC-SCs) as well as differentiated-like cells. EPHB2 and KRT20 immunohistochemistry in serial sections of human CRC. EPHB2+ (CSCs) are confined at the base of the crypt-like structures whereas differentiated KRT20+ cells are localized at the cells close to the gland lumen. From (Merlos-Suárez et al., 2011).

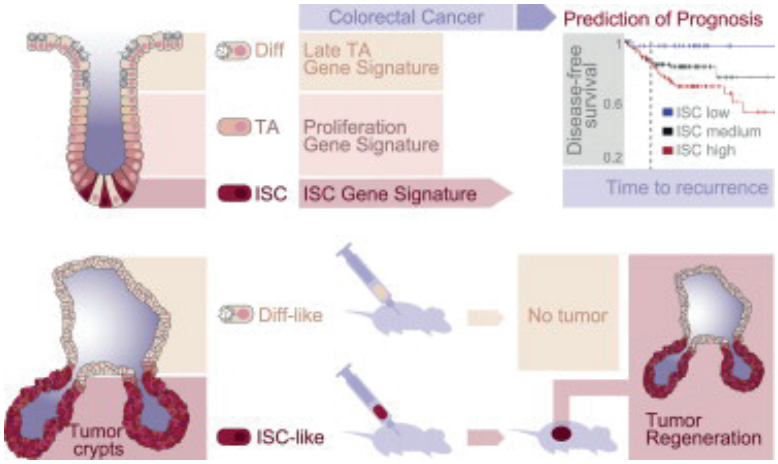

Figure 22: CRC-SCs are enriched in ISC genes and display tumor initiation capacity. EphB2 high tumor cells are enriched in ISC genes and display tumor initiation potential whereas the EphB2 low/negative expresses genes of intestinal differentiation and are not tumorigenic. Elevated expression of the ISC-specific genes associate with high risk of recurrent CRC. From (Merlos-Suárez et al., 2011).

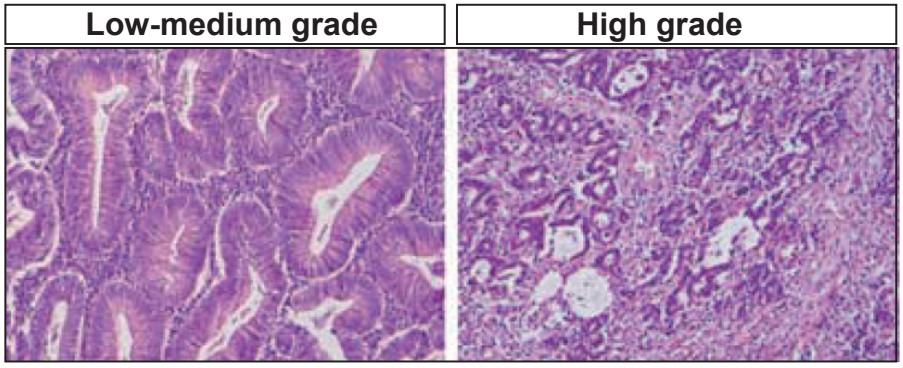

Figure 23: Histological organization of CRC. Comparison between low-medium and high grade tumors. The glandular structure is lost in high grade tumors as well as the EPHB2 expression. This correlates with the malignancy of the tumor. Adapted from (E Batlle et al., 2005).

7. rDNA transcription and ribosome biogenesis

Around 60% of the nascent RNA synthesis in a cell accounts for the transcription of ribosomal RNA (rRNA) genes, which direct and support the production of several millions of ribosomes. rDNA transcription is a highly coordinated and complex biological process that takes place in specific regions of the nucleus called nucleolus. Eukaryotic cells have developed a ribosomal DNA (rDNA) transcription machinery that includes the RNA Polymerase I (RNA Pol I) together with other essential factors that ensure this activity in the cell.

7.1 Ribosomal DNA gene structure

RNA Pol I directs rDNA synthesis from a single class of genes, rDNA genes, which are found in multiple tandem copies in the nucleolus of eukaryotic cells (Hadjiolov, 1980). In human cells, rDNA genes clusters are located on the short arm of the five pairs of acrocentric chromosomes (chromosomes 13, 14, 15, 21 and 22). Chromosomal regions containing these loci have been named “nucleolar organizer regions” (NORs). These NORs represent sites of active rDNA transcription and can be visualized with colloidal silver techniques (AgNORs). The AgNOR number is known to correlate with the proliferative activity of the cell population and the AgNOR score of cancer cells such as lung, breast or colorectal has been a good predictor of patient’s prognosis (Derenzini et al., 2000).

The structure of a single rDNA repeated unit can be divided into two major regions: the rRNA precursor and the intergenic spacer sequences . Once transcribed, the rRNA precursor generates a single rRNA transcript

termed pre-rRNA, which is processed by endonucleases and exonucleases to produce the final mature rRNA subunits (28S, 18S and 5.8S). The intergenic spacer region is not transcribed and includes all the sequences responsible for proper RNA Pol I transcription such as proximal promoters, spacer promoters and terminators (Hadjiolov, 1980) (**Figure 24**).

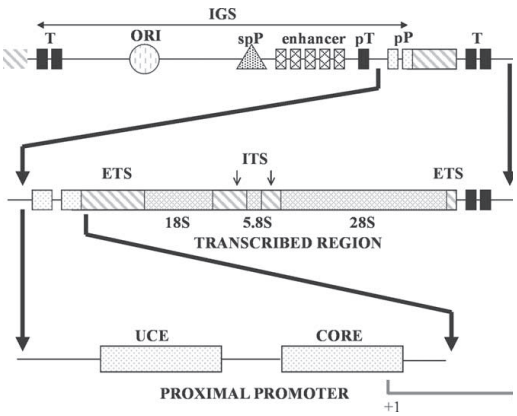

Figure 24: Schematic representation of eukaryotic rDNA gene. The rDNA genes are composed by the rRNA precursor and the non-transcribed intergenic spacers. The rRNA precursor region generates the pre-rRNA molecule whereas the intergenic spacers contain the regulatory elements such as promoters, spacers and terminators. From (Comai, 2004).

7.2 Factors involved in rDNA transcription

The development of cell-free transcription systems together with column fractionation analyses of cell extracts from a variety of organisms, led to the identification of several factors required for efficient and accurate rDNA transcription.

7.2.1 RNA Polymerase I

Ribosome biogenesis is a central biological process that in eukaryotes requires the coordination of three nuclear, RNA polymerases. RNA Pol I transcribes the rRNA precursor gene and is the most active eukaryotic RNA polymerase contributing up to 60% of the total transcriptional activity (Viktorovskaya & Schneider, 2015). RNA Polymerase II (RNA Pol II) synthesises messenger RNA and RNA Polymerase III (RNA Pol III) is mainly involved in transfer RNA synthesis. RNA Pol II and III also contribute to ribosome biogenesis by providing mRNAs encoding ribosomal proteins and 5S rRNA, respectively.

The yeast RNA Pol I enzyme has a total mass of 589 kDa and consists of 14 subunits. RNA Pol I core includes the two largest subunits, A190 and A135 (POLR1A and POLR1B in mammals), forming the DNA binding cleft, plus five subunits present in all nuclear RNA polymerases. These largest subunits, that are required for the catalytic function, are shared among bacteria, Achaea and eukaryotes suggesting that they probably have evolved from a common ancestral progenitor (Comai, 2004; Fernández-Tornero et al., 2013) (**Figure 25**).

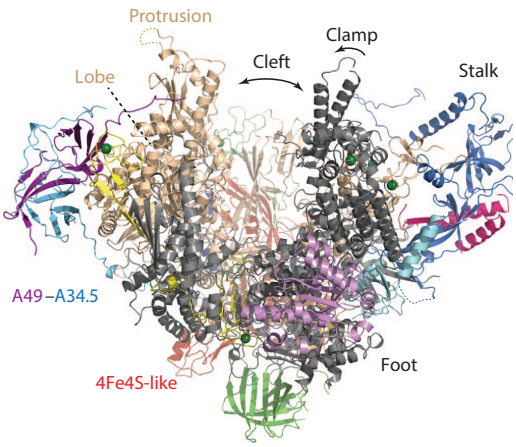

Figure 25: RNA Polymerase I crystal structure. The crystal structure of the yeast RNA polymerase I reveals a 14-subunit enzyme. Extracted from (Fernández-Tornero et al., 2013).

7.2.2 RNA Polymerase I transcription factors

In order to start transcription RNA Pol I has to interact with other transcription factors to from the pre-initiation complex (PIC). Three essential factors has been described: TIF-IA/RRN3, UBF and SL1.

-TIF-IA/RRN3: is a direct interactor of RNA Pol I core enzyme. Dimerization between TIF-IA and RNA Pol I is essential for initiation of the transcriptional process. When RNA Pol I switches from initiation to elongation, the RNA Pol I-TIF-IA complex is disrupted (Engel, Plitzko, & Cramer, 2016). TIF-IA specifically binds to the yeast RNA Pol I subunit A43 (TWISTNB in mammals) through an interface that contains a patch of serine residues. Phosphorylation of this serine patch represses RNA Pol I transcription because it prevents RNA Pol I interaction with TIF-IA. Both ERK-MAPK and mTOR signalling cascades have been implicated in the control of TIF-IA activity and its interaction with RNA Pol I (Mayer, Bierhoff, & Grummt, 2005; Mayer, Zhao, Yuan, & Grummt, 2004) (**Figure 26**).

-UBF: The upstream binding factor (UBF) is a DNA-binding protein that recognizes the rDNA promoter. By binding to the DNA, UBF functions as a scaffold protein, which facilitates the formation of the transcriptional initiation complex at the ribosomal DNA promoter (Grummt, 2010). UBF can be phosphorylated by casein kinase 2 (CK2) and this contributes to transcriptional activation (Comai, 2004) (**Figure 26**).

-Selective factor SL1: is a multisubunit complex composed of TATA-binding proteins (TBP) and TBP-associated factors (TAFs). SL1 does not bind specifically to the rDNA promoter but in the presence of UBF, it forms a strong cooperative DNA-binding complex at the ribosomal DNA promoter that is essential for initiation of transcription. The interactions between UBF and its DNA recognition sequence, and between UBF and SL1, play a major role in RNA Pol I transcription (Comai, 2004) (**Figure 26**).

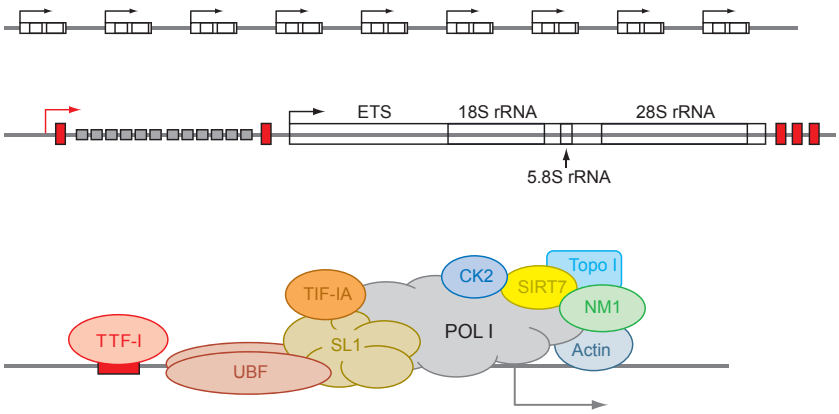

Figure 26: Basal factors required for transcription initiation. UBF, SL1 and TIF-IA associate with RNA Pol I and form the pre-initiation complex (PIC) required to initiate the rDNA transcription from the rDNA promoter. From (Drygin, Rice, & Grummt, 2010).

7.3 The RNA Pol I transcription cycle

7.3.1 Pre-initiation complex formation

Transcription starts with the recruitment and assembly of RNA Pol I together with the other transcription factors into a pre-initiation complex (PIC) at the rDNA gene promoter. Mammalian rDNA gene promoters contain a CORE element, which is required for accurate transcription initiation, and an upstream control element (UCE), which plays a modulatory role. In addition to these elements, there are distal enhancer-like sequences which function by helping the stable PIC formation on the rRNA gene promoter.

The initial step required for the formation of the pre-initiation complex is the binding of the UBF dimer to the UCE and core elements. Once bound, UBF will recruit the SL1 factor to the rDNA promoter. The subsequent recruitment of the RNA polymerase core enzyme appears to be mediated by multiple protein-protein interactions. The RNA Pol I associated factor TIF-IA bridges RNA Pol I to the SL1 complex. The assembly of the initiation complex on the promoter and the transition from a closed to an open DNA structure is then followed by RNA PL Itranscription elongation (**Figure 27**).

7.3.2 Initiation and promoter escape

Once transcription is initiated, UBF and SL1 remain bound to the promoter ready to recruit a new TIF-IA/Pol I complex for a new round of transcription. On the contrary, TIF-IA is released from the polymerase and inactivated. The RNA

polymerase moves over the synthesis of the first few nucleotides until escapes the promoter to continue with the elongation of the transcript (**Figure 27**).

7.3.3 Elongation of transcription

As RNA Pol I escapes and clears the promoter, UBF and SL1 remain bound into the promoter in order to recruit the next RNA Pol I complex from the same promoter suggesting multiple rounds of transcription from the same promoter. Unlike RNA polymerase II system, RNA polymerase I transcription does not require a form of energy such as ATM for initiation and elongation. (**Figure 27**).

7.3.4 Termination and reinitiation of transcription

Transcription termination elements are located at 3' end of the transcribed region of the rRNA gene and upstream of the rDNA transcription start site. The mammalian transcription termination factor I (TTF-I) binds the termination site at 3' end of the transcribed region, forces RNA Pol I to pause, induces transcription termination and dissociates the elongating RNA Pol I and transcript from the DNA template. Following termination of transcription, the components of the released polymerase are likely to be recycled to generate new RNA Pol I (**Figure 27**) (Russell & Zomerdijk, 2005).

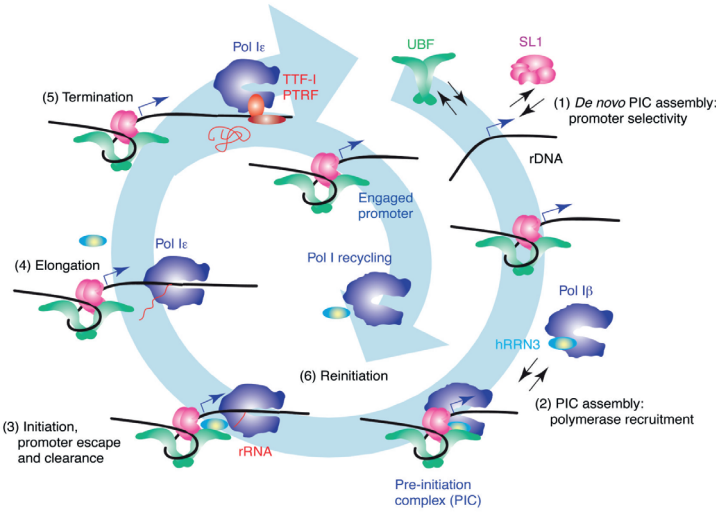

Figure 27: The RNA polymerase I transcription cycle. (1-2) pre-initiation complex formation (PIC), (3) transcription initiation, promoter escape and clearance, (4) elongation and (5) termination. From (Russell & Zomerdijk, 2013).

7.4 rRNA processing and ribosomal particle assembly

There are six important steps in ribosome biogenesis: (i) synthesis of components (rRNAs, ribosomal proteins (RPs), assembly factors (AFs) and small nucleolar ribonucleoproteins particles (snoRNPs); (ii) processing of pre-rRNAs (cleavage); (iii) covalent modification of pre-RNAs, RPs and AFs; (iv) assembly; (v) transport (nuclear import of RPs and AFs and export of pre-ribosomes to the cytoplasm); and (vi) quality controls and surveillance mechanisms (**Figure 28**) (Lafontaine, 2015).

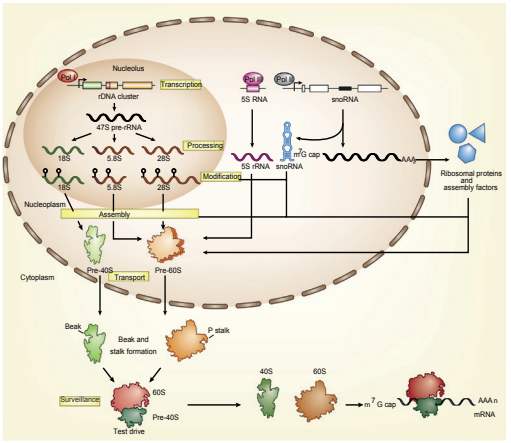

Figure 28: Eukaryotic ribosome biogenesis. Ribosome biogenesis encompasses six important steps (yellow boxes): (i) transcription of rRNAs, mRNAs encoding ribosomal proteins (RPs) and assembly factors (AFs); (ii) cleveage of pre-RNAs; (iii) modification of pre-RNAs, RPs and AFs; (iv) assembly; (v) transport (nuclear import of RPs and AFs; pre-ribosome export to the cytoplasm); and (vi) quality control and surveillance. From (Lafontaine, 2015).

The first rRNA molecule generated after transcription is called pre-rRNA and needs to be processed before constituting mature ribosomes. The eukaryotic pre-rRNA transcript is composed by the 18S, 5.8S and 28S rRNAs, which are separated by internal transcribed spacers 1 (ITS1) and 2 (ITS2) and flanked by 5' and 3' external transcribed spacers (5'-ETS and 3'-ETS). In order to be processed, pre-rRNA associates with several ribosomal proteins (RPs) and small nucleolar ribonucleoproteins particles (snoRNPs).

During pre-rRNA processing, transcribed spacers are sequentially eliminated through a complex series of endonucleolytic and exonucleolytic cleavages. In addition to these cleavages, pre-rRNA is also extensively modified mostly by methylation of the 2'-hydroxil group of specific riboses and conversion of specific uridine residues to pseudouridine. The positions of cleavage sites in pre-rRNA, the specific sites of 2'-o-methylation and pseudouridine formation are determined by approximately 150 different snoRNAs (**Figure 29**). Three different types of snoRNAs have been involved in the processing of pre-rRNA transcripts (Lafontaine, 2015).

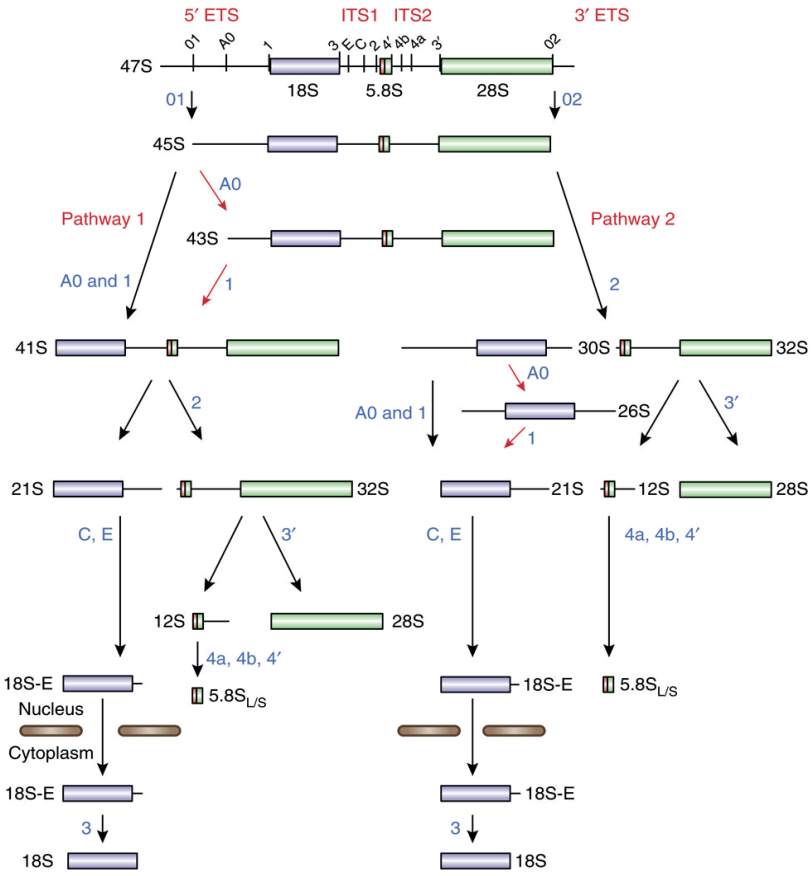

Figure 29: pre-rRNA processing pathways. 18S, 5.8S and 28S are produced from a single RNA Pol I transcript (47S). The mature sequences are embedded in noncoding 5' and 3' external transcribed spacers (ETS) and internal transcribed spacers (ITS1 and ITS2). 47S is cleaved at sites 01 and 02 on both sides of the molecule to generate the 45S pre-rRNA, which is processed by two alternative pathways pathway 1 and 2) depending on the cleavage sites. Extracted from (Lafontaine, 2015).

-The U3 snoRNAs are non-coding RNAs that guide the site-specific cleavage of pre-rRNA at ETS and ITS regions.

-The C/D box snoRNAs contain two short conserved motifs, C (RUGAUGA) and D (CUGA) located near the 5' and 3' ends of the snoRNA respectively. These snoRNAs are associated with specialized proteins such as Fibrillarin, NOP58, NOP50 and Snu13 that are involved in the 2'-o-methylation of the pre-rRNA.

-The H/ACA box snoRNAs contain conserved sequences motifs known as H box and ACA box. In this case, H/ACA box snoRNAs are associated with four evolutionary conserved and essential proteins, Dyskerin, GAR1, NHP2 and

NOP10 that carry the conversion of uridine nucleotides into pseudouridine by enzymatic reactions.

Once the pre-rRNA has been processed and modified, the formation of ribosomes involves the assembly of mature rRNAs with both ribosomal proteins and the 5S rRNA. The genes that encode ribosomal proteins are transcribed outside the nucleolus by RNA polymerase II. The ribosomal proteins are then transported from the cytoplasm to the nucleolus, where they are assembled with rRNAs to form preribosomal particles.

The association of ribosomal proteins with rRNA begins while the pre-rRNA is still being synthesized, and more than half of ribosomal proteins are in complex with the pre-rRNA prior to its cleavage. The remaining ribosomal proteins and the 5S rRNA are incorporated as cleavage of the pre-rRNA proceeds.

Finally, mature ribosomes are composed by two ribosomal subunits. The 40S or small ribosomal subunit that contains only the 18S rRNA and 33 ribosomal proteins and the large subunit composed by the 28S, 5.8S and 5S rRNAs together with 50 additional ribosomal proteins. The final stages of ribosome maturation follow the export of the preribosomal particles to the cytoplasm forming the active 40S and 80S subunits of eukaryotic ribosomes (Raza & Galili, 2012) (**Figure 30**).

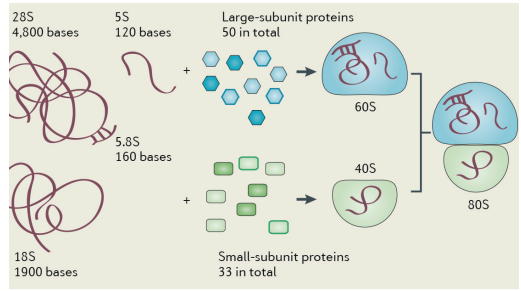

Figure 30: Ribosomal assembling. Once the pre-rRNA has been processed and modified the mature RNA subunits (18S, 28S and 5.8S) are rapidly transported to the cytoplasm where final processing and incorporation of additional proteins to generate the mature 40S and 60S subunits is completed. From (Raza & Galili, 2012).

8. Regulation of rRNA transcription

Regulation of rDNA transcription is tightly linked to both general cellular metabolism and specific environmental challenges. Signalling pathways that affect cell growth and proliferation regulate rDNA synthesis by modulating individual steps of the transcription cycle.

It has also been shown that rDNA transcription is altered under oncogenic conditions. Many oncogenes and tumor suppressor genes exert their effect by modulating the rDNA transcriptional activity of tumor cells. Indeed, it is thought that cancer cells might achieve a proliferative advantage by elevating

the level of specific oncogenes which in turn raise the production of rRNA.

All these factors impinge in a short-term regulation that mainly occurs at the level of transcription initiation, elongation and RNA processing. Many of the proteins participating in these processes such as UBF, SL1 or TIF-IA can serve as potential targets to modulate rDNA transcription rates by these signalling pathways.

8.1 Proliferation, growth and cell cycle

Different signalling pathways such as MAPK pathway or mTOR are involved in the regulation of rDNA transcription in response to growth, energy consumption and proliferation. Their effect impinge on the activity of key transcriptional factors required for RNA Pol I transcription.

One of the main factors involved in the short-term regulation of rDNA synthesis is the UBF protein through post-transcriptional modifications. In this case, the extracellular signal-regulated protein kinase (ERK) is essential for activation of rDNA transcription by growth factors. For instance, ERK is involved in the phosphorylation of UBF at specific serine residue (Ser484) upon serum stimulation whereas transcriptional silencing in quiescent cells correlates with its hypophosphorylation (Stefanovsky et al., 2001). mTOR is another signalling pathway that impinges on the regulation of UBF in response to proliferation. mTOR stimulates RNA Pol I transcription through phosphorylation of the C-terminal activation domain of UBF (Hannan et al., 2003).

SL1 transcriptional factor is also regulated during rDNA transcription changes. In this case, acetylation of the specific SL1 factor TAFI68 stimulates transcription initiation (Muth, Nadaud, Grummt, & Voit, 2001). This acetylation is counteracted by SIRT1, a member of a family of highly conserved NAD+-dependent histone deacetylases, termed sirtuins. As the activity of sirtuins depends on the level of cellular NAD+, changes in the cellular energy status are translated into changes in rRNA synthesis and ribosome production.

Another key player in growth-dependent regulation of rDNA transcription is TIF-IA that is regulated by diverse signals in response to cell growth and proliferation. Specific phosphorylation of TIF-IA either facilitates or impairs the interaction with RNA Pol I, indicating that reversible phosphorylation of TIF-IA is an effective way to rapidly and efficiently modulate rDNA transcription in response to growth factors, nutrient availability or external stress. Conditions that support growth

and proliferation also activate TIF-IA by mTOR-dependent and ERK-dependent phosphorylation (Mayer et al., 2004). Conversely, stress-induced activation of c-Jun N-terminal kinase (JNK)2 triggers an inhibitory phosphorylation signal (Mayer et al., 2005). In addition, rDNA transcription and ribosome biogenesis are also regulated by the intracellular ATP levels. The key enzyme that translates changes in energy levels into adaptive cellular responses is the AMP-activated protein kinase (AMPK). Activation of AMPK under low levels of energy, phosphorylates TIF-IA at Ser635 which in turn inactivates TIF-IA and inhibits rRNA synthesis (Hoppe et al., 2009).

Aside from growth-dependent regulation, RNA Pol I transcription also oscillates during cell cycle progression. In early G1-phase rDNA transcription remains low and it is progressively recovered during progression through the G1-phase and S-phase when UBF is activated by phosphorylation of Ser484 by Cdk4-cyclin D and Ser388 by Cdk2-cyclin E and Cdk1-cyclein A (Voit, Hoffmann, & Grummt, 1999). The maximum peak of rDNA transcription is achieved during the S and G2 phases of the cell cycle. Then, at entry into mitosis Cdk1-cyclin B phosphorylates the SL1 complex leading to repression of Pol I transcription during mitosis (Heix et al., 1998). At the exit of mitosis Cdc14B dephosphorylates again SL1 leading to rDNA transcription recovery (**Figure 31**).

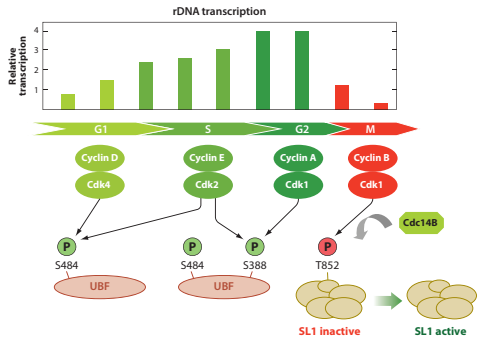

Figure 31: Regulation of rDNA transcription. Regulation of RNA Pol I transcription during cell cycle progression. From (Drygin et al., 2010).

8.2 rDNA transcription and cancer

At the end of the last century pathologists already realized that the hypertrophy of the nucleolus was one of the most consistent cytological features of cancer cells. Nucleolar size might thus represent a morphological parameter of the cell proliferation rate in cancer tissue. Derenzini and colleagues demonstrated a direct correlation between the size and function of the nucleolus and the cell proliferation rate of the cancer tissues using silver staining of AgNOR proteins to label the nucleolus of tissue sections of tumor xenografts (Derenzini et al., 2000) (**Figure 32**).

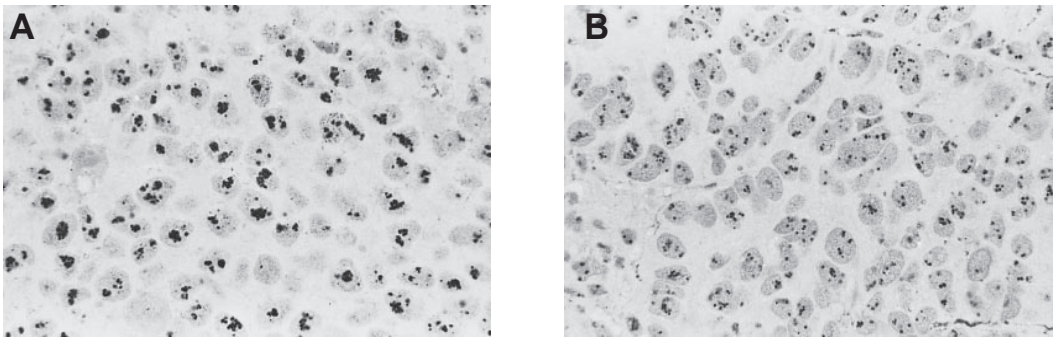

Figure 32: Nucleolar size in normal and tumor cells. Sections from the same xenograft stained by AgNor proteins. (**A**) A large amount of AgNOR proteins are present within the nucleolus of the rapidly proliferating tumor mass. (**B**) Only few silver stained dots are present within cancer cells of the slowly proliferating mass. Adapted from (Derenzini et al., 2000).

There has been a growing realization that the expression and activity of many of the components involved in ribosome production and translational control are directed by signal transduction pathways, which are often deregulated in cancer. Indeed, RNA Pol I transcription is regulated by a balanced interplay between oncogene products and tumor suppressors.

8.2.1 Tumor suppressors

In healthy cells RNA Pol I transcription is restrained by tumor suppressors such as pRB, p53, and PTEN. For instance pRb and the related pocket proteins p107 and p130 restrict cell growth and proliferation. It has been shown that UBF is a target for pRb-induced repression of RNA Pol I transcription. pRB accumulates in the nucleoli of differentiated or cell cycle-arrested cells and causes downregulation of rDNA transcription (Cavanaugh et al., 1995). Binding of pRb to UBF leads to its dissociation from the rDNA therefore impairing transcription complex formation (Voit, Schäfer, & Grummt, 1997).

Similar to pRb and p130, the tumor suppressor p53 has been shown to repress Pol I transcription. Cancers with deleted pRb and mutated p53 exhibit much higher rates of rDNA transcription and are generally more aggressive than those with intact Rb and p53. In accordance with its role restricting cell proliferation, p53 inhabits ribosome biogenesis by repressing RNA Pol I and RNA Pol III transcription (Budde & Grummt, 1999; Zhai & Comai, 2000). P53 interacts with the transcription factor SL1 interfering with the formation of the pre-initiation complex consisting of SL1 and UBF.

PTEN is another example of tumor suppressor gene that is able to regulate RNA Pol I transcriptional activity. PTEN acts upon mTOR, triggering the activation of several downstream signalling events that inhibit cell proliferation. PTEN impinges in Pol I activity by disrupting the TATA binding protein SL1 from the rDNA promoter preventing the assembly of the transcription initiation complex. In Ras transformed cells PTEN was found at the rDNA promoter in a complex with the glycogen synthase kinase GSK3B. Indeed, inhibition of GSK3B upregulates rRNA synthesis (Vincent, Kukalev, Andäng, Pettersson, & Percipalle, 2008) (**Figure 33**).

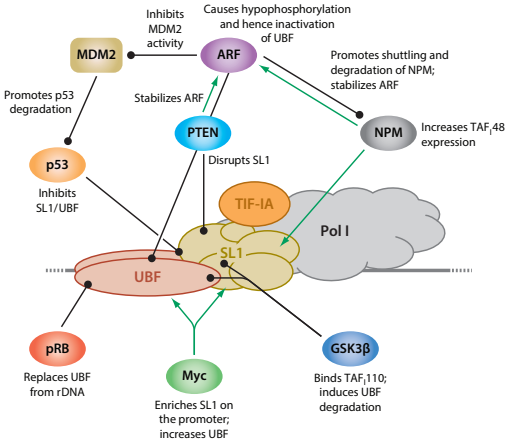

Figure 33: Oncogenes and tumor suppressors that control RNA Pol I transcription. Oncogenes activate rRNA synthesis by upregulating the level of transcription factors and/or stabilizing protein-protein or protein-DNA interactions (green arrows), whereas tumor suppressors inhibit rRNA synthesis by interfering with essential transcription factors required for initiation complex assembly (black lollipops). From (Drygin et al., 2010).

8.2.2 Oncogenes

The PI3K (phosphoinositide 3-kinase)-AKT-mTOR (mammalian target of rapamycin) signalling pathway has been shown to be an exquisite regulator of the translation machinery and the ribosome biogenesis process. Chan et al. uncovered that the protein kinase AKT, in addition to its role in controlling translation initiation, also modulates ribosome biogenesis, specifically by promoting RNA Pol I loading during rDNA transcription initiation, rDNA transcription elongation and rRNA processing (Chan et al., 2011). This suggests that AKT-mediated rRNA synthesis could be a direct effect and active participant in the AKT-mediated oncogenic program.

Another oncogene that impinges in a signalling pathway that can influence in the rDNA transcription activity is the GTPase Ras. Upon mitogenic stimulation, the epithermal growth factor receptor (EGFR) triggers a signalling cascade involving Ras, the kinases Raf, MEK, and ERK. Consistent with its positive effect on cell growth and proliferation, MAPKs have been found to activate rRNA synthesis by targeting the factors TIF-IA and UBF leading to upregulation of rDNA transcription (Victor Y. Stefanovsky, Frédèric Langlois, David Bazett-Jones, Guillaume Pelletier, & Tom Moss*, 2006

8.3 Epigenetic control of rDNA transcription

Transcription of rDNA is also modulated by epigenetic mechanisms. Approximately half of the several hundred copies of rDNA genes exhibit an heterochromatic chromatin structure and are transcriptionally silent. The number of active rDNA genes varies between different cell types, indicating that the fraction of active gene copies varies during development and differentiation. Thus, long-term changes in rDNA transcription can be modulated by regulating the number of rDNA genes that are transcriptionally active.

DNA methylation is an epigenetic mechanism that regulates rDNA gene transcription. Methylation at cytosine is an epigenetic mark associated with gene silencing. Initial studies using methylation sensitive and insensitive restriction enzymes revealed a correlation between the proportions of active and inactive versus unmethylated and methylated rRNA genes. Moreover, these methylation marks were found in the promoter and enhancer regions of inactive genes. Analysis of the methylation profile of human hepatocellular carcinomas or the colon cancer cell line HCT116 showed significant hypomethylation of the rDNA promoter compared with normal tissues evidencing the elevated rDNA synthetic activity of rapidly proliferating cells (Grummt & Pikaard, 2003; McStay & Grummt, 2008).

Another important epigenetic modulation of the transcriptional state of rDNA genes is histone modification. Most epigenetic modifications localize at specific positions within the N- and C-terminal histone tail. Whereas lysine acetylation correlates with chromatin accessibility and transcriptional activity, lysine methylation can have different effects, depending on which residue is modified. These key modifications distinguish silent heterochromatin from permissive euchromatin and correlate with the activity status of rDNA repeats (McStay & Grummt, 2008).

Despite the existent evidence about the epigenetic regulation of rDNA transcription, there are many questions still to be addressed. For instance, how do cells select the fraction of genes to be activated or silenced, what is the relationship between short-term transcriptional activity and long-term chromatin structure or which are the mechanisms that allow switching between transcriptional states.

9. MYC signalling in intestinal homeostasis, colorectal cancer and ribosome biogenesis

Human c-MYC was the second proto-oncogene identified and encodes a basic helix-loop-helix leucine zipper transcription factor. MYC proteins dimerize with MAX, and MYC-MAX heterodimers can activate or repress a large number of biological functions such as proliferation, cell growth, differentiation and apoptosis in different cell types (Murphy, Wilson, & Trumpp, 2005).

9.1 MYC signalling in the intestinal epithelium

Myc oncogene was one of the first genes identified as a β-catenin/Tcf-4 transcriptional target. Subsequent studies identified binding sites for TCF4 in the c-Myc promoter, suggesting that c-MYC was a bona fide direct target of canonical Wnt signalling pathway (He et al., 1998). Indeed, endogenous c-Myc is expressed in the proliferative zone of the crypts and colocalizes with nuclear β -catenin, indicative of active WNT signalling (Sansom et al., 2004).

Van de Wetering, Sancho and colleagues showed that in CRC cells, disruption of β-catenin /TCf-4 activity induced rapid G1 arrest and blocked the genetic program that is active in the proliferative compartment of colon crypts (Van de Wetering et al., 2002). At the same time, an intestinal differentiation programme was induced. They suggested that the TCF-4 target gene c-MYC played a central role in this switch by direct repression of the p21CIP1/WAF1 promoter. This work suggested that c-MYC blocks the expression of the differentiation program by directly regulating p21 expression, and thus the proliferative status of the cell.

In line with these observations, transgenic mice ectopically expressing the WNT inhibitor Dkk1 showed a reduction of epithelial proliferation, which coincided with the loss of intestinal crypts. In this model, disruption of Wnt signalling by Dkk1 expression resulted in the inhibition of c-Myc expression and subsequent up-regulation of the cell cycle inhibitor p21 (Pinto et al., 2003).

A key role for MYC in ISC homeostasis was further demonstrated when conditional depletion of this gene in homeostatic ISCs resulted in crypt loss within weeks. The c-Myc deficient crypts were replaced by c-Myc proficient crypts that had escaped gene deletion (Muncan et al., 2006). Of note, this study also showed that Myc depletion affected the biosynthetic capacity of ISCs by reduction of their rRNA synthesis capacity (**Figure 34**).

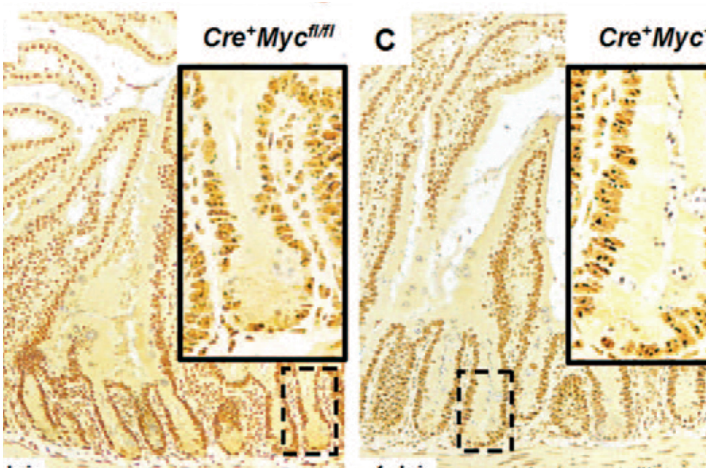

Figure 34: Loss of biosynthetic capacity in intestinal c-Myc-deficient cells. Intestinal crypts lacking c-Myc expression show a reduction in ribosomal gene synthesis evidenced by a decrease of AgNor staining compared to WT crypts. From (Muncan et al., 2006).

Overall, these studies demonstrate that c-Myc plays a central role in promoting proliferation of intestinal progenitors at the same time it maintains their undifferentiated state.

9.2 MYC signalling in colorectal cancer

Expression of MYC as direct target of the WNT pathway is also found during CRC development. The oncogene MYC has been identified as a WNT target gene both in colorectal cancer cell lines *in vitro* (Van de Wetering et al., 2002) as well as in intestinal epithelial crypts after conditional deletion of Apc *in vivo* (Sansom et al., 2004). The latter study identified Myc as one of the main upregulated genes upon Apc deletion together with other well-known WNT targets such as *AXIN2*, *CD44* or *EPHB3*. Alongside with these genetic changes, loss of Apc in the intestinal epithelium altered the normal pattern of cell differentiation and proliferation. This phenotype is in agreement with the notion that MYC could play a role by blocking differentiation through p21 inhibition (Van de Wetering et al., 2002).

Finally, a breakthrough study carried out by Sansom and colleagues demonstrated that Myc deletion rescued the Apc deficiency phenotype in the small intestine. They showed that Myc is required for the majority of WNT target gene activation following Apc loss (Sansom et al., 2007). These results demonstrated that Myc is one of the major drivers of the progenitor/crypt like phenotype observed during CRC development.

9.3 MYC: regulator of rDNA transcription and ribosome biogenesis

MYC has been described as a global regulator of various cellular processes, which include transcription, regulation of chromatin structure, translation, DNA replication and ribosome biogenesis. It is clear that MYC overexpression results in tumorigenesis that is associated with global deregulation of many of these processes.

Multiple observations suggest that MYC regulates multiple stages of ribosome biogenesis through the transcription of rRNA, recruitment of RNA Pol I cofactors, RNA Pol II-dependent transcription of structural ribosomal protein genes, factors for rRNA processing and ribosomal subunit export (**Figure 35**).

MYC directly binds to rDNA loci and activates the transcription of rRNA through two mechanisms. On one hand, chromatin immunoprecipitation experiments revealed that MYC occupies E-box sequences in the promoters of active rDNA clusters. Binding of MYC in these loci correlates with increased presence of transcription domain-associated proteins (TRRAP) and consequently increased acetylation of nucleosomal histones H3 and H4 upstream the rDNA promoter region.

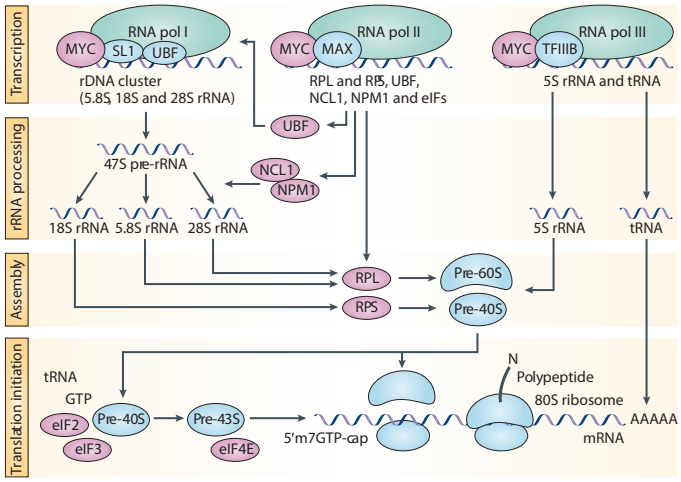

Figure 35: MYC controls multiple components of ribosome biogenesis. MYC directly regulates the expression of several ribosomal proteins, RNA components, and auxiliary factors that are required for ribosomal RNA (rRNA) processing, ribosome assembly, the export of mature ribosomal subunits from the nucleus into the cytoplasm, as well as factors that control the initiation of mRNA translation. MYC also facilitates RNA pol I transcription from ribosomal DNA (rDNA) clusters that encode the 5.8S, 18S and 28S rRNAs, which requires upstream binding transcription factor (UBF) and selectivity factor (SL1). Finally, MYC activates transcription of 5S rRNA and transfer RNA (tRNA) through RNA pol III. From (van Riggelen, Yetil, & Felsher, 2010).

This suggests that MYC facilitates rDNA transcription by opening the chromatin structure near rDNA loci (Arabi et al., 2005; Grandori et al., 2005; Shiue, Berkson, & Wright, 2009).

On the other hand, MYC also enhances the expression and recruitment of the RNA Pol I cofactors UBF and SL1. Indeed, UBF is a Myc target gene, which is upregulated in a RNA pol II-dependent manner. Interaction of MYC with UBF regulates promoter clearance during rDNA transcription. Moreover, MYC also interacts with SL1 factor and enhances RNA Pol I recruitment to target promoters (Grandori et al., 2005). Therefore, MYC activates RNA Pol I-dependent rDNA transcription both through chromatin remodelling and cofactor recruitment.

MYC also regulates the transcription of ribosomal proteins through RNA Pol II-dependent transcription. MYC has been shown to increase the levels of many RPL and RPS proteins (Boon et al., 2001). In addition, MYC coordinates the transcription of genes that encode proteins involved in the processing of rRNA precursors such as nucleolar protein 56 (NOP56), fibrillarin (FBL), dyskerin (DKC1), nucleolin (NCL) and nucleophosmin (NPM1). The latter has been reported to directly interact with MYC and its overexpression stimu-lates MYC-dependent hyperproliferation and transformation. Indeed, NPM1 cooperates with MYC-induced proli-feration and transformation by directly interacting with Myc at target promoters (Z Li & Hann, 2013; Zhaoliang Li, Boone, & Hann, 2008).

Overall these studies suggest that MYC directly impinges on ribosome biogenesis. We will further discuss whether the oncogenic phenotype driven by MYC upregulation can be explained to a certain extent by the stimulation of this cellular process.

Results

1. Characterization of EPHB2 cell populations based on their biological functions

Previous work in our laboratory showed that colorectal tumors are heterogeneous and are formed by a hierarchical cell architecture similar to the one found in the normal intestinal epithelium (Merlos-Suárez et al., 2011). This hierarchy can be readily appreciated by analysing the EPHB2 marker that it is expressed heterogeneously in a large proportion of colorectal cancers (CRCs).

Analogous to what occurs in normal tissue, EPHB2 is enriched in colorectal cancer stem cells (CRC-SCs) in tumors. Genetic analyses and functional assays showed that EPHB2-high CRC-SCs displayed long-term self-renewal as well as differentiation capacity. More importantly, these EPHB2-high CRC-SCs are the only population in CRCs that retains tumor-initiation properties. On the contrary, tumor cells with low EPHB2 levels represent a non-tumorigenic population that expresses markers of intestinal differentiation (Merlos-Suárez et al., 2011). These data indicate that despite having acquired a large range of genetic alterations not all tumor cells are equally tumorigenic.

Although this study has led to the identification of a clinically relevant CRC-SC population, the biological functions that explain the differential tumor-initiation capacities of CRC-SCs and differentiated tumor cells remain unknown. To tackle this question, we generated refined gene expression signatures of distinct tumor populations in primary colorectal tumors together with paired normal tissue samples. Comparison of EPHB2-high vs. -low populations from both tumor and normal tissues allowed us first, to identify genes and functions enriched in the overall EPHB2 high expressing cells and second, to further infer cancer stem cell-specific functions when comparing CRC-SCs to normal mucosa (NM) SCs.

1.1 Stratification of normal and tumor cell populations from CRC patients based on EPHB2 expression

Fresh colorectal tumors or normal tissues were obtained from Hospital Clinic and Hospital del Mar (Barcelona). Samples were first disaggregated and then single cells stained for epithelial selection (EPCAM+) and for EPHB2 (see methods section for details) (**Figure 1**).

By Fluorescence Activated Cell Sorting (FACS) we isolated epithelial cells expressing distinct levels of EPHB2 from both normal and tumor samples of 13 different patients (**Table 1**). Although the overall expression levels of EPHB2

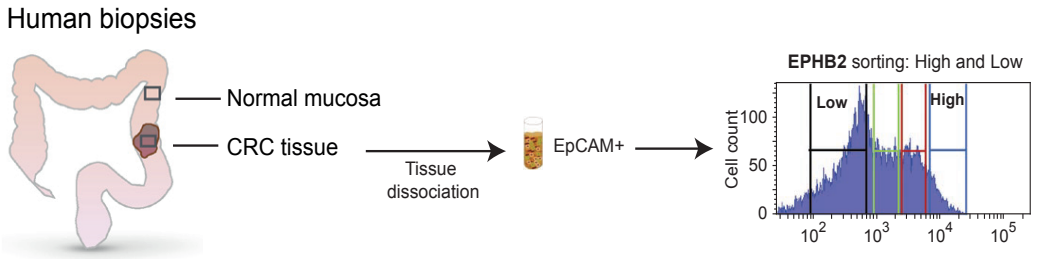

Figure 1: Experimental workflow. Isolation of normal and tumor epithelial cells based on their EPHB2 surface expression levels. Biopsies are thoroughly dissociated following various steps (described in methods) until a single cell solution is obtained. Cells are then labelled with EpCAM antibodies to mark cells of epithelial origin and then sorted on the basis of their EphB2 protein levels. Different populations are subsequently used for global gene expression analysis.

Paired samples		Individual samples	
SAMPLE CODE	TISSUE	SAMPLE CODE	TISSUE
P1	Normal	N1	Normal
P2		N2	
P1	Tumor	N3	
P2		P3	Tumor
		P4	
		P5	
		HMT	
		53	
		56	
		59	
		61	

Table 1: Primary normal and tumor samples analysed. 15 different samples (including normal and tumor tissues) from 13 colorectal cancer patients were used in this study. Two normal and tumor samples (P1 and P2) were obtained from the same patient (paired samples).

varied between tumor samples, the expression of this surface marker was heterogeneous in tumor cells. In order to simplify the analysis we defined two types of epithelial cells based on their EPHB2 expression in both tissues: The EPHB2^{hi} (top 10%-15% brightest cells) and EPHB2^{lo} displaying low/negative EPHB2 surface expression. We isolated 2000 cells of each EPHB2^{hi} and EPHB2^{lo} populations from tumor and normal samples. Because of the low cell number obtained from each population, cDNA was amplified from sorted cells through methodology developed by the Functional Genomics core facility at our institution (Gonzalez-Roca et al., 2010).

1.2 Global gene expression analysis of EPHB2 tumor and normal cell populations

To ensure we had purified and analysed the appropriate cell populations, we validated by RT-qPCR that EPHB2^{hi} cells from tumor and normal mucosa (NM) were enriched in well-known intestinal stem cell markers (*LGR5* and *SMOC2*). In addition, we corroborated that the EPHB2^{lo} cells showed a differentiated phenotype by the

expression of well- established markers of intestinal differentiation such as *KRT20* (**Figure 2**).

We next analysed the global gene expression profile of the 4 isolated populations: EPHB2^{hi} normal, EPHB2^{hi} tumor, EPHB2^{lo} normal and EPHB2^{lo} tumor cells. To this end, we hybridized EPHB2^{hi} and EPHB2^{lo} cells from a total of 5 normal mucosa and 10 tumor samples. This collection contained two paired NM and tumor samples from same patient (P1 and P2), allowing their paring for statistical analysis, whereas the rest of normal samples were from independent patients (**Table 1**).

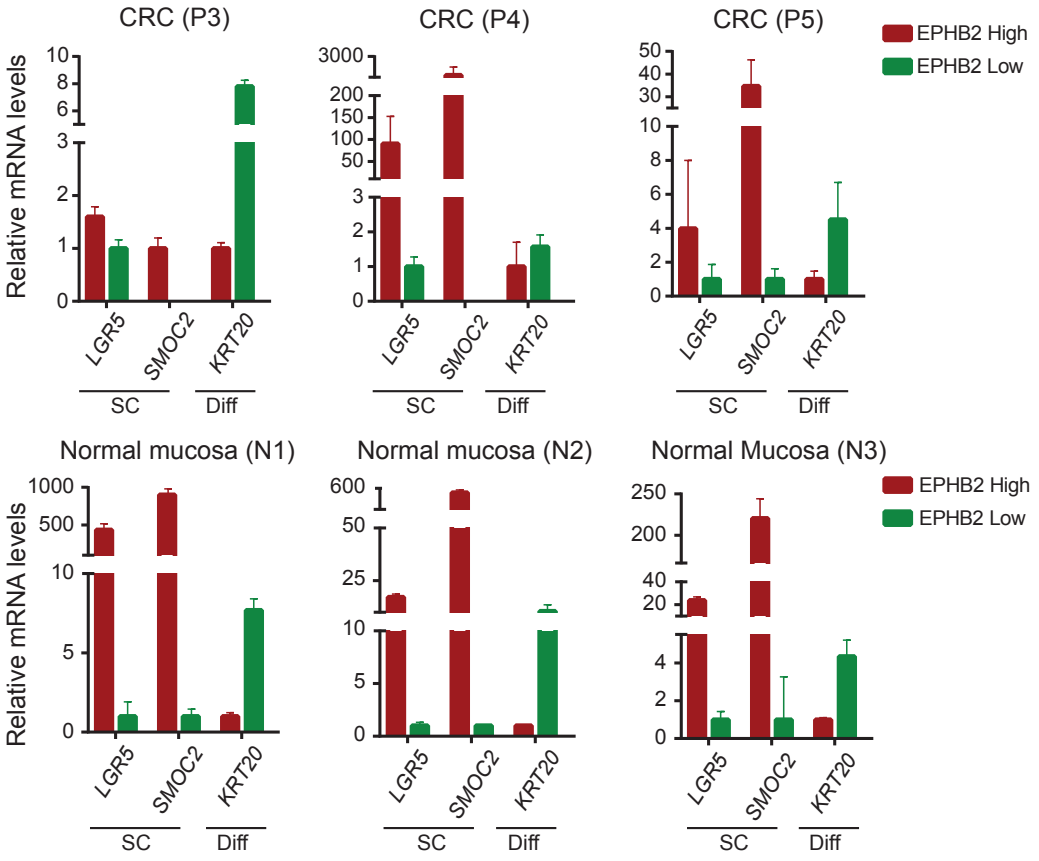

Figure 2: Expression analysis of stem cell and differentiation genes in EPHB2 isolated cell populations from primary samples. RT-qPCR analysis of stem cell and differentiation genes in EPHB2 populations (high and low) sorted from 3 different primary tumors (upper panel) and 3 normal colon mucosa (lower panel). Values show mean ± SD of three measurements.

Principal component analysis (PCA) of global gene expression clearly segregated the samples in 4 groups according to two principal components (**Figure 3**). The first component was related to the tissue of origin (tumor or NM) and explained 50% of the variability in gene expression. The second component was related to EPHB2 expression and explained 17% of the variation in gene expression. These results suggest the existence of two distinct cell populations both in tumor and normal intestine that can be isolated by the surface marker EPHB2. This observation also reinforces the notion that EPHB2 defines populations with similar characteristics both in normal and tumor tissues (**Figure 3**).

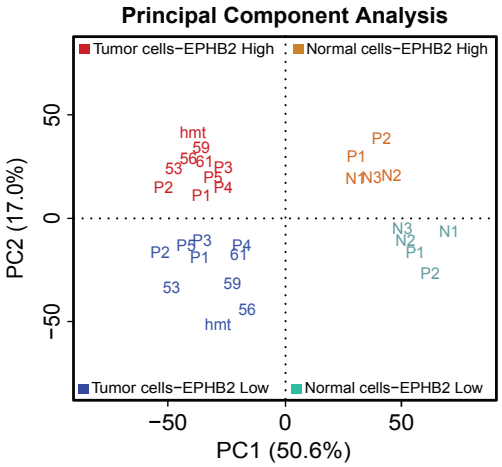

Figure 3: EPHB2 expression segregates two distinct cell populations in normal and tumor primary tissues. Principal component analysis (PCA) reflecting the distribution of EPHB2^{hi} and EPHB2^{lo} expressing cells purified from normal and tumor tissues.

In order to functionally characterize these 4 cell functionally we performed gene set enrichment analysis (GSEA). We analysed gene sets related to gene ontology (GO Slim) and signalling pathways (KEGG). Gene sets enriched in the EPHB2^{hi} normal (CoSCs) and tumor cell populations (CRC-SCs) compared to their EPHB2^{lo} counterparts revealed a group of biological functions commonly enriched in these two types of stem-like cells. The first top enriched category were gene ontologies associated to proliferation such as *mitosis*, *cell cycle,* or *chromosome segregation* (**Figure 4A**). These results were not surprising, considering that the intestinal epithelium is one of the tissues with the highest cell turnover, which includes very high rates of stem cell division. Interestingly, the second most enriched category were gene sets related to ribosome biology. Examples of these gene sets were *Ribosome*, *Structural constituent of ribosome,* or *Nucleolus* (**Figure 4A**).

Since these gene sets were associated to stem cell-enriched (EPHB2^{hi}) populations from both sample types, we next wanted to find biological functions that could be specific for tumor stem cells. Thus, we looked for gene sets that were upregulated in the EPHB2^{hi} tumor samples when compared to the EPHB2^{hi} from NM. We found that CRC-SCs were enriched in gene sets

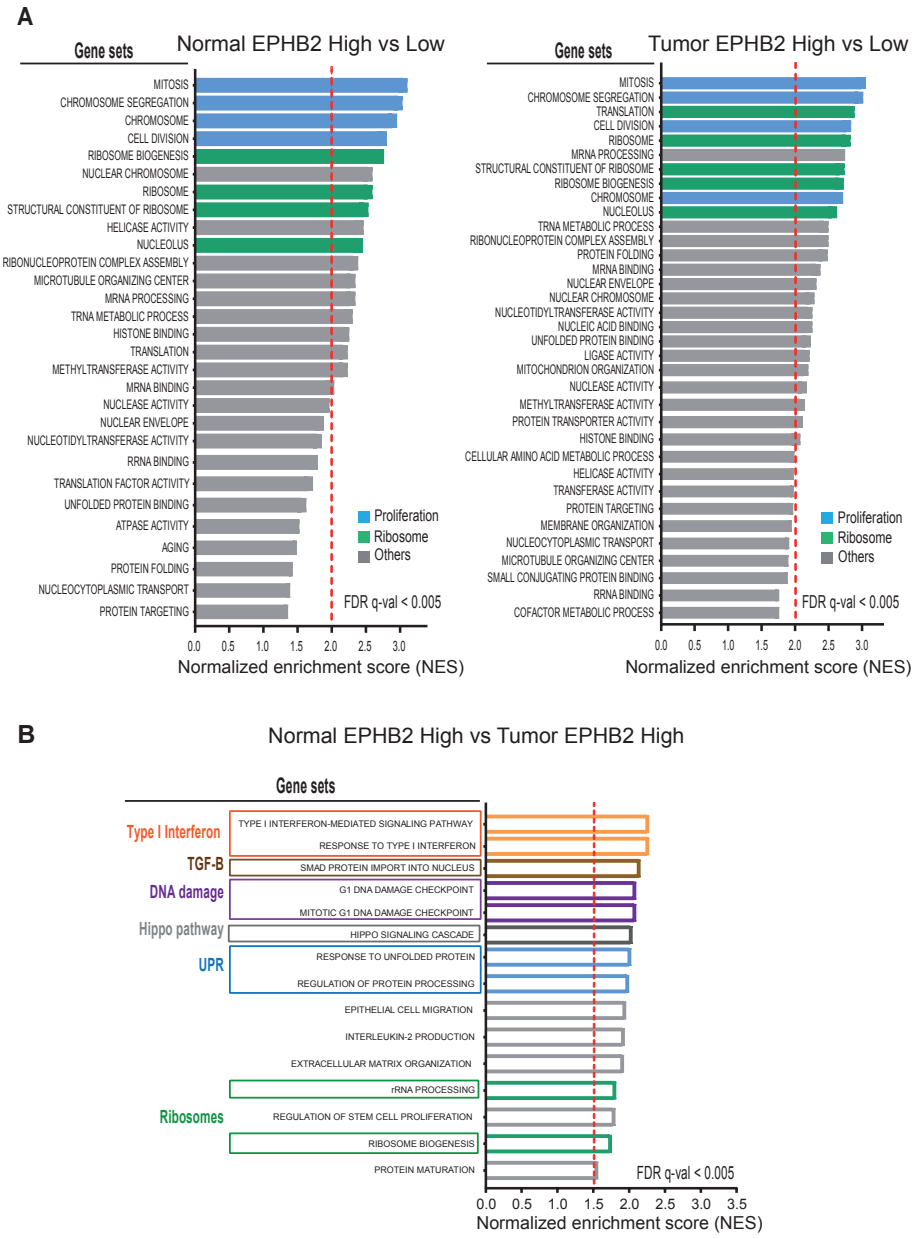

Figure 4: Gene set enrichment analysis comparing the EPHB2^{hi} and EPHB2^{lo} normal and tumor cell populations. (**A**) Summary of gene sets enriched in EPHB2^{hi} cells compared to EPHB2^{lo} cells in normal (left) and tumor (right) tissues. The red vertical dotted line denotes a Normalized enrichment score (NES) > 2. Gene sets represented show a FDR q-val <0.005. Note that proliferation (in blue) and ribosome biogenesis (in green) related gene sets are commonly enriched in EPHB2^{hi} cells both in normal and in tumor cells. (**B**) List of gene sets enriched in EPHB2^{hi} tumor cells when compared with EPHB2^{hi} normal cells. The red vertical dotted line denotes a Normalized enrichment score (NES) > 1.5. Gene sets represented show a FDR q-val <0.005.

comprising recognized tumor-specific features (**Figure 4B**). *Interferon type I signalling response* was one of the gene sets upregulated in tumor stem cells. This signalling pathway is usually engaged by various ligands during immune responses (Ivashkiv & Donlin, 2013). We also observed that gene sets related to TGF-β signalling were enriched in CRC-SCs that correlated with the well-known role of TGF-β signalling as a tumor promoter in CRCs (Calon et al., 2012). These analyses also revealed that DNA damage response through TP53 signalling was upregulated in CRC-SCs compared to normal stem cells. In addition, gene sets related to Hippo pathway or unfolded protein response (UPR) were also enriched in this population.

Finally, we also observed upregulation of ribosome biogenesis related genes in this population, suggesting that tumor cells might enhance ribosome production to sustent the high metabolic demands due to the elevated proliferation rates (Quin et al., 2014). (**Figure 4B**).

1.2.1 Genes encoding nucleolar functions and ribosome biogenesis are enriched in tumor stem cells.

Amongst the top categories enriched in normal and tumor stem cells we found gene ontologies related to ribosome biogenesis. In particular, *Ribosome Biogenesis* and *Nucleolus* were commonly enriched in the EPHB2^{hi} tumor and normal populations. The KEGG pathway database also showed *Ribosome Biogenesis* as one of the most enriched pathways in these populations (**Figure 5A**). Whereas ribosomal biogenesis and rDNA transcription are well-known general cellular functions (Comai, 2004; I Grummt, 2010; Lafontaine, 2015), their preferential association to stemness is poorly described. Therefore, we focused our attention to this phenomenon as a potential determinant of normal and cancer stem cells.

Ribosome biogenesis and nucleolus gene sets included genes related to rDNA transcription, processing and maturation as well as genes codifying for ribosomal proteins. As RNA Polymerase I is they key protein in rDNA transcription, we investigated the specific expression of genes coding for the main structural subunits of the enzyme, (POLR1A, POLR1B and POLR1C) (Fernández-Tornero et al., 2013). Expression of RNA Pol I subunits was enriched in the EPHB2^{hi} populations, both in tumors and normal samples. The same applied to essential genes involved in the processing of pre-rRNA, such as the rRNA methyl-transferase fibrillarin (*FBL*) or the RNA helicase *DDX21* (Calo et al., 2014; Marcel et al., 2013). (**Figure 5B**).

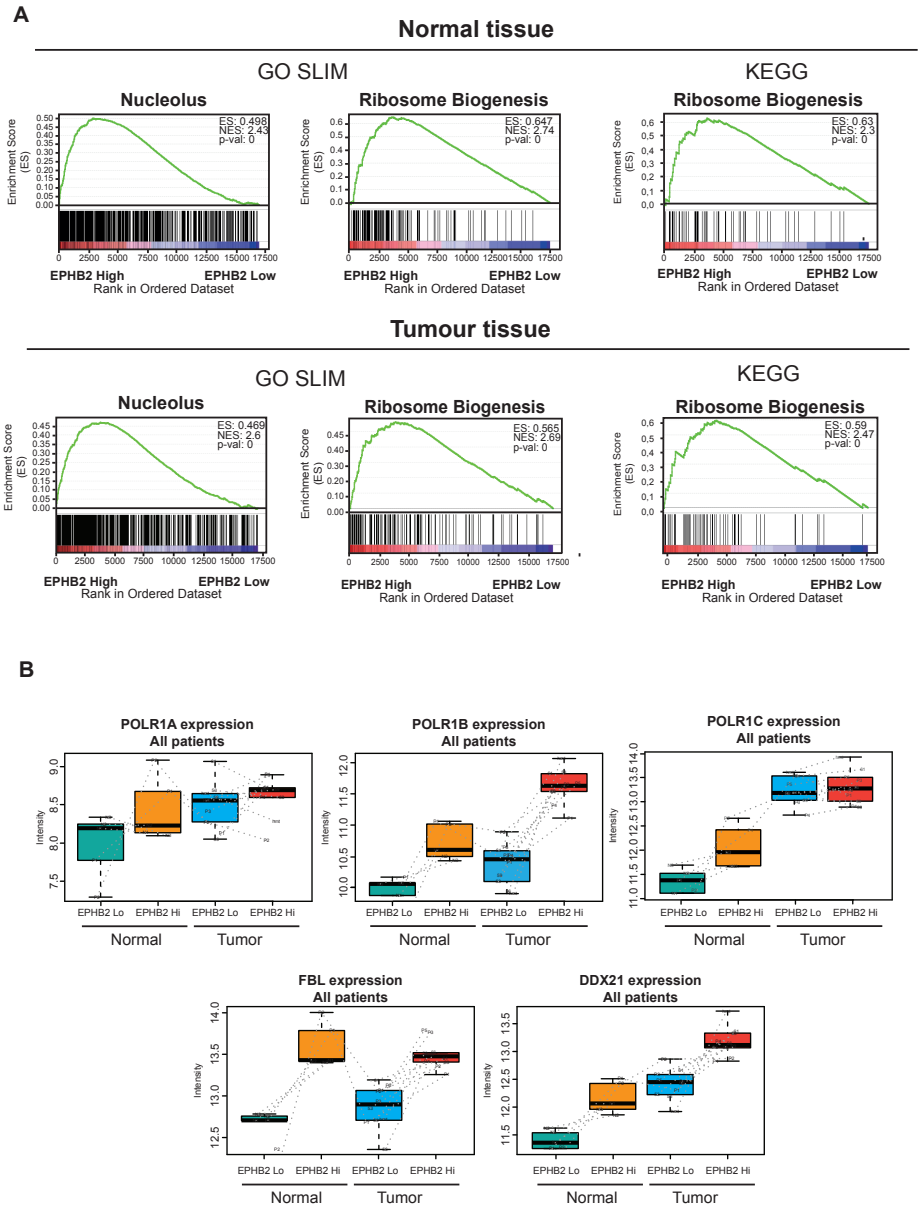

Figure 5: Gene sets related to nucleolus and ribosome biogenesis are enriched in normal and tumor stem cells. (**A**) Examples of the expression of gene sets related to nucleolus and ribosome biogenesis that are upregulated in normal and tumor stem cells (EPHB2^{hi}) when compared with differentiated counterparts (EPHB2^{lo}). KEGG analysis also reveals upregulation of signaling pathways associated with ribosome biogenesis in these populations. (**B**) Boxplots representing the mRNA expression of RNA Polymerase I main structural subunits (*POLR1A*, *POLR1B* and *POLR1C*) and rRNA processing genes in EPHB2^{hi} and EPHB2^{lo} of normal and tumor cell populations.

Interestingly, we also found that ribosome-related gene sets were enriched in tumor versus normal ISC-like cells as illustrated in Figure 5B except for *FBL* (cf. red vs. orange). We tentatively conclude that the rDNA synthesis and ribosome biogenesis, at least at the transcriptional level, define normal and cancer stem cells. This function appears to be amplified in tumor versus normal stem cells, possibly to sustain higher proliferative demand.

1.3 rDNA transcriptional activity is reduced in normal and tumor differentiated cells

To functionally validate the results obtained from the transcriptomic analysis we analysed rDNA transcriptional activity *in vivo* in tumor cells expressing different levels of EPHB2. As rRNA constitutes the vast majority of RNA synthesized in a cell (Comai, 2004; I Grummt, 2010), we took advantage of a chemical method to detect RNA synthesis in cells based on the biosynthetic incorporation of the uridine analogue 5-ethynyluridine (EU) into newly transcribed RNA (Jao & Salic, 2008). Cellular RNA is labelled by EU in very short periods and with high sensitivity by means of a copper (I)-catalysed azide-alkyne cycloaddition reaction - a type of “click” chemistry - with fluorescent azides. This chemical label can be followed by flow cytometry detection or microscopy.

This analysis was performed on tumors derived from a collection of patient derived organoids (PDOs). Organoids or 3D cell cultures derived from patients are powerful tools in cancer research. When injected in mice, these *in vitro* cultures reproduce colorectal tumor heterogeneity *in vivo* (Calon et al., 2015; Van De Wetering et al., 2015). For these studies we used the PDO lines 7, 18 and 19b, which mutational profiles are described in **Table 2**.

PDO	WNT pathway	KRAS pathway	PI3K pathway	TP53/ ATM	TGF-beta Pathway
7	APC STOP (R787*)/STOP (K1438*)	KRAS (G13/+)	WT	ATM (V182L / N1983S)	SMAD4 (L536R /L536R)
18	WT	WT	WT	ATM spliced	WT
19b	APC (W)T ARIDA (FS)	BRAF (V600E)	PIK3CA (H1047R) PIK3R1 (STOP)	ATM (N471T) TP53 (Q331splice/ R273C)	TGFBR2 (L323P)

Table 2: Status of CRC driver mutations in the patient derived organoids (PDOs) used in this study.

Mice bearing PDO 7, 18 and 19b xenografts were injected with EU 2 hours before sacrifice to allow its incorporation into tumor cells. After this period, tumors were disaggregated and stained for EPHB2 to separate cancer stem cells and differentiated tumor cells (**Figure 6A**). We then analysed the fraction of EU positive cells of each population using flow cytometry. The percentage of EU positive cells within the EPHB2^{hi} populations was 3 fold higher than in EPHB2^{med} cells and 5 fold higher than in in EPHB2^{lo} cells. Similar results were obtained for independent PDOs. (**Figure 6B**).

We also analysed the histological pattern of EU incorporation in paraffin sections from these same xenografts. We combined EU staining with immunofluorescence (IF) using EPHB2 and KRT20 antibodies to mark stem-like and differentiated cells. EU labelled mainly the nucleolus of tumor cells. Most EU positive cells were located in domains exhibiting high EPHB2 levels. In fact, we could hardly detect EU incorporation in differentiated tumor areas positive for KRT20 (**Figure 6C**).

These results demonstrated that rDNA transcription in tumor cells correlated with EPHB2 expression levels. Most rDNA transcription occurred in EPHB2^{hi} cells within tumors. EPHB2^{med} cells were labelled with EU albeit at lower levels, suggesting that EU incorporation was not completely restricted to CRC-SCs. In contrast, the differentiated population (EPHB2^{lo}) did not display detectable rDNA transcription. These findings, in combination with data obtained from transcriptomic analysis, led us to conclude that rDNA transcription is heterogeneously regulated among tumor cells and is strongly downregulated in the differentiated tumor cells.

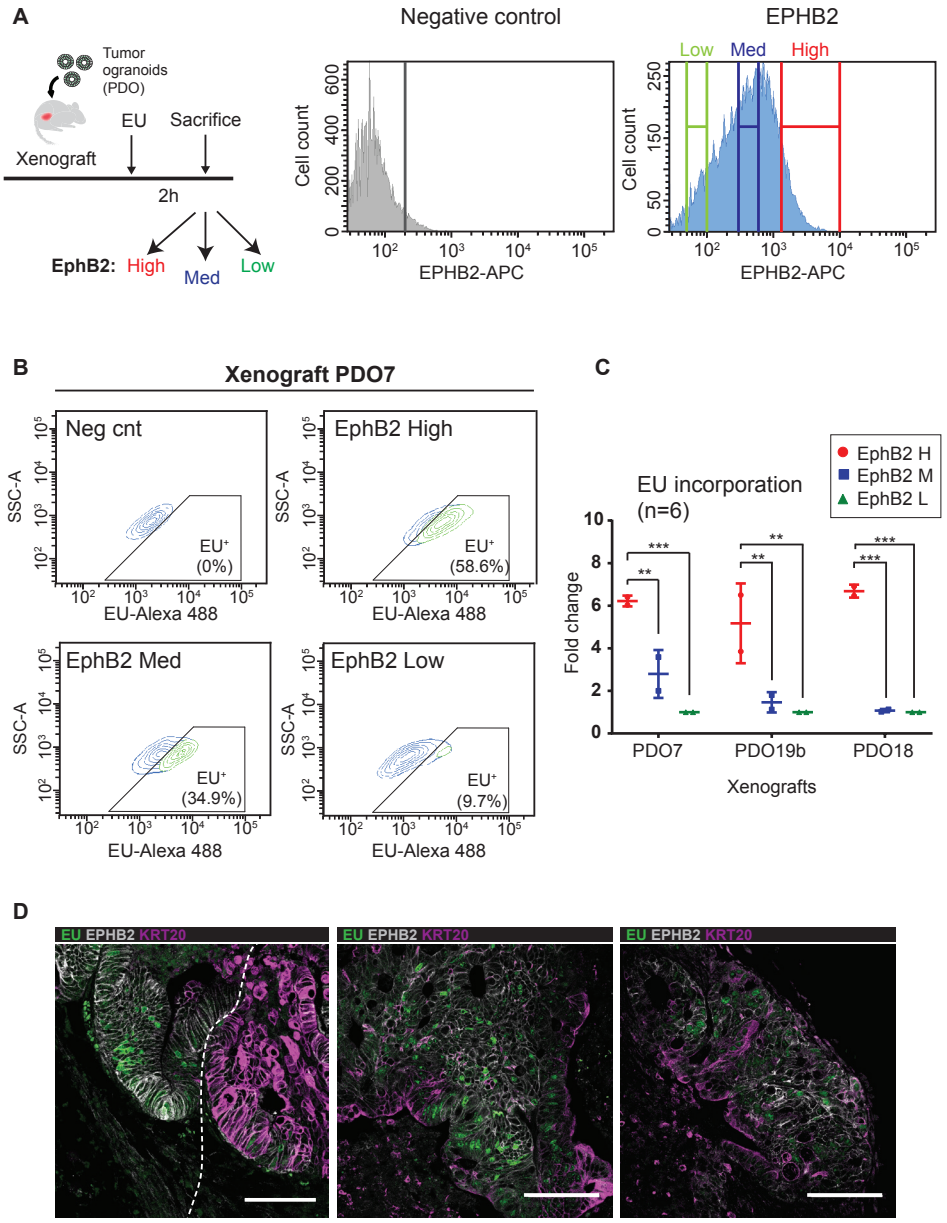

Figure 6: EU incorporation analysis in EPHB2 sorted cell populations from tumor xenografts. (**A**) Scheme depicting the experimental protocol followed (left) and representative EPHB2 staining FACS profile of PDO7 derived xenograft (right). (**B**) Representative FACS plots of EU incorporation in EPHB2 sorted tumor cells from PDO7 derived xenograft. (**C**) Quantification of EU positive cells among the different EPHB2 populations in 3 different patient derived xenografts (PDX). Each PDX represents two replicates. Data are represented as mean ± SD. ** p≤0.01, *** p≤0.001 in one way ANOVA. (**D**) Immunofluorescence of EU (green), EPHB2 (grey) and KRT20 (magenta) in histological sections of tumor xenografts. Most of the EU signal is confined in the EPHB2+ glands and absent in KRT20+ areas. Scale bar represents 100µm.

1.4 Analysis of the ribosomal content in CRC histological sections

To assess whether the reduced rDNA transcriptional activity found in differentiated tumor cells (EPHB2 low) was also reflected on their ribosomal content, we used an antibody (Y10B) that detects the 5.8S rRNA. This is a monoclonal anti-rRNA antibody obtained from a panel of anti-nucleic acid antibodies generated using a genetic mouse model of autoimmune disease (Lerner, Lerner, Janeway, & Steitz, 1981). Previous experiments demonstrated that Y10B antibody recognizes a cytoplasmic epitope in chick neurons (G. Garden, Canady, Lurie, Bothwell, & Rubel, 1994). Indeed, Y10B antibody specifically labels free ribosomes, polysomes, and endoplasmatic reticulum-associated ribosomes (G. A. Garden, Hartlage-Rübsamen, Rubel, & Bothwell, 1995). Thus, we use this marker as an indirect measurement of rDNA transcription rate.

5.8S rRNA immunofluorescence (IF) stained mainly the cytoplasm of tumor cells (**Figure 7)** in sections of human CRC samples. These stainings revealed that not all tumor cells expressed equivalent 5.8S rRNA levels: its expression was heterogeneous and followed a clustered-like pattern. In accordance with data obtained by EU labelling, combination of immunostaining of 5.8S with the differentiation marker KRT20 evidenced that KRT20 highly positive tumor areas showed reduced 5.8S rRNA signal compared to non-differentiated areas, and vice versa (**Figure 8A;** white and yellow arrowheads respectively, in upper panel). Yet, we observed a smaller proportion of cells that expressed both markers, suggesting the existence of apparently differentiated cells with

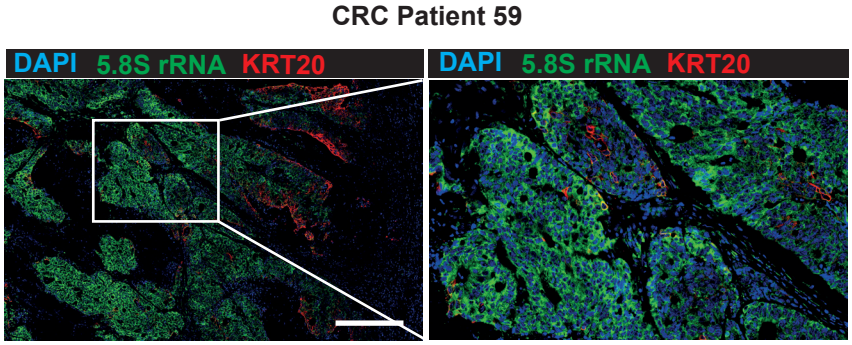

Figure 7: 5.8S rRNA antibody labels ribosomes in the cytoplasm of tumor cells. Immunostaining of 5.8S rRNA (green) and KRT20 (red) in primary CRC histological sections. Right, magnified inset. Expression of KRT20 and 5.8S rRNA follows in general a mutually exclusive pattern. However, few cells are found with both marks. Scale bar represents 100μm.

relatively high rDNA transcriptional activity (**Figure 8A**; stars in lower panel). Consistent with these findings, we observed that most of the EPHB2 high tumor areas showed high 5.8S rRNA staining (**Figure 8B**). Again, there was a minority of EPHB2 low regions that stained positive for the 5.8S rRNA. Occasionally, we also observed EPHB2 and KRT20 negative areas displaying some elevated 5.8S rRNA staining (yellow arrowheads in **Figure 8B**).

CRC primary tissue sections frequently contain adjacent normal colon mucosa. Analysis of the 5.8S signal in these areas revealed a general upregulation of the staining in tumor areas compared with the normal tissue, supporting the previous observations that ribosome biogenesis might be upregulated in tumor compared to normal cells (section 1.2) (**Figure 9A**).

Interestingly, 5.8S rRNA staining pattern in the NM followed a decreasing gradient of expression from the crypt base to the upper part of the villus (**Figure 9B**). We observed that crypt base cells were highly positive both for EPHB2 and 5.8S staining. However, the EPHB2 gradient was sharper than the 5.8S gradient, which also labelled part of the transit-amplifying compartment above the stem cell niche. As in CRC, the ribosomal signal was not undetectable in the differentiated area on top of the crypts, positive for KRT20 (**Figure 9B**).

To further support this observations, we isolated by FACS colon crypt cells according to surface expression of EPHB2 as described in Merlos-Suárez et al. (Merlos-Suárez et al., 2011) and subsequently assessed protein levels of RNA Pol I (POLR1A) by Western blot on cell lysates. This experiment showed that POLR1A gradually decreased in human colon crypt cell populations as cells migrate from the crypt base towards the top (i.e. EPHB2-high to negative). Terminally differentiated (EPHB2-low) cells expressed low POLR1A levels, which may account for the absence of ribosomal content in this cell population (**Figure 9B**). Thus, in accordance with transcriptomic analysis and EU incorporation studies (sections 1.2 and 1.3), ribosomal load negatively correlates with the differentiation state of normal and tumor cells. It appears that differentiated cells shut down nucleolar and ribosomal activity.

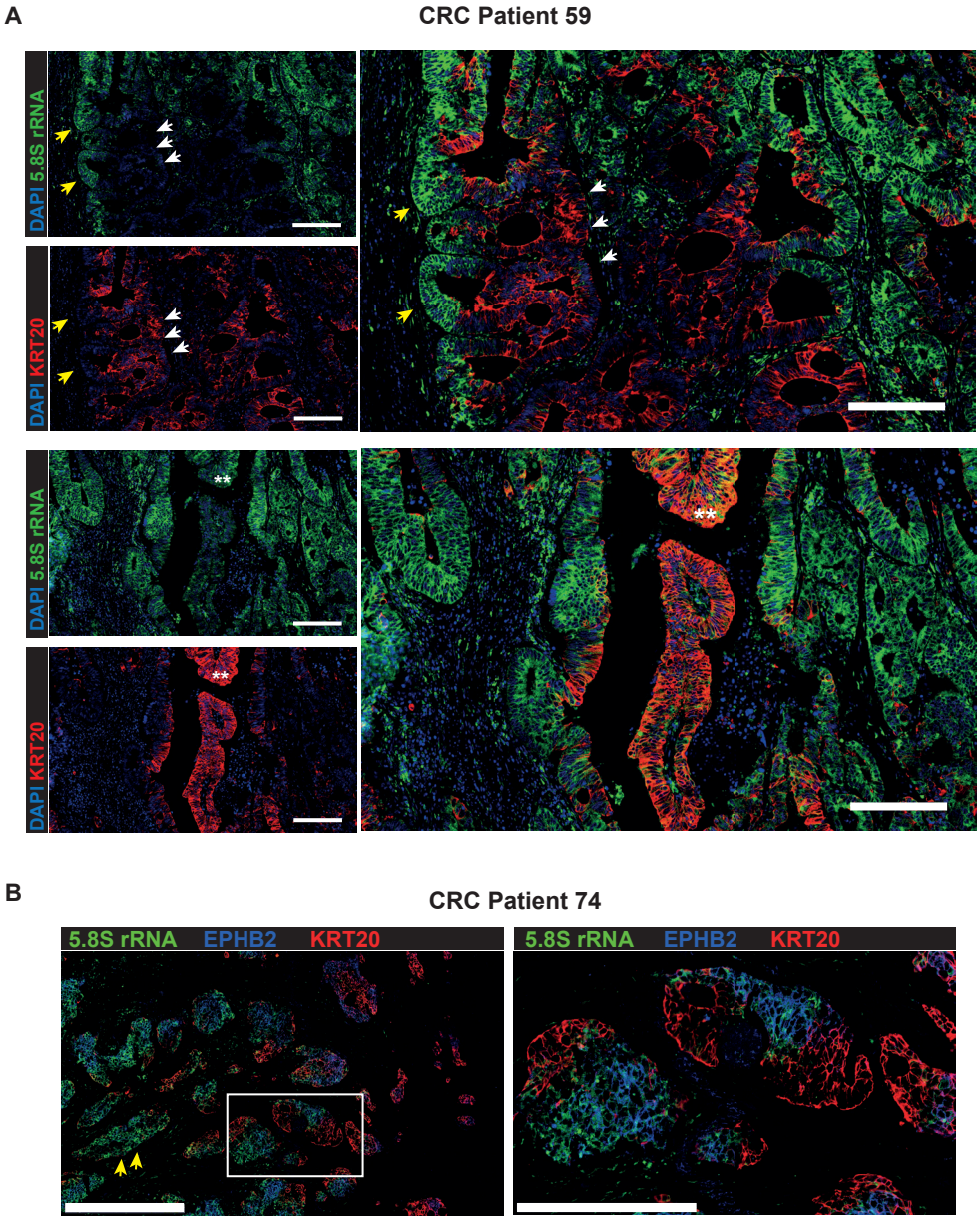

Figure 8: Analysis of ribosomal content and KRT20 expression in histological sections of primary CRC tumors. (**A**) Immunostaining of 5.8S rRNA (green) and KRT20 (red) of primary CRC histological sections. Yellow arrowheads indicate glands positive for 5.8S rRNA staining and white arrowheads indicate differentiated areas positive for KRT20 staining. Stars represent tumor cells positive for both marks. Scale bar represents 100µm. (**B**) Immunostaining of 5.8S rRNA (green), EPHB2 (blue) and KRT20 (red) in primary CRC histological sections. Yellow arrows point to areas that are rich in ribosomal activity, yet are devoid of EPHB2 and KRT20 positivity. Right panel: inset magnification. Scale bar represents 500µm and 250µm, respectively.

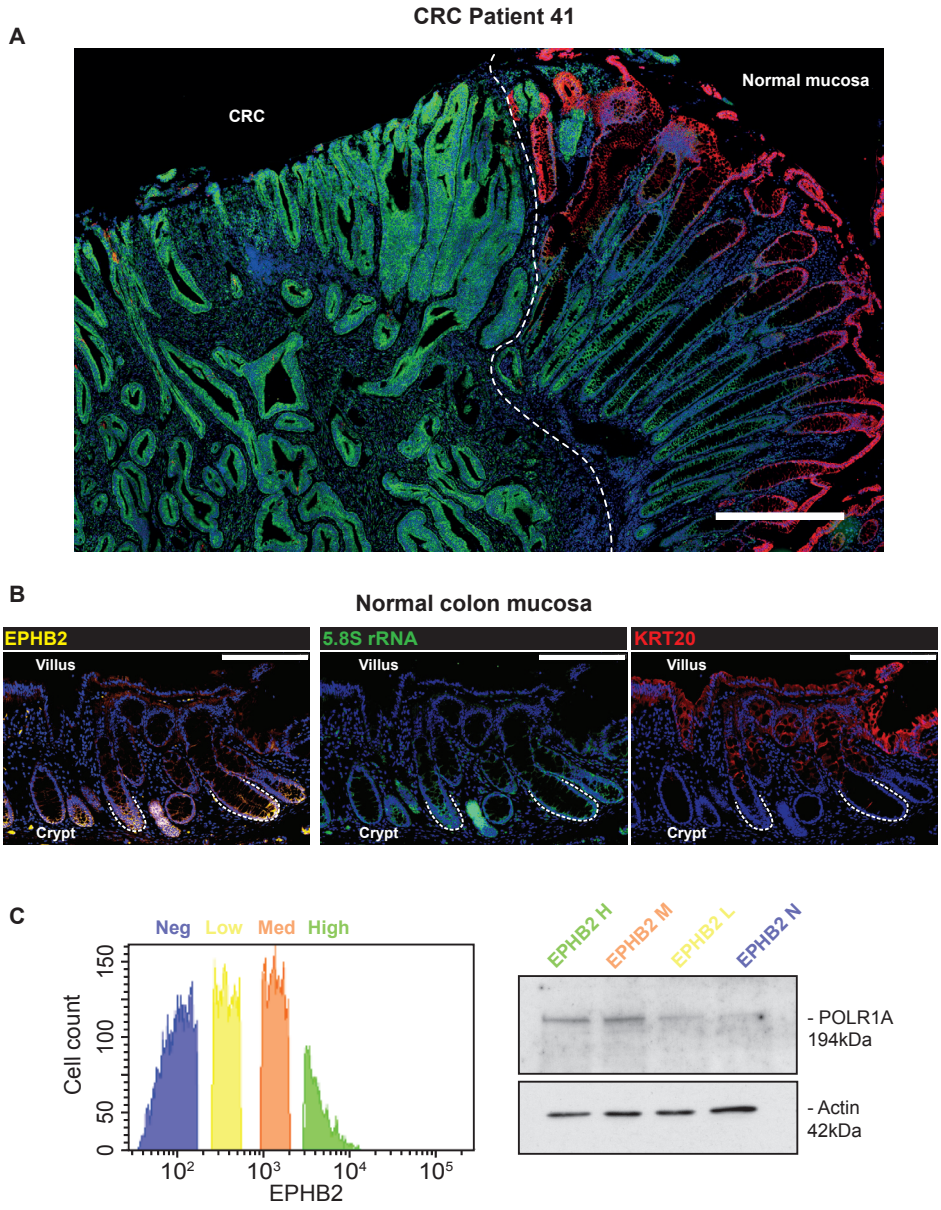

Figure 9: Analysis of ribosomal content and POLR1A expression in normal colon mucosa. (**A**) IF 5.8S rRNA (green) and KRT20 (red) staining on a histological section of a primary CRC that contains normal mucosa and tumor tissue (CRC). Note that tumor cells express higher levels of 5.8S rRNA staining compared to normal cells. Scale bar located at the upper right corner of the figure represents 100µm. (**B**) Immunostaining of 5.8S rRNA (green), EPHB2 (yellow) and KRT20 (red) in normal colon mucosa. Scale bar represents 250µm. (**C**) Representative FACS profile of single-cell suspensions from normal human colonic crypts stained with EPHB2 antibody (left) and POLR1A protein analysis by Western blot in sorted EPHB2 populations from normal human colonic crypts (right).

2. *In vivo* characterization of CRC cells based on their rDNA transcriptional activity

We next wanted to further characterize tumor cells displaying distinct rDNA transcriptional activity *in vivo*. As RNA Polymerase I is the main driver of rDNA transcription, we set out a strategy to use this enzyme as a surrogate of the rRNA synthesis rate in a cell. RNA Polymerase I is a large holocomplex localized in the nucleolus, a substructure in the nucleus. The intracellular localization of this complex impairs the use of antibodies for cell sorting experiments. To overcome this limitation, we exploited the CRSPR-Cas9 genome editing technique that has recently been set up in our laboratory (Cortina et al., 2017) to label endogenous RNA Polymerase I in PDOs.

2.1 Endogenous labelling of RNA Pol I in CRC organoids by CRISPR-Cas9 technology

PDO7 and PDO18 were selected to target RNA Pol I. PDO7 was derived from a stage IV CRC patient and carries genetic alterations in the major signalling pathways altered in CRC such as WNT, EGFR and TGFβ. PDO18 is a non-hypermutated organoid that among the common driver genes only carries alterations in the ATM protein (see details in **Table 2**).

The targeting strategy that we followed to label RNA Pol I at the endogenous genomic locus was to generate a N-terminal fusion protein between POLR1A (the main RNA Pol I subunit) and the EGFP fluorescent protein. To this end, we designed Cas9 guide RNAs complementary to sequences overlapping the ATG start codon of the POLR1A locus and generated a donor vector that contained POLR1A transcription start site homology arms flanking an ATG-EGFP reporter cassette so that EGFP is inserted in frame (**Figure 10**).

We nucleofected organoid cells with an RFP+ donor vector together with a guide-RNA-Cas9-iRFP encoding plasmid and after 48 hours we sorted cells that had incorporated both plasmids (RFP+ and iRFP+ cells). After 20 days in culture, we re-analysed these cells and we observed that 6.5% in PDO18 and 15% in PDO7 expressed EGFP (**Figure 11**). Next, we generated single cell-derived organoids from EGFP+ cells and assessed correct EGFP integration by PCR and southern-blot (example in **Figure 12**). The efficiency of integration differed depending on the PDO. For PDO7, 18,5% of the analysed clones had correctly integrated the EGFP. From those, 80% had no additional off-target incorporations. However, in PDO18 the integration efficiency rose up to 63%, of which 66,6% corresponded to a single integration (**Table 3**).

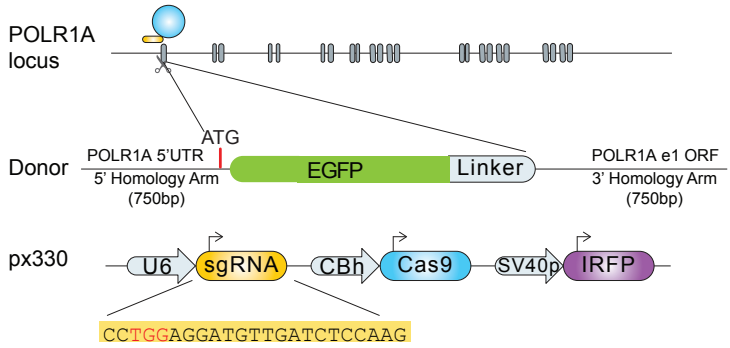

Figure 10: Labeling of endogenous POLR1A in colorectal cancer organoids using CRISPR-Cas9 technology. Targeting strategy for the generation of EGFP-POLR1A organoids. The blue circle above the POLR1A locus represents the CRISPR/Cas9 protein complex and the yellow box underneath the guide RNA. Detailed design of POLR1A-EGFP donor and CRISPR/Cas9 sgRNA vectors.

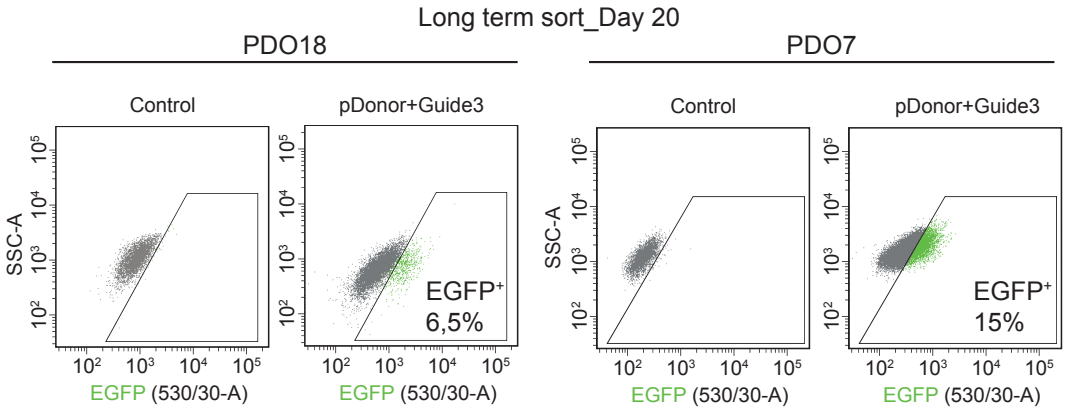

Figure 11: Long term selection of tumor cells with integrated EGFP reporter cassette. FACS plots analysis of EGFP expression in PDOs 20 days after nucleofection with pDONOR and px330 guide plasmids. Two different PDOs (PDO18 and PDO7) were nucleofected. The percentage of EGFP positive cells in each PDO at long term selection is indicated.

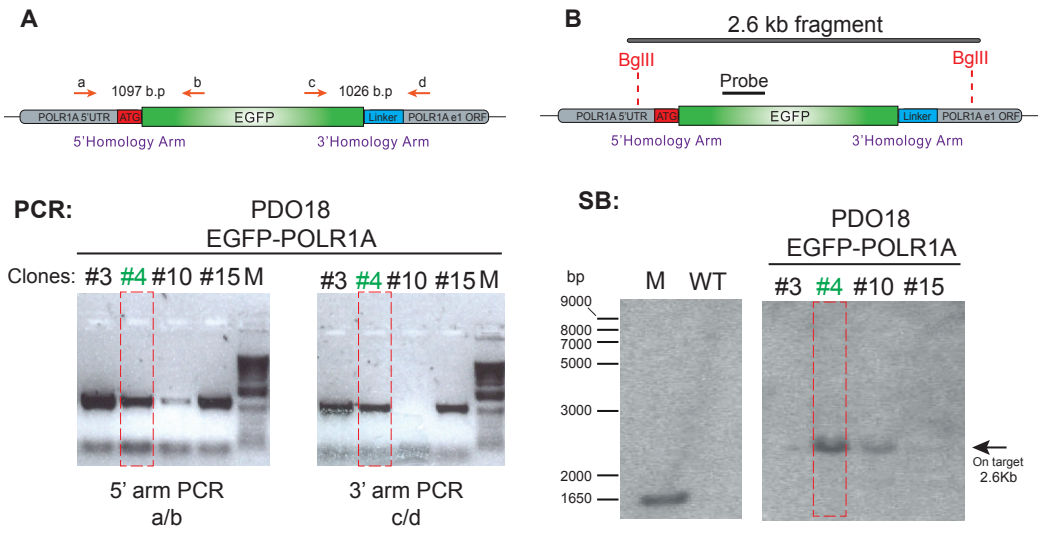

Figure 12: Validation of EGFP integration in knock-in derived clones. (**A**) Scheme depicting primer location (in orange) for detection of specific integration by PCR. Integration PCR products from PDO18 derived clones using the primers shown in the scheme is shown below. Primer pair a/b detected knock-in of the 5' arm and the primer pair c/d detected knock-in of the 3' arm. (**B**) Scheme depicting southern blot detection of on target integrations at the EGFP-POLR1A locus. Southern blot results in PDO18 derived clones using probes spanning part of the EGFP sequence are shown below. Numbers in green represent positive clones.

Table 3: CRISPR/Cas9 Knock-in efficiency

Knock-in locus	Tumoroid	% Positive long-term sort (3)	Single cells on-target clones (4)	Clones without off-target integration (5)
EGFP-POLR1A	PDO7	15%	18,5 % (5/27)	80% (4/5)
	PDO18	6,5%	63% (9/11)	66,6% (6/9)

Table 3: CRISPR/Cas9 knock-in efficiencies. The percentage of cells positive for the EGFP reporter 20 days after nucleofection is indicated in Column 3. Column 4 indicates the proportion of single cell derived clones from the sorted pool at day 20 that scored positive by integration PCR. Column 5 shows the percentage of integrated clones without off-targets integrations assessed by southern blot.

Several correctly integrated clones were analysed by confocal microscopy, which revealed a punctate EGFP signal consistent with a nucleolar localization that overlapped with POLR1A immunostaining (**Figure 13A** and **13B**).

Next, we asked whether levels of the labelled protein correlated with POLR1A mRNA expression.

To this end, we isolated cells expressing EGFP^{hi} and EGFP^{lo} from *in vitro* grown targeted PDOs by FACS. EGFP high cells expressed higher levels of both EGFP and POLR1A mRNA (**Figure 14**). These results demonstrated that we had successfully targeted endogenous RNA Pol I by CRISPR-Cas9 technology in CRC PDOs.

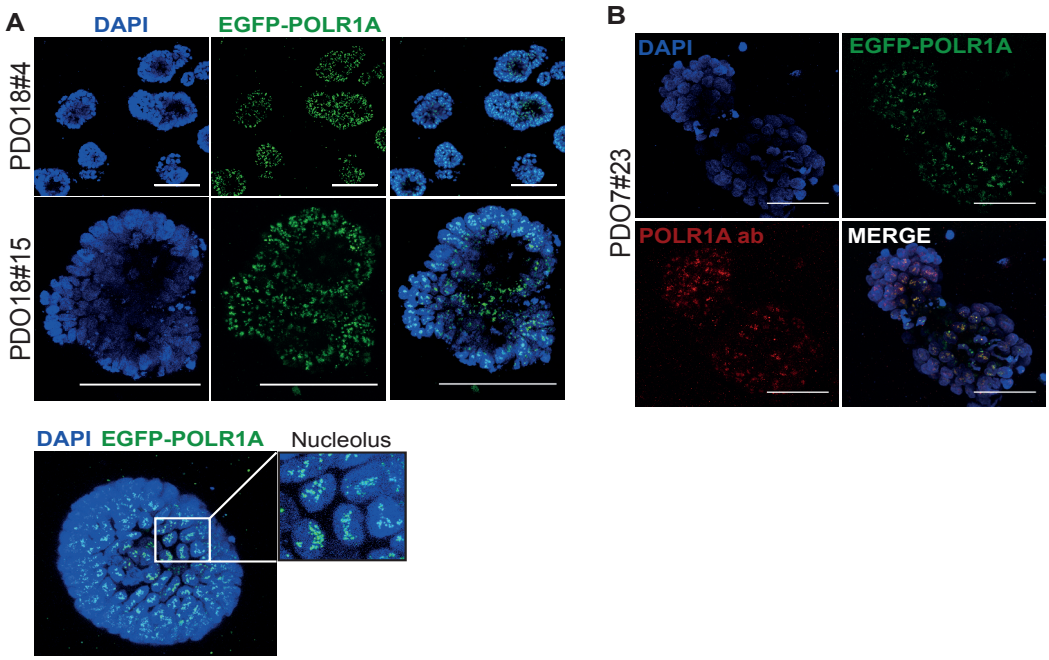

Figure 13: Analysis of endogenous EGFP-POLR1A expression in knock-in PDO derived clones. (**A**) Confocal images of EGFP-POLR1A endogenous expression of knock-in PDO18 derived clones #4 and #15. Inset shows EGFP expression in the nucleolus of tumor cells. Scale bar represents 100µm. (**B**) IF analysis of POLR1A antibody (red) in EGFP-POLR1A (green) knock-in PDO7 clone #23. Note that the EGFP signal colocalizes with POLR1A endogenous pattern. Scale bar represents 50µm.

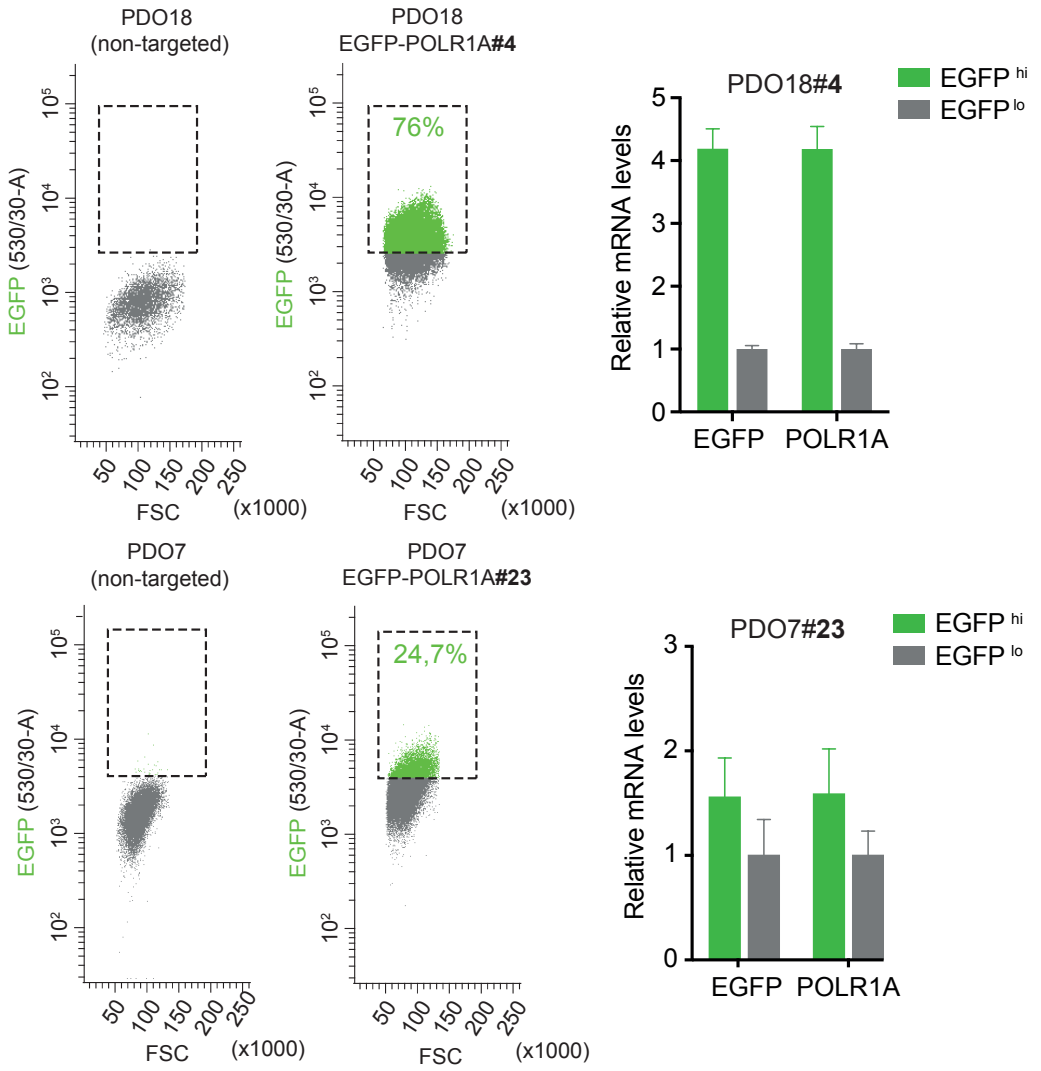

Figure 14: *In vitro* EGFP-POLR1A expression analysis of knock-in PDOs. FACS analysis of EGFP expression of EGFP-POLR1A labeled PDOs (left) and RT-qPCR of *EGFP* and *POLR1A* mRNA levels in EGFP high and low sorted cells from EGFP-POLR1A targeted PDOs (right). Values show mean ± SD of three measurements. Note that EGFP protein levels report POLR1A mRNA.

2.2 *In vivo* characterization of RNA Pol I CRC cells

To study RNA POL I tumor cells *in vivo* we generated tumor xenografts by injecting EGFP-POLR1A knock-in PDOs into NOD/SCID mice. Two clones derived from two different PDOs lines, PDO7 clone 23 (PDO7#23) and PDO18 clone 4 (PDO18#4) were used in this analysis.

2.2.1 RNA Pol I is heterogeneously expressed in CRC derived xenografts

Histological analysis of xenografts derived from EGFP-POLR1A targeted PDOs revealed a heterogeneous EGFP expression pattern in the nucleolus of tumor glands (**Figure 15A** and **15B**). We observed marked variations in EGFP-POLR1A expression among tumor cells. Combination of EGFP staining with markers of differentiation

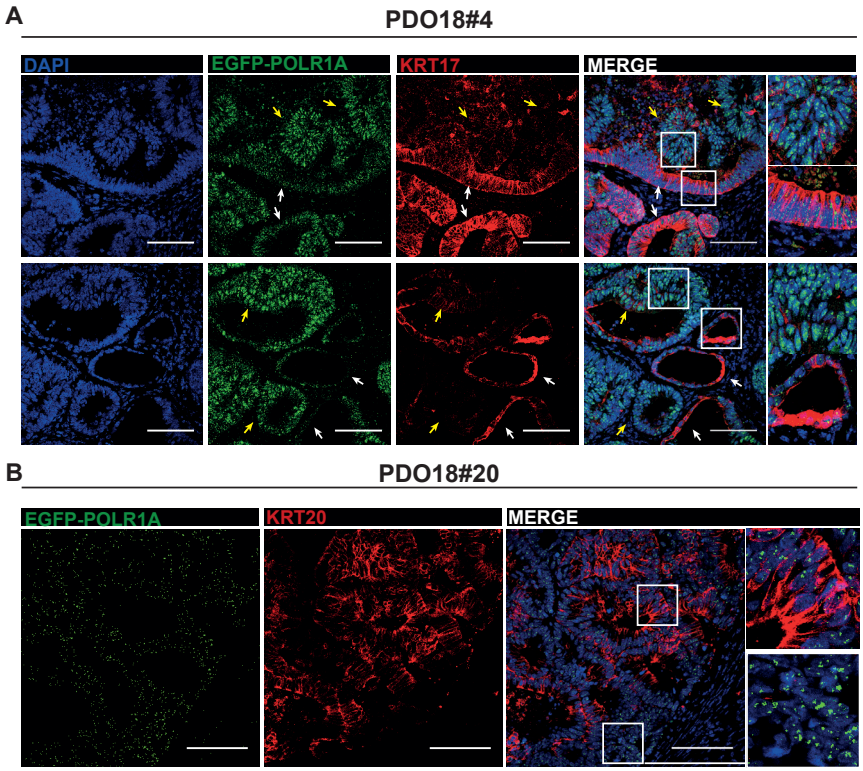

Figure 15: *In vivo* EGFP-POLR1A expression analysis of tumor xenografts derived from knock-in PDOs. (**A**) Immunostaining of EGFP (green) and KRT17 (red) in histological sections of xenografts derived from subcutaneously injected EGFP-POLR1A PDO18 clone #4. Scale bar represents 100µm. (**B**) Immunostaining of EGFP (green) and KRT20 (red) in histological sections of xenografts derived from subcutaneously injected labeled EGFP-POLR1A PDO18 clone #20. Scale bar represents 100µm.

such as KRT17 or KRT20 revealed that cells expressing high levels of these differentiation markers showed EGFP-POLR1A labelling of reduced size and intensity (white arrowheads) compared to cells expressing low or negative levels of these markers (yellow arrowheads) (**Figure 15A** and **15B**). EGFP-POLR1A differential expression pattern in knock-in xenografts was reminiscent of that found for POLR1A in primary CRCs (examples in **Figure 16**). These results suggested that –as the endogenous protein – EGFP-POLR1A reporter correlates with the differentiation state of the cells.

2.2.2 Gene expression analysis and functional characterization of RNA Pol I tumor cell populations *in vivo*

We next assessed whether EGFP-POLR1A levels correlated with transcriptional rRNA activity. In order to demonstrate that EGFP-POLR1A^{hi} tumor cells represented a population with high rDNA transcriptional activity, we measured EU incorporation rates. As detailed in the matherials and methods section, animals bearing xenografts derived from POLR1A labelled PDOs were injected with EU (**Figure 17A**). Two hours after EU incorporation we disaggregated the xenografts and stained these cells with the epithelial marker EpCAM to select for the epithelial tumor cell population. We subsequently analysed EGFP expression in the EPCAM+ fraction and isolated POLR1A-EGFP^{hi} and POLR1A-EGFP^{lo} tumor cells (**Figure 17B**). By FACS, we interrogated the EU signal emanating from each population. EGFP^{hi} tumor cells had actively incorporated the EU molecule whereas the EGFP^{lo} cells did not (**Figure 17C**). These results demonstrate that rDNA transcriptional activity directly correlated with expression levels of RNA Pol I in tumor cells *in vivo*.

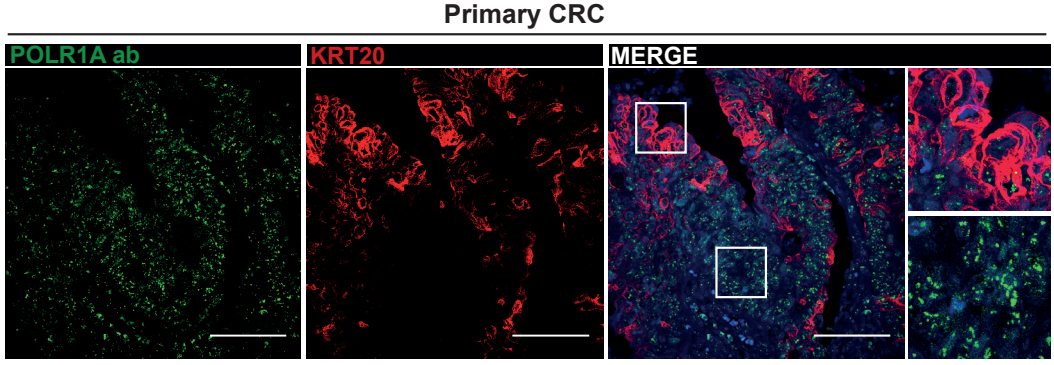

Figure 16: Endogenous POLR1A expression in primary CRCs is reminiscent of the EGFP-POLR1A pattern of tumor xenografts derived from knock-in PDOs. Immunostaining of endogenous POLR1A (green) and KRT20 (red) in primary histological sections of CRCs. Scale bar represents 100µm.

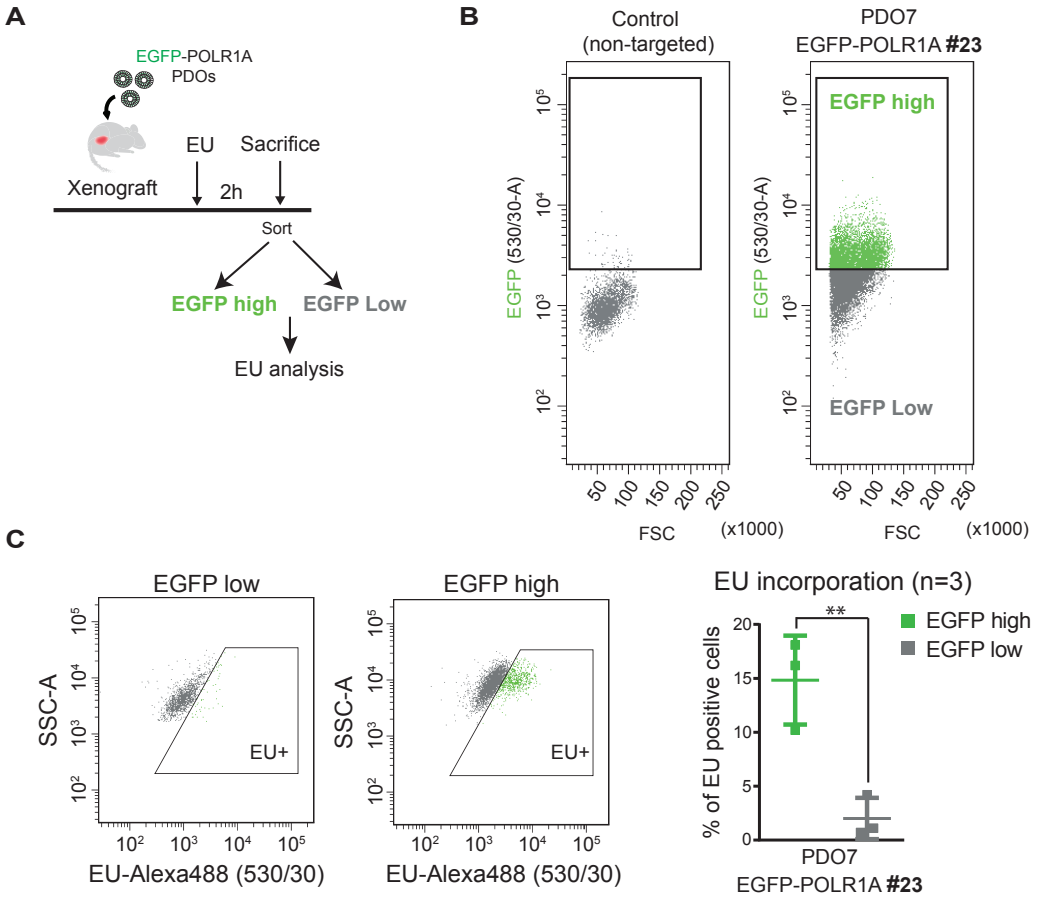

Figure 17: POLR1A high expressing tumor cells display rDNA transcriptional activity. (**A**) Experimental design of *in vivo* EU incorporation analysis. (**B**) FACS analysis of EGFP-POLR1A expression of tumor xenografts derived from injected PDO7 clone #23. (**C**) FACS analysis of EU signal in purified EGFP high and EGFP low cells from labelled EGFP-POLR1A tumor xenografts in A (left). Quantification of EU positive cells in EGFP high and EGFP low populations analyzed from 3 replicates of PDO7 clone 23 derived xenografts (right). Data are represented as mean ± SD. ** p≤0.01. Unpaired t-test was used for statistical analysis.

To further functionally characterize tumor cells on the basis of their rDNA transcriptional activity, we analysed marker gene expression of tumor cells expressing different levels of RNA Pol I *in vivo*. EGFP-POLR1A^{hi} cells represented between 11-30% (depending on the PDO) of the epithelial population in dissociated xenografts (**Figure 18A**). We confirmed that EGFP^{hi} cells expressed over 3 fold higher level of EGFP and POLR1A than EGFP^{lo} cells by RT-qPCR validation analysis (**Figure 18B**).

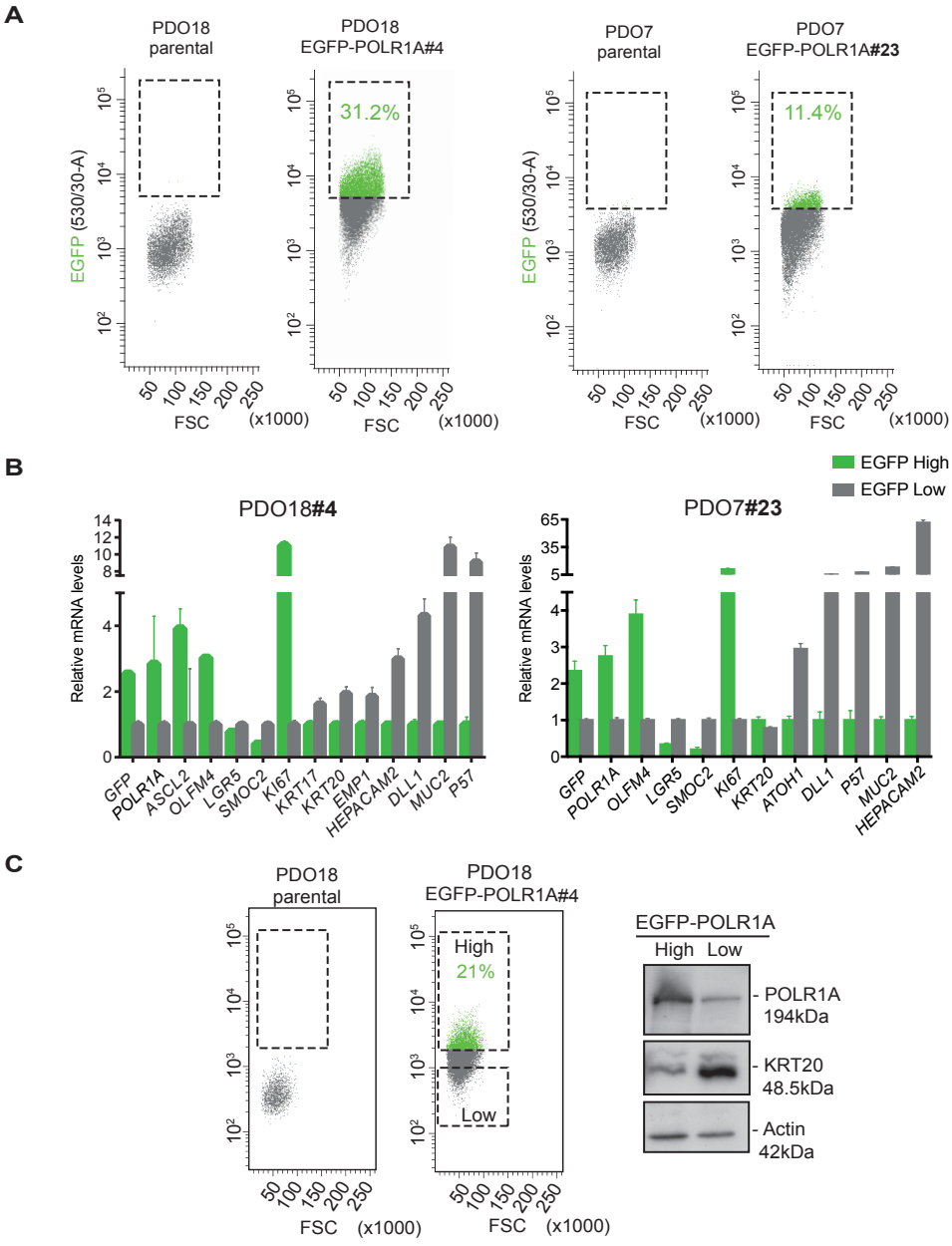

Figure 18: Gene expression analysis of POLR1A tumor cell populations. (**A**) FACS analysis of EGFP-POLR1A cells from disaggregated tumor xenografts derived from PDO18 clone #4 and PDO7 clone #23. The gate represents the EGFP high population. (**B**) RT-qPCR analysis of selected genes in EGFP high and EGFP low populations sorted from EGFP-POLR1A tumor xenografts in A. Values show mean ± SD of three measurements. (**C**) Analysis of POLR1A and KRT20 protein expression in EGFP-POLR1A high and low purified cell populations from tumor xenografts derived from PDO18 clone #4.

We then interrogated the expression of stem cell and differentiation programmes in these two cell populations. Unexpectedly, we observed that *LGR5* and *SMOC2* stem cell markers where not enriched in EGFP^{hi} cells suggesting that the stem cell programme was similarly expressed in both POLR1A-hi and -low populations. In contrast, the expression of genes related to the differentiation secretory lineage such as *MUC2*, *ATOH1* and *DLL1* where highly enriched in the EGFP^{lo} population, indicating that EGFP^{lo} cells represented a mix of populations or a population of mixed phenotypes. We also observed that the differentiation marker KRT20 didn't enrich in the EGFP^{lo} population at mRNA level. We then explored its expression at protein level. To do so, we isolated EGFP^{hi} and EGFP^{lo} tumor cells from xenografts and we observed that there was an upregulation of KRT20 at protein level in the POLR1A-EGFP^{lo} tumor cell population by Western-blot (**Figure 18C**). These results reinforce the notion that POLR1A-low cells represent a differentiated population in CRCs.

Since it is well-known that rDNA transcriptional activity is coupled with the proliferation state of cells we also assessed the expression of the proliferation marker *KI67*. EGFP^{hi} cells where enriched up to 10 fold in *KI67* mRNA levels compared to the EGFP^{lo} cells, which conversely expressed high levels of the cell cycle inhibitor *P57* (**Figure 18B**). Of note, *KI67* itself is a nucleolar protein and might be co-regulated together with other nucleolar proteins.

Our analyses show that the differentiation gene *MUC2* was clearly enriched in tumor cells expressing low levels of POLR1A. To validate this result, we analysed by IF POLR1A levels in MUC2 positive cells from primary tumor sections. Indeed, POLR1A was barely detectable in tumor cells expressing high levels of MUC2 (differentiated-like) compared with tumor cells positive for EPHB2 (stem-like) (**Figure 19**). These results reinforce the notion that the differentiation phenotype correlated with low levels of POLR1A expression.

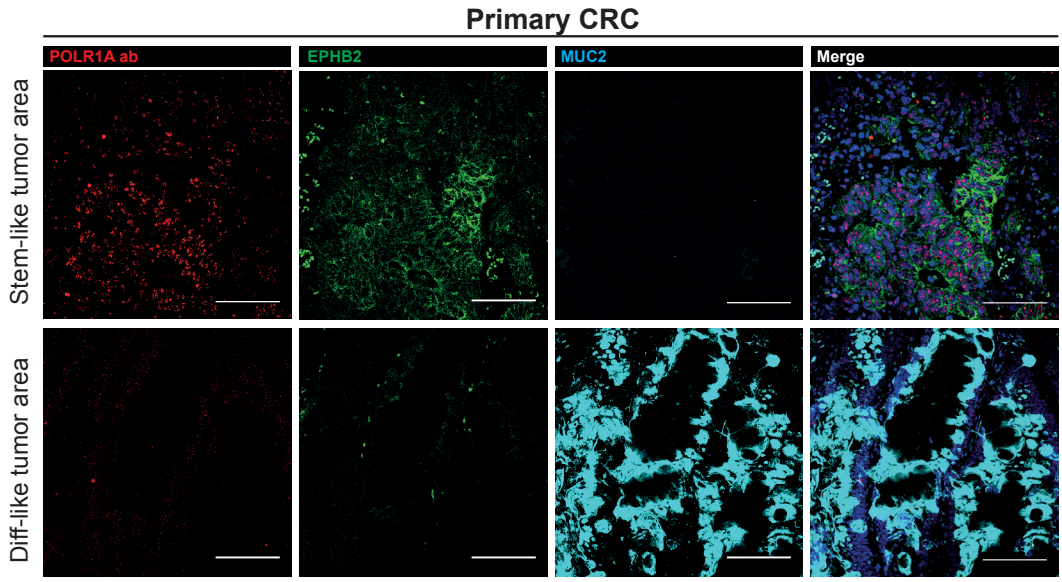

Figure 19: Endogenous POLR1A levels are reduced in tumor differentiated cells. (**A**) Immunostaining of endogenous POLR1A (red), EPHB2 (green) and MUC2 (cyan) in primary CRC histological sections. Stem-like and differentiated -like (diff-like) areas from the same tumor section are represented. Scale bar represents 100µm.

Finally, we assessed the clonogenic and tumorogenic potential of POLR1A CRC cells. EGFP-POLR1A^{hi} cells purified from xenografts displayed higher efficiency in forming organoids than the EGFP-POLR1A^{lo} CRC cells (**Figure 20A**). Both number and size of organoids were smaller in the latter population. Interestingly, the few organoids that grew from the EGFP^{lo} cells recovered POLR1A-GFP expression to similar levels as those derived from EGFP^{hi} cells (**Figure 20A**). This could be explained by either a possible contamination of a small fraction of EGFP^{hi} cells in the EGFP^{lo} population or by tumor cell plasticity.

To assess the tumorigenic capacity of these cells we inoculated 200 or 5000 epithelial tumor cells isolated from xenografts from each EGFP population into immunodeficient hosts. EGFP-POLR1A^{hi} cells were much more efficient generating tumor xenografts than the EGFP-POLR1A^{lo} population in tumors derived from both knock-in PDO7#23 and PDO18#4 (**Figure 20B**). Thus, the tumorigenic potential of tumor cells segregated with their rDNA transcriptional activity. This fits well with a model in which high rDNA transcription is a requirement for cancer stem cells as assessed by xenograft transplantation assays.

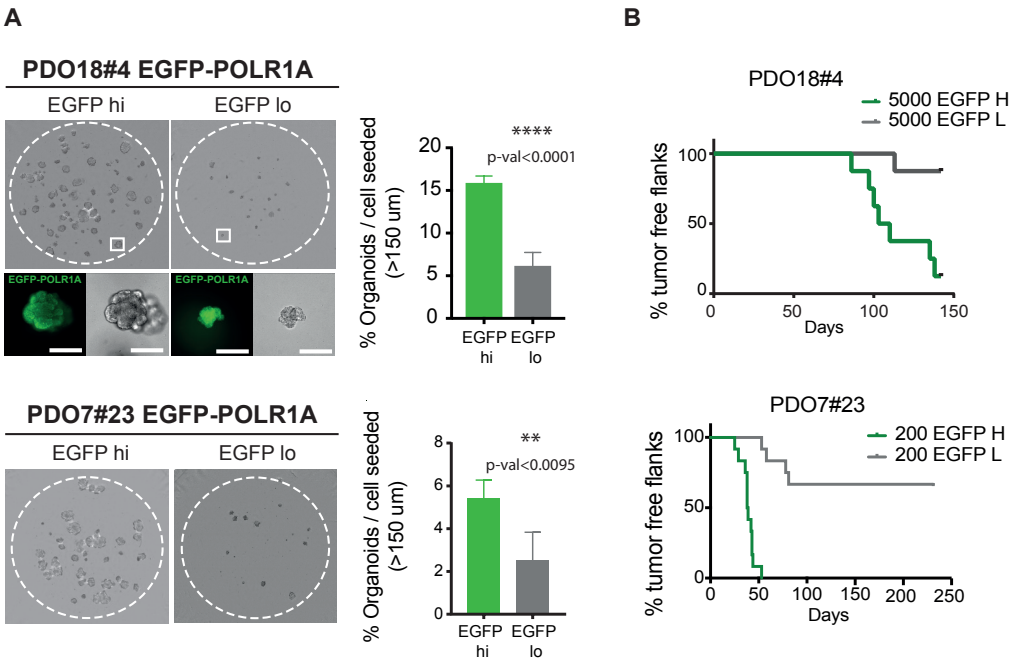

Figure 20: POLR1A high expressing cells display *in vitro* organoid formation capacity and tumor initiation potential. (**A**) Representative images of *in vitro* organoid formation of purified EGFP-POLR1A populations (high and low) from tumor xenografts of two different modified PDOs. The insets represent confocal analysis of a single derived organoid from each EGFP high and EGFP low population. Graph bar represents percentage of grown organoids in each condition (n=5 wells per condition). Data are represented as mean ± SD. ** p≤0.01, *** p≤0.001. Unpaired t-test was used for statistical analysis. (**B**) Subcutaneous growth of tumor EGFP-POLR1A populations in NOD/Scid mice (for PDO7 clone#23) and NSG mice (for PDO18 clone#4). 5000 cells EGFP high and EGFP low were injected from PDO18 clone #4 and 200 from PDO7 clone #23. Tumor growth was assessed for a maximum of 8 months period. Log-rank test was used for statistics.

3. Inhibition of rDNA transcription induced tumor cell differentiation *in vitro*

We have shown that cell differentiation coincides with the decrease of rDNA transcriptional activity. The key question is whether this activity is essential to maintain an undifferentiated, stem-like state of CRC cells. To this end, we analysed the effect of modulating rDNA transcription in tumor cells by using the RNA Pol I specific inhibitor BMH-21. This chemical compound has been shown to directly cause proteasome-dependent destruction of POLR1A, the large catalytic subunit protein of RNA Pol I holocomplex (Peltonen et al., 2014). The mechanism of action of BMH-21 entails preferential intercalation in DNA GC rich regions, preferentially in rDNA promoter regions. This triggers loss of RNA Pol I binding to these regions, leading to its degradation by the proteasome. It has been described

that BMH-21 reduces rRNA synthesis in treated cancer cell lines and induces cell cycle arrest (Colis et al., 2014; Peltonen et al., 2014).

We first treated EGFP-POLR1A CRISPR-Cas9 knock-in PDOs to validate the efficiency of the inhibitor by following the EGFP signal as readout of POLR1A expression. FACS analysis revealed that a 24h treatment with BMH-21 in PDO7#23 resulted in a 50% reduction in EGFP levels compared with non-treated cells, suggesting that indeed the inhibitor affected POLR1A protein stability (**Figure 21A**). Western blot analysis of parental, untargeted PDO7 treated with the inhibitor confirmed POLR1A downregulation in these cells (**Figure 21B**). We next analysed the expression of the stem and differentiated programmes and observed that after BMH-21 treatment there was a clear downregulation of stemness genes such as *LGR5*, *SMOC2*, *OLFM4* and *ASCL2*, accompanied by the expression of a differentiation gene signature (**Figure 21C**).

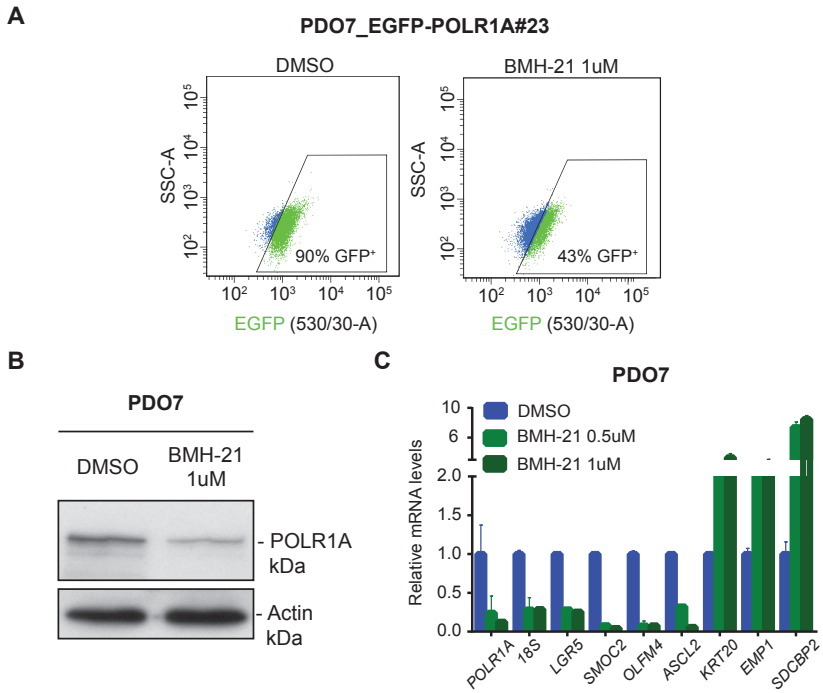

Figure 21: BMH-21 inhibitor downregulates POLR1A levels and induces *in vitro* differentiation of PDOs. (**A**) FACS analysis of EGFP-POLR1A expression in control or BMH-21 treated EGFP-POLR1A tumor organoids. (**B**) Analysis of POLR1A protein levels in parental PDO7 after 24 hours of BMH-21 *in vitro* treatment. (**C**) RT-qPCR of selected genes in control or BMH-21 treated PDO7 at 0.5uM and 1uM during 24 hours. Values show mean ± SD of three measurements.

To validate further the differentiation phenotype obtained in PDOs treated with BMH-21, we analysed the effect of the inhibitor in colorectal cell lines. LS174T cells represent a well-known cell line that can be used to study CRC differentiation (Van de Wetering et al., 2002). LS174T cells treated for 24h with BMH-21 showed a reduction in POLR1A protein levels which was accompanied by upregulation of differentiation markers similarly to what was observed in PDO7 (**Figure 22A** and **22B**).

To ensure that changes observed on Wnt signalling were a direct consequence of RNA Pol I reduction and to preclude a possible unspecific effect of BMH-21 we depleted specifically POLR1A mRNA in LS174T CRC cells using siRNA.

Although induction of the differentiation programme was not complete, we observed an upregulation of differentiation markers such as *KRT17* and *MUC2*. Yet, we observed only a mild downregulation of *LGR5* and no changes in *SMOC2* or *ASCL2*. (**Figure 23**). Thus, downregulation of POLR1A in this CRC cell line did not fully reproduce the changes in gene expression observed previously with BMH-21 treatment. It is thus possible that BMH-21-induced differentiation was not a direct consequence of RNA Pol I downregulation but rather of the intercalation of the drug in GC-rich promoters other that those driving rDNA transcription.

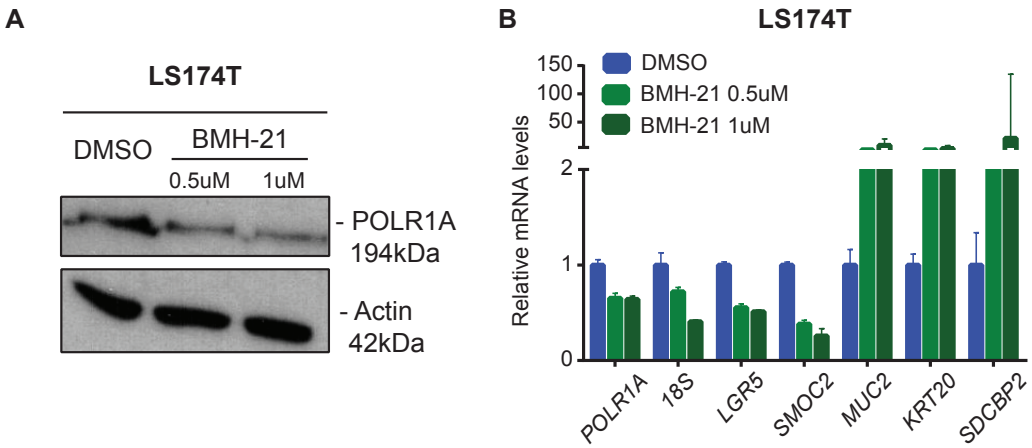

Figure 22: BMH-21 inhibitor downregulates POLR1A levels and induces *in vitro* differentiation of colorectal cancer cell lines. (**A**) Analysis of POLR1A protein levels in LS174T colorectal cancer cell line after 24 hours of BMH-21 *in vitro* treatment. (**B**) RT-qPCR of selected genes in control or BMH-21 treated LS174T colorectal cancer cell line at 0.5uM and 1uM during 24 hours. Values show mean ± SD of three measurements.

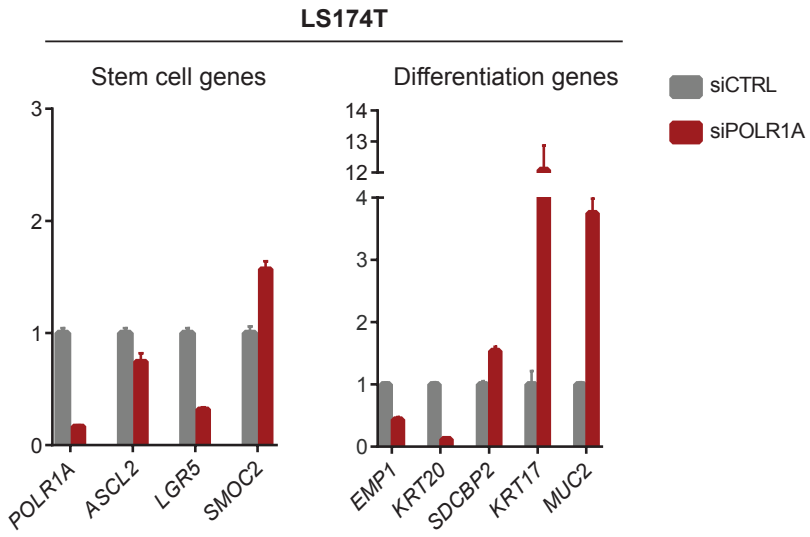

Figure 23: Genetic depletion of *POLR1A* mRNA induces *in vitro* differentiation of colorectal cancer cell lines. RT-qPCR of stem cell and differentiation genes in LS174T after depletion of *POLR1A* mRNA by siRNA. Values show mean ± SD of three measurements.

4. Ribosome biogenesis is regulated by WNT signalling

We have demonstrated that rRNA synthesis is regulated during cell differentiation both in tumors and in normal mucosa. Moreover, we have also shown that the tumorigenic potential of CRC cells relies, at least to some extent, on their ability to maintain high levels of rDNA transcription. However, how this process is regulated remains unresolved. Given that WNT signals represent the switch between the proliferative and the differentiated compartments in crypt and cancer cells (van de Wetering et al., 2002), we hypothesized that WNT may control rDNA transcription in stem and differentiated cells. We took advantage of an *in vitro* tumor cell differentiation model to further explore the role of WNT signalling in this biological process.

4.1 Induction of *in vitro* tumor cell differentiation by genetic WNT blockade

A collection of genetically modified CRC cell lines were previously engineered in our laboratory to modulate WNT signalling. These cancer cell lines are derived from late stage tumors that carried activating mutations in the WNT signalling pathway. In brief, each cell line was modified to stably express the beta-catenin-binding domain of TCF4 (N-TCF, amino acids 1 to 90) fused to a tamoxifen-inducible version

of the hormone-binding domain of the estrogen receptor (ERT2). Under basal conditions, the chimeric protein is retained in the cytoplasm (Gavin Whissell and colleagues, unpublished). Addition of 4-hydroxytamoxifen (4-OHT) shuttles the N-TCF-ERT2 fusion into the nucleus where it competes with endogenous TCFs for the binding to beta-catenin (Whissell et al., 2014) (**Figure 24A**).

To verify whether this represented a suitable cellular system for our purposes, we profiled changes in gene expression in CRC cells displaying mutational activation of the WNT pathway treated or not with 4-OHT during 48 or 96 hours. In these experiments we used LS174T cells – a cell line that carries an activating mutation in beta-catenin – and SW403 cells, which bears APC mutant alleles. Modified LS174T and SW403 (LS174T NE and SW403 NE) CRC cell lines showed a clear transcriptional response after disruption of beta-catenin/TCF4 transcriptional activity.

Activity of the TCF transcriptional reporter TOP (Korinek et al., 1997) was decreased in 4-OHT treated cells (**Figure 24B**) concomitant with a strong downregulation of the main WNT targets *LGR5*, *ASCL2* and *SMOC2*. On the contrary, genes related to the differentiation programme (*KRT20*, *KRT17* and *MUC2*) were upregulated (**Figure 25A**). We also analysed by immunofluorescence the expression of differentiation markers in 4-OHT treated tumor cells. We confirmed that untreated cells were negative for the expression of differentiation genes. However, 1 week after WNT blockade, these cells became positive for markers of differentiation such as KRT20 (**Figure 25B**). Of note, LS174T NE (but not SW403 NE) exhibited a heterogeneous KRT20 expression pattern after beta-catenin/TCF4 blockade (**Figure 25B**).
A possible explanation is that not all cells responded to the WNT off switch. Nevertheless, altogether these results indicated that N-TCF inducible CRC cell lines were a powerful resource to induce *in vitro* tumor cell differentiation in an efficient and reproducible manner.

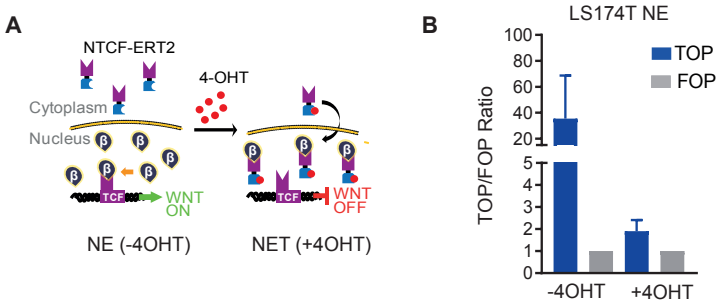

Figure 24: *In vitro* system of tumor cell differentiation. (**A**) Schematic representation of genetically engineered inducible WNT signaling disruption system in CRC cell lines. The addition of Tamoxifen (4-OHT) induces the translocation of the N-TCF-ERT2 fusion protein to the nucleus where it binds nuclear beta-catenin outcompeting TCF, and thus inhibiting transcriptional activity. (**B**) TOP/FOP ratio activity of colorectal cancer cell lines in control conditions or 48h after 4-OHT treatment. Note that TOP activity is reduced after 48h of WNT blockade. Values show mean ± SD of three measurements.

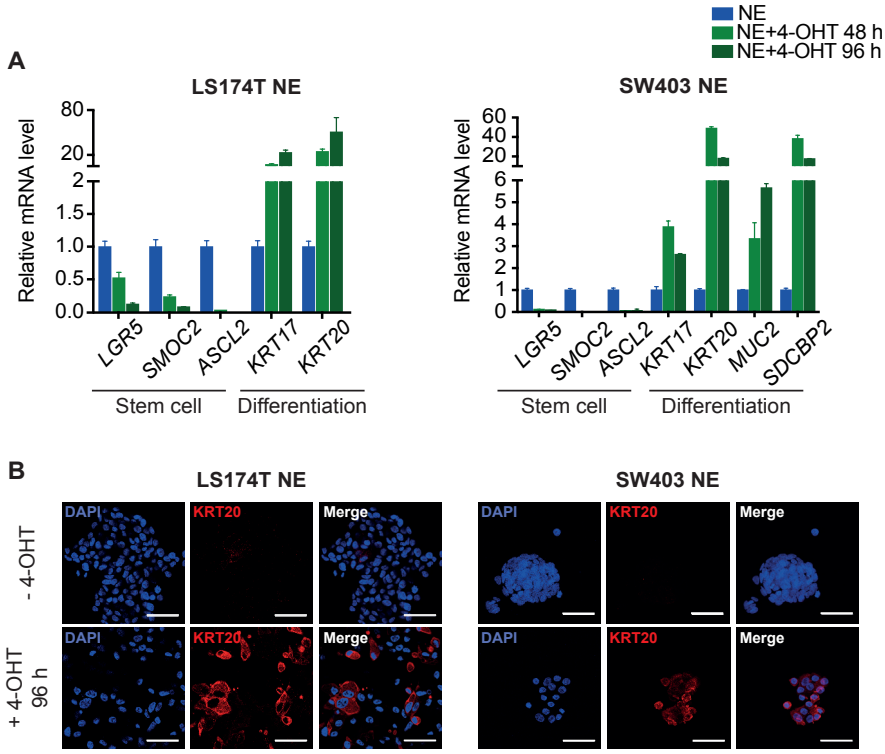

Figure 25: WNT blockade induces *in vitro* differentiation of colorectal cancer cell lines. (**A**) Gene expression analysis by RT-qPCR of stem cell and differentiated genes in LS174T NE and SW403 NE colorectal cancer cell lines in control conditions or after induction of differentiation by 4-OHT treatment during 48 and 96 hours. Values show mean ± SD of three measurements. n=3 (**B**) Confocal analysis of KRT20 (red) expression by immunofluorescence in LS174T NE and SW403 NE in control conditions or 96h after 4-OHT treatment. Scale bar represents 50µm.

4.2 Tumor cell differentiation induced cell cycle arrest and loss of tumorigenic potential in CRC cell lines

We next investigated the proliferative capacity of CRC cell lines after induction of differentiation upon WNT blockade. Cell cycle analysis demonstrated that control cells were actively proliferating whereas cells treated 72 hours with 4-OHT were largely arrested into G1/G0 phase of the cell cycle (**Figure 26A**).

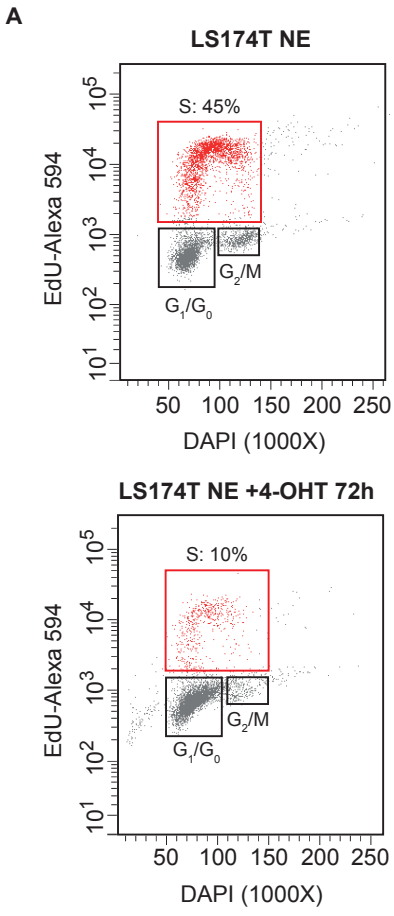

We then further investigated whether induction of differentiation modulated the tumorigenic capacity of these cells as it occurs *in vivo* (Merlos-Suárez et al., 2011). To this end, we injected subcutaneously LS174T NE into NOD SCID mice and treated mice or not with 4-OHT every two days. Only non-treated animals developed tumor xenografts (**Figure 26B**). These results demonstrated that induction of differentiation by WNT blockade in CRC cell lines does not only affect the proliferation capacity of these cells *in vitro* but also impaired their tumor initiation potential *in vivo*.

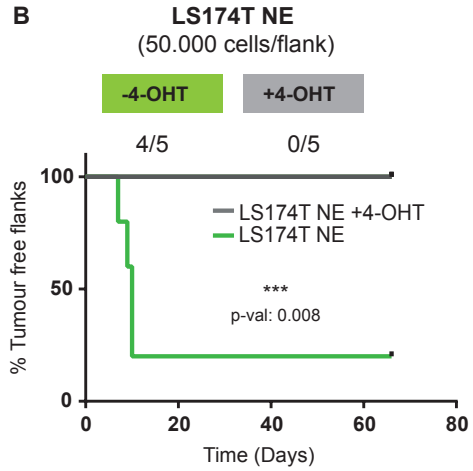

Figure 26: WNT blockade induces cell cycle arrest and loss of tumorigenic potential in colorectal cancer cell lines. (**A**) Cell cycle analysis by EdU incorporation in LS174T NE under control conditions or 72h after 4-OHT treatment. (**B**) Subcutaneous growth of injected LS174T NE in NOD/Scid mice treated or not with 4-OHT every two days. Tumor growth was monitored over a period of 66 days. Statistics are done using log-rank test.

4.3 RNA Pol I expression is reduced in differentiated CRC cell lines

Taking advantage of the *in vitro* tumor cell differentiation model described above, we next studied the rDNA transcription machinery and its activity in CRC cells during this process.

We first analysed the expression of *POLR1A* by RT-qPCR (the main subunit of the RNA Polymerase I) in LS174T NE and SW403 NE cells treated 48 or 96 hours with 4-OHT. We observed a progressive decrease, up to 5-fold at 96h, of *POLR1A* expression in treated cells compared to the control (**Figure 27A**). We also analysed the expression of other RNA Pol I subunits such as *POLR1B* or *POLR1C* and obtained identical results (data not shown), suggesting that the entire holocomplex was downregulated upon WNT blockade. Since POLR1A is known to be regulated post-transcriptionally, we assessed whether the decrease at transcriptional level was also reflected at protein level. Western blot analysis showed a clear reduction of the protein in cells after 96 hours treatment (**Figure 27B**). Of note, 72 hours of induction were required to observe changes at protein level suggesting that POLR1A protein is relatively more stable than the RNA.

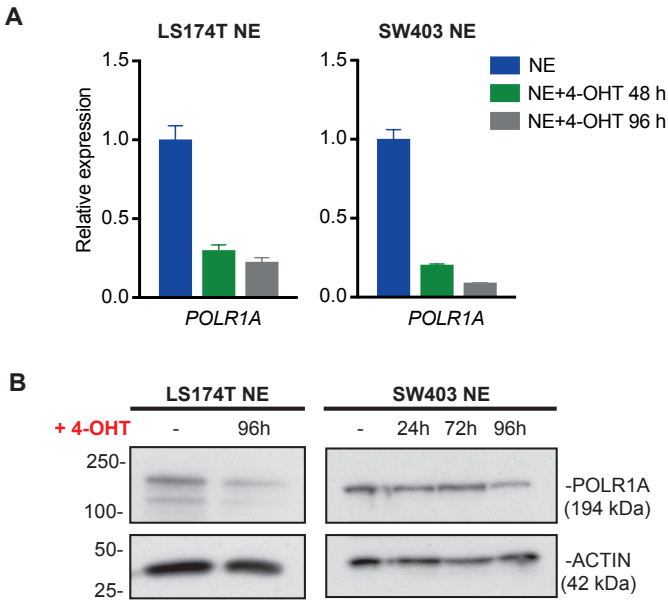

Figure 27: POLR1A is downregulated upon WNT blockade. (**A**) RT-qPCR of *POLR1A* mRNA in LS174T NE and SW403 NE tumor cell lines in control conditions or after induction of differentiation by 4-OHT treatment during 48 or 96 hours. Values show mean ± SD of three measurements. n=2 (**B**) POLR1A protein levels by Western blot in LS174T NE and SW403 NE cell lines upon 4-OHT treatment at indicated time points.

We also performed IF to visualize POLR1A in control and differentiated cell nucleoli, where rDNA is transcribed. Interestingly, the nucleolar morphology of non-treated cells showed a reticulated POLR1A pattern, whereas treated cells presented a smaller, more compacted and condensed POLR1A arrangement (**Figure 28A**). Reduction of POLR1A nucleolar label in 4-OHT treated cells was reminiscent of what we had observed previously in the differentiated areas of primary tumors and xenografts. We quantified these changes and demonstrated that the total number of POLR1A foci per nuclear area and the % of nuclear area occupied by this protein were reduced by inhibition of beta-catenin-TCF activity (**Figure 28B**). Thus, levels of RNA Polymerase I are reduced upon tumor cell differentiation induced by WNT blockade.

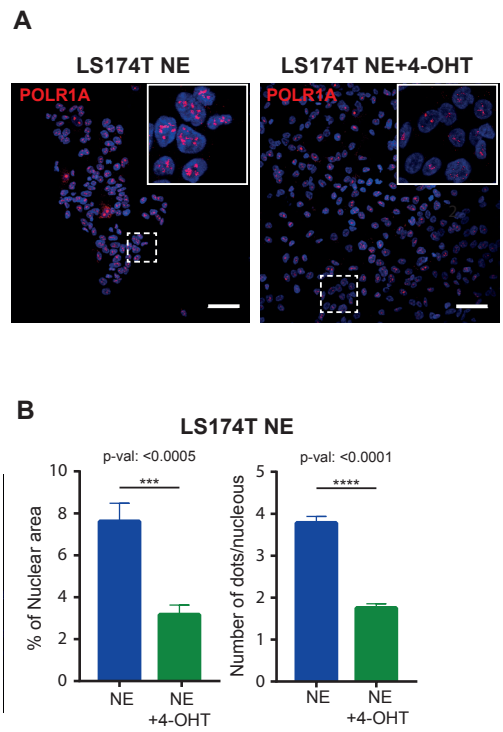

Figure 28: Downregulation of POLR1A upon WNT blockade is reflected by a decrease in nucleolar size. (**A**) Immunofluorescence of endogenous POLR1A (red) in CRC cell lines under control conditions or treated with 4-OHT during 1 week. Scale bar represents 50μm. (**B**) Quantification of percentage of total nuclear area occupied by POLR1A protein and number of POLR1A foci within the nucleus. Unpaired t-test was used for statistical analysis.

4.4 Transcription factors involved in rRNA biogenesis are downregulated during tumor cell differentiation

Downregulation of RNA Pol I subunits is a key event to explain the decrease of rRNA synthesis observed in differentiated cells. However, it is known that rDNA transcription is a highly coordinated and complex process that requires the involvement of many other proteins to cooperate with RNA Pol I to accomplish its rDNA transcription activity (Drygin, Rice, & Grummt, 2010; Ingrid Grummt, 2010). Therefore, we asked whether other components of the transcriptional machinery were also downregulated during differentiation. To this end, we performed RNA-seq of LS174T expressing N-TCF4-ERT2 dominant negative construct (LS174T NE) before and after induction with 4-OHT. We observed a clear downregulation of WNT target genes (WNT ON) such as *ASCL2*, *LGR5* or *SMOC2*. On the contrary, there was a clear upregulation of the differentiation gene program (WNT OFF). Interestingly, we identified several components of rDNA transcription machinery downregulated by inhibition of the WNT pathway (POL I) such as *NCL*, *DDX21*, *RRN3/TIF-IA, POLR1A* or *POLR1B* (**Figure 29A**). Consistently GSEA showed *Ribosome biogenesis* amongst the main activities downregulated by the dominant negative TCF4 factor. We also observed a clear downregulation of genes involved in the rDNA transcriptional apparatus (*RNA POL I*) upon disruption of WNT signalling (**Figure 29B**).

A prime example is RRN3/TIF-IA, which is an essential protein of the pre-initiation complex apparatus destined to recruit RNA Pol I at the rDNA promoter (Blattner et al., 2011; Miller et al., 2001; Peyroche et al., 2000). Indeed, TIF-IA and RNA Pol I dimerization is the first essential step that allows for the initiation of the transcriptional process. In particular, TIF-IA interacts with two subunits of the RNA Pol I holocomplex, POLR1A and RPA43 (Engel, Plitzko, & Cramer, 2016; Miller et al., 2001; Peyroche et al., 2000) (**Figure 30A**). We investigated if TIF-IA levels were also altered after WNT blockade in CRC cell lines. Analysis of *TIF-IA* expression levels upon 72h of 4-OHT treatment in LS174T NE cells showed a clear decrease similar to the one observed for *POLR1A* (**Figure 30B**). These results suggested that the rDNA transcriptional silencing observed during WNT blockade comprises the downregulation of not just RNA Pol I but also of a large fraction of the rRNA synthesis machinery.

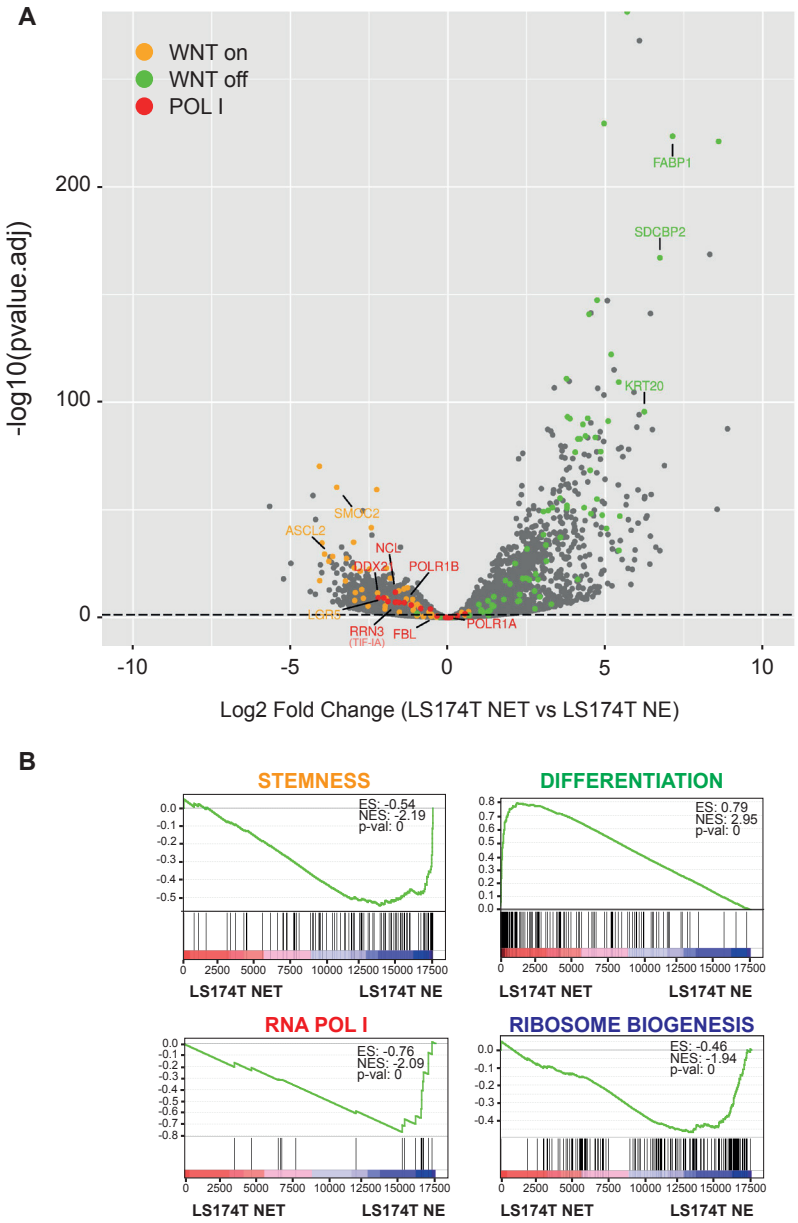

Figure 29: RNA-seq analysis reveals global downregulation of RNA Pol I transcription factors upon WNT blockade in colorectal cancer cell lines. (**A**) Volcano plot representing gene expression profile of LS174T NE versus LS174T NE treated with 4-OHT for 72h. Orange dots represent genes positively regulated by WNT signaling (WNT ON), green dots depict genes upregulated upon WNT blockade (WNT OFF) and red dots represent genes that belong to RNA Pol I transcriptional apparatus. (**B**) Gene set enrichment analysis comparing LS174T NE and LS174T NE treated with 4-OHT for 72h. The gene sets represented belong to the stem cell and differentiation programs. Gene sets related to the RNA Pol I transcriptional apparatus and ribosome biogenesis are also represented in this analysis.

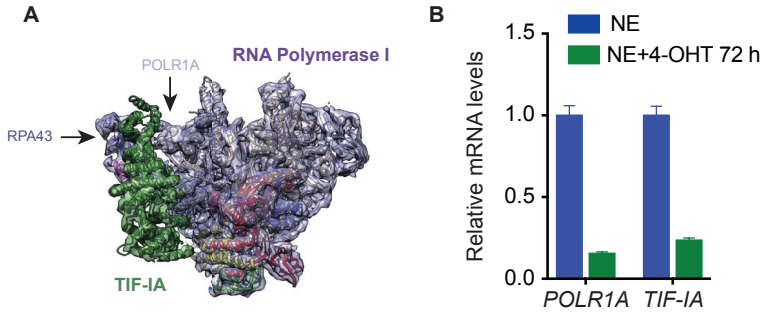

Figure 30: TIF-IA levels are downregulated upon WNT blockade. (**A**) Crystal structure of RNA Pol I and TIF-IA dimer. (**B**) RT-qPCR of *POLR1A* and *TIF-IA* mRNAs in LS174T NE control or treated with 4-OHT during 72 hours. Values show mean ± SD of three measurements. n=2

4.5 rDNA transcription, ribosome production and protein synthesis are downregulated in differentiated tumor cells

To investigate if reduction of POLR1A levels during differentiation had an impact on rDNA transcription, we performed EU incorporation assays to measure the rDNA transcriptional activity of tumor cells under stem or differentiation conditions. As RNA Pol I levels were clearly decreased after 96h of WNT blockade, we measured EU incorporation at the same time point in LS174T NE and SW403 NE cell lines.

We observed that in both cell lines, close to 100% of non-treated control cells were positive for EU, reflecting the high rDNA transcription rate of these cells *in vitro*. In contrast, only 5% of treated SW403 NE and 15% of the LS147T NE cells had actively incorporated EU, demonstrating a dramatic decrease of rDNA transcriptional activity in these cells upon WNT blockade and subsequent induction of differentiation (**Figure 31**).

As mentioned before, rDNA transcription is destined to produce ribosomes. We used the 5.8S rRNA antibody to analyse whether WNT blockade and differentiation reduced the ribosomal content in these cell lines. We stained LS174T NE and SW403 NE cells treated with 4-OHT for 24h, 48h and 7 days with the antibody detecting 5.8S rRNA. We combined the ribosomal staining with the differentiation marker KRT20. 24h of treatment induced a slight decrease of the 5.8S ribosomal signal. At 48h the reduction of the ribosomal content was more obvious and coincided with the emergence KRT20 expression. Finally, one week of blockade resulted in the complete loss of the ribosomal signal together with high expression of KRT20 (**Figure 32A** and **32B**).

WNT blockade for 1 week is required to exhaust the 5.8S signal probably because the lifetime of ribosomes is around 6 days (Nikolov, Dabeva, & Nikolov, 1983). Thus, despite 72 hours of blockade are sufficient to switch off rDNA transcription, cells might cope with existent ribosomes until their exhaustion days later. Indeed, this time frame appears to allow cellular differentiation, which goes in line with what we observed regarding the ribosomal content in the crypt-villus axis of the normal mucosa.

Because the final outcome of rRNA production is to generate ribosomes for protein synthesis, we wondered if a decrease in rDNA transcription also had an effect on the protein synthesis rates of differentiated cells. To this end we took advantage of another chemical method similar to the EU labelling that enables measurements of protein synthesis *in vitro* or i*n vivo*. In brief, changes in protein expression were detected by addition of Click-it OPP (O-propargyl-puromycin) to cultured cells, which incorporates in newly translated proteins. Similar to EU incorporation experiments, we incubated SW403 NE cells 30 min with OPP after being treated or not for 96h with 4-OHT. We then analysed the percentage of OPP positive cells by flow cytometry. 50% of non-treated cells had incorporated OPP. This percentage was clearly decreased to just 5% in treated cells (**Figure 33**).

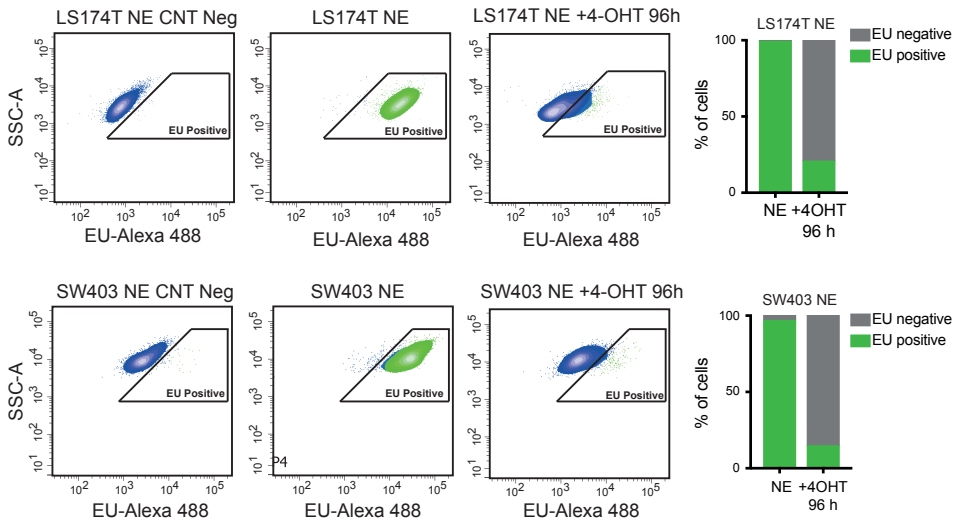

Figure 31: rDNA transcription is downregulated in CRC cell lines upon induction of differentiation. (**A**) FACS analysis of EU signal in LS174T NE and SW403 NE upon induction of differentiation by 4-OHT treatment during 72h. Quantification is shown on the right.

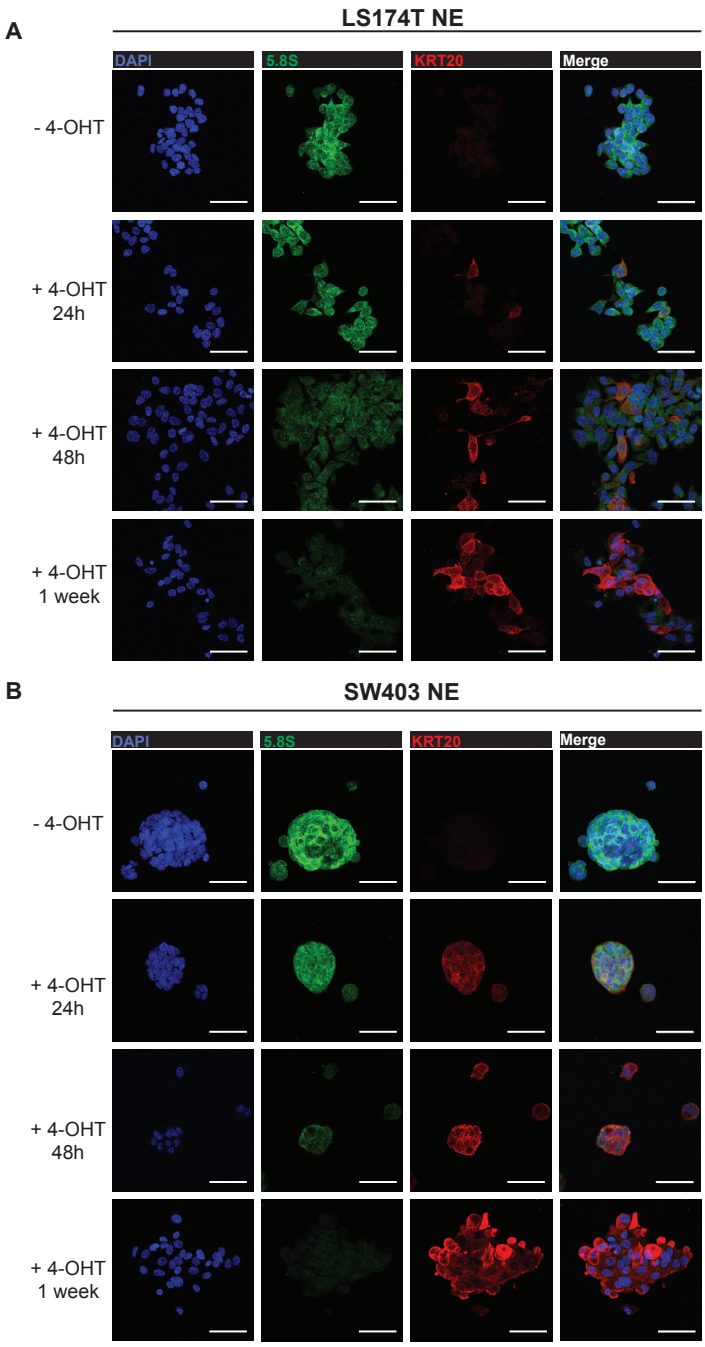

Figure 32: Ribosomal content decreases in CRC cell lines upon induction of differentiation. (**A**) Immunofluorescence of 5.8S rRNA (green) and KRT20 (red) in LS174T NE cells after 24h, 48h and 1 week of 4-OHT treatment. (**B**) Immunofluorescence of 5.8S rRNA (green) and KRT20 (red) in SW403 NE cells after 24h, 48h and 1 week of 4-OHT treatment. Scale bar represents 50µm.

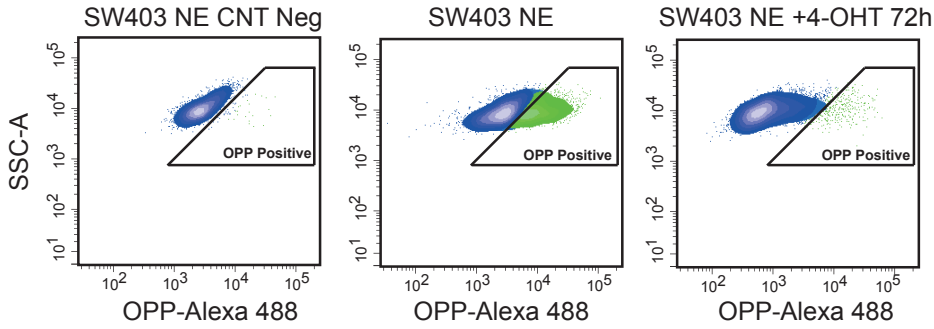

Figure 33: Analysis of protein synthesis in CRC cell lines upon induction of differentiation. FACS analysis of OPP signal in SW403 NE upon induction of differentiation by 4-OHT treatment for 72h.

5. Elucidating the mechanism underling rDNA transcription during CRC cell differentiation

As shown in previous sections, differentiation of CRC cells is accompanied by downregulation of the ISC signature and expression of the differentiation programme. Phenotypically, these transcriptional changes translate in a loss of proliferation capacity as well as in a reduction of tumorigenic potential. Moreover, decrease in rDNA transcription is another outcome of the differentiation process. Not only rRNA synthesis activity is affected but also overall ribosome biogenesis. It is also known that WNT signalling is the major driver of normal and tumor cell differentiation. Although we have not formally proven that WNT regulates rDNA synthesis, we have shown that this biological activity is clearly inhibited upon WNT blockade.

5.1 Overexpression of POLR1A and TIF-IA is not sufficient to restore the rDNA transcriptional activity of differentiated cells

A key open question is whether the phenotypic consequences (proliferation and tumorigenesis) observed in differentiated cells depend only on transcriptional changes (stem versus differentiated gene expression) or whether the loss of their rDNA transcriptional capacity plays a causal role in this process. To address this question, we explored whether restoration of rDNA transcriptional activity in differentiated tumor cells was sufficient to reinstate proliferation and tumorigenic properties independently (or not) of their differentiation status.

Grummt and colleagues demonstrated that overexpression of recombinant TIF-IA or POLR1A was sufficient to induce rDNA transcription in nuclear extracts *in vitro* (Mayer, Bierhoff, & Grummt, 2005; Mayer, Zhao, Yuan, & Grummt, 2004). Thus, we generated LS174T expressing NTCF4-ERT2 (NE) that in addition overexpressed essential factors for the rDNA transcription machinery. Two different lines were engineered to constitutively express either POLR1A (LS174T NE_POLR1A) or TIF-IA (LS174T NE_TIF-IA) under the CMV promoter. RT-qPCR and Western blot analysis demonstrated overexpression of both POLR1A and TIF-IA in transgenic cells compared to the controls carrying an empty vector (LS174T NE_EMPTY) (**Figure 34A** and **34B**). Upon 72h of 4-OHT, overexpressed POLR1A or TIF-IA levels were each maintained compared to the controls (red dashed lines) (**Figure 35**). Yet, POLR1A overexpression was not sufficient to maintain TIF-IA levels upon blockade of WNT signalling and vice versa (**Figure 35**).

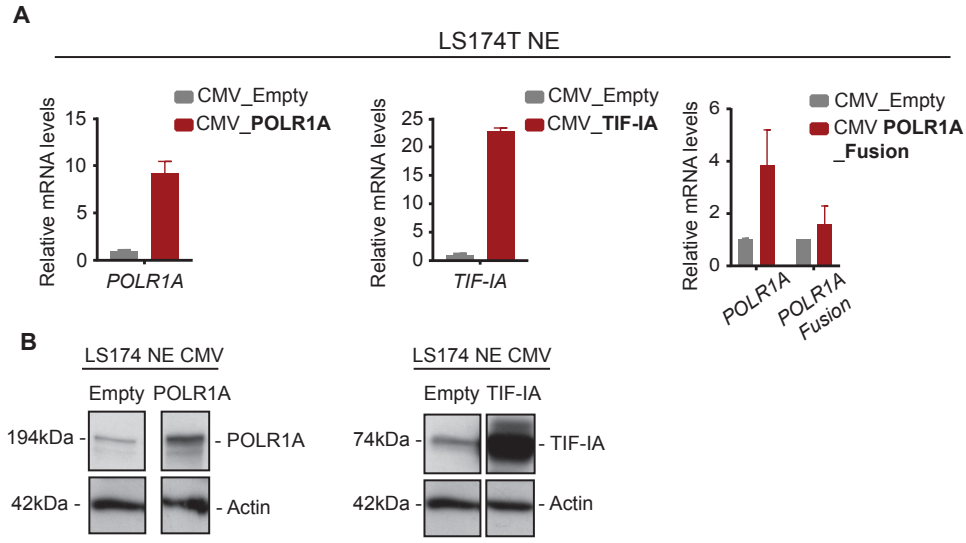

Figure 34: Generation of LS174T NE overexpressing POLR1A, TIF-IA or POLR1A_Fusion constructs under CMV promoter. (**A**) RT-qPCR showing mRNA upregulation of each gene in overexpressing cells compared to control cells carrying an empty vector. Values show mean ± SD of three measurements. (**B**) Protein levels of POLR1A and TIF-IA in overexpressing cells compared to control cells.

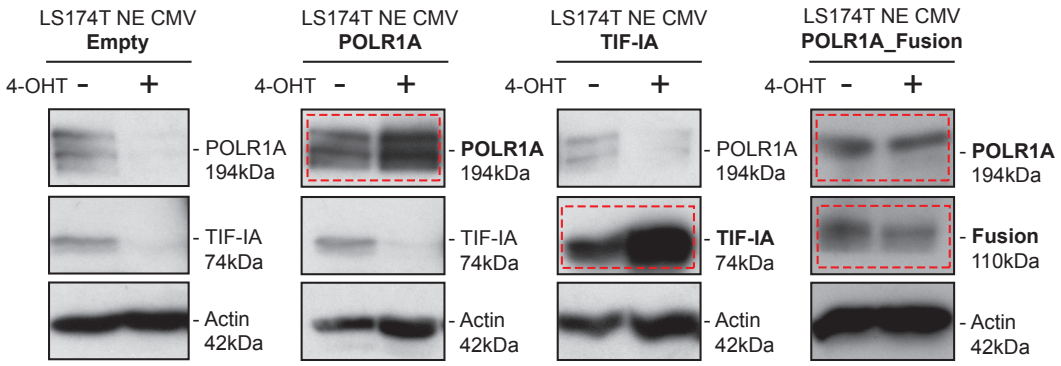

Figure 35: Overexpression of POLR1A, TIF-IA or POLR1A_fusion rescues the levels of these proteins upon induction of WNT blockade with 4-OHT treatment. Western blot showing protein levels of POLR1A, TIF-IA and POLR1A_Fusion in control cells (empty) and in overexpressing cells under control conditions of after treatment with 4-OHT for 72h.

We then asked if POLR1A or TIF-IA overexpression restored rDNA transcription activity in differentiated tumor cells. EU incorporation experiments revealed that maintenance of POLR1A or TIF-IA levels were not sufficient to retain rDNA transcription activity in the differentiated cells (**Figure 36**). The differentiation state of treated cells overexpressing POLRIA or TIF-IA was not altered regardless of POLR1A and TIF-IA overexpression (**Figure 37**). Also, cell cycle analysis revealed that POLR1A or TIF-IA overexpressing cells treated with 4-OHT remained arrested in the G1/G0 phase of the cell cycle (**Figure 38**).

Since dimerization of TIF-IA with RNA Pol I is an essential process for the onset of rDNA transcription activity, we speculated that both factors could be required to enhance the rDNA transcription activity. In fact, it has been previously reported that yeast strains expressing a fusion protein between TIF-IA and the RNA Pol I subunit RPA43 were able to maintain high levels of rDNA transcription (Laferté et al., 2006). Based on this finding, we modified LS174T NE CMV_POLR1A cells in order to re-introduce a fusion protein between TIF-IA and the subunit RPA43 (indicated as POLR1A+Fusion).

We confirmed by Western blot analysis that anti-TIF-IA antibody recognized a protein of 110 kDa that corresponded to the molecular weight of TIF-IA and RPA43 fusion (**Figure 34**). Levels of both POLR1A and TIF1A-RPA43 construct were kept constant upon induction with 4-OHT (red dashed lines) (**Figure 35**). Overexpression of both factors only induced a marginal rescue in nucleolar activity based on EU incorporation assays (**Figure 36**). LS174T-NE_POLR1A+Fusion cells downregulated the stem cell program and switched on the expression of differentiation genes upon induction with 4-OHT (**Figure 37**). Cell cycle arrest was equivalent to that of control cells (**Figure 38**). Therefore, we failed to restore nucleolar activity upon WNT blockade which precluded any conclusion about a causal role of rDNA synthesis in driving the tumorigenic phenotype in CRC.

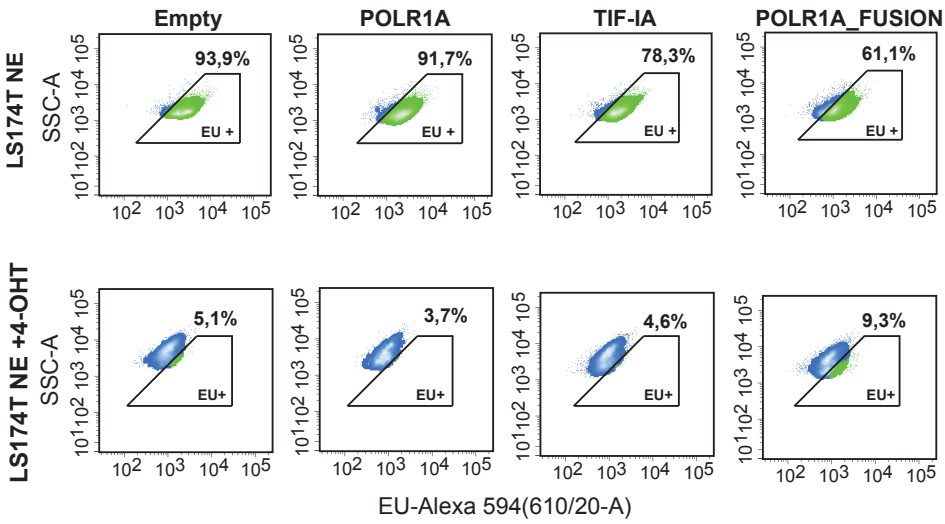

Figure 36: Restoration of POLR1A, TIF-IA or POLR1A_fusion is insufficient to rescue the rDNA transcription activity in colorectal cell lines upon WNT blockade. FACS analysis of EU incorporation in LS174T NE overexpressing POLR1A, TIF-IA and POLR1A_fusion in control conditions or after 72h of 4-OHT treatment.

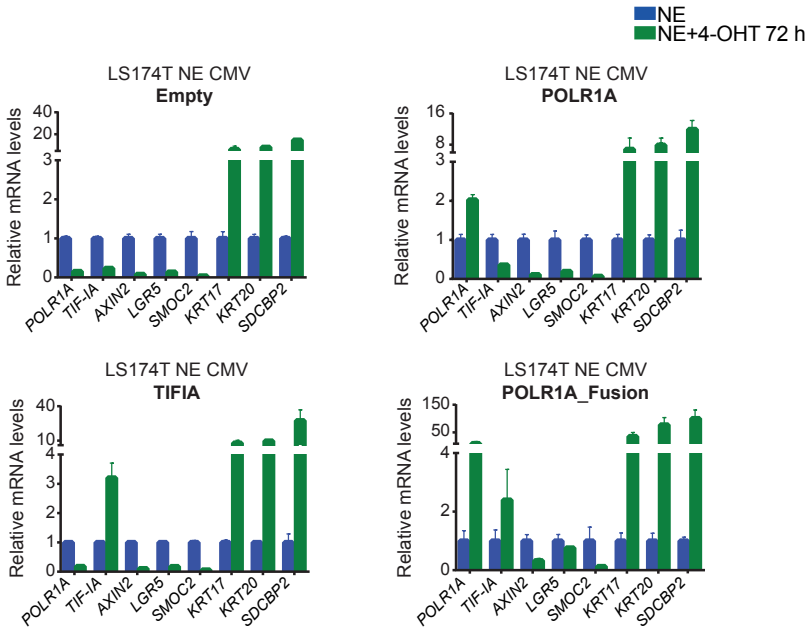

Figure 37: Gene expression analysis of the stem and differentiation programs in LS174T NE cells overexpressing PolR1A, TIF1A or fusion protein upon 4-OHT treatment. RT-qPCR of selected genes in control (empty) or overexpressing cells in control conditions or after treatment with 4-OHT for 72h. Values show mean ± SD of three measurements. N=2

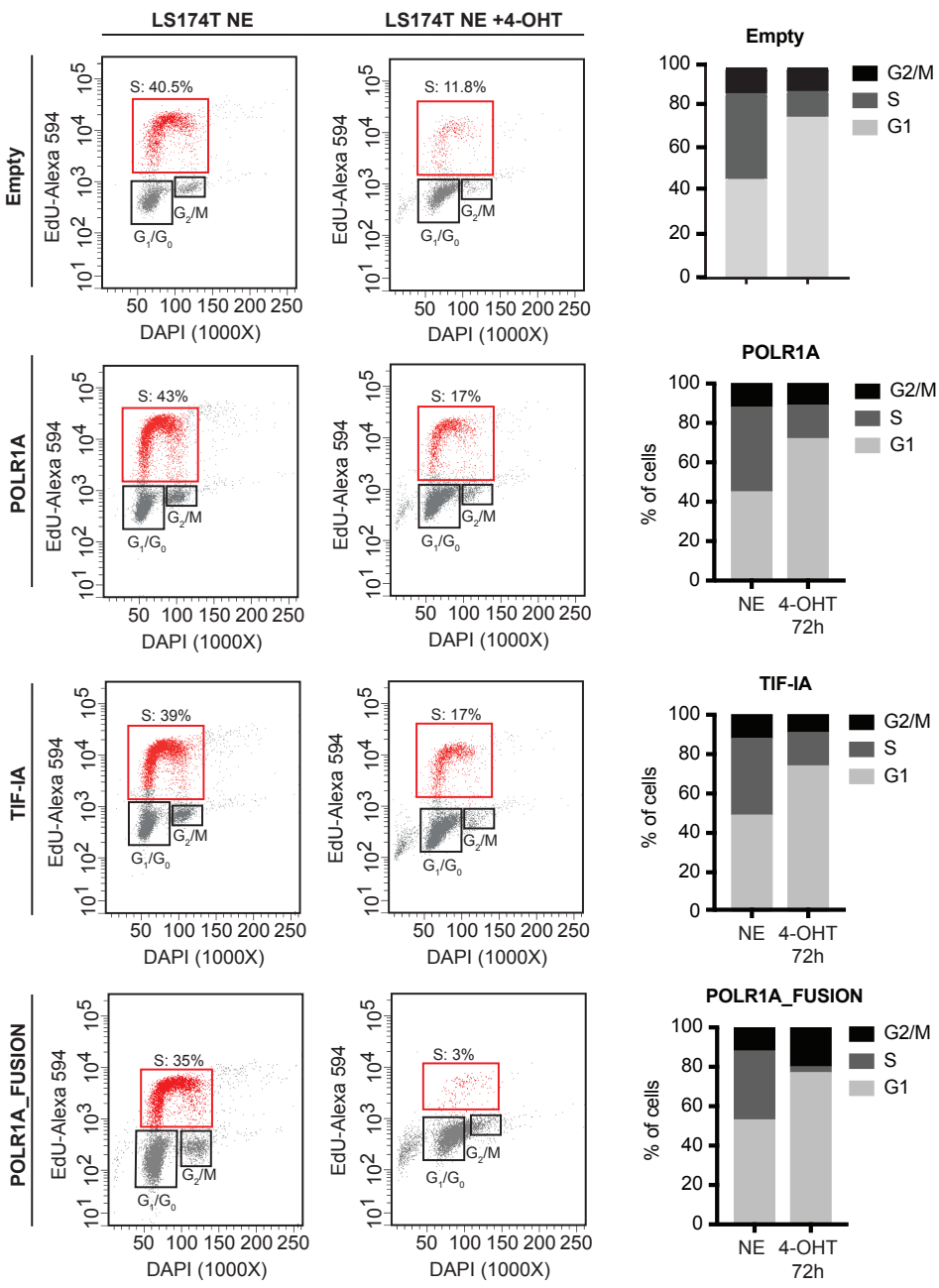

Figure 38: Restoration of POLR1A, TIF-IA or POLR1A-FUSION is insufficient to rescue the proliferation capacity of colorectal cancer cell lines upon WNT blockade. Cell cycle analysis by EdU incorporation in overexpressing tumor cells lines in control conditions or after 72h of 4-OHT treatment. Quantification of percentage of cells in G1, S and G2/M phases of the cell cycle in each condition is shown.

5.2 MYC: a possible regulator of rDNA transcription during tumor cell differentiation

The oncogene MYC was identified as one of the major targets of the Wnt pathway (He et al., 1998). In 2002, Sancho and Van der Wetering demonstrated that MYC expression was required to maintain the proliferation capacity of CRC tumor cells and that this was sufficient to rescue the cell cycle blockade induced after disruption of the beta-catenin/TCF4 transcriptional activity. This effect was attributed to direct repression of the negative cell cycle regulator p21 by MYC (Van de Wetering et al., 2002). *In vivo*, Myc deficiency bypasses the tumorigenic effect of APC mutations in the intestinal epithelium (Sansom et al., 2007).

Interestingly, several studies have reported that MYC regulates directly rDNA transcription. Gandori et al., demonstrated that MYC binds to the promoter region of rDNA genes and promotes rDNA transcription by recruiting essential factors of the transcriptional machinery (Grandori et al., 2005). It has also been shown that MYC coordinates protein synthesis by regulating the transcription of ribosomal components, genes involved in processing the rRNA and controlling the initiation of mRNA translation (van Riggelen, Yetil, & Felsher, 2010). Furthermore, the group of Davide Ruggero showed that single allele depletion of a ribosomal protein restores normal levels of protein synthesis in Emu-Myc/+ mice and this is sufficient to supress MYC oncogenic potential (Barna et al., 2008). All these observations prompted us to explore the possibility that MYC restoration in differentiated cells could rescue rDNA transcription activity.

We first analysed levels of MYC during WNT blockade in LS174T NE cells. 72 hours after induction of differentiation we observed that MYC levels were clearly decreased both at transcriptional and protein level (**Figure 39A**). This data confirmed that MYC is a target of the WNT signalling pathway in this system. Next, we generated LS174T NE cells constitutively expressing MYC under a CMV promoter (LS174T NE_MYC). RT-qPCR and Western blot analysis demonstrated a clear overexpression of MYC in these cells (**Figure 39B**).

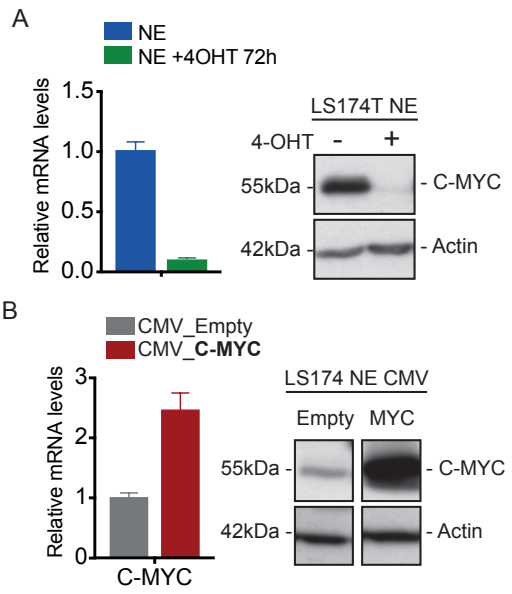

Figure 39: MYC is downregulated upon WNT blockade in colorectal cancer cell lines. (**A**) Analysis of *MYC* mRNA and MYC protein in LS174T NE after 72h of 4-OHT treatment. (**B**) Analysis of *MYC* mRNA and MYC protein levels in LS174T NE overexpressing MYC cells compared to LS174T NE control cells carrying an empty vector. Values show mean ± SD of three measurements.

We next investigated the effects of MYC overexpression in the context of tumor cell differentiation. LS174T NE CMV_MYC cells treated for 72 hours with 4-OHT were able to maintain MYC expression. Importantly, we found that whereas in control cells POLR1A and TIF-IA proteins were downregulated after 4-OHT treatment, their levels were maintained in treated cells overexpressing MYC (red dashed line) (**Figure 40A**).

When we looked at transcriptional changes we observed that although *POLR1A*, *TIF-IA* and *MYC* mRNAs were maintained in treated cells, these cells showed upregulation of the differentiation programme together with a decrease in the stem cell gene signature induced by the WNT blockade (**Figure 40B**). Therefore, MYC expression is not sufficient to completely prevent the loss of stemness and upregulation of the differentiation program imposed by inhibition of the beta-catenin/TCF4 activity.

Immunofluorescence analysis of MYC overexpressing cells confirmed that while in control cells (LS174T NE CMV_Empty) both POLR1A and MYC were decreased upon induction of differentiation, in LS174T NE CMV_MYC expressing cells the levels were maintained upon 4-OHT treatment despite the expression of differentiation markers (**Figure 40C**). EU incorporation analysis demonstrated that 4-OHT treated tumor cells were now able to maintain the rDNA transcription capacity although the induction of the differentiation programme (**Figure 41**). These results show that restoration of MYC in the differentiated population is sufficient to keep the rDNA transcription active in these cells.

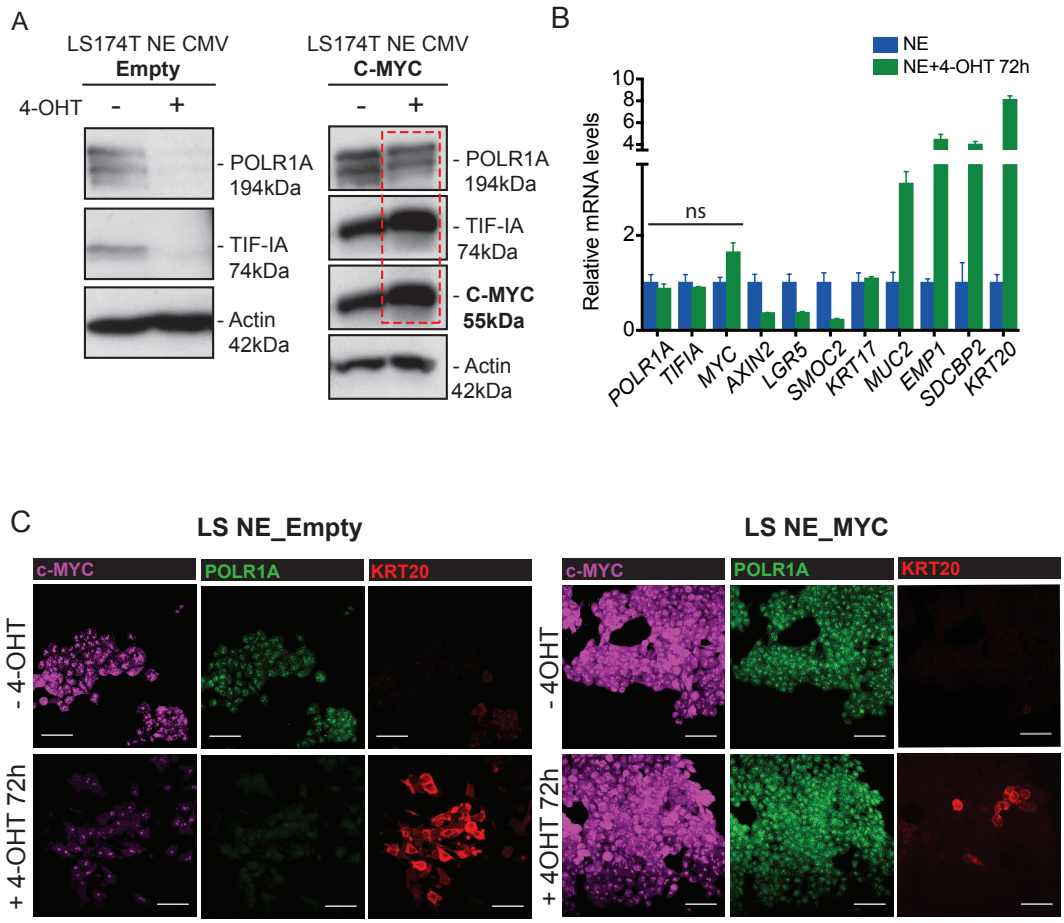

Figure 40: MYC overexpression is able to rescue POLR1A and TIF-IA levels in differentiated tumor cell lines. (**A**) Protein levels of POLR1A and TIF-IA are maintained upon induction of differentiation by 4-OHT treatment in LS174T NE MYC overexpressing cells (red dash lines). (**B**) RT-qPCR analysis of stem cell and differentiation gene expression in LS174T NE MYC overexpressing cells after 4-OHT treatment. Note that MYC overexpression also recues *POLR1A* and *TIF-IA* mRNAs in differentiated cells. Values show mean ± SD of three measurements. n=2 (**C**) Immunofluorescence analysis of POLR1A (green), MYC (magenta) and KRT20 (red) proteins in LS174T NE empty or MYC overexpressing cells under control conditions or after 72h of 4-OHT treatment. Scale bar represents 50µm.

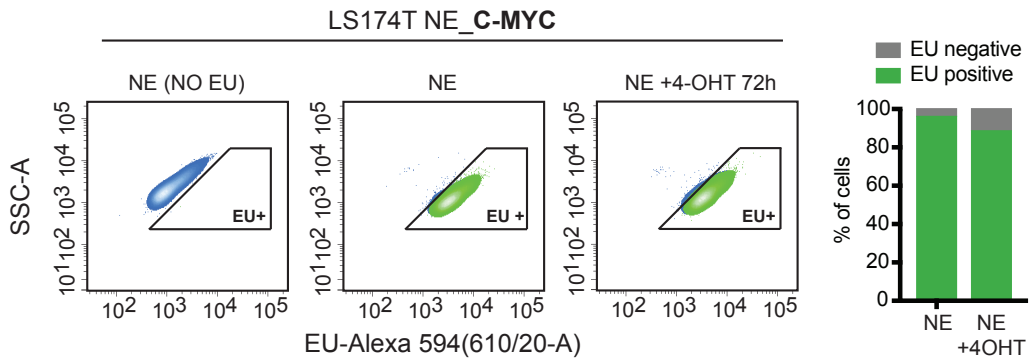

Figure 41: MYC overexpression is able to rescue rDNA transcription in differentiated colorectal cancer cell lines. FACS analysis of EU incorporation in LS174T NE overexpressing MYC cells. In this case, 4-OHT treated cells incorporated similar levels of EU signal compared to non-treated cells.

We next investigated to what extent MYC restoration affects the expression of genes related to the rDNA transcriptional process (besides from POLR1A and TIF-IA). We performed RNA seq analysis in control (Empty) and overexpressing MYC (MYC) cells treated or not with 4-OHT. We first interrogated the expression of gene sets such as *RNA Polymerase I* or *Ribosome biogenesis* in these four populations. The *RNA Polymerase I* gene set included all the genes codifying for essential subunits of the RNA Polymerase I enzyme as well as genes related to transcriptional factors of the rDNA transcription pre-initiation complex. The gene set *Ribosome biogenesis* included genes related to the processing and maturation of the pre-rRNA transcript. In both cases, we observed that while in the control cells their expression was downregulated after 4-OHT treatment, in MYC overexpressing cells their expression was completely rescued after induction of differentiation (**Figure 42A**). When looking at single gene expression, we confirmed that all the main RNA Pol I structural subunits (*POLR1A-POLR1E*) were downregulated in control cells treated with 4-OHT cells but not in MYC treated overexpressing cells. Similar results were obtained for genes codifying for factors of the pre-initiation complex (*UBTF*) or rRNA processing proteins (*FBL* and *NCL*) (**Figure 42B**). These results demonstrate that restoration of MYC is sufficient to rescue the expression of all these factors and therefore to maintain the rDNA transcriptional activity of the cells.

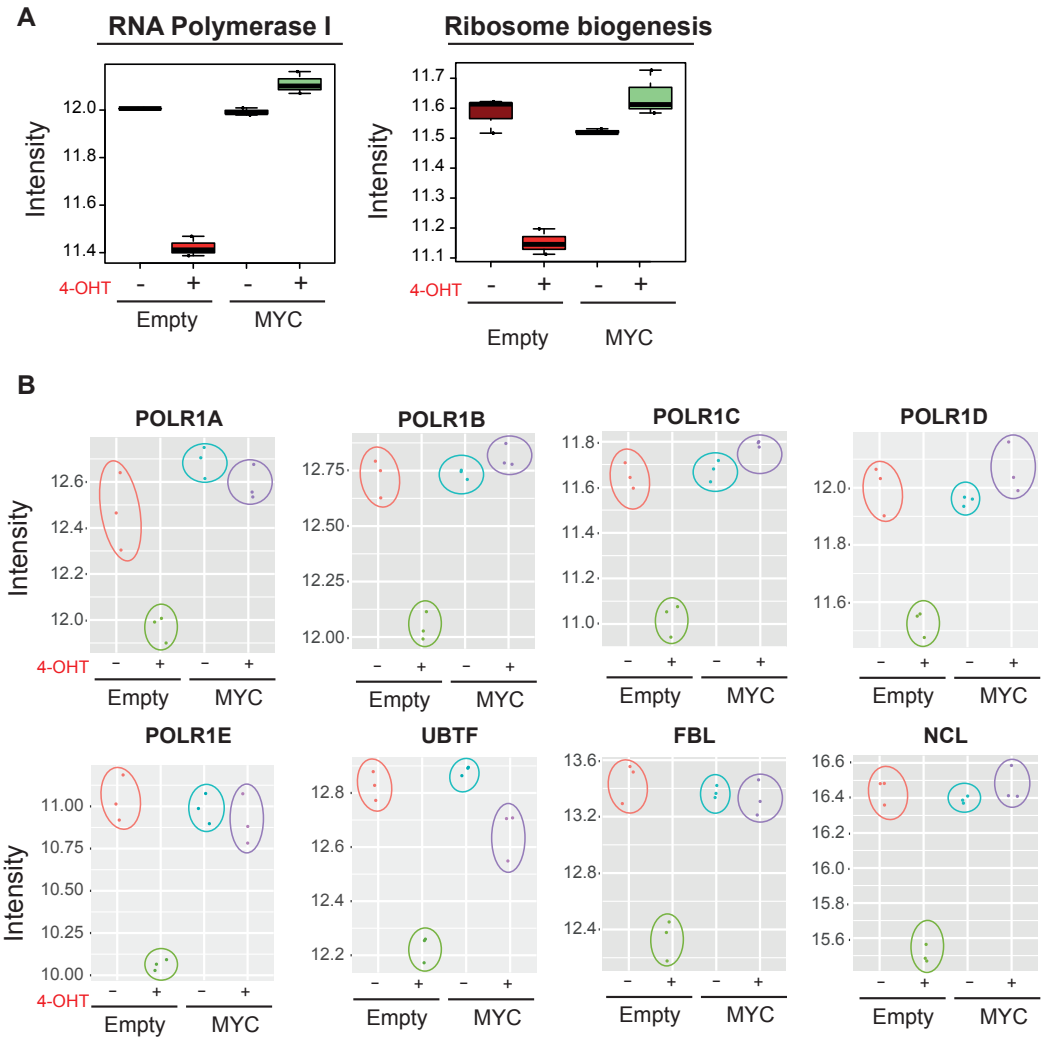

Figure 42: MYC overexpression rescues the expression of genes related to the RNA Pol I transcription machinery and ribosome biogenesis in differentiated colorectal cancer cell lines. (**A**) Expression of RNA polymerase I and Ribosome biogenesis gene sets in LS174T NE empty or MYC overexpressing cells under control or after 72h of 4-OHT treatment. (**B**) Stripcharts representing the mRNA expression of RNA Pol I structural subunits (*POLR1A-POLR1D*), the rDNA transcriptional factor *UBTF* and the rRNA processing genes *FBL* and *NCL* in LS174T NE empty or MYC overexpressing cells in control conditions or after 72h of 4-OHT treatment.

We have previously shown that downregulation of rDNA transcription also has an effect on the ribosomal content of the differentiated cells. Thus, we assessed if the rescue of rRNA synthesis by MYC overexpression also restored the ribosomal load in differentiated tumor cells. Immunofluorescence analysis of the 5.8S rRNA revealed that tumor cells overexpressing MYC maintained their ribosomal content after 4-OHT treatment (**Figure 43A**). Indeed, when we interrogated the expression of genes codifying for ribosomal proteins constituents of mature ribosomes, we found that their expression was also downregulated in 4-OHT treated control cells but restored in MYC overexpressing differentiated cells (**Figure 43B**).

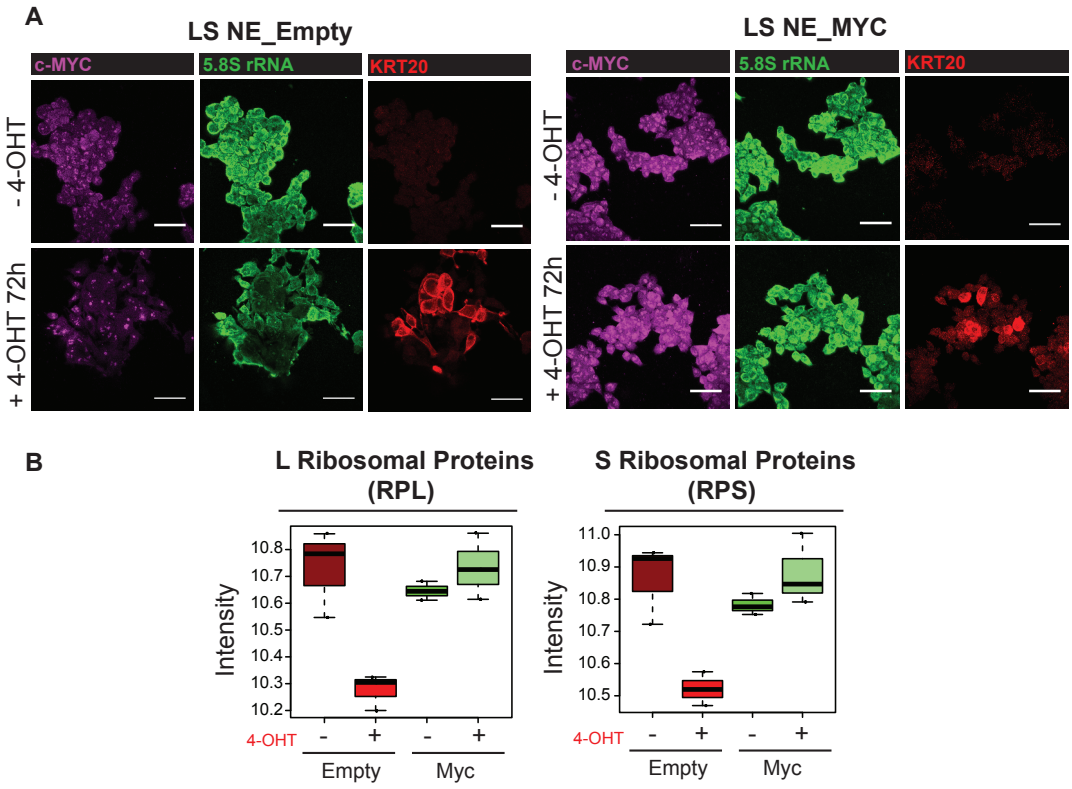

Figure 43: MYC overexpression rescues ribosome production in differentiated colorectal cancer cell lines. (**A**) Confocal images of the 5.8S rRNA (green), MYC (magenta) and KRT20 (red) staining in LS174T NE empty or MYC overexpressing cells in control conditions or after 72h of 4-OHT treatment. Scale bar represents 50µm. (**B**) Expression of ribosomal genes in the same conditions. Overexpression of MYC rescues the expression of this class of genes in differentiated tumor cells.

Next, we investigated the effect of MYC overexpression on the downregulation of the stem cell programme as well as on the induction of differentiation after WNT blockade. We found that while expression signatures that define ISC (WNT ON or hCoSC) were similarly downregulated in both control and MYC overexpressing cells after treatment, induction of differentiation was partially reduced in MYC overexpressing cells upon WNT signalling blockade (**Figure 44A**). As a case in point, the ISC genes *LGR5* and *AXIN2* were downregulated in control and MYC cells to a similar extent upon induction of N-TCF4 activity (**Figure 44B**). In contrast, the expression of differentiation genes such as *KRT20* or *FABP1* in MYC overexpressing cells after 4-OHT treatment was lower than in differentiated-induced control cells (**Figure 44B**).

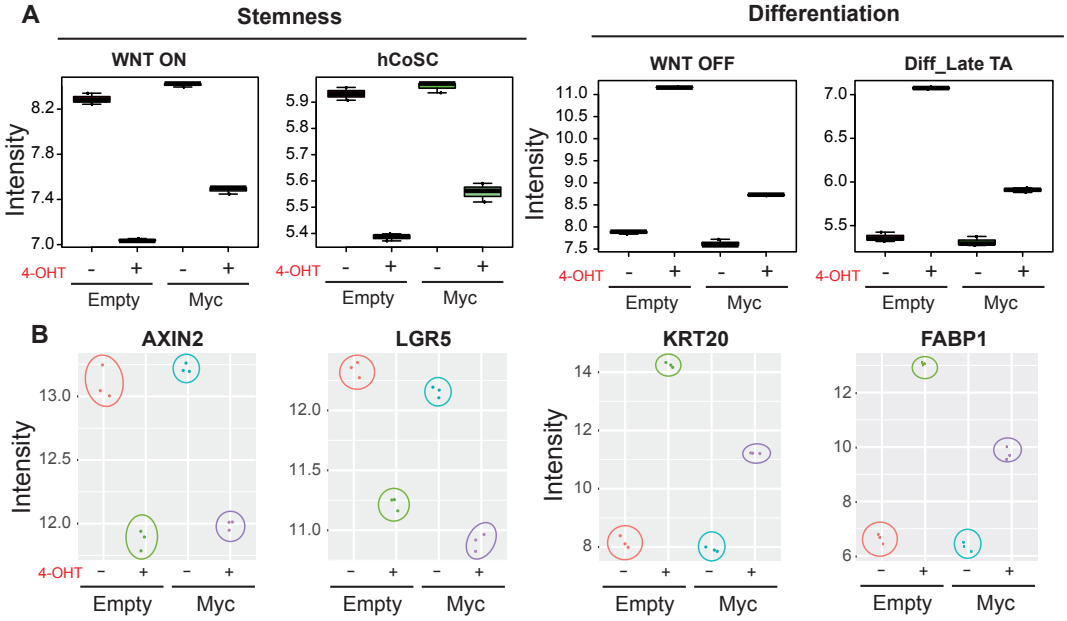

Figure 44: Induction of the differentiation program is partially reduced in MYC overexpressing cells upon WNT blockade. (**A**) Expression of stem cell and differentiation gene signatures in LS174T NE empty or MYC overexpressing cells in control conditions or after 72h of 4-OHT treatment (upper panel). (**B**) mRNA expression of single stem cell genes (*AXIN2*, *LGR5*) and differentiation genes (*KRT20*, *EMP1*) in LS174T NE control or MYC overexpressing cells after induction of differentiation (lower panel).

5.3 rDNA transcription is necessary to sustain proliferation during MYC-driven rescue of WNT activity in CRC cells

Another consequence of tumor cell differentiation besides the downregulation of rDNA transcription is the loss of the proliferation capacity. MYC rescued the proliferation of CRC lacking WNT signalling as previously shown (Van de Wetering et al., 2002). Consistently, RNA-seq analysis revealed that the expression of the proliferation signature was rescued in MYC overexpressing cells after 4-OHT treatment (**Figure 45A**). Indeed, cell cycle analysis and colony formation assays revealed that induction of differentiation upon WNT blockade did not affect the proliferation capacity LS174T NE overexpressing MYC cells (**Figure 45B** and **45C**).

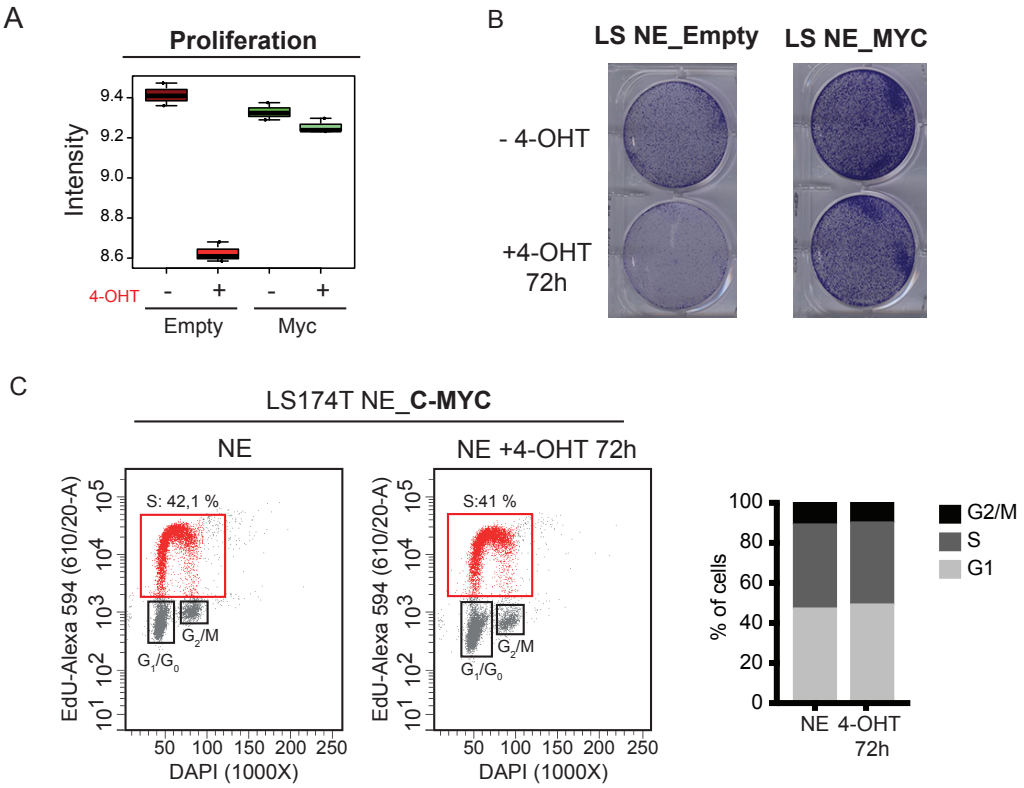

Figure 45: MYC overexpression rescues the proliferation capacity of differentiated colorectal cancer cell lines. (**A**) Expression of the proliferation gene signature in LS174T NE empty or MYC overexpressing cells after induction of differentiation by 4-OHT treatment during 72h. (**B-C**) Cristal violet staining and cell cycle analysis of LS174T NE empty or MYC overexpressing cells in control conditions or after induction of differentiation by 4-OHT treatment for 72h.

We thus asked whether rRNA synthesis was required to maintain the proliferation state of differentiated tumor cells induced by MYC overexpression. To this end, we depleted both *POLR1A* and *TIF-IA* mRNAs in LS174T NE_CMV_ MYC cells by siRNA. Downregulation of these proteins was sufficient to induce cell cycle arrest in MYC overexpressing cells (**Figure 46**).

Overall, these findings support the notion that MYC downregulation during tumor cell differentiation is the main cause of the rDNA transcriptional reduction observed in differentiated tumor cells. Our data suggest that MYC regulates the expression of essential machinery required for rNA synthesis downstream of WNT signalling.

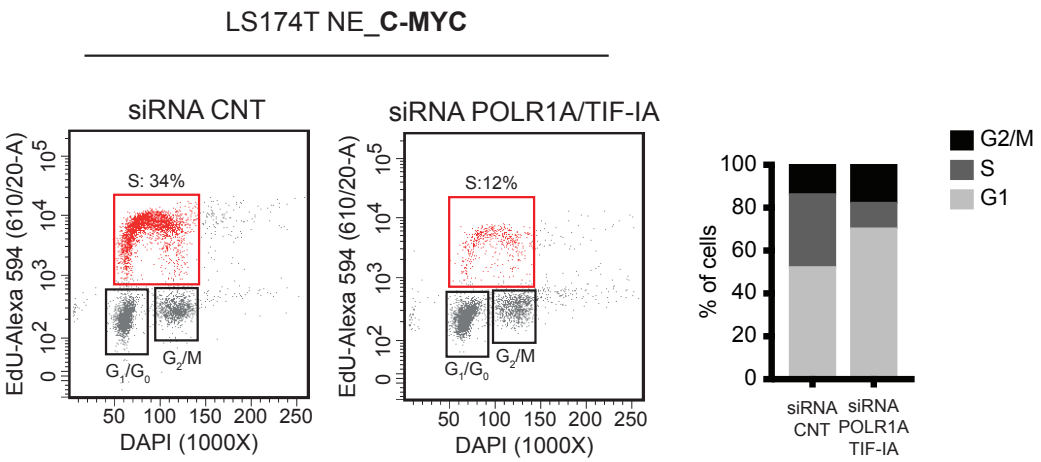

Figure 46: Downregulation of POLR1A and TIF-IA is sufficient to induce cell cycle arrest in MYC overexpressing colorectal cancer cell lines. Cell cycle analysis of MYC overexpressing cells transfected with control siRNA or POLR1A and TIFI-IA siRNAs for 3 days. Downregulation of *POLR1A* and *TIF-IA* mRNAs induces cell cycle arrest in LS174T NE MYC overexpressing tumor cells.

Discussion

Identification of colorectal cancer stem cells (CRC-SCs) has been a major step forward to understand the driving forces behind CRC maintenance and progression. This project has focused on the identification of biological functions underlying the tumor-fueling behavior of CRC-SCs. In the following pages we will discuss the important role of rDNA transcription and nucleolar activity as essential biological functions for the tumorigenic nature of CRC-SCs and the relationship between these cellular activities and the differentiation process. We aim to connect our findings with recent discoveries that evidence the important contribution of tumor cells other that CSCs for CRC growth and regeneration.

EPHB2 expression identifies CoSCs and CRC-SCs

Previous work by our laboratory had described EPHB2 as a marker of ISCs, CoSCs and CRC-SCs (Eduard Batlle et al., 2002; Jung et al., 2011; Merlos-Suárez et al., 2011). In CRCs, EPHB2 levels distinguish tumor cells with particular transcriptional and functional features (Merlos-Suárez et al., 2011). To build a refined EPHB2 gene expression signature, we made use of EPHB2 expression to isolate CRC-SCs and CoSCs directly from primary tumor samples isolated from patients.

When analysing the transcriptional distribution of the distinct EPHB2 expressing cell populations from normal and tumor tissues, we found that the most evident segregation was tissue dependant (normal *vs* tumor). The reason behind this arrangement is probably the large accumulation of mutations harboured by tumor cells. These genetic aberrations result in a largely divergent transcriptional profile between normal and cancer cells. Nevertheless, we observed that EPHB2 levels were still able to dissociate two distinct groups, $EPHB2^{hi}$ and $EPHB2^{lo}$, within each tissue. Certainly, $EPHB2^{hi}$ expressing cells enriched for the expression of ISC genes in both normal and tumor samples. The same applied for the expression of intestinal differentiation genes in the $EPHB2^{lo}$ populations. These results largely confirm what was observed regarding the similarities between normal and tumor SCs and further reinforce the notion that EPHB2 is a robust marker to isolate CoSCs and CRC-SCs in a reproducible and reliable manner.

Ribosome biogenesis and nucleolar related genes are enriched in CoSCs and CRC-SCs

Transcriptomics analysis revealed that the expression of gene ontologies related to ribosome biogenesis and nucleolar function appeared clearly

enriched in the EPHB2^{hi} compared to EPHB2^{lo} normal and tumor cells. These gene sets included hundreds of genes encoding for proteins involved in several steps of ribosome biogenesis such as rDNA transcription, maturation and ribosomal assembly. Many ribosomal genes encoding for ribosomal proteins required for the formation of mature ribosomes were also included in these gene sets. Interestingly, we found that expression of these gene sets was commonly enriched in the EPHB2^{hi} cells of both tissues. Thus, we hypothesise that ribosome biogenesis could represent a distinctive biological function of the stem cell population. It is to be noted that the expression of these genes was overall higher in tumor compared to normal cells, probably reflecting the high demand for protein synthesis of transformed cells. However, besides the elevated expression of this class of genes in tumor cells, we found a consistent upregulation in EPHB2^{hi} compared to EPHB2^{lo} cancer cells suggesting that this biological activity is also differentially regulated among tumor cells.

These observations were initially surprising since it is common knowledge that ribosome biogenesis is a fundamental and indispensable cellular activity present in all cell types. Moreover, EPHB2^{lo} cells represent a differentiated population supposed to be well-off in protein production to ensure specialized intestinal functions, i.e. enzymes involved in nutrient absorption, mucosecretion, hormone secretion, etc. By contrast, our results suggest that differentiated cells display very low ribosomal activity. A possible explanation behind this contradictory finding is that in normal intestinal epithelium differentiated cells do not need to synthesize new ribosomes because they inherit ribosomes previously generated by the stem cells. The few remaining ribosomes in differentiated cells are sufficient to produce proteins ensuring their specific cellular functions. Considering that the architecture and cell heterogeneity of CRCs is reminiscent of the normal colon epithelium, it is plausible that ribosomes of tumor-differentiated cells are also inherited from CSCs. Because of low capacity to synthesize proteins, we speculate that these tumor cells show reduced proliferation capacity and decrease tumorigenic properties. Therefore, ribosomal activity could account for the distinct tumorigenic capacity of CSCs and non-CSCs.

At the time this project was conceived there was almost no supporting literature relating ribosome biogenesis and intestinal biology. However, alongside the development of the project single cell transcriptomic studies have shed light to the differential expression

of ribosomal genes between stem cells and differentiated progenitors (Grün et al., 2015; Li et al., 2017). Li et al., have shown that although ribosomal protein coding genes are overall highly expressed compared to other transcripts, their expression is enriched in the stem cells/TA population compared to differentiated cells both in normal intestine and CRCs (Li et al., 2017).

CRC-SCs display high rDNA transcription activity compared to differentiated-like tumor cells

An essential processes for the production of ribosomes is transcription of ribosomal RNA (rRNA). Indeed, 60% of nascent RNA in a cell accounts for the transcription of rRNA genes, which direct and support the production of several millions of ribosomes per cell (Comai, 2004; I Grummt, 2010; Lafontaine, 2015).

By measuring EU incorporation we have shown that EPHB2^{hi} tumor cells exhibit higher rDNA transcriptional activity that the EPHB2^{lo} cells. The latter show reduced or almost absent rDNA transcription capacity. These results support the transcriptomics data obtained indicating that EPHB2^{hi} cells are enriched in gene sets related to ribosome biogenesis and nucleolar function. Because of the broad EPHB2 expression in CRC tumor xenografts, we were able to interrogate the rDNA transcriptional activity of tumor cells expressing medium levels of EPHB2.

In normal colon crypts EPHB2^{med} cells represent the TA population which is undifferentiated and actively proliferating. EU incorporation revealed that although these cells were not as active as the EPHB2^{hi} population, they showed an increased rDNA transcription activity compared to the EPHB2^{lo}. These results indicate that rRNA synthesis is not restricted to CRC-SCs (EPHB2^{hi}), yet decreases gradually along the differentiation path of tumor cells.

We have also used *in vitro* models of tumor cell differentiation to further confirm the decrease of rRNA synthesis in differentiated cells. In line with the i*n vivo* results, induction of differentiation through genetic WNT blockade causes a prominent reduction in the rDNA transcriptional activity in CRC cell lines. We note that cells had to be maintained under differentiation conditions up to three days to achieve a complete rDNA transcriptional silencing implying a relatively slow kinetics. Reduction of the rRNA synthesis was accompanied by cell cycle arrest, which reinforces the notion that the ribosomal activity is tightly coupled to cell cycle progression and proliferation.

Although we have not explored rDNA transcription activity in normal intestinal cells *in vivo*, our preliminary data suggest that the downregulation of ribosome biogenesis-related genes in the EPHB2^{lo} crypt cells is probably translated into a decrease of rRNA synthesis. Indeed, preliminary experiments showed that *in vitro* differentiation of mouse intestinal organoids reduces EU incorporation (data not shown), suggesting that differentiated normal intestinal cells also display low rDNA transcriptional activity.

Decrease of rDNA transcription reflects low ribosomal content of differentiated normal and tumor cells

Analysis of the number of mature ribosomes in normal and tumor primary tissue sections revealed that terminally differentiated cells contained less ribosomal load. Again, these results are in agreement with previous observations showing that these cells express low levels of ribosome biogenesis related genes and display low rDNA transcriptional activity.

In particular, ribosomal content in normal colon epithelium was labelled by an antibody that detects 5.8S subunit ensemble in the ribosome, which marked the colon crypt base cells. The signal was also present in transient amplifying cells at lower intensity and was only absent in the more differentiated cells close the villus top. This fits with a model that the rDNA transcriptional activity is gradually switched off throughout the process of cell differentiation, probably linked with the proliferative capacity of these cells.

When exploring the ribosomal content in tumor sections we found a striking reduction of 5.8S rRNA staining in tumor cells expressing high levels of the differentiation marker KRT20. This is in agreement with the idea that KRT20+ cells represent a post-mitotic differentiated population with low rDNA transcriptional activity. Of note, we also found a small proportion of tumor cells expressing both marks, which indicates the presence of differentiated cells with high ribosomal content. We have not analysed the role of these cells. However, a recent publication by the Sato group performed experiments of lineage tracing of CSCs and non-CSCs in human CRCs by means of a CRISPR/Cas9 based approach similar to the one recently use by our group (Cortina et al., 2017). They found that unlike Lgr5+ CSCs cells, most of the KRT20+ cells in human CRCs do not display long-term proliferation potential *in vivo* and therefore do not contribute to tumor growth. Yet, they observe the presence of a rare (about 4%) fraction of KRT20+ CRC cells with clonal expansion

capacity. These cells were able to generate large clones after tracing that contained Ki67+ cells (Shimokawa et al., 2017). This observation reinforces the notion of an existing small subset of differentiated cells in tumors with long term regeneration potential. It would be interesting to find out if these tumor cells are rDNA transcriptional active and display tumorigenic capacities.

On the other hand, we found that the expression of EPHB2 was more restricted than that of 5.8S rRNA in CRC. Although most of the EPHB2+ tumor cells were also positive for ribosomal content, we also noticed the existence of some cells with medium levels of EPHB2 that maintained substantial numbers of ribosomes. These results fit with the observations that the EPHB2^{med} population also displays rDNA transcription activity measured by EU incorporation.

Another aspect worth mentioning is the existence of a fraction of tumor cells negative for both EPHB2 and KRT20 but with elevated ribosomal content. One current hypothesis is that these cells comprise an intermediate state between the ISC-like and differentiated-like cells although we do not have formal evidences to prove it. Another possible explanation would be that these cells have silenced EPHB2 expression. Indeed, our laboratory has shown that EPHB2 can play a tumor suppressor role in the intestinal epithelium and overall low levels correlate with tumor malignancy during tumor progression (E Batlle et al., 2005).

An important aspect to consider is that the ribosomal content represents an indirect assessment of the rDNA transcription of the cells. While rDNA transcription activity can be switched off relatively fast, the ribosomal content requires more time to become extinguished upon differentiation. A plausible explanation is the long lifetime of a ribosome which oscillates between 6-7 days. Thus, there must be cells with decreased rDNA transcriptional activity but relatively high ribosomal content. It is tempting to speculate that a clear reduction of ribosomal content only occurs in terminally differentiated cells. This hypothesis is further supported by results obtained with *in vitro* models of tumor cell differentiation, which showed that whereas the rDNA transcription was completely downregulated after 3 days of induction of differentiation, the 5.8S ribosomal signal took up to 7 days to be completely washed out. Two independent studies in *Drosophila* encounter equivalent findings. Zhang and colleagues showed that the *Drosophila* ovarian germ line stem cells (GSC) displayed high levels of rDNA transcription compared to their differentiated daughters (Zhang et al.,

2014) . By contrast, a later study using this same animal model showed that despite progressive decrease of both nucleolar size and rDNA transcription during germline differentiation, there was an enhanced protein synthesis during the transition from self-renewal to differentiation (Sanchez et al., 2016). They hypothesised that enhanced rRNA synthesis in undifferentiated cells may prime differentiating daughters with an abundance of ribosomes, enough to sustain an enhanced translation rate during differentiation stages. A similar kinetic of rDNA transcription and protein translation could explain our observations in the normal intestinal epithelium and CRC.

Nucleolar heterogeneity linked to differentiation

Nucleolar size has been a well-studied parameter to characterize tumor cells. For many years pathologists realised that in general, cancer cells present bigger nucleoli compared to normal cells reflecting their high proliferative and growth demands (Derenzini et al., 2000).

In this study we have evidenced the presence of nucleolar size heterogeneity within tumors. We have shown that small nucleolar size positively correlates with the differentiation state of tumor cells. Nucleolar morphology visualized by POLR1A expression in both primary tumors and xenografts sections revealed that differentiated areas (KRT20+ and MUC2+) presented smaller nucleoli compared with non-differentiated ones. Since differentiated tumor areas also showed a decreased ribosomal content we hypothesise that small nucleolus reflects low rDNA transcription and ribosome production in these cells. In line with these observations we have also found that in our system of *in vitro* tumor cell differentiation there was a clear reduction of nucleolar size upon 4-OHT treatment in both LS174T and SW403 tumor cell lines.

Intriguingly, already in the 80s two biologists – Altmann and Leblond - denoted that the size of the nucleolus was gradually reduced from the crypt base to villus top of rat's small intestine. They concluded that gradual decrease taking place during stem cells migration correlated with their differentiation and the loss of their ability to synthesize rDNA. (Altmann & Leblond, 1982) (**Figure 1**). These observations suggest that reduced rRNA production is also a feature of normal differentiated cells, which goes in line with our own findings.

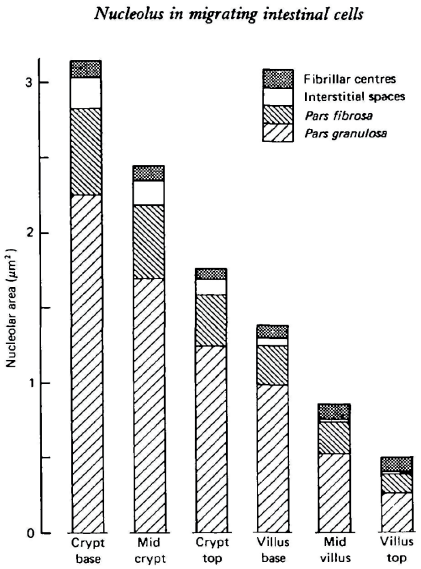

Figure 1: Nucleolar size is decreased from the crypt base to the villus top in rat's small intestine. Representation of the mean area of the nucleolus size at six successive levels along crypt and villus. The area of the nucleolus is divided in four compartments: *Fibrillar centers*, *intersticial spaces*, *pars fibrosa* and *pars granulosa*. All compartments are gradually reduced except for the fibrillary centers which remain constant from the crypt to villus axes. Adapted from (Altmann & Leblond, 1982).

Other recent studies reinforce these observations showing that ESCs are characterized for presenting both large nucleoli as well as high expression of nucleolar markers such as fibrillarin. On the contrary, ESC differentiation induced by Activin treatment downregulates the expression of nucleolar markers and correlates with a small and compact nucleolar structure (Watanabe-Susaki et al., 2014).

Characterization of RNA Pol I activity in CRC cells

POLR1A is a surrogate of rDNA transcription

rDNA transcription takes place in the nucleolus of the cell and is driven by the activity of the RNA Polymerase I (Pol I). This protein is a holocomplex made of different subunits. Our previous transcriptomics results showed that the expression of RNA Pol I main subunits (POLR1A-POLR1D) is upregulated in the EPHB2^{hi} normal and tumor cells and that the expression of these proteins correlates with their high rDNA transcription activity. In addition, we have also shown that protein levels of POLR1A subunit are enriched in the EPHB2$^{hi/med}$ compared to the EPHB2$^{lo/neg}$ cells from normal human colon mucosa. We have also observed that in tumor cell lines downregulation of rDNA transcription upon induction of differentiation is accompanied by a decrease of POLR1A. Overall, these experiments indicate that RNA Pol I levels correlate with the rDNA transcriptional activity of the cells. Therefore, we concluded that RNA Pol I could be a good surrogate of the transcriptional activity of tumor and normal cells.

POLR1A expression in tumor xenografts

By means of CRISPR-Cas9 technology, we genetically edited tumor organoids to express endogenous POLR1A fused to an EGFP reporter protein. Our results showed expression of EGFP in the nucleolus of these knock-in organoids where the rRNA is transcribed.

EU incorporation experiments confirmed that indeed EGFP-POLR1A^{high} (EGFP^{hi}) tumor cells represent an active rDNA transcription population whereas EGFP-POLR1A^{low} (EGFP^{lo}) displayed virtually no rDNA transcriptional activity.

Similar to what was previously observed with the 5.8S ribosomal staining analysis, we could not find tumor cells completely negative for POLR1A expression. However, we denoted that both the intensity and the amount of EGFP signal in the nucleus differed among tumor cells. Detailed analysis of nucleolar morphology and size revealed two clear distinguishable patterns that correlated with the differentiated state of tumor cells. We found that in most cases undifferentiated cells presented EGFP expression marking high proportion of the nucleus. On the contrary, tumor cells positive for differentiation markers such as KRT20 or KRT17 showed low EGFP signal usually found as small and condensed dots inside the nucleus. This pattern was also observed when we interrogated POLR1A expression pattern in primary tumor sections. Furthermore, these results are in line with the reduction of nucleolar size observed in CRC cell lines upon induction of differentiation suggesting that small nucleolus in differentiated cells reflects low POLR1A levels and reduction of rRNA synthesis capacity.

The absence of POLR1A negative cells suggest that a minimum level of this protein is required even in differentiated cells. Indeed, a recent publication has shown that under stress conditions such as nutrient starvation cells are able to reduce their rDNA transcription activity by inducing a rapid clearance of RNA Pol I-TIF-IA dimers, followed by the assembly of inactive RNA Pol I homodimers. This dual repressive mechanism is reverted upon nutrient addition, thus restoring cell growth (Torreira et al., 2017). These results evidence that RNA Pol I is highly regulated and cells have mechanisms to ensure low levels of this protein even in a scenario of silenced rDNA transcription. Based on these observations, we speculate that under specific conditions differentiated cells could switch from an inactive to active state by re-activating their rDNA transcription activity. Perhaps this mechanism is linked to plasticity of non-CSC, by which they are able to

regenerate the CSC pool as recently shown (Melo et al., 2017; Shimokawa et al., 2017).

Transcriptional characterization of POLR1A tumor cells

The genetic labelling of endogenous POLR1A in tumor organoids allowed us to purify tumor cells from xenografts expressing different EGFP-POLR1A levels by FACS. Whereas EGFP expression was found expressed in almost all epithelial tumor cells by immunofluorescence staining, by FACS the percentage of positive cells oscillated between 20-50% of the total epithelial population. We suspect that the focal localization of the EGFP in the nucleolus complicates its detection by flow cytometry.

When we interrogated the genetic expression of POLR1A populations we found that ISC genes such as *LGR5* or *SMOC2* were not enriched in the $EGFP^{hi}$ fraction. Although other stem cell genes such as *OLFM4* and *ASCL2* showed discrete enrichment in the $EGFP^{hi}$ population, the overall ISC gene signature was not significantly differentially expressed in the EGFPhi compared to the $EGFP^{lo}$ cells. Instead, the proliferative marker *KI67* was highly expressed in $EGFP^{hi}$ tumor cells as well as other cell cycle genes such as *CDC25*. Indeed, immunofluorescence analysis revealed high POLR1A expression in KI67 positive areas of tumor xenografts (**Figure 2**). A possible explanation for the lack of differential expression of the ISC gene signature among POLR1A populations is that POLR1A high expressing cells represent an actively proliferating population whereas the POLR1A low cells encompass both differentiated and stem cell quiescent tumor cells. Our laboratory recently showed that about half of the CRC-SCs labelled by LGR5 are negative for the expression of Ki67, suggesting the existence of a quiescent tumor stem cell population in CRCs (Cortina et al., 2017). These results are also in agreement with the expression of RNA binding protein Mex3A in the POLR1A low population, which in normal intestinal epithelium marks a slow proliferating stem cell population (Barriga et al., 2017).

On the other hand, the $EGFP^{lo}$ cell fraction showed a clear enrichment for markers of intestinal differentiation such as *MUC2*, *DLL1*, *KRT20* suggesting that POLR1A low cells represent a population of mature differentiated cells from both mucosecriting and enterocyte lineages.

Another factor to consider is the cell cycle regulation of rDNA transcription. It is known that the rRNA synthesis is a cell cycle regulated process that

is maximal during S- and G2-phase, subsides during mitosis, and then slowly recovers during G1-phase (Comai, 2004; Ingrid Grummt, 2010). Part of this regulation is through the inhibition of the transcriptional factors UBTF and SL1 through several phosphorylation events. Although we have not explored whether levels of RNA Pol I are also decreased in early G1 or mitotic phases, we cannot fully rule out the possibility that our EGFP^{lo} fraction of cells encompasses cells in these cell cycle phases. This would mask the differential expression of stem and differentiation programmes between POLR1A populations.

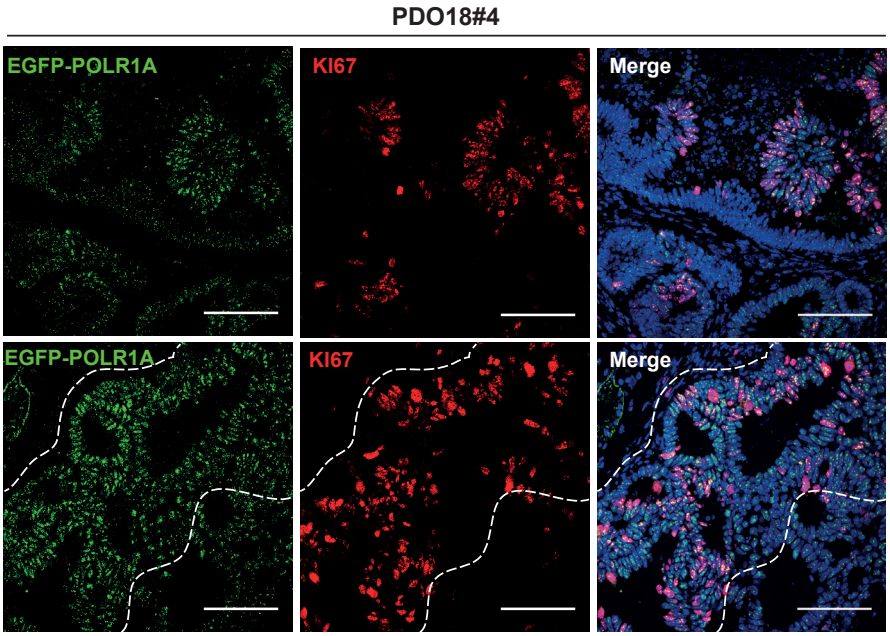

Figure 2: KI67 expression is restricted to POLR1A high areas in tumor xenografts. Confocal images of EGFP-POLR1A (green) and KI67 (red) expression in tumor xenografts derived from EGFP-POLR1A knock-in PDO18 clone #4. Note that most of the Ki67+ cells are located in EGFP-POLR1A-high tumor glands. Scale bar represents 100µm.

Functional characterization of POLR1A tumor cells

We found that POLR1A high cells were more efficient generating organoids *in vitro* than the POLR1A low. Of note, the few organoids that grew from POLR1A low cells regained the EGFP expression at similar levels of the POLR1A high derived organoids. This could simply be due to technical limitations (i.e. suboptimal purification of EGFP+ cells by FACs) or explained by the existence of tumor cell plasticity. This concept has been also evidenced in Shimokawa et al., where re-appearance of LGR5+ cells was observed in single LGR5-GFP- cell-derived organoids or LGR5-ablated organoids. Moreover, plasticity effect was also observed *in vivo*, where KRT20+ cells reverted to LGR5+ cancer stem cells (CSCs) and contributed to tumor regrowth after LGR5+ CSC ablation (Shimokawa et al., 2017). The high clonogenic capacity of POLR1A high tumor cells was also reflected on their tumorigenic potential. Subcutaneous injection of FACS-sorted POLR1A populations revealed that tumor-initiating capacity was enriched in the POLR1A high fraction.

These results led us to hypothesise that the tumorigenic capacity of cancer cells substantially relies on high rDNA transcription activity, which segregates with the non-differentiated state. We think that rDNA transcriptionally active cells encompass both CSCs (Lgr5+) and Lgr5- tumor cells. Although CRC-SCs cells display tumor initiation properties and drive tumor growth, we speculate that colorectal tumors are also sustained by the contribution of other tumor cells with elevated rDNA transcriptional potential. This idea has been supported by another recent study showing that mouse colorectal tumors are maintained by proliferating Lgr5- cells after genetic ablation of Lgr5+ CSCs in mouse models of CRC (Melo et al., 2017). Interestingly gene expression analysis of these CRCs before and after 24h of Lgr5+ ablation indicate an upregulation of gene signatures related to DNA replication as well as rRNA processing and metabolism, suggesting that the remaining tumor cells that sustain CRC growth after CSCs ablation display proliferative and rDNA transcriptional properties.

rDNA transcription and cell differentiation: chemical versus genetic RNA Pol I inhibition

Our results demonstrate that rDNA transcriptional is downregulated during the process of normal and tumor cell differentiation. This transcriptional silencing seems to be a consequence of the differentiation process and probably linked to a proliferation shut down, the

question is whether rDNA synthesis is required to maintain the undifferentiated state of tumor cells.

We found that inhibition of RNA Pol I at protein level using BMH-21 induced differentiation in tumor cell lines as well as in colorectal cancer organoids *in vitro*. However, transcriptional downregulation of POLR1A mRNA by siRNA did not completely reproduce the differentiation effect observed with BMH-21 treatment. One possible explanation to justify this incongruence is that BMH-21 unexpectedly acts as an inhibitor of other transcriptional mechanism required to sustain the CSC phenotype such as WNT-driven transcription. Considering that this molecule intercalates into the GC rich regions of the DNA, it feasible to think that BMH-21 could impair the β-catenin/TCF4 complex binding to the promoter region of target genes turning into a shutdown of the pathway.

Another possibility is that BMH-21 induces a global transcriptional silencing in which β-catenin and TCF4 transcription are also affected. However, in contrast to our scepticism with respect to BMH-21 effect, a recent published study have shown that treatment of human embryonic stem cells (hESCs) with the RNA Pol I inhibitor CX-5461 resulted in a reduced expression of specific stem cell markers and increased expression of specific germ layer markers (Woolnough, Atwood, Liu, Zhao, & Giles, 2016) suggesting that downregulation of rDNA transcription by RNA Pol I inhibition induces ESC differentiation.

WNT signalling as a possible mechanism controlling rDNA transcription during cellular differentiation

Our model of *in vitro* tumor cell differentiation showed that WNT silencing induces downregulation of POLR1A expression that, in turn, decreases the rDNA transcription activity in differentiated cells.

RNA sequencing analysis revealed that after WNT blockade not only POLR1A expression is downregulated but also the transcription of multiple genes related to ribosome biogenesis process including several RNA Pol I structural subunits as well as transcription factors required for rRNA synthesis. In addition, we also found a general downregulation of genes codifying for proteins involved in the processing of pre-rRNA as well as ribosomal proteins constituents of the mature ribosomes. These data suggest that induction of differentiation by WNT blockade impinges on the overall expression of nucleolar related genes and could potentially explain why we were unable to restore the rDNA

transcriptional activity in differentiated cells by overexpressing only POLR1A and the transcription factor TIF-IA.

WNT signalling is the main pathway maintaining stem cell identity by enhancing transcription of stem cell genes and blocking the expression of the differentiation program. ChIP sequencing analysis of β-catenin in mouse intestinal stem cells revealed a clear binding of this transcription factor in the promoter region of TIF-IA (Schuijers et al., 2015) (**Figure 3A**). Although we haven't extensively explored this possibility, our preliminary ChIP data shows that both β-catenin and TCF4 probably bind to the promoter region of TIF-IA in CRC cell lines (**Figure 3B**). These preliminary results suggest that regulation of rDNA transcription during cellular differentiation is directly driven by WNT signalling and imply that one of the main functions of beta-catenin/TCF transcription in normal and tumor stem cells is to ensure elevated rDNA synthesis.

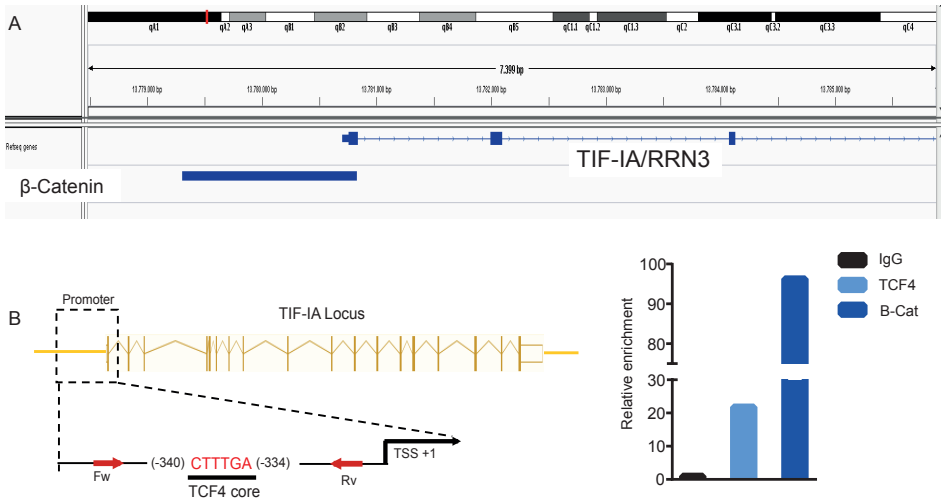

Figure 3: β-catenin binds to the promoter region of TIF-IA/RRN3. (**A**) ChIP seq analysis of β-catenin in mouse normal intestinal cells. Data obtained from (Schuijers et al., 2015) (**B**) Schematic representation of primer design used for ChIP analysis. ChIP results showing the relative enrichment of β-catenin and TCF4 binding in TIF-IA/RRN3 promoter.

A role for MYC in WNT-driven ribosome biogenesis

The downregulation of rDNA transcription upon WNT blockade is linked to the decrease of the proliferation rate of differentiated cells. It has been reported that part of the proliferative effects that WNT exerts on its target cells is through the activation of its own target MYC (Van de Wetering et al., 2002). Certainly, we have shown that *in vitro* differentiation of CRC cell lines led to a decrease of MYC expression both at mRNA and protein levels. On the other hand, several studies have reported the role of MYC controlling different aspects of the ribosome biogenesis process. Interestingly, two independent studies have shown that MYC is able to directly enhance rDNA transcription through its binding to the rDNA promoter by recruiting transcriptional factors required for rDNA transcriptional initiation and also enhancing histone acetylation for the establishment of an open and accessible chromatin state in rDNA promoters (Arabi et al., 2005; Grandori et al., 2005). Bringing all this data together, we sought to explore whether regulation of rDNA transcription by WNT signalling could be MYC mediated.

Our results show that MYC restoration in differentiated CRC cell lines rescued not only POLR1A and TIF-IA expression but also the expression of genes required for rDNA transcription and maturation, including all the RNA Pol I structural subunits, factors of the pre-initiation complex as well as pre-rRNA processing proteins. Indeed, MYC overexpression resulted in a complete recovery of the rDNA transcription activity of CRC cells upon induction of differentiation.

We also found that MYC restoration also rescued the ribosomal content of the differentiated cells. This was observed by immunofluorescence analysis of the 5.8 rRNA staining as well as by interrogating the expression of genes encoding for the ribosomal proteins (RPS and RPL). While differentiated control cells displayed a general decrease of ribosomal gene expression, this was rescued in differentiated overexpressing MYC cells. In line with these findings, several studies have reported that MYC also regulates the transcription of genes encoding for ribosomal proteins through RNA pol II-dependent transcription (Boon et al., 2001; Schlosser et al., 2003). Furthermore, suppression of MYC expression in a mouse model of osteosarcoma causes reduced expression of a multitude of ribosomal protein genes (Wu et al., 2008). Therefore, in addition to controlling nucleolar function, MYC may directly coordinate the RNA pol II-dependent

transcription of a substantial number of genes that encode for RPS and RPL proteins.

Another important observation was related to the differentiated state of MYC overexpressing cells. We found that although the downregulation of the stem cell genes was similar in both control and overexpressing MYC cells upon induction of differentiation, the transcriptional increase of differentiation targets was reduced in MYC overexpressing cells compared to controls. One possible explanation is that for unknown reasons the WNT blockade exerted by the dominant negative form NTCF4 in MYC overexpressing cells is not as robust as in control cells. To explore this possibility we measured the TOP/FOP activity in LS174 NE (WT), LS174T NE_Empty and LS174T NE_MYC treated or not with 4-OHT for 48h and 72h. We observed that in all cases the TOP activity was decreased after 4-OHT treatment (reflecting the WNT blockade) (**Figure 4**).

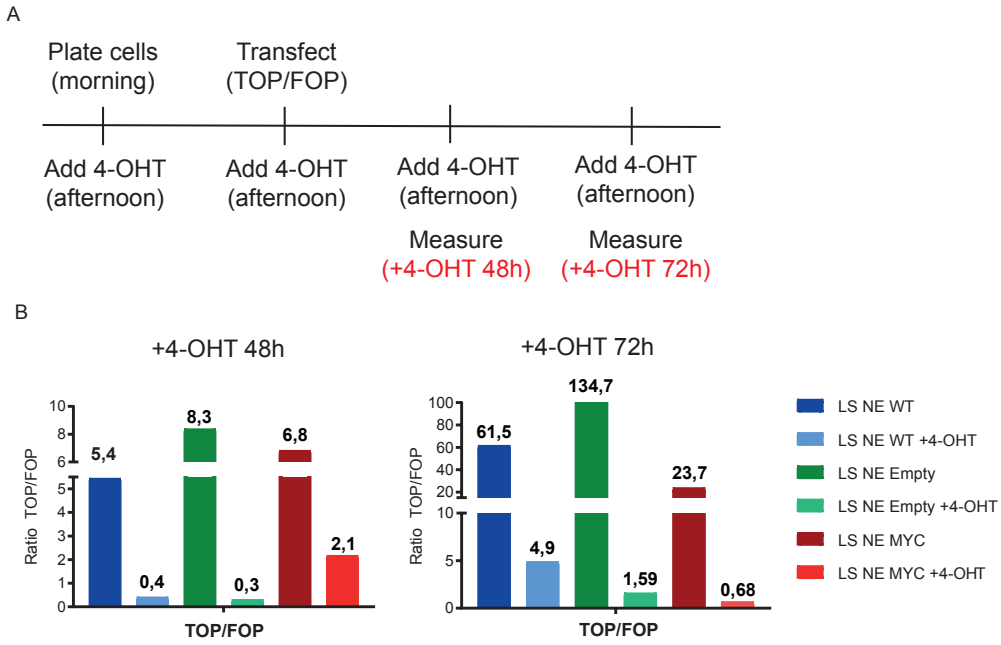

Figure 4. TOP/FOP activity is reduced after 4-OHT treatment in control and MYC overexpressing LS174T colorectal cancer cell lines. (**A**) Experimental design. (**B**) Representation of the TOP/FOP ratio in LS174T WT, LS174T NE_Empty and LS174T NE_MYC before and after 4-OHT treatment during 48h and 72h. n=1.

The second possibility is that somehow MYC expression is partially inhibiting the induction of differentiation by repressing the expression of differentiation target genes.

One consequence of MYC expression in differentiated tumor cells was the complete recue of the proliferation capacity in these cells. We found that the expression of proliferation related genes was maintained upon induction of differentiation in MYC overexpressing cells. Cell cycle analysis confirmed that MYC overexpressing CRC cell lines were able to maintain their proliferative state despite the loss of stem cell gene expression and gain of the differentiation program. This results are in line with published observations *in vitro* and *in vivo* (Sansom et al., 2007; Van de Wetering et al., 2002).

To explore whether the proliferation rescue observed in MYC overexpressing cells upon induction of differentiation was related to reactivation of rRNA synthesis we sought to block this activity in these cells. We show that knocking down both POLR1A and TIF-IA mRNAs is sufficient to block the proliferative capacity of MYC overexpressing cells *in vitro*. These findings are in line with the observation that in Eu-MYC transgenic mice, loss of one allele of the ribosomal protein Rpl24 or Rpl38 is sufficient to inhibit the tumorigenic effect exerted by MYC overexpression (Barna et al., 2008). Overall, these observations are in agreement with the hypothesis that part of the oncogenic effects driven by MYC overexpression is caused due to an enhancement of the rDNA transcription activity as well as ribosomal production in tumor cells. Interestingly, in experiments of CSC ablation in mouse and human CRCs it was found that the regenerative response that replenishes the CSC pool correlates with increase MYC signalling. It would be interesting to understand to which extent high nucleolar activity driven by MYC expression drives this process (Melo et al., 2017).

We are currently exploring whether the rescue of the rDNA transcription and proliferation capacity in differentiated tumor cells by MYC overexpression is also translated in a reestablishment of their tumorigenic capacity. We envision that the rDNA transcription activity of tumor cells is an indispensable requirement to maintain their tumorigenic property besides the genetic programme expressed.

Implications of our results for the CSC hierarchical model

Overall, our observations indicate that CRCs are composed by cells displaying distinct rDNA transcriptional activity. This property segregates with distinct

numbers of ribosomes and differential protein synthesis. We show that there is a strong link between increased rDNA transcription and ribosome biogenesis and the expression of the stem cell program in CRC. Our data indicate that CSCs are characterized by elevated nucleolar activity and capacity to produce ribosomes. In contrast, differentiated tumor cells appear to be able to synthesize less proteins. The heterogeneity of nucleolar activity is reminiscent of that present in the intestinal epithelium, which suggest that it is tightly controlled by stem/differentiation transition. WNT signalling, the main pathway involved in this switch appears to control nucleolar activity at multiple levels. It would be interesting to analyse nucleolar patterns in other tissues and tumors that expand thanks to the activity of WNT+ stem cells.

Tumorigenic capacity is driven by genetic and epigenetic alterations in oncogenes and tumor suppressor genes. CSC and non-CSCs within a given tumor share these mutations yet long-term tumorigenic potential is restricted to CSCs. The reasons that explain decreased tumorigenicity of non-CSCs are not well understood. We propose a model in which the loss of tumorigenic potential of differentiated tumor cells is directly the result of loss of their capacity to synthesize new proteins due to lack of ribosomes. Although still speculative, the implications of this model are multiple. First, tumor initiating potential (a surrogate for stemness) could in principle be uncoupled from the expression of the stem cell genes as differentiated cells that retain nucleolar functions might be as tumorigenic as CSCs. Second, targeting CSCs through specific surface markers such as LGR5 (Melo et al., 2017; Shimokawa et al., 2017) triggers a subsequent regeneration of the CSC pool. We speculate that this regenerative response may occur through LGR5- cells that retain nucleolar activity and thus could proliferate and revert. Third, therapies aimed at blocking nucleolar activity may be considered as anti-CSC therapies. In this regard, a recent work has shown that oxaliplatin, a drug commonly used to treat CRC patients, acts by blocking rDNA transcription (Bruno et al., 2017). Fourth, the relevance of WNT pathway in CRC is to sustain high nucleolar activity and protein synthesis that enable oncogene function in tumor cells. Without nucleolar activity, the function of oncogenes will not be fully penetrant. MYC appears to be the key mediator of this process as it can substitute the function of WNT-driven transcription. We are currently performing experiments to address the validity of all these hypotheses.

Conclusions

The main conclusions extracted from this research project are:

1. CoSCs and CRC-SCs purified from primary CRCs based on their EPHB2 surface levels are enriched in nucleolar and ribosome biogenesis related genes.

2. CRCs are composed by cells displaying distinct rDNA transcriptional activities. This property also correlates with different ribosomal content and protein synthesis capacity.

3. Tumor cells displaying high rDNA transcription activity represent an undifferentiated and proliferative population within CRCs. On the contrary, differentiated tumor cells appear to be rDNA transcriptional inactive with dismal capacity to produce ribosomes and synthesize proteins.

4. Elevated rDNA transcriptional capacity segregates with high *in vitro* clonogenic potential and *in vivo* tumorigenic capacity.

5. The heterogeneity of nucleolar activity is reminiscent of that present in the intestinal epithelium.

6. WNT signaling appears to be the main signaling pathway regulating nucleolar activity in normal and tumor cells.

7. The WNT target MYC occurs to modulate several nucleolar related processes connecting WNT signaling and nucleolar biology.

8. MYC overexpression in differentiated tumor cells is able to rescue the expression of nucleolar related genes as well as the rDNA transcription activity.

9. Restoration of rDNA transcription in differentiated tumor cells by MYC overexpression rescues their proliferation capacity.

10. Inhibition of rDNA transcription by downregulation of RNA Pol I is sufficient to induce cell cycle arrest in MYC overexpressing cells.

Methods

Cell culture

HEK-293T and colorectal cancer (CRC) cell lines LS174T and SW403 used in this study were obtained from the American Type Culture Collection (ATCC, USA). Cells were cultured in standard conditions in DMEM (Gibco) supplemented with 10% FBS (Gibco). Lentiviral-transduced cells were selected by adding puromycin (Invivogene, 2 µg/mL), hygromicin B (Thermo Fisher, 200 µg/mL) or blasticidin (Invivogene, 10 µg/mL) to the media to select the stable expression of the transgene.

Vector constructs and viral production

FUW-CMV-ERT2 was constructed by PCR amplifying the ERT2 domain from pCMV-CRE-ERT2 (Feil et al. 1996) and cloning it into a modified FUGW (Lois et al. 2002) lentiviral vector backbone. To obtain FUW-CMV-NTCF-ERT2, NTCF was then PCR amplified from the pCDNA3.1-NTCF-NLS (Van de Wetering et al. 2002) and cloned in frame upstream of ERT2 from FUW-CMV-ERT2. The vector is bicistronic as it possesses an IRES sequence downstream of the ERT2 followed by a puromycin resistance cassette for selection of transduced cells.

The pLenti-CMV-POLR1A and pLenti-CMV-TIF-IA were constructed by PCR amplifying the POLR1A and TIF-IA genes from the pCR4-TOPO-POLR1A (Biocat, ref. BC143345-TCH1003-GVO-TRI) and GFP-RRN3/TIF-IA (Addgene, ref. 17661) vectors respectively. The both genes were amplified with Gateway adaptors using the Phusion High-fidelity Polymerase (NEB). The PCR products were cloned first into the pDONOR221 and then into the pLenti-CMV-Blast DEST (Adggene, ref. 17451) by Gateway recombination reaction following the manufacturer's protocol (Invitrogene). The control vector pLenti-CMV-Empty was obtained from Addgene (ref. 17486). pLenti-CMV-MYC, was generated by sequential Gateway recombination reaction of pTRIPZ_MYC (kindly given by Peter Jung), with pDONOR221 and the final destination vector pLenti-CMV-Blast DEST (Adgene, ref. 17451).

Viral production was accomplished by transient transfection of HEK-293T producer cells wiht the lentiviral construct together with viral envelope vector (pCAGGS_VSVG), packaging vector (pCAG_KGPIR) and retrotranscriptase vector (pCAG_RTR2) in the following proportions (Hanawa et al. 2002): 50% lentiviral construct, 10% envelope vector, 30% packaging vector and 10% retrotranscriptase vector. Polyethylenimine (PEI)

(Polysciences Inc. 23966) was used as a transfection reagent at 1 µg/cm^2. DNA and PEI were mixed at 1:5 ratio and diluted in 150 mM NaCl up to 20 µL/cm^2, incubated at room temperature for 20 min and added to HEK-293T cells. Viral supernatants were collected at 48h and 72h post-transfection, filtered using 0.45 µm PVDF filters, supplemented with polybrene (8µg/mL) (Sigma, Ref. H9268), FBS 10% and used to transduce target cells by O/N incubation. Cell lines stably expressing the corresponding constructs were maintained under antibiotic selection.

In vitro treatments

4-hydroxytamoxifen (4-OHT, Sigma H7904): CRC cell lines expressing the NTCF-ERT2 construct were seeded in 6-well plates at 10% confluence. 24 h after seeding 1 µM of 4-OHT was added to the medium. After 72 h of incubation, gene expression, cell cycle and rDNA transcription analysis were performed. For cristal violet experiments the treatment was extended up to 7 days. 4-OHT was daily added.

BMH-21: The BMH-21 inhibitor (Sigma, SML1183) was added to the cells at 0,5 or 1 µM during 48 hours. After treatment cells were collected for gene and protein expression analysis.

CRISPR/Cas9 plasmids construction

Donor plasmid

The donor plasmid for the knock-in of EGFP at the N-terminus of POLR1A by CRISPR/Cas9 was generated as follows: the insertion cassette EGFP-linker flanked by two homology arms (HA) of 750 bp was synthetized (Thermo Fisher). The 5' and 3' HA were designed to specifically recombine and insert the cassette at the ATG site of the POLR1A locus in order to generate a N-terminus EGFP-linker-POLR1A fusion protein. The insertion cassette contained the Gateway adaptors to facilitate the cloning into the pDONR-RFP destination vector. Finally, by Gateway recombination the construct was cloned into the pDONR-RFP vector.

sgRNA design

Small guide RNAs were designed using the http:// crispr.mit.edu web tool. To select for the most suitable sgRNAs, the following criteria were applied: i. localization of the sgRNA as close as possible to the desired site of insertion to maximize homologous recombination efficiency, ii. Cas9-mediated double strand break upstream of the ATG codon to prevent NHEJ-induced indels in the ORF, iii. guides selected to anneal at the intersection between the 5' homology arm and 3' homology

arm so that the donor plasmid is protected from Cas9 cut, iv. minimum off-target score according to http://crispr.mit.edu and maximum Doench activity score (Doench et al. 2014). To target the POLR1A locus the following guide was used: sgRNA guide3 (CTTGGAGATCAACATCCTCC).

px330-IRFP Cas9 plasmid

px330 Cas9 plasmid from Feng Zhang's laboratory was obtained from Addgene (ref. 42230) and was modified by the introduction of a SV40promoter-IRFP expression cassette downstream of Cas9 by FseI - EcoRI. In addition, the BbsI site of IRFP was silenced by site-directed mutagenesis. SgRNAs were cloned in px330-IRFP as described in http://www.genome-engineering.org/crispr/wp-content/uploads/2014/05/CRISPR-Reagent-Description-Rev20140509.pdf

Culture and expansion of patient-derived tumor organoids (PDOs)

Primary colorectal tumor cells were grown as organoids embedded in 30µL drops of BME2 (Basement Membrane Extract 2, AMSbio). PDO18 and PDO19b PDOs were kindly provided by Dr Hans Clevers and cultured with the media described by the Clevers lab (Van de Wetering et al. 2002). PDO7 was given by G. Stassi (University of Palermo) and cultured using the following media recipe (Advanced DMEM/F12, 10 mM HEPES, 1× Glutamax; 1× B-27 without retinoic acid (Life technologies), 20 ng/mL bFGF (Invitrogene); 50 ng/mL EGF (Prepotech), 1 µM LY2157299 and 10 µM Y27632 (Sigma), recombinant R-SPONDIN1 (1 µg/mL) (home-made) and recombinant Noggin (100 ng/mL) (Preprotech). All cells were tested weekly for mycoplasma contamination with negative results.

For expansion, organoids embedded in BME drops were mechanically disaggregated and incubated with trypsin during 10 min at 37ºC. To obtain single cells, organoids were pipetted up and down until single cells were microscopically observed. Cells were washed twice with Wash Buffer (WB: Advanced DMEM/F12, 10 mM HEPES and 1xGlutamax) single cell pellets were resuspended in a mixture of 70% BME / 30% PBS (phosphate buffered saline) suplemented with 10 mM HEPES and 1XGlutamax. Subsequently cells were plated in 30 µL drops in a pre-warmed 6-well plate format. Drops were polymerized at 37ºC 15 min and finally the organoid medium was added.

CRISPR/Cas9 knock-in generation in PDOs

Two PDOs (PDO7 and PDOP18) were CRISPR/Cas9 modified to generate tumor cells expressing an EGFP-POLR1A fusion protein from the endogenous locus.

Nucleofection

PDOs were trypsinized to obtain singles cells. 2 millons of single cells were nucleofected with 7 µg of pDONR-RFP plasmid and 2 µg of px330-IRFP Cas9 corresponding plasmids using Lonza nucleofector kit V (VVCA-1003) and program A-32 in an Amaxa-II nucleofector following manufacturer protocol.

FACS strategy and generation of single cell-derived organoids

Nucleofected cells were embedded in BME2 drops and cultured for 2-3 days in organoid medium. To select the cells containing both plasmids, double positive cells (RFP+ and IRFP+) were isolated by FACS and cultured again in 3D for about 18-20 days. After this period it was observed the emergence of a cell population that expressed the EGFP marker gene suggesting that some cells had integrated the reporter construct. Then, the EGFP positive cells were again isolated by FACS and seeded in a 96-well format in 5 uL BME2 drops to derive single-cell clones. Wells with more than one cell per drop were discarded.

Specific genotyping PCRs

Single-cell derived clones were lysed in buffer consisting of 10 mM Tris, 1 mM EDTA, 1 % Tween 20 and 0.4 mg/mL proteinase K for 1 h at 55 °C. The lysate was directly used in the specific integration PCR. For the 5' specific integration PCR a forward primer upstream of the 5' homology arm and a reverse primer at the beginning of the inserted cassette were used. Similarly, for the 3' specific integration PCR a forward primer at the end of the inserted cassette and a reverse primer downstream of the 3' homology arm were used. The PCR conditions were as follows: DNA Polymerase (BioTools #10012-4103) 95 ºC 2 min (95 ºC 30 s – 55 ºC 30 s – 72 ºC 1:30 min) x 38 72 ºC 5 min - hold 16 ºC. Used primer sequences are shown in **Table 1**.

Locus-insertion		Primer
EGFP-POLR1A	5' specific	F: CTGATAACTTCTTTAGCCAAAGT
		R: GCTGAACTTGTGGCCGTTTA
	3' specific	F: ACATGGTCCTGCTGGAGTTC
		R: AAGATGTACAGACAGCTGAACAAAT

Table 1: Primers used for the specific integration PCR

Southern blot

Clones that were correctly targeted, based on 5' and 3' specific integration PCRs, were further checked for off-target cassette insertions by southern blot. Genomic DNA was extracted using the GenElute Mammalian Genomic DNA Miniprep Kit (Sigma G1N70-1KT). 10 ug of genomic DNA were digested overnight with the appropriate restriction enzyme (**Table 2**) and separated on a 0.8 % agarose gel. DNA fragments were transferred by capillarity to a Hybond-N+ membrane (GE Healthcare RPN303B) overnight. Probes were generated by PCR (protocol as described in the previous section, primers in **table 2**) and radioactively labelled with α-[32P]dCTP using the MegaPrime labelling kit (GE Healthcare RPN1604). Hybridization with the probe was carried out overnight at 60 ºC. Probes were detected using a Phosphoimager plate.

Locus-insertion	Primer	Restriction enzyme
EGFP-POLR1A	F: CCACCATGGTGAGCAAGGGCGAGG R: TTACTTGTACAGCTCGTCCATGCC	BglII

Table 2. Primers used for southern blot probe generation and restriction enzyme used to digest the construct.

Confocal imaging of CRISPR/Cas9 labeled PDOs

EGFP-POLR1A labeled PDOs were grown for 2 weeks without trypsinization and then harvested using Matrisperse Cell Recovery Solution (Corning, 354253) in order to remove the BME. PDOs were seeded at 100.000 cells per well in microscopy chamber slides in thin layers of BME (20 µL per chamber). Organoids were incubated at 37 ºC for 30 min with Hoechst 33342 1:1000 (Molecular Probes, R37605) to stain the nucleus. Images were taken with a LEICA SP5 confocal microscope.

Disaggregation of normal and tumor human samples

Fresh tumor samples together with their corresponding normal tissue were obtained from CRC patients treated at Hospital del Mar or Hospital Clinic (Barcelona, Spain).

Tumor samples were incubated for 20-30 min at RT in PBS containing 100X penicillin/streptomycin (Gibco). Tumor pieces were then minced with a sterile razor blade to generate small pieces and subsequently incubated during 15 min at 37ºC with HBSS (Lonza) containing 166 U/mL of Collagenase IV (Sigma; 100 U/mL). Pieces were homogenized by pipetting and incubated for an additional 15 min at 37ºC. Pieces were mechanically homogenized and consecutively passed through consecutive 18G and 21G needles. Single cells were collected by sequential filtering through cell strainers of 100 µm → 70 µm → 40 µm (BD Falcon). After centrifugation at 1500 rpm for 5 min, cells were resuspended in 5 mL ammonium chloride (0.15M; Sigma Aldrich) and incubated 3 min at room temperature to lyse erythrocytes. After two washes with HBSS single cells were resuspended in wash buffer (WB: ADVANCE DMEM/F12, 10mM HEPES and 1xGlutamax).

The protocol used for disaggregation of normal colon samples is described in detail in (Jung et al. 2011). Briefly, normal mucosa was minced with a sterile blade into small pieces and incubated with a mixture of antibiotics Normocin 1:250 (Invivogen), Antibiotic-Antimycotic 1:100 (Thermo Fisher Scientific)) for 15 min at room temperature. After incubation, pieces were washed twice with PBS and then incubated in 10mM DTT (Sigma) in 30 mL of PBS for 5 min at RT. Samples were transferred to 30 mL ice-cold 8 mM EDTA in PBS and slowly rotated for 60 min at 4ºC (cold room). The supernatant was replaced with fresh ice-cold PBS samples were shaken vigorously to yield a supernatant enriched in colonic crypts. The supernatant was transferred to a new 15 mL falcon tube and FBS (Gibco) was added to a final concentration of 5% to

minimize aggregation of the crypts.

After centrifugation at 40xg supernatant was discarded and replaced by WB with 5% FBS (Gibco), this washing procedure was repeated 3 times). Finally, to obtain single cells, crypts were incubated for 15 min at RT with disaggregation media: ADF, 10 mM HEPES, 1xGlutamax, N-2, B-27 without retinoic acid (Invitrogen), 10 µM Y-27632 (MedChem Express), Optional: 2.5 µM PGE2 (Sigma), 0.4 mg/mL Dispase (354235, BD Biosciences). Crypts were gently syringe through a 1.2 mm needle until a single-cell enriched population was observed microscopically. Finally, cells were sequentially passed through 100, 70, and 40 µm mesh filters (BD Biosciences) and washed with WB.

Generation and disaggregation of tumor xenografts

For the generation of tumor xenografts, wild type PDOs or EGFP-POLR1A CRISPR/Cas9 engineered PDOs were grown *in vitro* in BME drops for 7 days. PDOs were incubated with cell recovery solution during 30 min at 4ºC in order to dissolve the BME. (One drop of BME was separated, tripsinized and counted in order to have an estimation of the number of single cells per BME drop.) PDOs were washed twice with PBS to assure the complete removal of the BME. A range between 150,000 - 2 million cells per flank (depending the PDO) were injected subcutaneously as 7-days grown organoids into NOD/SCID female mice in 50% BME2-HBSS with a maximum of 4 xenografts per animal. Tumor volume was measured with manual calipers and using the formula (length x width x height)/2. Mice were sacrificed when tumors reached a maximum of 300 mm^3 the animal displayed ulceration in one of the xenografts or showed symptoms of distress. Xenografts were resected and disaggregated as previously described in (Merlos-Suárez et al. 2011). Briefly, tumor xenografts were cut in small pieces using a sterile blade, disaggregated with collagenase IV during 30 min at 37ºC and filtered through 100, 70, and 40 µm mesh filters (BD Biosciences). Tumor cells were incubated with ammonium chloride in order to remove blood cells. Finally single tumor cells were counted and resuspended with WB (described in the previous section).

Staining and isolation of EPHB2 tumor cell populations

One millon of normal or tumor single cells from primary tumor samples were resuspended in 0,5 mL of staining buffer (SB: Advanced DMEM/F-12, 10 mM HEPES, 1 x Glutamax and 10 µM Y-27632 (MedChem Express) with anti-EpCAM (1:150 ref. R&D

AF660) and anti-EPHB2 (1:50) primary antibodies during 1 hour at 4ºC. Cells were then washed three times with WB and incubated with the secondary antibodies α-goat-Alexa488 (1:250; ref. Invitrogene A11055) and α-mouse-APC (1:250; ref. Invitrogen A31571) for 1 hour at 4ºC.

EPHB2 staining of tumor cells from xenografts was performed using primary coupled antibodies, hEPCAM-PeCy7 (1:150 ref. eBioScience 25-9326-42) and hEPHB2-APC (1:100, Genentech, Mab 2H9). Fluorescence Activated Cell Sorting (BD Aria Fusion FACS or Aria FACS) was used to separate 2000 cells fror each population of interest. Briefly, debris were discarded by FSC-A/SSC-A gating, aggregates by FSC-A/FSC-W gating, alive cells by DAPI negative signal and human EPCAM positive cells were selected. Within the EPCAM positive cells the EPHB2 high and low expressing populations were sorted directly into 45 µL of picoprofile lysis buffer. RNA and cDNA was extracted and amplified as previously described in (Gonzalez-Roca et al. 2010).

Isolation of EGFP-POLR1A tumor cell populations

EGFP-POLR1A CRISPR/Cas9 engineered PDOs were disaggregated as is described previously and stained with hEPCAM-PeCy7 in order to select for epithelial tumor cells. From EPCAM positive cells EGFP levels were analyzed and 2000 cells of each population were sorted directly into picoprofile lysis buffer. RNA and cDNA was extracted and amplified as previously described in (Gonzalez-Roca et al. 2010).

RNA extraction, cDNA reaction and RT-qPCR

For CRC cell lines total RNA was extracted using TRIzol (Invitrogen) followed by RNA column purification using the RNA PureLink Kit (Ambion). Briefly, cells were scraped from cell culture dishes (Costar) and homogenized by pipetting in TRIzol solution. After phase separation with chloroform, the RNA from the aqueous phase was purified with the RNA PureLink Kit and quantified by Nanodrop spectrophotometer. cDNA was produced with the High-Capacity cDNA Reverse transcription Kit (Applied Biosystems) following the manufacturer's instructions.

To analyze gene expression changes RT-qPCR was performed using 5 ng of cDNA per each real-time qPCR well. Real-time qPCRs were performed with TaqMan assays (ThermoFischer) and TaqMan Universal PCR Master Mix in triplicates following manufacturer's instructions (Applied Biosystems 4369016). The TaqMan assays used in this study are listed in table 3. Gene expression levels were normalized using the endogenous control PPIA and B2M for each sample and differences in target gene expression were determined using SDS 2.4 or StepOne 2.2 plus software. Error bars represent standard deviation of samples performed in triplicate.

Gene	Taqman probe
B2M	Hs99999907_m1
PPIA	Hs99999904_m1
EGFP	Mr04097229_mr
LGR5	Hs00173664_m1
SMOC2	Hs0159663_m1
ASCL2	Hs00270888_s1
MYC	Hs00905030_m1
MKI67	Hs01032443_m1
POLR1A	Hs00209909_m1
POLR1B	Hs00219263_m1
RRN3/TIF-IA	Hs04398176_m1
KRT20	Hs00300643_m1
KRT17	Hs00356958_m1
EMP1	Hs00608055_m1
SDCBP2	Hs00210404_m1
HEPACAM2	Hs01650957_m1
MUC2	Hs03005094_m1
DLL1	HS00194509_m1
ATOH1	HS00944_s1

Table 3: RT-qPCR Taqman probes

Gene expression analysis

Microarray processing

A total of 30 samples were analyzed in this study, which were hybridized in two different Affymetrix platforms: Human Genome U133 Plus 2.0 Array and PrimeView Human Gene Expression Array (see **Table 4**). Samples were processed for each platform using packages affy (Gautier et al. 2004) and affyPLM (Bolstad et al. 2005) from R (https://www.R-project.org/) and Bioconductor (Gentleman et al. 2004). In order to remove technical variability, an a priori adjustment by batch of scanning and/or quality metrics described in (Eklund and Szallasi 2008) was carried out when necessary; for doing so, a linear model was used in which individual, tissue type, EPHB2 level and the interaction of tissue type and EPHB2 level were included in the model as covariates. Expression data were summarized at the gene level by selecting the most variable probeset within each annotated gene in each platform as measured by median absolute deviation. Data were then merged in a unique expression matrix after quantile normalization (Bolstad et al. 2003) using the common set of genes present in both platforms.

Probeset annotation was performed using the information available in Affymetrix web page (https://www.affymetrix.com/analysis/index.affx).

Sample ID	Patient	Platform	Tissue	EPHB2 levels
765 2009	N1	hug133plus2	Normal	High
763 2009	N1			Low
795 2009	N2			High
793 2009	N2			Low
803 2009	N3	Primeview		High
801 2009	N3			Low
564 2014	P1		Normal	High
574 2014	P1			Low
568 2014	P1		Tumor	High
570 2014	P1			Low
572 2014	P2		Normal	High
574 2014	P2			Low
576 2014	P2		Tumor	High
578 2014	P2			Low
241 2014	P3		Tumor	High
243 2014	P3			Low
245 2014	P4			High
247 2014	P4			Low
189 2014	P5			High
191 2014	P5			Low
792 2013	53			High
794 2013	53			Low
797 2013	56			High
799 2014	56			Low
814 2013	59			High
816 2013	59			Low
817 2013	61			High
819 2013	61			Low
820 2013	HMT			High
821 2013	HMT			Low

Table 4: Primary human samples used in this study

PCA and sample visualization

For visualization purposes, a Principal Component Analysis (PCA) was performed on the samples under analysis after a priori correction by technical and individual variability. For doing so, a mixed-effect model was fit to the data gene-wise in which platform, tissue, EPHB2 levels and the interaction between tissue and EPHB2 level were included as fixed effects and the sample specimen was modelled as a random effect. Expression data were corrected using the coefficients from the fixed effects and the imputations of the random effect derived from the models. Next, a PCA was performed on the resulting corrected data matrix. Samples were then represented in a two-dimensional space using the first two principal components as coordinates. All these analyses were carried out using R (https://www.R-project.org/) and the R package lme4 (Bates et al. 2014).

Biological significance analysis

Pathway enrichment was assessed through the pre-ranked version of Geneset Enrichment Analysis (GSEA) (Subramanian et al. 2005). GSEA was applied to the ranking defined by the t-statistics obtained from differential expression analyses using limma (Smyth 2004); again, the models in such analyses included platform (fixed effect) and individual (random effect) as adjusting variables (Smyth, Michaud, and Scott 2005). Genesets derived from the KEGG pathway database (Kanehisa and Goto 2000) and those annotated under the Gene Ontology (GO) (Ashburner et al. 2000) terms as collected in the MsigDB (Subramanian et al. 2005) were used for these analyses, as well as the GO slim version of the GO database (Ashburner et al. 2000).

RNA sequencing analysis

Reads were aligned to the hg19 version of the human genome using STAR with default parameters (Dobin et al. 2013). Counts per feature were computed with the R (http://www.R-project.org) package Rsubread (Liao, Smyth, and Shi 2013), function feature Counts. Differential expression between conditions was performed using the DESeq2 R package (Love, Huber, and Anders 2014). Stripcharts were plotted using the function plotCounts from DESeq2 and the ggplot2 package (Wickham 2009). We used the regularized log transformed matrix for boxplots and heatmaps. Gene set enrichment analysis (GSEA) was performed using the Broad Institute's implementation (Subramanian et al. 2005). Gene lists were sorted by the differential expression test statistic.

Public gene sets were downloaded from the Broad Institute's website, and custom gene sets from referenced literature (**Table 5**). Gene sets from mouse experiments were translated to human using the biomaRt package (Durinck et al. 2009). Ribosomal genes were defined as those with gene symbol starting with "RPL" or "RPS". The ribosome biogenesis GO term corresponds to id GO:0042254.

Gene Name	Symbol	Reference
RNA Polymerase I		
RNA Polymerase I subunit A	POLR1A	(Fernández-Tornero et al. 2013)
RNA Polymerase I subunit B	POLR1B	
RNA Polymerase I subunit C	POLR1C	
RNA Polymerase I subunit D	POLR1D	
RNA Polymerase I subunit E	POLR1A	
TWIST neighbor	TWISTNB	
Transcription factors		
RRN 3 homolog, RNA Polymerase I transcription factor	RRN3/TIF-IA	(Blattner et al. 2011; I Grummt 2010; Mayer, Bierhoff, and Grummt 2005)
Upstream binding transcription factor	UBTF	(Comai 2004)
TATA-box binding associated factors	TAF1A	(Comai 2004; Ingrid Grummt 2010)
	TAF1B	
	TAF1C	
	TAF1D	
rRNA processing factors		
Fibrillarin	FBL	(Marcel et al. 2013)
NOP56 ribonucleoprotein	NOP56	(Wu et al. 2013)
Dyskerin pseudouridine synthase	DKC1	(Ge et al., 2010)
DEAD/H-box helicases	DDX11	(Calo et al. 2014)
	DDX21	

Table 5: RNA Polymerase I custom gene sets

Protein extraction and Western blot analysis

For protein expression analysis cells were scraped from 6 well-plates and homogenized with lysis buffer 1:1:1 (1mM EDTA, 1mM EGTA, 1% SDS) supplemented with protease and phosphatase inhibitors (Sigma Aldrich) and heated at 99ºC for 10 min. Cell lysates were pipetted several times to break up gDNA and later centrifuged at 13200 rpm for 15 min. The supernatant was kept as the protein extract. Protein content was quantified with the Protein Assay (BioRad), based on the Bradford method. Equal amounts of protein per sample were separated by standard SDS-PAGE and transferred to PVDF membranes. The membranes were incubated in TBS-T 0.2% supplemented with 5% milk for 30 min at RT to block unspecific antibody binding. Primary antibodies were incubated overnight at 4 ºC (see **Table 6** for antibody details).

Secondary antibodies were diluted 1/10000 and incubated for 1 hour at RT with the membranes. After antibody incubations membranes were washed at least 3 times with TBS-T 0.2% for 10 min. Immuno-complexes were visualized with SuperSignal West Pico Chemiluminescent Substrate (Thermo Scientific, Ref. #34080).

Primary antibody	Species	Source	Reference	Dilution
RPA194 (POLR1A)	Mouse	Santa Cruz	SC-48385	1:500
RRN/(TIF-IA)	Rabbit	Sigma	HPA049837	1:500
c-MYC	Rabbit	Abcam	ab3207	1:10000
KRT20	Mouse	DAKO	M701929-2	1:500
ACTIN	Mouse	Abcam	ab20272	1:20000

Table 6: Primary antibodies for Western blot

ChIP

Cells seeded the day before were washed with warm PBS and then cross-linked for 10 minutes at 37°C with 1% formaldehyde in serum free DMEM. To stop the reaction, cells were incubated for 2 minutes more after adding glycin at final concentration of 0.125 M. Cells were washed twice with cold PBS scrapped off with cold soft lysis buffer (50mM Tris pH 8.0, 2 mM EDTA, 0.1% Nonidet P-40, 10% glycerol). Lysates were incubated 10 minutes on ice and then centrifuged for 15 minutes at 3000rpm in cold. Pellet was resuspended in SDS lysis buffer (1% SDS, 10 mM EDTA, 50mM Tris pH 8.0) and sonicated using 40% of the sonicator's amplitude (Branson DIGITAL Sonifier® UNIT Model S-450D) in order to generate DNA fragments ranging from 200 to 1000 kb in length. Lysates were incubated for 20 minutes on ice and centrifuged at maximum speed for 10 minutes. Optionally, the length of the fragments was confirmed running a small volume of the sample on 0.5% agarose gel.

Protein concentration was determined by Lowry and the desired amount of protein per immunoprecipitation (usually between 250 µg and 1 mg) was diluted ten times in dilution buffer (0.001% SDS, 1.1% Triton X-100, 16.7 mM Tris pH 8.0, 2 mM EDTA, 2 mM EGTA, 167 mM NaCl). In order to reduce background, samples were incubated for 3 hours at 4°C with IgGs of the same species as the used antibody and protein G or protein A magnetic beads (Upstate). Beads were removed using magnetic racks, 100 µl for the input was kept apart and the samples were divided in half and incubated with either the specific antibody or the IgG of the same species overnight at 4°C with agitation. Magnetic beads that were blocked overnight with BSA and sheared salmon sperm were added to all the samples and incubated 1 hour at 4°C with agitation. Afterwards, five washes were performed on ice with each in each of the given buffers: low salt buffer (0.1% SDS, 1% Triton X-100, 2 mM EDTA, 20 mM Tris, pH 8.0, and 150 mM NaCl), high salt buffer (the same as low salt but with 500 mM NaCl), LiCl Buffer (250 mM LiCl, 1% Nonidet P-40, 1% Sodium deoxycholate, 1 mM EDTA, and 10 mM Tris, pH 8.0), and TE buffer. Beads were recovered using magnetic racks and samples were eluted with the elution buffer (100 mM Na2CO3, 1% SDS) at 37°C. Elutes were recovered by centrifugation (3 minutes, 2000 rpm). To each sample and to the inputs NaCl was added at final concentration of 250 mM and both the samples and the inputs were decrosslinked by incubation at 65°C overnight, following by digestion with proteinase K for additional 2 hours. DNA was purified using GFX PCR

DNA and Gel Band Purification kit (GE healthcare) and quantitative PCR was performed. Primers used for ChIP analysis are listed in **Table 7**

Gene Name
RRN3/TIF-IA
Primers 5'-3'
FW: AATCCCCTTTCCTCCGTGAA
RV: ATGTGCTAAGCTGTGGCCG

Table 7: Primers used for ChIP qPCR

Cell cycle analysis

In vitro: CRC cell lines were seeded and treated with 4-OHT (see *in vitro* treatments section). After treatment, 1μM of EdU was added to the cell media and incubated for 1 hour at 37ºC. Cells were trypsinized and fixed with 3,7% formaldehyde (Sigma) in PBS during 15 min at RT. Cells were then washed twice with 1% BSA in PBS and incubated with 1X Click-iT saponin-based permeabilization and wash reagent during 15 min. To stain the EdU positive cells, Click-iT Alexa-488 cocktail reagent (Life Technologies, C10425) was prepared following the manufacturer's protocol and added to the cell pellet and incubated for 30 min at RT protected from light. Finally, cells were washed twice with 1% BSA in PBS, followed by the addition of 1μM DAPI and incubation for 1 hour. Cell cycle was analyzed using the BD aria fusion FACS.

In vivo: For *in vivo* cell cycle analysis of EGFP-POLR1A tumor cells, mice bearing subcutaneous xenografts from CRISPR/Cas9 modified PDOs were injected with 80 mg/kg EdU 3 hours before their sacrifice. Xenografts were resected, disaggregated and stained with hEPCAM-PeCy7 1/150 (eBioScience 25-9326-42) and DAPI at 1μg/mL as is described in the disaggregation of tumor xenografts section. 100.000 epithelial tumor cells (EPCAM+) were sorted according to their EGFP positivity. Sorted cells were fixed, permeabilized and EdU stained as is described above. Finally, cell cycle profile of EGFP-POLR1A tumor cell populations was analyzed using a BD aria fusion FACS.

Cristal violet staining

CRC cell lines were seeded in 6 well-plate format and treated with 4-OHT (See *in vitro* treatment section for details). After treatment plates were placed on ice and washed with ice-cold 1X PBS and then fixed with ice-cold methanol for 10 min. Methanol was aspirated and samples were incubated with 0.5% crystal violet solution at RT for 10 min. Plates were thoroughly rinsed with PBS and photographed.

rDNA transcription analysis

In vitro: rDNA transcription studies were performed by analyzing the incorporation of 5-Ethynyl Uridine (EU) (Jao and Salic 2008) (Invitrogen, Ref. E10345) into the RNA. CRC cell lines were seeded and treated with 4-OHT (see *in vitro* treatments section). 30 min before cell collection EU was added at final concentration of 1 mM. Cells were trypsinized and fixed with 3,7% formaldehyde (Sigma) in PBS during 15 min at RT. For permeabilization, cells were incubated with 0,5% Triton-100X in PBS during 15 min. To stain EU positive cells, Click-iT Alexa-488 or Alexa-594 cocktail reagent (Life Technologies, C10329/C10330) was prepared following the manufacturer's protocol and added to the cell pellet and incubated during 30 min at RT protected from light. Finally cells were washed twice with PBS and EU positive cells were analyzed using the BD Aria Fusion FACS.

In vivo: To analyze the EU incorporation of the EPHB2 tumor cells, mice bearing subcutaneous xenografts (PDO7, P18 or P19b) were injected with EU (80 mg/Kg) 2 h before their sacrifice. Xenografts were resected, disaggregated and stained (see tumor xenograft disaggregation section). 100.000 epithelial tumor cells (EPCAM+) were sorted according to their EPHB2 positivity. To analyze the EU incorporation of the EGFP-POLR1A tumor cells, mice bearing subcutaneous xenografts of CRISPR/Cas9 modified PDO7 and PDO18 were injected with EU as is described above. 100.000 epithelial tumor cells (EPCAM+) were sorted according to their EGFP positivity. Sorted tumor cells were fixed, permeabilized, EU stained and analyzed following the same protocol described for the *in vitro* rDNA transcription analysis.

Tumor initiation assays

Viable (DAPI negative) human EPCAM positive single cells from disaggregated xenografts were sorted according to their EGFP positivity and subsequently transplanted into new recipient mice at limiting dilutions. 200 or 1000 cells were injected per flank in 100 µl of BME2-HBSS 50 % - 50 % (n=12). Tumor volume was measured twice a week. When a xenograft reached 300 mm^3, it was resected from the animal. The experiment finished when all xenografts were grown or when the animals were 21 weeks old. Differences were assessed with Log-Rank (Mantel Cox) test.

Organoid Formation assays

Human EPCAM positive alive single cells from disaggregated xenografts were isolated by FACS according to their EGFP positivity as described before and seeded *in vitro* in 25 µL BME2 drops containing 1000 cells/drop (n=5) per condition. Then, plates were scanned with a ScanR inverted microscope at day 1 post-seeding to quantify the exact number of cells seeded per drop and at the experimental endpoint (day 14 post-seeding). Full drops were scanned taking overlapping pictures at 4x magnification and at 8 different z-stacks with a separation of 200 µm among them. Z-stacks of each field of view were projected in a single image and the full drop was digitally reconstructed by stitching the different image projections using an Image J custom-made macro developed for this purpose. Total number and mean size of cells (i.e. any object with a diameter larger than 5 µm) or organoids (diameter larger than 400 µm) were counted. Differences were assessed with Student´s t-test.

Immunofluorescences

In vitro CRC cell lines

CRC cell lines grown on ethanol sterilized glass coverslips were washed three times with PBS and incubated with 4% paraformaldehyde (PFA) for 15 minutes at room temperature, washed again with PBS and incubated for 5 minutes more with 50mM NH_4Cl to quench PFA's autofluorescence. Blocking and permeabilization were performed simultaneously for 1 hour at room temperature in PBS containing 3% BSA and 0.3% Triton X-100. Coverslips were first incubated in a humid chamber overnight at 4ºC with the primary antibody diluted in the blocking/permeabilization solution. After extensive washing the incubation with the secondary antibody was done for 1 hour in the dark. In case of the co-staining, both primary and secondary antibodies were mixed and used at the same time. Coverslips were mounted with DAPI-Fluoromount-G (SouthernBiotech. Ref. 0100-20).

In paraffin sections

Whole xenografts or primary CRC tumor samples were cut in halves and fixed in formalin ON. The fixative was removed and tissue was washed for 2 hours in PBS before paraffin embedding. Immunostainings were performed on 4 µm tissue sections according to standard procedures. Briefly, antigen retrieval was carried out with boiling Tris-EDTA buffer for 20 min, then samples were blocked with Peroxidase-Blocking Solution (Dako: S202386) for 10 min at room temperature. The blocking was removed by 3 washes of 5 minutes

with wash buffer (DAKO, K800721). Afterwards, tissues were incubated 20 min at RT with 10% normal donkey serum (Jackson Immunoresearch, Ref: 017-000-121) in order to block the unspecific unions. Primary antibody was added and incubated ON at 4ºC. Washes were performed in between steps with wash buffer (Dako, K800721). Secondary antibodies were added for 1 hour at RT. After three more washes of 5 min with wash buffer the samples were incubated 10 min with sudan black solution to quench tissue autofluorescence. Sudan black was removed performing a fast wash with wash buffer. Finally DAPI was added at 1:2500 after secondary antibody incubation and slides were mounted with Fluoerescent mounting media (Dako 53023).

To detect EU incorporation in paraffin sections from tumor xenografts after fixative removal and antigen retrieval (see above), samples were incubated 30 min with freshly prepared click-it cocktail (see manufacturer's protocol) protected from light. After the click-it reaction staining with desired antibodies was performed as is described above.

Quantification of the nucleolar staining in CRC cell lines

CRC cell lines either 4-OHT treated or untreated were stained for POLR1A (see treatments and IF sections for details). Images were taken with confocal SP5 microscope. Quantification of the nuclear area occupied by POLR1A signal was done with ImageJ using a Macro developed by the microscopy facility at IRB. For quantification of POLR1A nuclear area in xenografts, paraffin sections were stained for POLR1A and combined with differentiation markers such as KRT17 and MUC2. For each image, POLR1A nuclear area was quantified in KRT17/MUC2 positive and negative areas using the same macro.

Primary antibody	Species	Source	Reference	Dilution
EPHB2	Goat	R&D	AF467	1:100
KRT20	Rabbit	Sigma	HPA024309	1:100
KRT20	Mouse	DAKO	M701929-2	1:100
KRT17	Rabbit	Sigma	HPA000453	1:100
EGFP	Goat	Abcam	Ab6673	1:100
MUC2	Rabbit	Santa Cruz	Sc-15334	1:100
Ribosomal 5.8S	Mouse	TF Scientific	MA1-13017	1:50
RPA194	Mouse	Santa Cruz	Sc-48385	1.200

Table 8: Primary antibodies for immunofluorescence

References

Akiyama, Junko, Ryuichi Okamoto, Michiko Iwasaki, Xiu Zheng, Shiro Yui, Kiichiro Tsuchiya, Tetsuya Nakamura, and Mamoru Watanabe. 2010. “Delta-like 1 Expression Promotes Goblet Cell Differentiation in Notch-Inactivated Human Colonic Epithelial Cells.” Biochemical and Biophysical Research Communications 393 (4). Elsevier Inc.: 662–67. doi:10.1016/j.bbrc.2010.02.048.

Altmann, GG, and CP Leblond. 1982. “Changes in the Size and Structure of the Nucleolus of Columnar Cells during Their Migration from Crypt Base to Villus Top in Rat Jejunum.” J. Cell Sci. 56 (1): 83–99. http://jcs.biologists.org/content/56/1/83.long.

Arabi, Azadeh, Siqin Wu, Karin Ridderstråle, Holger Bierhoff, Chiounan Shiue, Karoly Fatyol, Sara Fahlén, et al. 2005. “C-Myc Associates with Ribosomal DNA and Activates RNA Polymerase I Transcription.” Nature Cell Biology 7 (3): 303–10. doi:10.1038/ncb1225.

Ashburner, M, C A Ball, J A Blake, D Botstein, H Butler, J M Cherry, A P Davis, et al. 2000. “Gene Ontology: Tool for the Unification of Biology. The Gene Ontology Consortium.” Nature Genetics 25 (1): 25–29. doi:10.1038/75556.

Auclair, Benoit A, Yannick D Benoit, Nathalie Rivard, Yuji Mishina, and Nathalie Perreault. 2007. “Bone Morphogenetic Protein Signaling Is Essential for Terminal Differentiation of the Intestinal Secretory Cell Lineage.” Gastroenterology 133 (3): 887–96. doi:10.1053/j.gastro.2007.06.066.

Barker, Nick, Marc van de Wetering, Hans Clevers, Marc Van De Wetering, and Hans Clevers. 2008. “The Intestinal Stem Cell.” Genes & Development 22 (14): 1856–64. doi:10.1101/gad.1674008.1856.

Barker, Nick, Johan H van Es, Jeroen Kuipers, Pekka Kujala, Maaike van den Born, Miranda Cozijnsen, Andrea Haegebarth, et al. 2007. “Identification of Stem Cells in Small Intestine and Colon by Marker Gene Lgr5.” Nature 449 (7165): 1003–7. doi:10.1038/nature06196.

Barna, Maria, Aya Pusic, Ornella Zollo, Maria Costa, Nadya Kondrashov, Eduardo Rego, Pulivarthi H Rao, and Davide Ruggero. 2008. “Suppression of Myc Oncogenic Activity by Ribosomal Protein Haploinsufficiency.” Nature 456 (7224). Nature Publishing Group: 971–75. doi:10.1038/nature07449.

Barriga, Francisco M, Elisa Montagni, Miyeko Mana, Camille Stephan-otto Attolini, Ivo Gut, Francisco M Barriga, Elisa Montagni, Miyeko Mana, Maria Mendez-lago, and Xavier Hernando-momblona. 2017. “Mex3a Marks a Slowly Dividing Subpopulation of Article Mex3a Marks a Slowly Dividing Subpopulation of Lgr5 + Intestinal Stem Cells.” Stem Cell. Elsevier Inc., 1–16. doi:10.1016/j.stem.2017.02.007.

Barry Pierce, G, and Wendell C Speers. 1996. “Tumors as Caricatures of the Process of Tissue Renewal: Prospects

for Therapy by Directing Differentiation1." CANCER RESEARCH 48.

Bartholdy, Boris, Maximilian Christopeit, Britta Will, Yongkai Mo, Laura Barreyro, Yiting Yu, Tushar D. Bhagat, et al. 2014. "HSC Commitment–associated Epigenetic Signature Is Prognostic in Acute Myeloid Leukemia." Journal of Clinical Investigation 124 (3). American Society for Clinical Investigation: 1158–67. doi:10.1172/JCI71264.

Bates, Douglas, Martin Mächler, Ben Bolker, and Steve Walker. 2014. "Fitting Linear Mixed-Effects Models Using lme4," June. http://arxiv.org/abs/1406.5823.

Batlle, E, J Bacani, H Begthel, S Jonkeer, A Gregorieff, M van de Born, N Malats, et al. 2005. "EphB Receptor Activity Suppresses Colorectal Cancer Progression." Nature 435 (7045): 1126–30. doi:10.1038/nature03941.

Batlle, Eduard, Jeffrey T. Henderson, Harry Beghtel, Maaike M W Van den Born, Elena Sancho, Gerwin Huls, Jan Meeldijk, et al. 2002. "β-Catenin and TCF Mediate Cell Positioning in the Intestinal Epithelium by Controlling the Expression of EphB/EphrinB." Cell 111 (2): 251–63. doi:10.1016/S0092-8674(02)01015-2.

Bjerknes, Matthew, and Hazel Cheng. 2006. "Intestinal Epithelial Stem Cells and Progenitors." Methods in Enzymology 419 (2000): 337–83. doi:10.1016/S0076-6879(06)19014-X.

Blanpain, Cédric, and Elaine Fuchs. 2009. "Epidermal Homeostasis: A Balancing Act of Stem Cells in the Skin." Nature Reviews. Molecular Cell Biology 10 (3): 207–17. doi:10.1038/nrm2636.

Blattner, Claudia, Stefan Jennebach, Franz Herzog, Andreas Mayer, Alan C M Cheung, Gregor Witte, Kristina Lorenzen, et al. 2011. "Molecular Basis of Rrn3-Regulated RNA Polymerase I Initiation and Cell Growth." Genes and Development 25 (19): 2093–2105. doi:10.1101/gad.17363311.

Bolstad, B. M., F. Collin, J. Brettschneider, K. Simpson, L. Cope, R. A. Irizarry, and T.P. Speed. 2005. "Quality Assessment of Affymetrix GeneChip Data." In Bioinformatics and Computational Biology Solutions Using R and Bioconductor, 33–47. New York: Springer-Verlag. doi:10.1007/0-387-29362-0_3.

Bolstad, B M, R A Irizarry, M Astrand, and T P Speed. 2003. "A Comparison of Normalization Methods for High Density Oligonucleotide Array Data Based on Variance and Bias." Bioinformatics (Oxford, England) 19 (2): 185–93. http://www.ncbi.nlm.nih.gov/pubmed/12538238.

Bonnet, D, and J E Dick. 1997. "Human Acute Myeloid Leukemia Is Organized as a Hierarchy That Originates from a Primitive Hematopoietic Cell." Nature Medicine 3 (7): 730–37. http://www.ncbi.nlm.nih.gov/pubmed/9212098.

Boon, K, H N Caron, R van Asperen, L Valentijn, M C Hermus, P van Slui, I Roobeek, et al. 2001. "{N-Myc} Enhances

the Expression of a Large Set of Gene Functioning in Ribosome Biogenesis and Protein Synthesis." Embo J. 20 (6): 1383–93.

Breault, David T, Irene M Min, Diana L Carlone, Loredana G Farilla, Dana M Ambruzs, Daniel E Henderson, Selma Algra, Robert K Montgomery, Amy J Wagers, and Nicholas Hole. 2008. "Generation of mTert-GFP Mice as a Model to Identify and Study Tissue Progenitor Cells." Proceedings of the National Academy of Sciences of the United States of America 105 (30): 10420–25. doi:10.1073/pnas.0804800105.

Bruno, Peter M, Yunpeng Liu, Ga Young Park, Junko Murai, Catherine E Koch, Timothy J Eisen, Justin R Pritchard, Yves Pommier, Stephen J Lippard, and Michael T Hemann. 2017. "A Subset of Platinum-Containing Chemotherapeutic Agents Kills Cells by Inducing Ribosome Biogenesis Stress." Nature Medicine 23 (4). Nature Publishing Group: 461–71. doi:10.1038/nm.4291.

Budde, Andreja, and Ingrid Grummt. 1999. "p53 Represses Ribosomal Gene Transcription." Oncogene 18 (4). Nature Publishing Group: 1119–24. doi:10.1038/sj.onc.1202402.

Busch, Katrin, Kay Klapproth, Melania Barile, Michael Flossdorf, Tim Holland-Letz, Susan M Schlenner, Michael Reth, Thomas Höfer, and Hans-Reimer Rodewald. 2015. "Fundamental Properties of Unperturbed Haematopoiesis from Stem Cells in Vivo." Nature 518 (7540): 542–46. doi:10.1038/nature14242.

Cadigan, Ken M. 2008. "Wnt-β-Catenin Signaling." Current Biology 18 (20): 943–47. doi:10.1016/j.cub.2008.08.017.

Calo, Eliezer, Ryan A Flynn, Lance Martin, Robert C Spitale, Howard Y Chang, and Joanna Wysocka. 2014. "RNA Helicase DDX21 Coordinates Transcription and Ribosomal RNA Processing." Nature 518 (7538). Nature Publishing Group: 249–53. doi:10.1038/nature13923.

Calon, Alexandre, Elisa Espinet, Sergio Palomo-Ponce, Daniele V F Tauriello, Mar Iglesias, María Virtudes Céspedes, Marta Sevillano, et al. 2012. "Dependency of Colorectal Cancer on a TGF-β-Driven Program in Stromal Cells for Metastasis Initiation." Cancer Cell 22 (5): 571–84. doi:10.1016/j.ccr.2012.08.013.

Calon, Alexandre, Enza Lonardo, Antonio Berenguer-llergo, Elisa Espinet, Xavier Hernando-momblona, Mar Iglesias, Marta Sevillano, et al. 2015. "Stromal Gene Expression Defines Poor-Prognosis Subtypes in Colorectal Cancer." Nature Genetics 47 (February). Nature Publishing Group: 320–29. doi:10.1038/ng.3225.

Cavanaugh, a H, W M Hempel, L J Taylor, V Rogalsky, G Todorov, and L I Rothblum. 1995. "Activity of RNA Polymerase I Transcription Factor UBF Blocked by Rb Gene Product." Nature. doi:10.1038/374177a0.

Chan, Joanna C, Katherine M Hannan, Kim Riddell, Pui Yee Ng, Abigail Peck, Rachel S Lee, Sandy Hung, et al. 2011. “Suppl_AKT Promotes rRNA Synthesis and Cooperates with c-MYC to Stimulate Ribosome Biogenesis in Cancer.” Science Signaling 4 (188): ra56. doi:10.1126/scisignal.2001754.

Cheng, Hazel, and C. P. Leblond. 1974a. “Origin, Differentiation and Renewal of the Four Main Epithelial Cell Types in the Mouse Small Intestine III. Entero-Endocrine Cells.” American Journal of Anatomy 141 (4): 503–19. doi:10.1002/aja.1001410405.

Cheng, Hazel, and C. P. Leblond. 1974b. “Origin, Differentiation and Renewal of the Four Main Epithelial Cell Types in the Mouse Small Intestine V. Unitarian Theory of the Origin of the Four Epithelial Cell Types.” American Journal of Anatomy 141 (4). Wiley Subscription Services, Inc., A Wiley Company: 537–61. doi:10.1002/aja.1001410407.

Clarke, Michael F., John E. Dick, Peter B. Dirks, Connie J. Eaves, Catriona H M Jamieson, D. Leanne Jones, Jane Visvader, Irving L. Weissman, and Geoffrey M. Wahl. 2006. “Cancer Stem Cells - Perspectives on Current Status and Future Directions: AACR Workshop on Cancer Stem Cells.” Cancer Research 66 (19): 9339–44. doi:10.1158/0008-5472.CAN-06-3126.

Clevers, Hans. 2006. “Wnt/??-Catenin Signaling in Development and Disease.” Cell 127 (3): 469–80. doi:10.1016/j.cell.2006.10.018.

Clevers, Hans. 2006. 2015. “What Is an Adult Stem Cell?” 350 (6266): 4–6. doi:10.1126/science.aad7016.

Clevers, Hans, and Eduard Batlle. 2013. “SnapShot: The Intestinal Crypt.” Cell 152 (5). Elsevier: 1198–1198.e2. doi:10.1016/j.cell.2013.02.030.

Colis, Laureen, Karita Peltonen, Paul Sirajuddin, Hester Liu, Sara Sanders, Glen Ernst, James C Barrow, and Marikki Laiho. 2014. “DNA Intercalator BMH-21 Inhibits RNA Polymerase I Independent of DNA Damage Response.” Oncotarget 5 (12): 4361–69. doi:10.18632/oncotarget.2020.

Comai, By Lucio. 2004. “MECHANISM OF RNA POLYMERASE I TRANSCRIPTION” 67: 123–55.

Cortina, Carme, Gemma Turon, Diana Stork, Xavier Hernando-Momblona, Marta Sevillano, Mònica Aguilera, Sébastien Tosi, et al. 2017. “A Genome Editing Approach to Study Cancer Stem Cells in Human Tumors.” EMBO Molecular Medicine, e201707550. doi:10.15252/emmm.201707550.

Dalerba, P, SJ Dylla, IK Park, and R Liu. 2007. “Phenotypic Characterization of Human Colorectal Cancer Stem Cells.” Proceedings of the. http://www.pnas.org/content/104/24/10158.short.

Dalerba, Piero, Tomer Kalisky, Debashis Sahoo, Pradeep S Rajendran, Michael E Rothenberg, Anne a Leyrat, Sopheak Sim, et al. 2011. “Single-Cell Dissection of Transcriptional Heterogeneity in Human Colon Tumors.” Nature Biotechnology 29

(12). Nature Publishing Group: 1120–27. doi:10.1038/nbt.2038.

Date, Shoichi, and Toshiro Sato. 2015. “Mini-Gut Organoids: Reconstitution of the Stem Cell Niche.” Annual Review of Cell and Developmental Biology 31 (1): 269–89. doi:10.1146/annurev-cellbio-100814-125218.

de Lau, Wim, Nick Barker, Teck Y. Low, Bon-Kyoung Koo, Vivian S. W. Li, Hans Teunissen, Pekka Kujala, et al. 2011. “Lgr5 Homologues Associate with Wnt Receptors and Mediate R-Spondin Signalling.” Nature 476 (7360). Nature Research: 293–97. doi:10.1038/nature10337.

Derenzini, Massimo, Davide Trerè, Annalisa Pession, Marzia Govoni, Valentina Sirri, and Pasquale Chieco. 2000. “Nucleolar Size Indicates the Rapidity of Cell Proliferation in Cancer Tissues.” Journal of Pathology 191 (2): 181–86. doi:10.1002/(SICI)1096-9896(200006)191:2<181::AID-PATH607>3.0.CO;2-V.

Dick, John E. 2003. “Stem Cells: Self-Renewal Writ in Blood.” Nature 423 (6937): 231–33. doi:10.1038/423231a.

Dobin, Alexander, Carrie A Davis, Felix Schlesinger, Jorg Drenkow, Chris Zaleski, Sonali Jha, Philippe Batut, Mark Chaisson, and Thomas R Gingeras. 2013. “STAR: Ultrafast Universal RNA-Seq Aligner.” Bioinformatics (Oxford, England) 29 (1): 15–21. doi:10.1093/bioinformatics/bts635.

Doench, John G, Ella Hartenian, Daniel B Graham, Zuzana Tothova, Mudra Hegde, Ian Smith, Meagan Sullender, Benjamin L Ebert, Ramnik J Xavier, and David E Root. 2014. “Rational Design of Highly Active sgRNAs for CRISPR-Cas9–mediated Gene Inactivation.” Nature Biotechnology 32 (12): 1262–67. doi:10.1038/nbt.3026.

Drygin, Denis, William G Rice, and Ingrid Grummt. 2010. “The RNA Polymerase I Transcription Machinery: An Emerging Target for the Treatment of Cancer.” Annual Review of Pharmacology and Toxicology 50 (January). Annual Reviews: 131–56. doi:10.1146/annurev.pharmtox.010909.105844.

Durinck, Steffen, Paul T Spellman, Ewan Birney, and Wolfgang Huber. 2009. “Mapping Identifiers for the Integration of Genomic Datasets with the R/Bioconductor Package biomaRt.” Nature Protocols 4 (8): 1184–91. doi:10.1038/nprot.2009.97.

Eklund, Aron C, and Zoltan Szallasi. 2008. “Correction of Technical Bias in Clinical Microarray Data Improves Concordance with Known Biological Information.” Genome Biology 9 (2): R26. doi:10.1186/gb-2008-9-2-r26.

Engel, Christoph, Jürgen Plitzko, and Patrick Cramer. 2016. “RNA Polymerase I–Rrn3 Complex at 4.8 Å Resolution.” Nature Communications 7: 12129. doi:10.1038/ncomms12129.

Fearon, E R, and B Vogelstein. 1990. “A Genetic Model for Colorectal

Tumorigenesis.” Cell 61 (5): 759–67. http://www.ncbi.nlm.nih.gov/pubmed/2188735.

Feil, R, J Brocard, B Mascrez, M LeMeur, D Metzger, and P Chambon. 1996. “Ligand-Activated Site-Specific Recombination in Mice.” Proceedings of the National Academy of Sciences of the United States of America 93 (20): 10887–90. doi:10.1073/pnas.93.20.10887.

Fernández-Tornero, Carlos, María Moreno-Morcillo, Umar J. Rashid, Nicholas M. I. Taylor, Federico M. Ruiz, Tim Gruene, Pierre Legrand, Ulrich Steuerwald, and Christoph W. Müller. 2013a. “Crystal Structure of the 14-Subunit RNA Polymerase I.” Nature 502 (7473): 644–49. doi:10.1038/nature12636.

Ficara, Francesca, Mark J. Murphy, Min Lin, and Michael L. Cleary. 2008. “Pbx1 Regulates Self-Renewal of Long-Term Hematopoietic Stem Cells by Maintaining Their Quiescence.” Cell Stem Cell 2 (5): 484–96. doi:10.1016/j.stem.2008.03.004.

Fre, Silvia, Mathilde Huyghe, Philippos Mourikis, Sylvie Robine, Daniel Louvard, and Spyros Artavanis-Tsakonas. 2005. “Notch Signals Control the Fate of Immature Progenitor Cells in the Intestine.” Nature 435 (7044): 964–68. doi:10.1038/nature03589.

Fuchs, Elaine. 2009. “The Tortoise and the Hair: Slow-Cycling Cells in the Stem Cell Race.” Cell 137 (5): 811–19. doi:10.1016/j.cell.2009.05.002.

Fuchs, Elaine, and Ting Chen. 2013. “A Matter of Life and Death: Self-Renewal in Stem Cells.” EMBO Reports 14 (1). Nature Publishing Group: 39–48. doi:10.1038/embor.2012.197.

Garden, G A, M Hartlage-Rübsamen, E W Rubel, and M A Bothwell. 1995. “Protein Masking of a Ribosomal RNA Epitope Is an Early Event in Afferent Deprivation-Induced Neuronal Death.” Molecular and Cellular Neurosciences. doi:10.1006/mcne.1995.1023.

Garden, GA, KS Canady, DI Lurie, M Bothwell, and EW Rubel. 1994. “A Biphasic Change in Ribosomal Conformation during Transneuronal Degeneration Is Altered by Inhibition of Mitochondrial, but Not Cytoplasmic Protein Synthesis.” The Journal of Neuroscience : The Official Journal of the Society for Neuroscience 14 (4): 1994–2008. http://www.ncbi.nlm.nih.gov/pubmed/8158254.

Gautier, Laurent, Leslie Cope, Benjamin M Bolstad, and Rafael A Irizarry. 2004. “Affy--Analysis of Affymetrix GeneChip Data at the Probe Level.” Bioinformatics (Oxford, England) 20 (3): 307–15. doi:10.1093/bioinformatics/btg405.

Ge, J., D. A. Rudnick, J. He, D. L. Crimmins, J. H. Ladenson, M. Bessler, and P. J. Mason. 2010. “Dyskerin Ablation in Mouse Liver Inhibits rRNA Processing and Cell Division.” Molecular and Cellular Biology 30 (2): 413–22. doi:10.1128/MCB.01128-09.

Gentleman, Robert C, Vincent J Carey, Douglas M Bates, Ben Bolstad, Marcel

Dettling, Sandrine Dudoit, Byron Ellis, et al. 2004. “Bioconductor: Open Software Development for Computational Biology and Bioinformatics.” Genome Biology 5 (10): R80. doi:10.1186/gb-2004-5-10-r80.

Gentles, Andrew J, Sylvia K Plevritis, Ravindra Majeti, and Ash A Alizadeh. 2010. “Association of a Leukemic Stem Cell Gene Expression Signature with Clinical Outcomes in Acute Myeloid Leukemia.” JAMA 304 (24): 2706–15. doi:10.1001/jama.2010.1862.

Gerbe, F, and P Jay. 2016. “Intestinal Tuft Cells: Epithelial Sentinels Linking Luminal Cues to the Immune System” 9. doi:10.1038/mi.2016.68.

Gonzalez-Roca, Eva, Xabier Garcia-Albéniz, Silvia Rodriguez-Mulero, Roger R Gomis, Karl Kornacker, and Herbert Auer. 2010. “Accurate Expression Profiling of Very Small Cell Populations.” PloS One 5 (12): e14418. doi:10.1371/journal.pone.0014418.

Grandori, Carla, Natividad Gomez-Roman, Zoe a Felton-Edkins, Celine Ngouenet, Denise a Galloway, Robert N Eisenman, and Robert J White. 2005. “C-Myc Binds to Human Ribosomal DNA and Stimulates Transcription of rRNA Genes by RNA Polymerase I.” Nature Cell Biology 7 (3): 311–18. doi:10.1038/ncb1224.

Gregorieff, Alex, Daniel Pinto, Harry Begthel, Olivier Destrée, Menno Kielman, and Hans Clevers. 2005. “Expression Pattern of Wnt Signaling Components in the Adult Intestine.” Gastroenterology 129 (2): 626–38. doi:10.1016/j.gastro.2005.06.007.

Grummt, I. 2010. “Wisely Chosen Paths--Regulation of rRNA Synthesis: Delivered on 30 June 2010 at the 35th FEBS Congress in Gothenburg, Sweden.” FEBS J 277 (22): 4626–39. doi:10.1111/j.1742-4658.2010.07892.x.

Grummt, Ingrid, and Craig S Pikaard. 2003. “Epigenetic Silencing of RNA Polymerase I Transcription.” Nature Reviews. Molecular Cell Biology 4 (8): 641–49. doi:10.1038/nrm1171.

Grün, Dominic, Anna Lyubimova, Lennart Kester, Kay Wiebrands, Onur Basak, Nobuo Sasaki, Hans Clevers, and Alexander van Oudenaarden. 2015. “Single-Cell Messenger RNA Sequencing Reveals Rare Intestinal Cell Types.” Nature 525 (7568): 251–55. doi:10.1038/nature14966.

Hadjiolov, A A. 1980. “Biogenesis of Ribosomes in Eukaryotes.” Sub-Cellular Biochemistry 7: 1–80. http://www.ncbi.nlm.nih.gov/pubmed/7003820.

Hanahan, D, and R A Weinberg. 2000. “The Hallmarks of Cancer.” Cell 100 (1): 57–70. doi:10.1007/s00262-010-0968-0.

Hanawa, Hideki, Patrick F Kelly, Amit C Nathwani, Derek A Persons, Jody A Vandergriff, Phillip Hargrove, Elio F Vanin, and Arthur W Nienhuis. 2002. “Comparison of Various Envelope Proteins for Their Ability to Pseudotype Lentiviral Vectors and Transduce Primitive Hematopoietic Cells

from Human Blood." Molecular Therapy : The Journal of the American Society of Gene Therapy 5 (3): 242–51. doi:10.1006/mthe.2002.0549.

Hannan, Katherine M, Yves Brandenburger, Anna Jenkins, Kerith Sharkey, Alice Cavanaugh, Lawrence Rothblum, Tom Moss, et al. 2003. "mTOR-Dependent Regulation of Ribosomal Gene Transcription Requires S6K1 and Is Mediated by Phosphorylation of the Carboxy-Terminal Activation Domain of the Nucleolar Transcription Factor UBF." Molecular and Cellular Biology 23 (23): 8862–77. doi:10.1128/MCB.23.23.8862-8877.2003.

Haramis, Anna-Pavlina G., Harry Begthel, Maaike van den Born, Johan van Es, Suzanne Jonkheer, G. Johan A. Offerhaus, and Hans Clevers. 2004. "De Novo Crypt Formation and Juvenile Polyposis on BMP Inhibition in Mouse Intestine." Science 303 (5664).

Hardwick, James C, Liudmila L Kodach, G Johan Offerhaus, and Gijs R van den Brink. 2008. "Bone Morphogenetic Protein Signalling in Colorectal Cancer." Nature Reviews. Cancer 8 (10): 806–12. doi:10.1038/nrc2467.

He, T C, A B Sparks, C Rago, H Hermeking, L Zawel, L T da Costa, P J Morin, et al. 1998. "Identification of c-MYC as a Target of the APC Pathway." Science (New York, N.Y.) 281 (5382): 1509–12. doi:10.1126/science.281.5382.1509.

Heix, Jutta, Andreas Vente, Renate Voit, Andreja Budde, Theologos M. Michaelidis, and Ingrid Grummt. 1998. "Mitotic Silencing of Human rRNA Synthesis: Inactivation of the Promoter Selectivity Factor SL1 by cdc2/cyclin B-Mediated Phosphorylation." EMBO Journal 17 (24): 7373–81. doi:10.1093/emboj/17.24.7373.

Hoppe, Sven, Holger Bierhoff, Ivana Cado, Andrea Weber, Marcel Tiebe, Ingrid Grummt, and Renate Voit. 2009. "AMP-Activated Protein Kinase Adapts rRNA Synthesis to Cellular Energy Supply." Proceedings of the National Academy of Sciences of the United States of America 106 (42): 17781–86. doi:10.1073/pnas.0909873106.

Ivashkiv, Lionel B., and Laura T. Donlin. 2013. "Regulation of Type I Interferon Responses." Nature Reviews Immunology 14 (1). Nature Publishing Group: 36–49. doi:10.1038/nri3581.

Jao, Cindy Y, and Adrian Salic. 2008. "Exploring RNA Transcription and Turnover in Vivo by Using Click Chemistry." Proceedings of the National Academy of Sciences of the United States of America 105 (41): 15779–84. doi:10.1073/pnas.0808480105.

Jung, Peter, Toshiro Sato, Anna Merlos-Suárez, Francisco M Barriga, Mar Iglesias, David Rossell, Herbert Auer, et al. 2011. "Isolation and in Vitro Expansion of Human Colonic Stem Cells." Nature Medicine 17 (10): 1225–27. doi:10.1038/nm.2470.

Kanehisa, M, and S Goto. 2000. "KEGG: Kyoto Encyclopedia of Genes and

Genomes." Nucleic Acids Research 28 (1): 27–30. http://www.ncbi.nlm.nih.gov/pubmed/10592173.

Klaus, Alexandra, and Walter Birchmeier. 2008. "Wnt Signalling and Its Impact on Development and Cancer." Nature Reviews. Cancer 8 (5): 387–98. doi:10.1038/nrc2389.

KLEINSMITH, L J, and G B PIERCE. 1964. "MULTIPOTENTIALITY OF SINGLE EMBRYONAL CARCINOMA CELLS." Cancer Research 24 (October): 1544–51. http://www.ncbi.nlm.nih.gov/pubmed/14234000.

Korinek, V, N Barker, P Moerer, E van Donselaar, G Huls, P J Peters, and H Clevers. 1998. "Depletion of Epithelial Stem-Cell Compartments in the Small Intestine of Mice Lacking Tcf-4." Nature Genetics 19 (4): 379–83. doi:10.1038/1270.

Korinek, V, N Barker, P J Morin, D van Wichen, R de Weger, K W Kinzler, B Vogelstein, and H Clevers. 1997. "Constitutive Transcriptional Activation by a Beta-Catenin-Tcf Complex in APC-/- Colon Carcinoma." Science (New York, N.Y.) 275 (5307): 1784–87. http://www.ncbi.nlm.nih.gov/pubmed/9065401.

Krings, Matthias, Cristian Capelli, Frank Tschentscher, Helga Geisert, Sonja Meyer, Arndt Von Haeseler, Göran Possnert, et al. 2000. "Mutations in AXIN2 Cause Colorectal Cancer with Defective Mismatch Repair." Nature 26 (october): 146–47. doi:10.1038/79859.

Laferté, Arnaud, Emmanuel Favry, André Sentenac, Michel Riva, Christophe Carles, and Stéphane Chédin. 2006. "The Transcriptional Activity of RNA Polymerase I Is a Key Determinant for the Leve of All Ribosome Components." Genes and Development 20: 2030–40. doi:10.1101/gad.386106.

Lafontaine, Denis L J. 2015. "Noncoding RNAs in Eukaryotic Ribosome Biogenesis and Function." Nature Structural & Molecular Biology 22 (1): 11–19. doi:10.1038/nsmb.2939.

Lane, Steven W, David a Williams, and Fiona M Watt. 2014. "Modulating the Stem Cell Niche for Tissue Regeneration." Nature Biotechnology 32 (8). Nature Publishing Group: 795–803. doi:10.1038/nbt.2978.

Lapidot, T, C Sirard, J Vormoor, B Murdoch, T Hoang, J Caceres-Cortes, M Minden, B Paterson, M A Caligiuri, and J E Dick. 1994. "A Cell Initiating Human Acute Myeloid Leukaemia after Transplantation into SCID Mice." Nature 367 (6464). Nature Publishing Group: 645–48. doi:10.1038/367645a0.

Lerner, E a, M R Lerner, C a Janeway, and J a Steitz. 1981. "Monoclonal Antibodies to Nucleic Acid-Containing Cellular Constituents: Probes for Molecular Biology and Autoimmune Disease." Proceedings of the National Academy of Sciences of the United States of America 78 (5): 2737–41. doi:10.1073/pnas.78.5.2737.

Li, Hua-Jung, Ferenc Reinhardt, Harvey R Herschman, and Robert A Weinberg. 2012.

"Cancer-Stimulated Mesenchymal Stem Cells Create a Carcinoma Stem Cell Niche via Prostaglandin E2 Signaling." Cancer Discovery 2 (9): 840–55. doi:10.1158/2159-8290.CD-12-0101.

Li, Huipeng, Elise T Courtois, Debarka Sengupta, Yuliana Tan, Kok Hao Chen, Jolene Jie Lin Goh, Say Li Kong, et al. 2017. "Reference Component Analysis of Single-Cell Transcriptomes Elucidates Cellular Heterogeneity in Human Colorectal Tumors." Nature Genetics, no. March. doi:10.1038/NG.3818.

Li, Z, and S R Hann. 2013. "Nucleophosmin Is Essential for c-Myc Nucleolar Localization and c-Myc-Mediated rDNA Transcription." Oncogene 32 (15): 1988–94. doi:10.1038/onc.2012.227.

Li, Zhaoliang, David Boone, and Stephen R Hann. 2008. "Nucleophosmin Interacts Directly with c-Myc and Controls c-Myc-Induced Hyperproliferation and Transformation." Proceedings of the National Academy of Sciences of the United States of America 105 (48): 18794–99. doi:10.1073/pnas.0806879105.

Liao, Y., G. K. Smyth, and W. Shi. 2013. "The Subread Aligner: Fast, Accurate and Scalable Read Mapping by Seed-and-Vote." Nucleic Acids Research 41 (10): e108–e108. doi:10.1093/nar/gkt214.

Lois, Carlos, Elizabeth J Hong, Shirley Pease, Eric J Brown, and David Baltimore. 2002. "Germline Transmission and Tissue-Specific Expression of Transgenes Delivered by Lentiviral Vectors." Science (New York, NY) 295 (5556): 868–72. doi:10.1126/science.1067081.

Lombardo, Ylenia, Alessandro Scopelliti, Patrizia Cammareri, Matilde Todaro, Flora Iovino, Lucia Ricci-Vitiani, Gaspare Gulotta, Francesco Dieli, Ruggero De Maria, and Giorgio Stassi. 2011. "Bone Morphogenetic Protein 4 Induces Differentiation of Colorectal Cancer Stem Cells and Increases Their Response to Chemotherapy in Mice." Gastroenterology 140 (1). Elsevier Inc.: 297–309. doi:10.1053/j.gastro.2010.10.005.

Love, Michael I, Wolfgang Huber, and Simon Anders. 2014. "Moderated Estimation of Fold Change and Dispersion for RNA-Seq Data with DESeq2." Genome Biology 15 (12): 550. doi:10.1186/s13059-014-0550-8.

Lu, Jia, Xiangcang Ye, Fan Fan, Ling Xia, Rajat Bhattacharya, Seth Bellister, Federico Tozzi, et al. 2013. "Endothelial Cells Promote the Colorectal Cancer Stem Cell Phenotype through a Soluble Form of Jagged-1." Cancer Cell 23 (2). Elsevier Inc.: 171–85. doi:10.1016/j.ccr.2012.12.021.

Marcel, V, S E Ghayad, S Belin, G Therizols, A P Morel, E Solano-Gonzalez, J A Vendrell, et al. 2013. "p53 Acts as a Safeguard of Translational Control by Regulating Fibrillarin and rRNA Methylation in Cancer." Cancer Cell 24 (3): 318–30. doi:10.1016/j.ccr.2013.08.013.

Marshman, Emma, Catherine Booth, and Christopher S. Potten. 2002. "The Intestinal Epithelial Stem Cell." BioEssays 24 (1): 91–

98. doi:10.1002/bies.10028.

Mayer, Christine, Holger Bierhoff, and Ingrid Grummt. 2005. “The Nucleolus as a Stress Sensor: JNK2 Inactivates the Transcription Factor TIF-IA and down-Regulates rRNA Synthesis.” Genes and Development 19 (8): 933–41. doi:10.1101/gad.333205.

Mayer, Christine, Jian Zhao, Xuejun Yuan, and Ingrid Grummt. 2004. “mTOR-Dependent Activation of the Transcription Factor TIF-IA Links rRNA Synthesis to Nutrient Availability.” Genes and Development 18 (4): 423–34. doi:10.1101/gad.285504.

McStay, B, and I Grummt. 2008. “The Epigenetics of rRNA Genes: From Molecular to Chromosome Biology.” Annu Rev Cell Dev Biol 24: 131–57. doi:10.1146/annurev.cellbio.24.110707.175259.

Melo, Felipe de Sousa e, Antonina V. Kurtova, Jonathan M. Harnoss, Noelyn Kljavin, Joerg D. Hoeck, Jeffrey Hung, Jeffrey Eastham Anderson, et al. 2017. “A Distinct Role for Lgr5+ Stem Cells in Primary and Metastatic Colon Cancer.” Nature 543 (7647). Nature Publishing Group: 676–80. doi:10.1038/nature21713.

Merlos-Suárez, Anna, Francisco M. Barriga, Peter Jung, Mar Iglesias, María Virtudes Céspedes, David Rossell, Marta Sevillano, et al. 2011. “The Intestinal Stem Cell Signature Identifies Colorectal Cancer Stem Cells and Predicts Disease Relapse.” Cell Stem Cell 8 (5): 511–24. doi:10.1016/j.stem.2011.02.020.

Milano, Joseph, Jenny McKay, Claude Dagenais, Linda Foster-Brown, Francois Pognan, Reto Gadient, Robert T Jacobs, Anna Zacco, Barry Greenberg, and Paul J Ciaccio. 2004. “Modulation of Notch Processing by Gamma-Secretase Inhibitors Causes Intestinal Goblet Cell Metaplasia and Induction of Genes Known to Specify Gut Secretory Lineage Differentiation.” Toxicological Sciences : An Official Journal of the Society of Toxicology 82 (1): 341–58. doi:10.1093/toxsci/kfh254.

Miller, G., K. I. Panov, J. K. Friedrich, L. Trinkle-Mulcahy, a. I. Lamond, and J. C B M Zomerdijk. 2001. “hRRN3 Is Essential in the SL1-Mediated Recruitment of RNA Polymerase I to rRNA Gene Promoters.” EMBO Journal 20 (6): 1373–82. doi:10.1093/emboj/20.6.1373.

Morin, P. J. 1997. “Activation of Beta -Catenin-Tcf Signaling in Colon Cancer by Mutations in Beta -Catenin or APC.” Science 275 (5307): 1787–90. doi:10.1126/science.275.5307.1787.

Morrison, Sean J., and Allan C. Spradling. 2008. “Stem Cells and Niches: Mechanisms That Promote Stem Cell Maintenance throughout Life.” Cell 132 (4): 598–611. doi:10.1016/j.cell.2008.01.038.

Morrison, Sean J, and Judith Kimble. 2006. “Asymmetric and Symmetric Stem-Cell Divisions in Development and Cancer.” Nature 441 (7097): 1068–74. doi:10.1038/nature04956.

Muncan, Vanesa, Owen J Sansom, Leon Tertoolen, Toby J Phesse, Harry Begthel, Elena Sancho, Alicia M Cole, et al. 2006. “Rapid Loss of Intestinal Crypts upon Conditional Deletion of the Wnt/Tcf-4 Target Gene c-Myc.” Molecular and Cellular Biology 26 (22): 8418–26. doi:10.1128/MCB.00821-06.

Muñoz, Javier, Daniel E Stange, Arnout G Schepers, Marc van de Wetering, Bon-Kyoung Koo, Shalev Itzkovitz, Richard Volckmann, et al. 2012. “The Lgr5 Intestinal Stem Cell Signature: Robust Expression of Proposed Quiescent ‘+4’ Cell Markers.” The EMBO Journal 31 (14). EMBO Press: 3079–91. doi:10.1038/emboj.2012.166.

Murphy, Mark J., Anne Wilson, and Andreas Trumpp. 2005. “More than Just Proliferation: Myc Function in Stem Cells.” Trends in Cell Biology 15 (3): 128–37. doi:10.1016/j.tcb.2005.01.008.

Muth, Viola, Sophie Nadaud, Ingrid Grummt, and Renate Voit. 2001. “Acetylation of TAF I 68 , a Subunit of TIF-IB / SL1 , Activates RNA Polymerase I Transcription.” The EMBO Journal 20 (6): 1353–62.

Neutra, M R. 1998. “Current Concepts in Mucosal Immunity. V Role of M Cells in Transepithelial Transport of Antigens and Pathogens to the Mucosal Immune System.” The American Journal of Physiology 274 (5 Pt 1): G785-91. http://www.ncbi.nlm.nih.gov/pubmed/9612256.

Ng, Stanley W. K., Amanda Mitchell, James A. Kennedy, Weihsu C. Chen, Jessica McLeod, Narmin Ibrahimova, Andrea Arruda, et al. 2016. “A 17-Gene Stemness Score for Rapid Determination of Risk in Acute Leukaemia.” Nature 540 (7633). Nature Publishing Group: 433–37. doi:10.1038/nature20598.

Nikolov, E N, M D Dabeva, and T K Nikolov. 1983. “Turnover of Ribosomes in Regenerating Rat Liver.” The International Journal of Biochemistry 15 (10): 1255–60. http://www.ncbi.nlm.nih.gov/pubmed/6628827.

O’Brien, Catherine A., Aaron Pollett, Steven Gallinger, and John E. Dick. 2007. “A Human Colon Cancer Cell Capable of Initiating Tumor Growth in Immunodeficient Mice.” Nature 445 (7123): 106–10. doi:10.1038/nature05372.

Park, In-kyung, Dalong Qian, Mark Kiel, Michael W Becker, Michael Pihalja, Irving L Weissman, Sean J Morrison, and Michael F Clarke. 2003. “Bmi-1 Is Required for Maintenance of Adult Self-Renewing Haematopoietic Stem Cells.” Nature 423 (6937): 302–5. doi:10.1038/nature01587.

Peltonen, Karita, Laureen Colis, Hester Liu, Rishi Trivedi, MichaelS Moubarek, HennaM Moore, Baoyan Bai, MichelleA Rudek, CharlesJ Bieberich, and Marikki Laiho. 2014. “A Targeting Modality for Destruction of RNA Polymerase I That Possesses Anticancer Activity.” Cancer Cell 25 (1). Elsevier Inc.: 77–90. doi:10.1016/j.ccr.2013.12.009.

Peyroche, G., P. Milkereit, N. Bischler, H. Tschochner, P. Schultz, A. Sentenac, C. Carles, and M. Riva. 2000. “The Recruitment of RNA Polymerase I on rDNA Is Mediated by the Interaction of the A43 Subunit with Rrn3.” The EMBO Journal 19 (20): 5473–82. doi:10.1093/emboj/19.20.5473.

Pinto, Daniel, Alex Gregorieff, Harry Begthel, and Hans Clevers. 2003. “Canonical Wnt Signals Are Essential for Homeostasis of the Intestinal Epithelium Service Canonical Wnt Signals Are Essential for Homeostasis of the Intestinal Epithelium,” 1709–13. doi:10.1101/gad.267103.

Potten, C S. 1977. “Extreme Sensitivity of Some Intestinal Crypt Cells to X and Gamma Irradiation.” Nature 269 (5628): 518–21. doi:10.1038/269518a0.

Powell, Anne E, Yang Wang, Yina Li, Emily J Poulin, Anna L Means, Mary K Washington, James N Higginbotham, et al. 2012. “The Pan-ErbB Negative Regulator Lrig1 Is an Intestinal Stem Cell Marker That Functions as a Tumor Suppressor.” Cell 149 (1): 146–58. doi:10.1016/j.cell.2012.02.042.

Raza, Azra, and Naomi Galili. 2012. “The Genetic Basis of Phenotypic Heterogeneity in Myelodysplastic Syndromes.” Nature Reviews. Cancer 12 (12). Nature Publishing Group: 849–59. doi:10.1038/nrc3321.

Reya, Tannishtha, and Hans Clevers. 2005. “Wnt Signalling in Stem Cells and Cancer.” Nature 434 (7035): 843–50. doi:10.1038/nature03319.

Ricci-Vitiani, Lucia, Dario G Lombardi, Emanuela Pilozzi, Mauro Biffoni, Matilde Todaro, Cesare Peschle, and Ruggero De Maria. 2007. “Identification and Expansion of Human Colon-Cancer-Initiating Cells.” Nature 445 (7123): 111–15. doi:10.1038/nature05384.

Russell, Jackie, and Joost C B M Zomerdijk. 2005. “RNA-Polymerase-I-Directed rDNA Transcription, Life and Works.” Trends in Biochemical Sciences 30 (2). Elsevier: 87–96. doi:10.1016/j.tibs.2004.12.008.

Sanchez, Carlos G, Felipe Karam Teixeira, Benjamin Czech, Colin D Malone, Gregory J Hannon, Ruth Lehmann, Carlos G Sanchez, et al. 2016. “Regulation of Ribosome Biogenesis and Protein Synthesis Controls Germline Stem Cell Resource Regulation of Ribosome Biogenesis and Protein Synthesis Controls.” Elsevier Inc., 276–90. doi:10.1016/j.stem.2015.11.004.

Sancho, Elena, Eduard Batlle, and Hans Clevers. 2004. “SIGNALING PATHWAYS IN INTESTINAL DEVELOPMENT AND CANCER.” Annual Review of Cell and Developmental Biology 20 (1): 695–723. doi:10.1146/annurev.cellbio.20.010403.092805.

Sansom, Owen J., Karen R. Reed, Anthony J. Hayes, Heather Ireland, Hannah Brinkmann, Ian P. Newton, Eduard Batlle, et al. 2004. “Loss of Apc in Vivo Immediately Perturbs Wnt Signaling, Differentiation, and Migration.” Genes and Development 18 (12): 1385–90. doi:10.1101/gad.287404.

Sansom, Owen J, Valerie S Meniel, Vanesa Muncan, Toby J Phesse, Julie a Wilkins, Karen R Reed, J Keith Vass, Dimitris Athineos, Hans Clevers, and Alan R Clarke. 2007. “Myc Deletion Rescues Apc Deficiency in the Small Intestine.” Nature 446 (7136): 676–79. doi:10.1038/nature05674.

Sato, Toshiro, Johan H. van Es, Hugo J. Snippert, Daniel E. Stange, Robert G. Vries, Maaike van den Born, Nick Barker, Noah F. Shroyer, Marc van de Wetering, and Hans Clevers. 2011. “Paneth Cells Constitute the Niche for Lgr5 Stem Cells in Intestinal Crypts.” Nature 469 (7330). Nature Publishing Group: 415–18. doi:10.1038/nature09637.

Sato, Toshiro, Robert G. Vries, Hugo J. Snippert, Marc van de Wetering, Nick Barker, Daniel E. Stange, Johan H. van Es, et al. 2009a. “Single Lgr5 Stem Cells Build Crypt–villus Structures in Vitro without a Mesenchymal Niche.” Nature 459 (7244): 262–65. doi:10.1038/nature07935.

Schlosser, Isabel, Michael Hölzel, Marlies Mürnseer, Helmut Burtscher, Ulrich H. Weidle, and Dirk Eick. 2003. “A Role for c-Myc in the Regulation of Ribosomal RNA Processing.” Nucleic Acids Research 31 (21): 6148–56. doi:10.1093/nar/gkg794.

Schuijers, Jurian, Jan Philipp Junker, Michal Mokry, Pantelis Hatzis, Bon Kyoung Koo, Valentina Sasselli, Laurens G. Van Der Flier, Edwin Cuppen, Alexander Van Oudenaarden, and Hans Clevers. 2015. “Ascl2 Acts as an R-Spondin/wnt-Responsive Switch to Control Stemness in Intestinal Crypts.” Cell Stem Cell 16 (2). Elsevier Inc.: 158–70. doi:10.1016/j.stem.2014.12.006.

Shimokawa, Mariko, Yuki Ohta, Shingo Nishikori, Mami Matano, Ai Takano, Masayuki Fujii, Shoichi Date, Shinya Sugimoto, Takanori Kanai, and Toshiro Sato. 2017. “Visualization and Targeting of LGR5+ Human Colon Cancer Stem Cells.” Nature. Nature Publishing Group, 1–21. doi:10.1038/nature22081.

Shiue, C-N, Rg Berkson, and Aph Wright. 2009. “C-Myc Induces Changes in Higher Order rDNA Structure on Stimulation of Quiescent Cells.” Oncogene 28 (16). Nature Publishing Group: 1833–42. doi:10.1038/onc.2009.21.

Smyth, Gordon K. 2004. “Linear Models and Empirical Bayes Methods for Assessing Differential Expression in Microarray Experiments.” Statistical Applications in Genetics and Molecular Biology 3 (1): 1–25. doi:10.2202/1544-6115.1027.

Smyth, Gordon K, Joëlle Michaud, and Hamish S Scott. 2005. “Use of within-Array Replicate Spots for Assessing Differential Expression in Microarray Experiments.” Bioinformatics (Oxford, England) 21 (9): 2067–75. doi:10.1093/bioinformatics/bti270.

Stefanovsky, Victor Y., Guillaume Pelletier, Ross Hannan, Thérèse Gagnon-Kugler, Lawrence I. Rothblum, and Tom Moss.

2001. “An Immediate Response of Ribosomal Transcription to Growth Factor Stimulation in Mammals Is Mediated by ERK Phosphorylation of UBF.” Molecular Cell 8 (5): 1063–73. doi:10.1016/S1097-2765(01)00384-7.

Subramanian, A., P. Tamayo, V. K. Mootha, S. Mukherjee, B. L. Ebert, M. A. Gillette, A. Paulovich, et al. 2005. “Gene Set Enrichment Analysis: A Knowledge-Based Approach for Interpreting Genome-Wide Expression Profiles.” Proceedings of the National Academy of Sciences 102 (43): 15545–50. doi:10.1073/pnas.0506580102.

Sun, Jianlong, Azucena Ramos, Brad Chapman, Jonathan B Johnnidis, Linda Le, Yu-Jui Ho, Allon Klein, Oliver Hofmann, and Fernando D Camargo. 2014. “Clonal Dynamics of Native Haematopoiesis.” Nature 514 (7522): 322–27. doi:10.1038/nature13824.

Takashima, Shigeo, David Gold, and Volker Hartenstein. 2013. “Stem Cells and Lineages of the Intestine: A Developmental and Evolutionary Perspective.” Development Genes and Evolution 223 (1–2). Springer-Verlag: 85–102. doi:10.1007/s00427-012-0422-8.

Takeda, Norifumi, Rajan Jain, Matthew R LeBoeuf, Qiaohong Wang, Min Min Lu, and Jonathan A Epstein. 2011. “Interconversion between Intestinal Stem Cell Populations in Distinct Niches.” Science (New York, N.Y.) 334 (6061): 1420–24. doi:10.1126/science.1213214.

Tauriello, Daniele V. F., Alexandre Calon, Enza Lonardo, and Eduard Batlle. 2016. “Determinants of Metastatic Competency in Colorectal Cancer.” Molecular Oncology, 1–23. doi:10.1002/1878-0261.12018.

Torreira, Eva, Jaime Alegrio Louro, Irene Pazos, Noelia González-Polo, David Gil-Carton, Ana Garcia Duran, Sébastien Tosi, Oriol Gallego, Olga Calvo, and Carlos Fernández-Tornero. 2017. “The Dynamic Assembly of Distinct RNA Polymerase I Complexes Modulates rDNA Transcription.” eLife 6: e20832. doi:10.7554/eLife.20832.

Van De Wetering, Marc, Hayley E. Francies, Joshua M. Francis, Gergana Bounova, Francesco Iorio, Apollo Pronk, Winan Van Houdt, et al. 2015. “Prospective Derivation of a Living Organoid Biobank of Colorectal Cancer Patients.” Cell 161 (4). Elsevier Inc.: 933–45. doi:10.1016/j.cell.2015.03.053.

Van de Wetering, Marc, Elena Sancho, Cornelis Verweij, Wim De Lau, Irma Oving, Adam Hurlstone, Karin Van der Horn, et al. 2002. “The β-catenin/TCF-4 Complex Imposes a Crypt Progenitor Phenotype on Colorectal Cancer Cells.” Cell 111 (2): 241–50. doi:10.1016/S0092-8674(02)01014-0.

van der Flier, Laurens G., Marielle E. van Gijn, Pantelis Hatzis, Pekka Kujala, Andrea Haegebarth, Daniel E. Stange, Harry Begthel, et al. 2009. “Transcription Factor Achaete Scute-Like 2 Controls Intestinal Stem Cell Fate.” Cell 136 (5). Elsevier Ltd: 903–12. doi:10.1016/j.cell.2009.01.031.

van Es, Johan H., Philippe Jay, Alex Gregorieff, Marielle E. van Gijn, Suzanne Jonkheer, Pantelis Hatzis, Andrea Thiele, et al. 2005. “Wnt Signalling Induces Maturation of Paneth Cells in Intestinal Crypts.” Nature Cell Biology 7 (4): 381–86. doi:10.1038/ncb1240.

van Riggelen, Jan, Alper Yetil, and Dean W Felsher. 2010. “MYC as a Regulator of Ribosome Biogenesis and Protein Synthesis.” Nature Reviews. Cancer 10 (4). Nature Publishing Group: 301–9. doi:10.1038/nrc2819.

Vermeulen, Louis, Felipe De Sousa E Melo, Maartje van der Heijden, Kate Cameron, Joan H. de Jong, Tijana Borovski, Jurriaan B. Tuynman, et al. 2010. “Wnt Activity Defines Colon Cancer Stem Cells and Is Regulated by the Microenvironment.” Nature Cell Biology 12 (5): 468–76. doi:10.1038/ncb2048.

Victor Y. Stefanovsky, ‡, ‡ Frédèric Langlois, § David Bazett-Jones, ‡ and Guillaume Pelletier, and ‡ Tom Moss*. 2006. “ERK Modulates DNA Bending and Enhancesome Structure by Phosphorylating HMG1-Boxes 1 and 2 of the RNA Polymerase I Transcription Factor UBF†.” American Chemical Society . doi:10.1021/BI051782H.

Viktorovskaya, Olga V., and David A. Schneider. 2015. “Functional Divergence of Eukaryotic RNA Polymerases: Unique Properties of RNA Polymerase I Suit Its Cellular Role.” Gene 556 (1). Elsevier B.V.: 19–26. doi:10.1016/j.gene.2014.10.035.

Vincent, T, a Kukalev, M Andäng, R Pettersson, and P Percipalle. 2008. “The Glycogen Synthase Kinase (GSK) 3beta Represses RNA Polymerase I Transcription.” Oncogene 27 (39): 5254–59. doi:10.1038/onc.2008.152.

Voit, R, M Hoffmann, and I Grummt. 1999. “Phosphorylation by G1-Specific Cdk-Cyclin Complexes Activates the Nucleolar Transcription Factor UBF.” The EMBO Journal 18 (7): 1891–99. doi:10.1093/emboj/18.7.1891.

Voit, R, K Schäfer, and I Grummt. 1997. “Mechanism of Repression of RNA Polymerase I Transcription by the Retinoblastoma Protein.” Mol Cell Biol 17 (8): 4230–37. doi:10.1128/MCB.17.8.4230.

Wang, Yang, Maryann Giel-Moloney, Guido Rindi, and Andrew B Leiter. 2007. “Enteroendocrine Precursors Differentiate Independently of Wnt and Form Serotonin Expressing Adenomas in Response to Active Beta-Catenin.” Proceedings of the National Academy of Sciences of the United States of America 104 (27). National Academy of Sciences: 11328–33. doi:10.1073/pnas.0702665104.

Watanabe-Susaki, Kanako, Hitomi Takada, Kei Enomoto, Kyoko Miwata, Hisako Ishimine, Atsushi Intoh, Manami Ohtaka, et al. 2014. “Biosynthesis of Ribosomal RNA in Nucleoli Regulates Pluripotency and Differentiation Ability of Pluripotent Stem Cells.” Stem Cells (Dayton, Ohio) 32 (12):

3099–3111. doi:10.1002/stem.1825.

Whissell, Gavin, Elisa Montagni, Paola Martinelli, Xavier Hernando-Momblona, Marta Sevillano, Peter Jung, Carme Cortina, et al. 2014. “The Transcription Factor GATA6 Enables Self-Renewal of Colon Adenoma Stem Cells by Repressing BMP Gene Expression.” Nature Cell Biology 16 (7): 695–707. doi:10.1038/ncb2992.

Wickham, Hadley. 2009. ggplot2. Elegant Graphics for Data Analysis. Edited by Springer.

Woolnough, Jessica L., Blake L. Atwood, Zhong Liu, Rui Zhao, and Keith E. Giles. 2016. “The Regulation of rRNA Gene Transcription during Directed Differentiation of Human Embryonic Stem Cells.” PLoS ONE 11 (6): 1–18. doi:10.1371/journal.pone.0157276.

Wu, Chi-Hwa, Debashis Sahoo, Constadina Arvanitis, Nicole Bradon, David L. Dill, and Dean W. Felsher. 2013. “Correction: Combined Analysis of Murine and Human Microarrays and ChIP Analysis Reveals Genes Associated with the Ability of MYC To Maintain Tumorigenesis.” Edited by Vivian G. Cheung. PLoS Genetics 9 (10). doi:10.1371/annotation/a0e06cef-a7e4-4ec9-9f35-9df5e50bf7a2.

Wu, Chi-Hwa, Debashis Sahoo, Constadina Arvanitis, Nicole Bradon, David L Dill, and Dean W Felsher. 2008. “Combined Analysis of Murine and Human Microarrays and ChIP Analysis Reveals Genes Associated with the Ability of MYC to Maintain Tumorigenesis.” Edited by Vivian G. Cheung. PLoS Genetics 4 (6): e1000090. doi:10.1371/journal.pgen.1000090.

Yarden, Yosef, and Ben-Zion Shilo. 2007. “SnapShot: EGFR Signaling Pathway.” Cell 131 (5): 1018. doi:10.1016/j.cell.2007.11.013.

Zhai, Weiguo, and Lucio Comai. 2000. “Repression of RNA Polymerase I Transcription by the Tumor Suppressor p53.” Molecular and Cellular Biology 20 (16): 5930–38. doi:10.1128/MCB.20.16.5930-5938.2000.Updated.

Zhang, Qiao, Nevine A Shalaby, Michael Buszczak, A. Spradling, D. Drummond-Barbosa, T. Kai, S. J. Morrison, et al. 2014. “Changes in rRNA Transcription Influence Proliferation and Cell Fate within a Stem Cell Lineage.” Science (New York, N.Y.) 343 (6168). American Association for the Advancement of Science: 298–301. doi:10.1126/science.1246384.

Zhong, W, J N Feder, M M Jiang, L Y Jan, Y N Jan, S Artavanis-Tsakonas, K Matsuno, et al. 1996. “Asymmetric Localization of a Mammalian Numb Homolog during Mouse Cortical Neurogenesis.” Neuron 17 (1): 43–53. doi:10.1016/S0896-6273(00)80279-2.